

UNIVERSITY OF SHEFFIELD  
Department of Civil and Structural Engineering

A LABORATORY STUDY OF THE  
SHAFT RESISTANCE OF BORED PILES

by

YONG KWET YEW 楊國柔  
B.Eng. (Shefd.)

A thesis submitted to the University  
of Sheffield for the degree of  
Doctor of Philosophy.

September, 1979

To my parents ....

.... for their love and encouragement.

## SUMMARY

The work presented in this thesis forms a pioneer study for future laboratory investigation into the behaviour of bored piles in clay. The research covered important aspects of installation and the factors affecting the development of pile shaft resistance. Total and effective stress approaches to pile design were examined using the test results.

A series of carefully controlled laboratory scale experiments was conducted on an elemental section of pile installed in a bed of anisotropically consolidated kaolin prepared to a known stress history. The tests were conducted in such a manner that the various stages of field pile construction were simulated as closely as possible.

To monitor the total stresses and pore water pressures in the soil and at the pile-soil interface, small-scale measuring devices were successfully developed.

Test results showed that the shaft resistance of bored piles in clay is primarily a function of the effective horizontal stress acting on the pile shaft and the effective angle of friction between the soil and the pile. For the variables investigated, the development of shaft resistance depended on the degree of moisture migration and soil softening close to the pile, the water-cement ratio of the pile, the time delay between boring and concreting, and the time lapse between casting and load testing.

## ACKNOWLEDGEMENTS

This research was carried out in the Department of Civil and Structural Engineering of the University of Sheffield, for which the author expresses his gratitude to the Head of Department, Professor D. Bond, for the use of the facilities. The author is also obliged to the University of Sheffield for the award of the University Grouped Scholarship in Engineering.

The author is indebted to Dr W. F. Anderson for his guidance, supervision and assistance in many ways. The help and encouragement from Professor T. Hanna and the Geotechnical Staff of the Department is gratefully acknowledged.

The skills of the technical staff in the fabrication of equipment and instrumentation is appreciated. In particular, the author wishes to acknowledge the assistance of Mr. J.D. Webster, Mr. V. Harrison, and Mr. S. Hill. The help of Mrs. D. Hutson for the photographic prints and Mr. Y. S. Chia for the assistance in preparing the drawings are acknowledged.

The author wishes to thank his colleagues, in particular, Mr. T. A. Ooi and Mr. Y. Tanaka for their constructive criticisms and helpful suggestions.

The author also acknowledges the contribution of many others whose names are not given individual mention here.

This thesis could not have completed without the support and encouragement of the author's parents and sisters. Finally, the author wishes to express his love and gratitude to his wife, Yoke Chin, for her patience and encouragement throughout the study as well as the help rendered in the preparation of this thesis.

## CONTENTS

	<u>Page</u>
Title	... i
Dedication	... ii
Summary	... iii
Acknowledgements	... iv
Contents	... v
List of tables	... xi
List of figures	...xiii
Notations	.. xviii
CHAPTER 1 <u>INTRODUCTION</u>	... 1
1.1    General	... 1
1.2    The need for investigation	... 1
1.3    Research objectives	... 3
1.4    Characteristics of laboratory-scale tests	... 4
CHAPTER 2 <u>LITERATURE REVIEW ON BORED PILES IN CLAY</u> ...	5
2.1    Introduction	... 5
2.2    Selection and use of bored piles	... 5
2.3    Current methods of construction	... 6
2.3.1 Introduction	... 6
2.3.2 Dry method	... 7
2.3.3 Slurry displacement method	... 8
2.3.4 Casing method	... 8
2.3.5 Underreaming of bored piles	... 10
2.3.6 General construction considerations..	10
2.4    Effects of installation and associated problems	... 12
2.4.1 Introduction	... 12
2.4.2 Stress changes in the vicinity of pile	... 12
2.4.3 Moisture migration and softening in soil	... 14
2.4.4 Swelling and stability of boreholes..	16
2.4.5 Mechanical disturbance	... 17
2.4.6 Defects in bored cast-in-situ piles..	18

	<u>Page</u>
2.5	Behaviour of bored piles under axial load ... 19
2.5.1	Load transfer and settlement ... 19
2.5.2	Adhesion factor $\alpha$ ... 21
2.5.3	Increase in shaft capacity with time ... 24
2.5.4	Effect of sustained loading ... 24
2.6	Other factors affecting shaft friction of bored piles ... 25
2.6.1	Introduction ... 25
2.6.2	Stresses in soil surrounding a pile ... 25
2.6.3	Physical characteristics of piles ... 26
2.6.4	Influence of bentonite ... 28
2.6.5	Effect of underreaming ... 28
2.6.6	Effect of construction procedure ... 29
2.7	Bored piles in difficult ground conditions .. 30
2.8	General comparisons of bored and driven piles. 32
2.9	A brief review of pile group behaviour ... 34
CHAPTER 3	<u>EFFECTIVE STRESS APPROACH IN PILE DESIGN</u> ... 35
3.1	Review of current design methods ... 35
3.1.1	Introduction ... 35
3.1.2	Adhesion or $\alpha$ -method ... 36
3.1.3	API-method ... 37
3.1.4	$\lambda$ -method ... 38
3.1.5	Effective stress method ... 38
3.1.6	Factors of safety ... 39
3.2	Effective stress methods of design ... 39
3.2.1	Concept of effective stress ... 39
3.2.2	Shaft resistance in terms of effective stress ... 40
3.2.3	Potential of the effective stress approach ... 43
3.2.4	Application of the effective stress method in pile design ... 44
3.3	Estimation of design parameters ... 47
3.3.1	Introduction ... 47
3.3.2	Total and effective vertical stress ... 47
3.3.3	Total and effective horizontal stress .. 48
3.3.4	Coefficient of lateral stress, $K_s$ ... 50
3.3.5	Effective stress parameters ... 51
3.4	Limitations of the effective stress approach. 51

		<u>Page</u>
CHAPTER 4	<u>TEST APPARATUS</u>	... 53
4.1	Introduction	... 53
4.2	Design and development of test cell	... 53
	4.2.1 Test requirements	... 53
	4.2.2 Design of test cell	... 55
	4.2.3 Construction details	... 55
4.3	Ancillary equipment	... 57
	4.3.1 Augering device	... 57
	4.3.2 Loading system	... 58
	4.3.3 Void forming device	... 58
	4.3.4 Convoluted rubber jack	... 59
	4.3.5 Borehole measuring device	... 60
4.4	Soil sampling and testing equipment	... 60
	4.4.1 General	... 60
	4.4.2 Vane shear apparatus	... 61
	4.4.3 Triaxial test apparatus	... 62
CHAPTER 5	<u>INSTRUMENTATION AND MEASUREMENTS</u>	... 64
5.1	Introduction	... 64
	5.1.1 General	... 64
	5.1.2 Fundamentals of instrumentation	... 65
5.2	Measurements required for test studies	... 65
5.3	Design and development of pressure cells	... 66
	5.3.1 Introduction	... 66
	5.3.2 Review of pertinent literature	... 67
	5.3.3 Factors influencing the performance of pressure cells	... 68
	5.3.4 Design considerations	... 69
	5.3.5 Design of pressure cells	... 70
	5.3.6 Construction details	... 71
	5.3.7 Strain gauge technique	... 72
	5.3.8 Calibration	... 74
	5.3.9 Summary	... 76
5.4	Pore water pressure piezometers	... 76
	5.4.1 Introduction	... 76
	5.4.2 Factors affecting pore water pressure measurement	... 77
	5.4.3 Development of piezometers	... 79
	5.4.4 De-airing of piezometer system	... 81

	<u>Page</u>
5.4.5 Calibration	... 82
5.5 Settlement measurements	... 83
5.5.1 Introduction	... 83
5.5.2 Tell tale arrangement	... 83
5.5.2 Calibration of displacement transducers (LVDT)	... 84
5.6 Data acquisition	... 84
 CHAPTER 6	
<u>TEST PROGRAMME AND EXPERIMENTAL PROCEDURES</u>	... 87
6.1 Test programme	... 87
6.2 General procedure	... 88
6.3 Preparation of clay beds	... 89
6.3.1 Introduction	... 89
6.3.2 Cell and soil instrumentation	... 89
6.3.3 Preparation procedure	... 91
6.4 Installation of 'model' concrete pile	... 94
6.4.1 Introduction	... 94
6.4.2 Use of microconcrete for 'model' piles.	... 95
6.4.3 Boring	... 96
6.4.4 Casting and curing	... 97
6.5 Pile testing procedure	... 99
6.5.1 Introduction	... 99
6.5.2 Loading procedure	... 99
6.6 Summary of experimental procedures	... 101
6.7 Observation after pile tests	... 101
6.7.1 Introduction	... 101
6.7.2 General observations	... 102
6.8 Experiments on factors affecting test performance	... 103
6.8.1 Introduction	... 103
6.8.2 Boundary effects	... 103
6.8.3 Stability of instrumentation	... 103
 CHAPTER 7	
<u>PRESENTATION AND INTERPRETATION OF TEST RESULTS</u>	... 105
7.1 Introduction	... 105
7.2 Properties of soil	... 105
7.2.1 Basic properties	... 105

	<u>Page</u>
7.2.2 Consolidation and swelling characteristics	... 106
7.2.3 Strength properties	... 107
7.2.4 Effective stress parameters	... 111
7.2.5 $K_0$ studies	... 111
7.3 Short term effects of installation on soil properties	... 114
7.3.1 General	... 114
7.3.2 Moisture migration study	... 114
7.3.3 Changes in undrained strength	... 116
7.3.4 General relationship between moisture migration and changes in soil strength	... 118
7.4 Long term installation effects on soil properties	... 120
7.4.1 General	... 120
7.4.2 Influence of curing time on moisture migration	... 121
7.4.3 Influence of curing time on shear strength	... 122
7.5 Results of load tests on piles	... 122
<b>CHAPTER 8</b> <u>GENERAL DISCUSSION ON TEST PERFORMANCE AND TEST RESULTS</u>	... 125
8.1 Introduction	... 125
8.2 General limitations of the experimental study	... 125
8.3 Performance and limitations of test apparatus	... 126
8.3.1 Performance of test equipment	... 126
8.3.2 Repeatability of test results	... 127
8.3.3 Boundary effects of test cell	... 128
8.3.4 Effects of temperature	... 129
8.3.5 Effects of creep in soil and concrete ..	131
8.4 Performance and limitations of instrumentation	... 132
8.4.1 Introduction	... 132
8.4.2 General performance of EP and IF pressure cells	... 132
8.4.3 Compatibility of theoretical and measured readings	... 134

	<u>Page</u>
8.4.4 Stability of strain gauges	... 135
8.4.5 Response of piezometers	... 137
8.4.6 Tell tale devices	... 140
8.5 Stress changes in the soil surrounding the pile	... 140
8.5.1 General	... 140
8.5.2 Consolidation and boring	... 140
8.5.3 Casting and curing	... 140
8.5.4 Pile loading	... 144
8.6 Analysis of load test results in terms of total and effective stress	... 146
8.6.1 Introduction	... 146
8.6.2 Total stress analysis	... 146
8.6.3 Effective stress analysis	... 149
8.6.4 General discussion on total and effective stress analysis	... 152
8.6.5 Comparison of design methods	... 156
8.6.6 Implications of the analysis	... 159
8.7 Factors influencing development of shaft resistance of bored piles	... 160
8.7.1 Introduction	... 160
8.7.2 Effect of stress history of soil	... 161
8.7.3 Effect of pile dimensions	... 161
8.7.4 Effect of delay between boring and concreting	... 162
8.7.5 Influence of moisture migration	... 164
8.7.6 Effect of long term curing of test piles	... 166
 CHAPTER 9	
<u>CONCLUSIONS AND RECOMMENDATIONS FOR FUTURE RESEARCH</u>	... 168
9.1 Main conclusions	... 168
9.2 Recommendations for future research	... 170
 REFERENCES	... 172
APPENDIX I Design of consolidation and test cell	... 183
II Manufacture of rubber jacks	... 186
III Design of earth pressure cell	... 187
IV Theoretical calculation of strain in the centre of the diaphragm	... 189
V Principles of strain gauging	... 190
VI Calculation of time lag for design purposes..	192

## LIST OF TABLES

<u>Table No.</u>	<u>Title</u>
2.1	Advantages and disadvantages in the use of bored piles.
2.2	Typical sizes and loads for bored piles
2.3	Recommended slump for bored cast-in-place piles
2.4	Working stresses and maximum working loads in compression on bored-and-cast-in-situ piles (including driven-in-tubes)
2.5	Summary of field studies on moisture migration
2.6	Summary of existing literature on adhesion factor of bored piles in clay
3.1	Empirical relationships of $K_0$ for normally consolidated clays
3.2	Empirical relationships of $K_0$ for overconsolidated clays
5.1	Measurements and instrumentation
5.2	Design guidelines for pressure cells
5.3	Types of IF pressure cells developed
5.4	Strain rosettes (manufacturer's specifications)
5.5	Typical characteristics of pressure cells developed
6.1	Main test programme
6.2	Complementary test programme
6.3	Details of main test programme
6.4	Basic properties of kaolin
6.5	Microconcrete mix design
6.6	Properties of microconcrete
7.1	Consolidation characteristics of kaolin
7.2	Strength properties
7.3	Pore pressure parameters
7.4	Measured values of $K_0$
7.5	Summary of reported $K_0$ measurements for kaolinite clay
7.6	Values of $K_0$ calculated from empirical relationships

<u>Table No.</u>	<u>Title</u>
7.7	Influence of initial moisture content on moisture migration
7.8	Influence of water-cement ratio on moisture migration
7.9	Influence of stress history on remoulding factor, $\alpha_r$
7.10	Influence of water-cement ratio on remoulding factor, $\alpha_r$
7.11	Influence of curing time on moisture migration
7.12	Influence of curing time on shear strength
7.13	Results of load tests
8.1	Repeatability of test results
8.2	Response of piezometers
8.3	Total stress analysis of load test results
8.4	Effective stress analysis of load test results
8.5	Comparison between predicted and measured shaft resistance
8.6	Effect of delay time on development of shaft resistance
8.7	Calculation of excess water in concrete available for moisture migration

## LIST OF FIGURES

<u>Figure No.</u>	<u>Title</u>
2.1	Classification of cast-in situ piles
2.2	Dry method
2.3	Slurry method
2.4	Casing method
2.5	Some equipment used in the construction of bored piles
2.6	State of stress and deformation around piles (after Kedzi, 1975)
2.7	Pattern of moisture movement
2.8	Moisture transfer between concrete and clay (after Taylor, 1966)
2.9	Strain caused by boring a 25mm hole in a kaolin specimen using two different techniques(after Eid, 1978)
2.10	Formation of cavities in bored pile construction
2.11	Typical load transfer of an axially loaded bored pile
2.12	Development of shaft and base resistance (after Burland and Cooke, 1974)
2.13	Histogram of adhesion values for bored piles (Kraft and Lyons, 1974)
2.14	Development of shaft friction on cylindrical and irregular pile shaft (after Fleming and Sliwinski, 1977)
3.1	Design curves for adhesion factors for piles driven into clay soils (after Tomlinson, 1977)
3.2	Frictional capacity coefficient, $\lambda$ , versus pile penetration (after Vijayvergiya and Focht, 1972)
3.3	State of stress in soil and at pile-soil interface at depth 'd'
3.4	Relationship between average shaft friction, $q_s$ , and average depth for driven piles in soft clay (after Burland, 1973)
3.5	Relationship between average shaft friction and average depth in clay for bored piles in London Clay (after Burland, 1973)
3.6	Relationship between average shaft friction and average depth in clay for driven piles in London Clay (after Burland, 1973)

<u>Figure No.</u>	<u>Title</u>
3.7	Relationship between $K_0$ , $\sigma'$ and OCR (after Brooker and Ireland, 1965)
3.8	Values of Poisson's Ratio for lightly overconsolidated soils (after Wroth, 1975)
4.1	Schematic diagram of test cell
4.2	Details of cell covers
4.3	Typical test cell
4.4	Arrangement of test cells
4.5	Augering devices
4.6	Loading system
4.7	Details of loading arrangement
4.8	Void forming device
4.9	Materials for making 'voids'
4.10	Equipment for manufacture of rubber jacks
4.11	Borehole measuring device
4.12	Moisture content sampling equipment
5.1	Approximate location of instrumentation used
5.2	Design relationship between diaphragm thickness and pressure
5.3	Details of pressure cells
5.4	Pressure cells
5.5	Materials for fabrication of pressure cells
5.6	Bonding of strain gauges
5.7	Dummy gauges
5.8	Calibration of pressure cells
5.9	Typical calibration curves for pressure cells
5.10	Types of probes
5.11	Materials for piezometer system
5.12	Details of probes
5.13	Piezometer arrangement
5.14	Calibration of pressure transducers
5.15	Tell tale arrangement
5.16	Calibration of displacement transducer
5.17	Tell tale device and LVDT calibrating apparatus
5.18	Terminal box

<u>Figure No.</u>	<u>Title</u>
5.19	Power supply, portable DVM and Junction box
5.20	Data logger
5.21	Flow diagram for computation of results
5.22	Flow diagram for data acquisition
6.1	Test arrangement
6.2	Test arrangement and set-up
6.3	Soil instrumentation
6.4	Simulation of shaft resistance on pile element
6.5	Pile instrumentation
6.6	Stress-strain curves for prototype and microconcrete (after Aldridge and Breen, 1968)
6.7	Stress surrounding the 'model' pile
6.8	Summary of experimental procedures
6.9	(Horizontal) EP pressure cell
6.10	Location of soil instrumentation
6.11	Exposed pile shaft and location of instrumentation
7.1	Relationship between water content and consolidation pressure (logarithm scale)
7.2	Typical consolidation curves
7.3	Relationship between void ratio and consolidation pressure
7.4	Plot of void ratio versus consolidation pressure at logarithm scale
7.5	Typical stress strain relationship
7.6	Plot of undrained shear strength obtained from vane shear tests and from consolidated-undrained triaxial tests
7.7	Variation of undrained shear strength with stress history
7.8	Plots of pore pressure parameter $A_f$ versus overcon- solidation ratio on (a) logarithm scale and (b) in- verse scale
7.9	Mohr stress circles for consolidated-undrained triaxial test
7.10	Typical variation of stresses and pore pressure

<u>Figure No.</u>	<u>Title</u>
	during consolidation (pressure increment 0 → 70 kN/m <sup>2</sup> )
7.11	Typical variation of stress and pore pressure during consolidation
7.12	Relationship between horizontal and vertical effective stresses measured at the end of primary consolidation
7.13	Variation of $K_0$ with stress history
7.14	Influence of initial moisture content on moisture migration in soil surrounding the pile (at mid-height of pile)
7.15	Influence of water-cement ratio on moisture migration in soil surrounding pile (at mid-height of pile)
7.16	Influence of stress history on the remoulding factor in soil surrounding the pile
7.17	Influence of water-cement ratio on the remoulding factor in soil adjacent to the pile
7.18	Relationship between remoulding factor and initial moisture content of the soil
7.19	Relationship between remoulding factor and average increase in moisture content of soil within 20mm from pile face
7.20	Variation of moisture content with curing time
7.21	Variation of remoulding factor and average increase in moisture content of soil close to the pile shaft with curing time
7.22	Typical load/settlement/time relationship
7.23	Typical plot of shaft resistance versus settlement in dimensionless quantity
7.24	Comparison of load-settlement characteristics with soil stress-strain behaviour
8.1	Repeatability of test results (variation of stresses during consolidation)
8.2	Repeatability of test results (load-settlement relationship)
8.3	Ambient temperature in the research laboratory for a complete year

<u>Figure No.</u>	<u>Title</u>
8.4	Zero drifts in strain gauges
8.5	Variation of total horizontal stress, pore water pressure and effective horizontal stress with time (Normally consolidated clays $p_o = 420 \text{ kN/m}^2$ )
8.6	Variation of total and effective horizontal stress and pore pressure with time (overconsolidated clay, OCR = 4)
8.7	Relationship between adhesion factor and undrained shear strength
8.8	Relationship between remoulding factor and adhesion factor for normally consolidated clay
8.9	Relationship between shaft resistance and effective horizontal stress
8.10	Correlation of $\alpha$ and $\beta$ values for lightly overconsolidated clay
8.11	Range of stress condition in normally consolidated and lightly overconsolidated soils where $\phi'$ is not fully mobilized [ after Parry and Swain, (1976)]
8.12	Comparison between shaft resistance predicted by total and effective stress method values (7 days after casting) for normally consolidated clay
8.13	Shaft resistance versus pile displacement for different stress histories
8.14	Shaft resistance versus pile displacement for various pile diameters
8.15	Effect of delay between completion of boring and casting on the adhesion factor
8.16	Changes in moisture content and shear strength after pile installation
8.17	Development of shaft resistance with time
8.18	Effect of age on adhesion factor

## NOTATIONS AND SYMBOLS

A	-	pore pressure parameter (after Skempton)
$A_f$	-	pore pressure parameter A at failure
B	-	pore pressure parameter (after Skempton)
$C_A$	-	cell action factor
$C_C$	-	compression index
$C_S$	-	swelling index
c	-	cohesion
$c'$	-	effective cohesion
$c_a$	-	pile adhesion
$c_u$	-	undrained shear strength
$C_v$	-	coefficient of consolidation
D	-	pile diameter
E	-	modulus of elasticity
e	-	void ratio
G	-	specific gravity
H	-	thickness of clay bed
$I_p$	-	plasticity index
K	-	strain gauge factor
$K_0$	-	coefficient of lateral earth pressure at rest
$K_s$	-	coefficient of lateral stress
k	-	coefficient of permeability
L	-	length of pile
$m_v$	-	coefficient of volume compressibility
$N_c$	-	bearing capacity factor
p	-	vertical consolidation or overburden pressure <i>total or effective</i>
$Q_b$	-	end bearing load
$Q_s$	-	shaft load
$Q_u$	-	total load
$q_b$	-	unit end bearing capacity
$q_s$	-	unit shaft resistance
$S_r$	-	degree of saturation
U	-	degree of primary consolidation
u	-	pore water pressure
w	-	water content
$\Delta w$	-	average increase in moisture content in the first 20mm from pile

- $\alpha$  - adhesion factor
- $\alpha_r$  - remoulding factor
- $\beta$  - empirical factor
- $\gamma_s$  - unit weight of soil
- $\gamma_w$  - unit weight of water
- $\delta$  - effective angle of friction between the soil and pile
- $\epsilon$  - linear strain
- $\lambda$  - frictional coefficient
- $\nu$  - Poisson's ratio
- $\sigma, \sigma'$  - normal total and effective stress respectively
- $\sigma_1', \sigma_3'$  - effective principal stresses
- $\sigma_H, \sigma_H'$  - total and effective horizontal stress
- $\sigma_m'$  - mean effective normal stress
- $\sigma_v, \sigma_v'$  - total and effective vertical stress
- $\tau$  - shear stress
- $\phi'$  - effective angle of shearing resistance of soil
- $\phi_p'$  - peak effective angle of shearing resistance
- $\phi_r'$  - residual effective angle of shearing resistance

## CHAPTER 1

### INTRODUCTION

#### 1.1 GENERAL

A bored pile is a deep foundation constructed by excavating a hole and casting concrete directly against the soil. For axial loads, the shaft provides vertical support by both shaft friction and end-bearing. The base of the shaft may be enlarged to increase the capacity of the pile.

Recent developments in drilling equipment and installation techniques have led to extensive application of bored piles for foundation work. The inherent advantages of relatively rapid, quiet and vibrationless installation have made bored piles ideally suited for foundation work in built-up areas.

#### 1.2 THE NEED FOR INVESTIGATION

A common problem in foundation engineering is the pre-determination of load bearing capacity in terms of the fundamental soil properties. In order to make such a prediction, a knowledge of state of stress which exists in the soil, immediately after pile installation and before loading, is essential. Unfortunately most literature on piles contains a substantial amount of pile performance records and load-settlement characteristics, but a lack of information on installation aspects and the stress changes within the supporting soil. Furthermore, very few published records exist on attempts to directly measure these stresses. Hence, little is known about the actual changes in soil properties as a result

of installation, and the way effective stresses at the soil-pile interface are likely to be affected by this process. Therefore, there is a need to gain information on the interaction of a bored pile with the supporting soil so that significant parameters related to the design can be treated rationally.

One of the phenomena governing the development of shaft resistance in bored piles is the migration of moisture and the associated softening of soil in the vicinity of the pile. Since water has a great influence on soil properties such as strength, the study of moisture migration between fresh concrete and the soil is important in developing an understanding of the behaviour of bored piles.

Most of the reported studies on moisture migration have been carried out in the laboratory using a shear box with a normal load applied to simulate the lateral pressure on the concrete surface. However, these tests did not consider the effects of boring, leading to stress relief in the soil. Therefore, the moisture distribution obtained from the above studies must be treated with caution. An alternative method of investigation, in which piles are formed in-situ and where field procedures are simulated as closely as practically possible, is required.

Factors influencing the long term behaviour of bored piles such as the drilling time, disturbance to the soil fabric at the interface, time delay between boring and concreting and the elapsed time after construction have not been quantitatively evaluated. These factors are presently reflected in design only by application of 'good engineering judgement'. Most of the pile tests reported took place in a relatively short span of time (between 7 to 28 days) after casting. It will be interesting to discern if any deviations exist between the shaft resistance mobilized after short and long curing times.

The design of piles is at present mostly achieved by means of semi-empirical rules and experience, supplemented by field tests on single piles. From an examination of pile tests reported in the literature, it is evident that in some cases, the design load is unduly conservative. There is a need to look at a different approach to the design problem, one which may give a more realistic prediction to the ultimate load.

### 1.3 RESEARCH OBJECTIVES

The principal objectives of this research study are:

1. To improve the understanding of the fundamental aspects of the behaviour of bored piles, in particular, the effects of installation,
2. To investigate the factors that influence the development of shaft resistance, and
3. To examine the effective stress approach as a design method.

Laboratory techniques were chosen for achieving the objectives of the investigation because soil properties, construction procedures and instrumentation could be closely controlled.

The key assumption made at the outset of the studies was that the behaviour of bored piles can be determined from engineering properties of soil, particularly in terms of effective stresses. Therefore, there is a need to develop reliable laboratory-scale instrumentation capable of monitoring stresses in the soil as well as stresses at the pile-soil interface.

### 1.4 CHARACTERISTICS OF LABORATORY-SCALE TESTS

Apart from the high cost involved in terms of equipment and labour, field tests also have a number of experimental

difficulties. Very often, it is difficult, almost impossible, to control variables in the field. On the other hand, small-scale laboratory tests have potential savings in time, materials and labour. Laboratory tests also permit certain investigations to be performed under more uniform soil conditions than would be found at most field test sites. The small-scale of the tests also enable a more detailed investigation of certain phases of the problem. The simplicity of test procedures and the ease of instrumenting the tests at relatively low costs are further advantages of laboratory-scale tests

However, for a 'model' or laboratory-scale test to be fully representative of field conditions, all gravity stresses in the soil should be reproduced. This is only possible in a centrifuge and access to this facility is very limited. Another practical difficulty associated with laboratory-scale tests is the time factor. For example, consolidation in the laboratory takes about a few days or weeks but in the field, the process is over a period of years. Therefore, differences in the behaviour of soil in the field and that prepared in the laboratory are likely.

Whilst recognising the limitations of a laboratory study, particularly in relation to the scale effect, the contributions of such investigations should not be overlooked.

## CHAPTER 2

### LITERATURE REVIEW ON BORED PILES

#### 2.1 INTRODUCTION

Bored piles were first used in Chicago and New York about 75 years ago as caissons to transmit the load of skyscrapers through deep deposits of sand or clay to rock, and also in Texas as foundations in expansive clays. At that time, excavation was carried out manually. The excavation for the drilled shafts by machine was first employed in the United States in the 1920's. Since then, especially over the last 20 years, there have been remarkable improvements in the installation techniques and drilling equipment covering a wide variety of soil conditions.

Field studies on the behaviour of bored piles are limited in view of the vast expense and time involved in the preparation of field tests. Most of the reported research studies relating to bored piles have been conducted in London clay and in Beaumont clay, Houston, Texas. Results from these studies and literature pertinent to the scope of this research investigation will be referred to in the appropriate sections of this chapter.

Studies by Chandler(1968), Burland (1973) and more recently by Kirby and Esrig (1979) and Searle (1979) have renewed interest in the application of the effective stress approach to the design of piles. The work of these authors will be reported in Chapter 3.

#### 2.2 SELECTION AND USE OF BORED PILES

There are many different types of piles described in various engineering literature and they may be classified in different

ways according to the material used, the method of installation and the performance. Further details can be found in Peck et al. (1974) and Tomlinson (1977), while Weltman and Little (1977) provides a comprehensive review of various pile types available in the United Kingdom.

There are no standard rules on the selection of piles. Important considerations influencing the choice are the soil and groundwater conditions, the type of structure to be supported, the site access and space, the environment and the cost.

The first consideration probably represents the most significant factor governing the selection. Ground conditions where shafts can be bored without using a lining and where the base can be enlarged easily by mechanical tools favour the use of bored piles. Such is the case for London clay where large diameter bored piles are frequently used. The other advantages of bored piles are listed in Table 2.1 together with some disadvantages. Typical dimensions of bored piles and the normal load ranges are compiled in Table 2.2 from technical brochures of piling firms and the reported literature of Weltman and Little (1977).

## 2.3 CURRENT METHODS OF CONSTRUCTION

### 2.3.1 Introduction

Based on published information including Tomlinson (1977), Weltman and Little (1977) and Reese (1978), and technical brochures of various piling firms, it can be seen that bored piles can be classified in two different ways - according to their method of construction or according to the type of equipment used. The two methods of classification are shown in Fig. 2.1 and does not include a number of specialised techniques patented by major piling firms.

In general, the construction procedure includes boring a hole with or without casing, inspecting the bored hole and back-filling the hole with fresh concrete with or without reinforcing steel. Bored piles are mostly vertical because the construction of inclined piles are difficult and expensive. Piles may be straight-shafted, deriving their support mainly from shaft friction or in suitable soils, they may have enlarged bases (underreams or bells), with the object of increasing the end bearing capacity.

There are several methods of constructing a bored pile as shown in Fig. 2.1(a). The choice depends on a number of factors, including properties of the soil, structural considerations and comparative economics. However, only the three most common methods are described : (a) dry method (b) slurry displacement method and (c) the casing method. Since there are many variations in these procedures in different countries, only the typical features will be covered. For further details on the pile construction practices in the United Kingdom, Tomlinson (1977) provides a comprehensive review of the techniques and equipment available.

### 2.3.2 The Dry Method

In stable ground, an unlined hole can be drilled by hand or auger in the dry. If reinforcement is required, a light cage can then be placed in the hole followed by concrete. The stages of construction by the dry method are illustrated in Fig. 2.2.

The dry method allows rapid construction of bored piles and is employed in the absence of water-bearing sands and when boring can be completed quickly enough to prevent collapse of the borehole walls. Homogeneous firm to stiff clay usually favours the use of this method.

### 2.3.3 Slurry Displacement Method

This method is commonly used in unstable soil conditions and involves the use of a drilling mud during the advancement of the hole. The drilling fluid, which can either be slurry or bentonite suspension, is carried to the full length of the excavation through the drilling tools. Reinforcing steel, if required, is placed directly in the drilling mud and concreting is accomplished by the use of a tremie pipe kept at the base of the shaft. The concrete displaces the drilling mud and concreting is stopped when good quality concrete appears at the ground surface. The procedure for the method of construction is shown in Fig.2.3.

The use of slurry or bentonite requires proper site supervision. Partial collapse can occur if proper drilling pressures are not maintained. On the other hand, excessive velocity of drilling fluid and excessive pumping rate relative to the borehole advancement rate can result in wash-out which could lead to a progressive collapse of the borehole, reduction in effective lateral stress or variation in pile diameter. Experience has shown that the amount and rate of fluid circulation to bore a proper hole must be determined by field experimentation for each type of soil condition.

It is good construction practice to ensure that all the slurry is completely displaced otherwise any slurry trapped between the soil and concrete will affect the carrying capacity of the pile. Fleming and Sliwinski (1977) provide a useful reference for the use of bentonite pile construction.

### 2.3.4 Casing Method

This is an alternative procedure to the slurry displacement method described above. It is employed in situations where the soil conditions are unstable for the dry method of construction. In water-bearing soils, casing is needed to sup-

port the sides of the borehole, this casing being withdrawn (for economic reasons) during or after placement of the concrete. In some very unstable soils, the casing is left permanently in the ground and forms an integral part of the pile

There are two methods of introducing casing into the soil when a stratum of unstable soil is reached during boring. If drilling fluid is used to facilitate the boring operation, casing is usually placed directly into the bored hole. In this case, the diameter of the borehole is slightly larger than the external diameter of the casing. The slurry is then removed and the boring continues with the casing in position until the required depth is reached. The hole is then concreted as casing is withdrawn. The various stages described are shown in Fig. 2.4.

An alternative method of introducing casing into the soil is by driving or vibrating it into position. However this is known to cause more disturbance than the method described in the previous paragraph. The soil in the casing is then removed with an auger and the hole concreted as casing is withdrawn.

It is important to arrange the construction procedure so as to avoid the formation of cavities behind the casing, particularly in water-bearing strata of low permeability. Boring below the bottom of casing in unstable soils may lead to the formation of large cavities which are concealed by casing. The withdrawal of the casing also requires care and expert supervision to prevent the surrounding soil and water from intruding into the space that should be occupied by concrete. In some cases, the use of slurry or bentonite provides an economic and practical alternative for temporary casings where considerable lengths are involved which might give rise to difficulties in extraction.

### 2.3.5 Underreaming of bored piles

Where heavy loads are carried, it is sometimes more economical to enlarge the bases of bored piles by underreaming than to extend the shafts. However, adoption of underreamed bases often implies the acceptance of an increase in settlement under working load, and it is usually preferable to increase the length of pile rather than to underream.

Conditions most favourable to underreaming are stiff clay capable of high end bearing capacity. However, if the stiff clay is silty or heavily fissured, underreaming may be impractical. A completed pile with an underream is shown in Fig. 2.4.

For reasons of economy and construction feasibility, the maximum diameter to which the base can be enlarged is limited to approximately three times the shaft diameter. The effects of underreaming on the development of shaft resistance are discussed in Section 2.6.5.

### 2.3.6 General Construction Considerations

In recent years, the construction industry increased its use of continuous flight auger boring systems for the construction of bored piles. Continuous flight augers have a considerable advantage over other boring tools in that the spoil is fed to the surface on a "screw elevator" and thus boring can be undertaken continuously. Furthermore, the "wiping" action of auger flights against the wall of the hole causes "packing" thus prolonging the stability of the exposed hole. Some equipment and tools used in the construction of bored piles is shown in Fig. 2.5.

Concreting is the most critical operation in the construction

of bored piles. Insistence on dry mixes is not consistent with good practice. The concrete must have adequate workability so that it can flow against the walls of the hole, as often, the only compaction available is the fall under gravity from the top of borehole. The use of vibrators is not recommended for compaction. Experience indicates that of all defects associated with this type of work, over half are traceable to the use of unworkable concrete mixes [Thorburn and Thorburn (1977)]. Therefore, high workability is of paramount importance in the construction procedure.

The basic minimum specification is for a workable mix designed to give a minimum strength of  $20\text{N/mm}^2$  at 28 days, containing not less than  $300\text{ kg/m}^3$  of cement. The water-cement ratio of concrete used in practice is usually in the range of 0.5 to 0.7 depending on the slump specified in Table 2.3. The working stresses for concrete in bored and cast-in-place pile required by various Codes of Practice are shown in Table 2.4.

Reinforcement is not usually required for bored piles. It is used only when required to resist uplift load due to shrinkage and swelling of clay near the ground surface or to withstand bending moments caused by any eccentricity in the application of the load.

Good construction practice also includes the removal of debris from the base of boring when end-bearing is important, and the need for careful tremie placing techniques especially in the early stages of concreting to avoid 'washout' at the shaft bottom. Monitoring of vertical holes can be done with the aid of a continuous reading inclinometer.

Other construction considerations are the time delay

between completion of boring and concreting and the control of augering procedures to reduce mechanical disturbance. In general, it is desirable to accomplish boring of the hole with as little inward strain as possible. These considerations are discussed further in the following sections.

## 2.4 EFFECTS OF INSTALLATION AND ASSOCIATED PROBLEMS

### 2.4.1 Introduction

The method of installation has a major influence on the behaviour of a pile through alteration in the soil properties. It is interesting to note that most of the difficulties that have occurred with the use of bored piles have been associated with the construction problems. The degree of disturbance depends on the type of soil and method of placement. In the case of bored piles in clay, the excavation of a hole and the placement of fresh concrete in it affects the properties of the soil in the vicinity of the pile. A knowledge of the factors affecting the changes in soil properties may lead to a more proficient control of installation procedures.

The factors which characterize the influence of installation include stress changes in the soil, moisture migration and softening, swelling and stability of the borehole, mechanical disturbance to soil fabric, and the influence of drilling mud. With the exception of the last factor which will be discussed in Section 2.6.4, the others are discussed in the following sections.

### 2.4.2 Stress changes in the vicinity of pile

Placing a pile in the soil will certainly change the stress state of the soil around it. These changes depend mainly on the method of pile installation and ground conditions. The state of stress and deformation of soil

around bored and driven piles are shown in Fig. 2.6.

The 'at-rest' condition of a semi-infinite soil mass is shown in Fig. 2.6(a). When the soil is removed, as in the case of a bored hole, stress relief occurs. There is a tendency for soil to move towards the excavated hole as a result of a decrease in the total horizontal earth pressure as shown in Fig. 2.6(b). This effect is time dependent.

After concreting, the total horizontal stress will increase but Chandler (1968) and Tomlinson (1977) both suggest that it is unlikely to reach its undisturbed value again. This is attributed to the arching of fresh concrete around the bored hole as well as to concrete shrinkage during curing. Furthermore, if concrete placement is undertaken in batches as in the case of long piles, concrete at lower part of the pile begins to set and inhibits the full hydrostatic pressure from being developed. Reese et al. (1968) reported some measurements of the development of total horizontal earth pressure in a bored pile and found that the limited data obtained appears to agree with the above suggestions.

For comparison, the state of stress and deformation around a driven cylindrical pile in clay are shown in Fig. 2.6(c). In the case of driven piles, the stress distribution shown is applicable for certain ranges of length to diameter ratio ( $L/D < 10$  to  $15$ ). For  $L/D > 30$ , Kedzi (1975) suggests that a constant stress increment will occur. In contrast with bored piles, the installation of driven piles will cause lateral displacement and sometimes surface heave. Total horizontal stress will increase as a result of soil displacement and high excess pore pressures are generated during the driving process.

### 2.4.3 Moisture migration and softening in soil

Studies on moisture migration associated with bored pile construction have been conducted in laboratory as well as in the field during pile testing. Important results from field studies are presented in Table 2.5. Various significant conclusions can be drawn from this summary.

Moisture content increases at the interface were found to range from 1.5 to 8% and the thickness of the affected zone did not exceed 50mm. However, Chandler (1977) observed in London Clay, an increase in water content from around 29% to about 35% close to the pile, but right against the pile there seems to be a fall off in water content. Most of the authors referred to in Table 2.5 also found that an increase of moisture content in the soil surrounding the shaft caused a decrease of soil strength along the pile shaft.

Laboratory tests have been carried out by Dubose (1956), Taylor (1966), Chuang and Reese (1969), O'Neill and Reese (1972) and Rice (1975). However, results from these studies must be treated with caution since test conditions were different from those occurring in the field. In some of these tests, the effects of stress relief due to boring, the effects of hydrostatic head of fresh concrete and the overburden pressure of the soil were not taken into account. Therefore stresses using the laboratory technique were different from the imposed stresses in the field.

Chuang and Reese (1969) poured cement mortar into a tube containing a sample of soil. The tube was then sealed and subjected to various pressures in a triaxial chamber. After a certain time period, the moisture contents of the cement mortar and soil were studied. O'Neill and Reese (1972) used a shear box, each half-filled with soil

and cement mortar, with a normal load applied. Both these tests considered the hydrostatic head of fresh concrete and stresses in the soil but neglected the effects of boring and the subsequent stress relief. Nevertheless, the trend of the results obtained by these authors appears to be consistent with field observations.

The pattern of moisture migration is best illustrated in Fig. 2.7. The cumulative effect of moisture migration is the softening of a relatively narrow zone of clay surrounding the pile shaft resulting in a loss of strength. Clearly, the time delay from boring to concreting, protection from the weather, soil properties and water-cement ratio all influence the degree of softening.

The water-cement ratio of concrete is usually in the range of 0.5 to 0.7, far in excess of the theoretical value of 0.38 required for complete hydration of cement [Neville (1973)]. For constructional reasons given in Section 2.3.6, extra water is added to give a high workability to the mix. Hydration of concrete is a gradual process and water which was surplus at the time of casting may later be required. As concrete matures, a crystalline structure is built up, and the size of pores is constantly reduced with time [Neville (1973)]. This gives concrete an increasing moisture suction capacity which enables it to draw in water. This observation was confirmed by Taylor (1966) who also found that the moisture content of the samples of great age was about 2.5% below the natural value.

Taylor used a simple mass-transfer balance in which a tube was half-filled with boulder clay and the remaining half with cement mortar with water-cement ratio of 0.5.

The ratio of weights in the mortar and soil was observed over a period of time and results are shown in Fig. 2.8. For the first four days, the weight of clay increased but then decreased steadily until the original balance was regained after 43 days; after which the concrete side became heavier.

From the studies of authors quoted in this section, it appears that the magnitude of moisture content changes in the soil and the thickness of the affected zone depend on the initial stress history and the magnitude of stress relief, the permeability of the soil, the pore water pressure parameters, the water-cement ratio, the hydrostatic head of fresh concrete, the initial moisture content of the soil and time.

#### 2.4.4 Swelling and stability of boreholes

As the hole is bored, total stress at the wall of the hole reduces to zero. Moisture from the adjacent soil mass seeps towards the stress relieved zone resulting in swelling. Associated with swelling is a reduction in soil strength. The magnitude of swelling depends on the magnitude of stress relief, the soil swelling potential, the soil permeability, the availability of excess water and the time lapse between completion of boring and casting. The higher the overburden pressure, the overconsolidation ratio and plasticity, the greater is the swell potential. The addition of water also increases swelling.

Swelling in a soil reduces its effective stress and may even result in the soil becoming unstable. Stability of an open borehole in soil was first analysed by Terzaghi (1943). Walls of a borehole may collapse under a horizontal earth pressure or a combination of earth pressure and hydrostatic pressure in the soil. Resisting the

collapse are the passive forces of soil arching around the hole. Based on this analysis and the theory of cavity expansion, Massarsch (1976) presented a method of calculating the critical depth at which a borehole will collapse.

Borehole stability is a common construction problem. Since swelling is time-dependent, the longer the hole remains open and the walls exposed, the greater are the chances of instability occurring. Therefore, the time lapse between completion of boring and concreting must be minimised as much as possible.

#### 2.4.5 Mechanical disturbance

The soil is subjected to mechanical disturbance from the boring tool over a thin zone immediately adjacent to the sides of the hole. The degree of disturbance to the soil fabric which affects the load-transfer from pile is influenced by the type of boring tool. Since the degree of disturbance is difficult to determine quantitatively in the field, a knowledge of the causes and their qualitative effects may be useful in the development of new boring devices or techniques. In this context, laboratory studies may prove useful.

Eid (1978) examined the effects of boring a 25mm diameter hole in a laboratory-prepared clay sample using two different boring tools - a polished brass sampling tube and a mild steel auger. Two pairs of strain coils were placed in the slurry prior to consolidation. After consolidation, these strain coils were about 25mm and 50mm from the centre of the borehole and at approximately mid-height. Readings monitored by strain coils during the process of boring are shown in Fig. 2.9 for the two techniques used. The author found that although the tube method produced a fairly

clean and straight hole in the clay specimen, there was relatively more disturbance in the soil than the augering method, as shown in the figure. However, it is worth noting that the soil specimens were uncased during the boring process. In this case, swelling in the soil resulting from stress relief may influence the strain readings.

The magnitude of strain observed by Eid (1978) which is about 1% for the augering method is slightly higher than that observed by Wroth and Hughes (1973). Using a radiographic technique the authors showed that the strain during boring was less than 0.5%.

#### 2.4.6 Defects in bored cast-in-situ piles

Most structural members can be inspected superficially, whereas a pile which satisfied a load-settlement test may contain hidden defects. These may affect the performance of the pile in the long term.

Baker and Khan (1971) listed various types of conditions that can lead to faulty piles including excess water at cold joints resulting in weak concrete; improper placement of concrete; development of voids in the shaft due to arching; and side or surface cave-in of soil resulting in contaminated concrete. These last two conditions are illustrated in Fig. 2.10(a).

Thorburn and Thorburn (1977) found that the principal cause for defects in bored piles is associated with the removal of temporary casings. Of these defects, the most important is the occurrence of overbreak cavities which can undermine the structural integrity of piles.

'Overbreak' is the term describing the removal of the soil material by physical or chemical forces resulting

in cavitation and discontinuity. Removal of the material can be caused by boring ahead of casing in unstable soil or the release of ground water as shown in Fig. 2.10(b). The ultimate result may be a contamination of the concrete, a reduction in cross-sectional area of the shaft and the exposure of the reinforcement to corrosion. Although such defects may not affect the pile performance in the short term, long term behaviour may be impaired, particularly when the pile may be subjected to bending.

There are a number of methods used for testing the integrity of piles, ranging from simple excavation and exploratory coring to more sophisticated methods such as sonic logging and radiometric techniques. Weltman (1977) provides a reference document which reviews the various methods available. Baker and Khan (1971) and Woodward et al. (1972) described in considerable detail various inspection methods to be considered in obtaining satisfactory piles as well as procedures to remedy any faults.

However, Thorburn and Thorburn (1977) stressed that failures caused by physical defects in bored cast-in-situ piles are rare and that the proportion of these defects is very small in relation to the total number of piles constructed. With proper understanding of the causes, adequate site supervision and good quality control, the majority of defects can be eliminated.

## 2.5 BEHAVIOUR OF BORED PILES UNDER AXIAL LOAD

### 2.5.1 Load transfer and settlement

The behaviour of an axially loaded pile in clay has been investigated by several authors such as Cummings et al. (1950), Seed and Reese (1957), Tomlinson (1957), Peck (1958), Coyle and Reese (1966), Reese and Hudson (1968), O'Neill

and Reese (1972). The results of these studies have provided some understanding of the mechanism of load transfer for piles in clay and will serve as a basis for a more knowledgeable evaluation of design parameters.

The transfer of axial load from a pile to the supporting soil is dependent on many interrelated factors including subsurface conditions, the physical characteristics of the pile, the method of construction and the elapsed time after construction. A typical curve of the distribution of load along the length of an axially loaded bored pile is shown in Fig. 2.11. Distribution of shaft resistance in practice is unlikely to be uniform over the full length of the shaft and the average value in the opinion of most authors is likely to be close to two-thirds of the maximum value mobilised. However, this approximation depends on the dimensions of the pile and the amount of settlement. The proportion of load transfer can be found from the slope of the load transfer curve. There is substantial evidence from the literature quoted above, to suggest that the reduced proportion of load transfer near the base is attributed to the reduced lateral stresses in the vicinity of the base due to soil arching.

There are a number of useful papers and discussions on bored piles in stiff clay such as Whitaker and Cooke (1966) and Burland et al. (1966). However, these papers contain no measurements of the distribution of friction along the shaft although they provide information on the relative magnitude of base and shaft loads, as well as displacement needed to mobilize these loads. A long shafted pile which carries its loads mainly by friction has a load-settlement curve of the form shown in Fig. 2.12(a). Relatively short piles with large underreams display the behaviour shown in Fig. 2.12(b).

Whitaker and Cooke (1966) reported that peak shaft resistance was mobilised at a very small displacement of about 0.5% of the shaft diameter, while full mobilization of the base loads occurred at a settlement of the order of 10 to 20% of the base diameter. These results were based on field tests in London Clay and suggest that most of the design load is carried by shaft friction and end-bearing only becomes significant as the ultimate load is approached. Similar trends were observed by O'Neill and Reese (1972) for pile tests in Beaumont Clay, Houston. On the basis of these tests, the authors suggest that settlement considerations may not be critical in the design of friction piles.

However, if theoretical computations of pile settlement are required, the methods of Poulos (1972, 1977) can be used. Another useful method is the finite element method for predicting load deformation characteristics for bored piles presented by Ellison et al. (1971). An approximation of the stress-strain curve obtained from undrained triaxial tests is sufficient to predict the entire load-deformation curve of a pile using this finite method.

#### 2.5.2 Adhesion factor, $\alpha$

In pile design and analysis, it is usual to relate the shaft resistance of the pile to the undrained shear strength of the soil by an adhesion factor  $\alpha$ . For bored piles,  $\alpha$  is usually less than unity and is a complex function of various factors such as the effects of installation, defects in pile construction and variation in soil properties. The determination of the average value of  $\alpha$  for piles in clay has been the subject of a number of field and laboratory studies. A summary of existing literature on the adhesion factors of bored piles in clay is presented in Table 2.6.

Typically, London Clay is overconsolidated and fissured over a wide area and depth, with a liquid limit of 70% and a water content near or slightly below the plastic limit of about 26%. Skempton (1959), Burland et al.(1966) and others have shown that the undrained shear strength of this clay increases with depth. Results of bored pile tests have shown that the value of  $\alpha$  varies from as low as 0.3 [Skempton(1959)] to as high as 1.0 [Meyerhof and Murdock(1953)]. Tomlinson (1975) even experienced adhesion factors as low as 0.1 for bored piles in very stiff to hard Lias Clay. The wide variation in the reported values reflects the influence of differences in construction procedure, pile testing method and soil testing technique, the duration of exposure of open shafts and the variation in soil properties.

Leach et al.(1976) carried out load tests of bored piles in weathered Keuper Marl and found that the adhesion factor can have two very different values depending on whether the undrained strength was based on laboratory tests or in-situ pressuremeter tests. For one pile,  $\alpha$  was 1.61 when based on undrained shear strength determined from unconsolidated-undrained triaxial tests and 0.53 when based on undrained strength measured by the pressuremeter. This example reflects the importance of obtaining a representative undrained strength value of the undisturbed soil mass.

Reese (1978) suggests that  $\alpha$  is low near the ground surface, has a maximum value near the mid-height of the shaft and is low again near the base of the shaft. The low value near the ground surface is probably due to low normal pressure at the interface of concrete and soil because of initial low hydrostatic pressure in the fresh concrete. The low value of  $\alpha$  near the base of the shaft is thought to be related to the mechanics of load transfer discussed in the previous section.

For bored piles in glacial till, Weltman and Healy(1978) analysed a number of reported pile test results and found that results of adhesion factors are scattered. However, the authors suggested a tentative relationship of  $\alpha$  equal to 0.90 at undrained strength of the order of 80 kN/m<sup>2</sup> falling to 0.35 at 200 kN/m<sup>2</sup>.

Kraft and Lyons (1974) carried out a statistical analysis of  $\alpha$  values for 65 bored piles in clay. The values of  $\alpha$  were obtained from field studies by a number of authors, some of which have been presented in Table 2.6. The analysis shown in Fig. 2.13 yielded an average adhesion factor of 0.45 and a standard deviation of 0.12. These values appear to support the design recommendation of Skempton (1959) who suggested that in the absence of previous field experience of adhesion factors in any particular type of clay, a value of 0.45 is appropriate provided there is adequate load testing to confirm the design value. The application of adhesion factors to the design of piles will be discussed further in Chapter 3.

Most of the data reported in Table 2.5 are related to bored piles in overconsolidated stiff clays with average shear strength between 70 kN/m<sup>2</sup> and 250 kN/m<sup>2</sup>. Very limited data is available on tests in normally consolidated clays. Eide et al.(1972) suggest that  $\alpha$  can be as high as 1.0 for normally consolidated marine clay with a shear strength of the order of 40 kN/m<sup>2</sup> measured with an in-situ vane test. In fact, there is no reason to suppose that the full shear strength of soft clay should not be mobilised in shaft friction provided that time is allowed for regaining the shear strength lost by remoulding during the boring operations.

### 2.5.3 Increase in shaft capacity with time

Tomlinson (1977) discussed the effects of time on the shaft resistance in clay and suggests that in general, piles experience a gradual increase in shaft capacity with time. However, he pointed out that the increase is relatively small and in most cases insignificant when compared with other uncertain effects.

Whitaker and Cooke (1966) reported an increase in frictional resistance of piles in London clay of the order of 13% over a period of about 500 days against a pile tested at about 100 days after casting. This increase is attributed to the increase in total lateral stress acting at the pile interface.

Taylor (1966) also reported an increase in bearing capacity of bored piles up to six months after casting, after which it remained constant some 28% above the 7-day old pile capacity.

Studies relating to the long term capacity of piles are limited in view of the high cost involved in conducting these tests.

### 2.5.4 Effect of sustained loading

Long term loading tests on short bored piles in London Clay were conducted by Green (1961) to simulate the service loading of piles in practice. The author found that piles which were loaded 1 year after casting continued to settle under the design loads for several years, although the rate of settlement was very small after the first three months. For the piles investigated (300 and 355mm diameter x 3.05m long), the overall settlement did not exceed 0.5% of the shaft diameters between

3 months and about 4 years after loading. Green also found that resistance to settlement increased with time after casting of the pile.

Wooley and Reese (1974) examined the long term phenomena of creep and consolidation resulting from sustained loading on a drilled shaft. From a literature research the authors found that creep can have the eventual effect of load shedding [Peck (1965)], i.e. a transfer of load to the lower regions of the shaft. This phenomenon can have the effect of increasing the settlement. However, from field observations and measurements, Wooley and Reese found that little load shedding had occurred. This is reasonable because present design methods keep the stress levels in the soil well below their actual capacity. Therefore, in general, creep does not present a serious problem.

## 2.6 OTHER FACTORS AFFECTING SHAFT RESISTANCE OF BORED PILES

### 2.6.1 Introduction

A number of factors influence the development of shaft resistance in a bored pile. Some of these factors such as the effects of installation and the mechanism of load transfer have been discussed in previous sections. This section considers the influence of the stresses in the soil surrounding the pile, the physical characteristics of piles, the use of bentonite and the effect of under-reaming.

### 2.6.2 Stresses in soil surrounding a pile

There is evidence to suggest that the shaft friction is primarily a function of the effective lateral pressure between the pile and the soil [Clark and Meyerhof (1973), Janbu (1976) and Flaate and Selnes (1977)]. Therefore,

the development of the effective lateral pressure after installation is of major interest. Stress changes in the vicinity of bored piles due to installation have been discussed in Section 2.4.2.

The total horizontal pressure acting at the shaft of a bored pile shortly after it is installed, depend mainly on the effect of the hydrostatic pressure of the fresh concrete on the sides of the borehole. After casting, lateral pressure in the soil will be gradually re-established around the pile shaft, although Chandler (1968) doubts if the initial at-rest horizontal stresses can ever be fully re-established. This is attributed to arching between the concrete and the wall of the borehole. Radial shrinkage associated with concrete curing may also reduce the effective stress on the shaft surface [Tomlinson(1977)]. However, it is difficult to evaluate these effects quantitatively in the field as evidenced by the absence of literature on this aspect.

### 2.6.3 Physical characteristics of piles

Load transfer and settlement are governed to a certain extent by the length to diameter ratio of the shaft and the relative stiffness of pile and surrounding soil. The influence of these parameters has been investigated by Mattes and Poulos (1969) using mathematical models of single "compressible" and "incompressible" piles embedded within an elastic isotropic medium. The authors found that for a pile in an elastic medium, the proportion of load transferred to the base increases with (i) an increase in the rigidity of the pile shaft and (ii) a decrease in the shaft length to diameter ratio.

From theoretical investigations of piles with enlarged bases in an ideal elastic medium, Poulos and Davis(1968)

found that the base diameter has a significant influence on pile behaviour only when the length to shaft diameter ratio is less than 25.

Potyondy (1961) investigated the skin friction between various soils and materials with different surface textures in a shear box apparatus, while Bea (1975) conducted experiments using direct shear tests and triaxial rod shear tests. The triaxial rod shear tests consisted of inserting a small diameter steel pipe pile into a large cylindrical soil sample, confining the sample triaxially and loading the pile axially to failure. Both authors found that surface roughness affected the load transfer characteristics. However, it is prudent to note that the observation is based only on laboratory experiments. Any roughness of the material in the laboratory tests may be exaggerated when compared to actual dimensions of pile in practice.

In the case of bored piles, it is more useful to consider the shaft irregularity rather than the roughness on the pile surface. The development of shaft friction on a cylindrical and irregular pile shaft is shown in Fig.2.14. Fleming and Sliwinski (1977) suggested that in practice, these two effects will be present at the same time in any one cast-in-place pile. The shaft irregularity is attributed to the localised variations in the properties of the strata in which the pile is formed and the excavation technique. The contribution of each type of resistance to load is dependent on the extent of the surface irregularities and soil type. The authors also suggested that the load-settlement relationship for any pile will reflect the relative proportions of each of these types of frictional behaviour and for design purposes, the diameter of a cylindrical shaft can be assumed.

#### 2.6.4 Influence of bentonite

Bentonite or any drilling fluid is used mainly to stabilize the hole during boring and to bring the spoil to the surface. Fleming and Sliwinski (1977) presented a 'state-of-the-art' review of the use and influence of bentonite on the load capacity of bored piles. Based on various published and unpublished information, the authors found no significant influence on the eventual pile performance. This observation was further supported by Fearenside and Cooke (1978) who tested seven piles constructed in London Clay; three concreted under bentonite and the remainder under dry conditions. The authors found no evidence to suggest that the use of bentonite adversely affected the shaft friction.

Reese, O'Neill and Touma (1973) also reported no significant differences in friction in clays between piles bored dry and piles bored under bentonite suspension. However, the authors drew attention to the risks of the mud being trapped between the concrete and the soil wall. This will contaminate the concrete and cause softening of the soil at the interface, resulting in a reduction in adhesion.

#### 2.6.5 Effect of underreaming

In the design of underreamed piles, considerations must be given to the influence of the underream on the load transfer along the shaft just above the underream. Tomlinson (1961) suggests that under working conditions, the development of shaft friction near the base of a pile may be inhibited by soil movement around an enlarged base. The author recommended that the length of shaft above the top of the underream equal to the underream diameter should be disregarded in calculating the shaft

friction. However, it is usual to treat the response of shaft and underream loads as being independent of each other and results by Burland et al.(1966) suggest that this will not lead to appreciable errors.

#### 2.6.6 Effect of construction procedure

It is interesting to note that most of the reported field tests on bored piles were based on piles constructed in the dry or piles constructed using the bentonite displacement method. Literature on field tests on bored piles constructed by the casing method is very limited. Therefore, the effects of casing withdrawal on the development of shaft resistance is unknown.

Frischmann and Fleming (1962) suggest that the value of  $\alpha$  for bored piles constructed by the casing method is less than that obtained if bored piles had been constructed in the dry.

O'Neill and Reese (1972) considered the effect of different construction methods and variables in the relationship,

$$\alpha_{avg} = (\alpha_{11} \cdot \alpha_{12} \cdot \alpha_{13})\phi \quad \dots (2.1)$$

where  $\alpha_{avg}$  is the average adhesion factor over the entire length of shaft,

$\alpha_{11}$  is associated with soil disturbance during pile installation,

$\alpha_{12}$  is associated with moisture migration,

$\alpha_{13}$  is associated with surface shrinkage,

$\phi$  is a factor which depends on the method of pile installation.

For a cylindrical pile,  $\alpha_{11}$  is taken as 0.65, and  $\alpha_{12}$  and  $\alpha_{13}$  can both be determined from  $(1 - 0.76/L)$  where  $L$  is the pile length in metres. For piles installed by the dry method,  $\phi$  is taken as 1.0 whereas for piles installed

by casing or bentonite displacement method,  $\phi$  is taken as 0.6.

If a pile length of 20m is assumed, then  $\alpha_{avg}$  will have a value of 0.6 for piles constructed in the dry and a value of 0.36 for the casing method. It is interesting to note that these values correspond to the upper and lower design limits of adhesion factor recommended by Skempton (1959).

## 2.7 BORED PILES IN DIFFICULT GROUND CONDITIONS

### 2.7.1 Introduction

Four types of difficult soil strata are discussed briefly in this section: cohesionless soil, soft compressible soil, expansive clay and heavily fissured soil. If any of these strata of soil are encountered during the construction of a bored pile, special measures are necessary.

### 2.7.2 Cohesionless soil

In the United Kingdom, bored piles are seldom used in deep granular soils because of the high load capacities which can be provided by driven precast jointed piles formed of high strength concrete. In fact, driven piles are generally used in granular medium in preference to bored piles because of the former's ability to develop a high shearing resistance as the pile is forced into the ground. In addition practical difficulties limit the use of bored piles in a cohesionless soil.

If a stratum of cohesionless soil is present, bored piles will probably have to be constructed using the casing method.

### 2.7.3 Soft compressible or underconsolidated soil

Consolidation or remoulding of a soft compressible or underconsolidated clay around a pile after installation causes 'negative skin friction' or 'downdrag'. This phenomenon is used to describe the additional load transferred to a pile due to the gradual settlement of soft clay under the influence of self weight or of a surcharge pressure, for example, fill placed over the site. Due to the adhesion of soil to the pile, a downward force develops and allowance must be made for this in the design calculations. However, negative friction is unlikely to be important for bored piles since reconsolidation after installation is likely to be relatively small.

### 2.7.4 Expansive clay

Another soil in which piles should be designed with caution is expansive clay. This clay undergoes large volume changes as moisture content changes. When exposed to abundant supplies of water, these soils can greatly increase their volume and when completely desiccated, they shrink excessively. This behaviour has obvious implications in bored pile construction where excess water is present.

When soil expands, it can exert great tensile forces on the shaft and these tensile forces can have a detrimental effect on the unreinforced sections of the drilled shafts [Wooley and Reese (1974)]. When clay shrinks, soil may crack and separate from the shaft in the upper portions of the soil-pile interface, resulting in a reduction in load capacity.

Mohan and Chandra (1961) found that reduction in frictional resistance of bored piles in expansive clay is due partly

to softening of the clay adjacent to the pile and partly to loss of adhesion between concrete and soil.

#### 2.7.5 Heavily fissured soil

The presence of fissures in clay increases the rate of water from the soil mass towards the stress-relieved zone of soil after boring, thus enhancing softening within this zone. Another problem with fissured clay is the selection of a consistent shear strength value, inherently scattered due to the fissuring. In their studies of bored piles in fissured clay, Meyerhof and Murdock (1953), Williams and Colman (1965) and O'Neill and Reese (1972) found that the shear strength decreased rapidly with time after sampling, due to the opening of fissures which could not be closed sufficiently by large cell pressures in the triaxial compression tests. One method of choosing design values, proposed by O'Neill and Reese (1972), is to draw a minimum envelope to the data points expressing shear strength as a function of depth. This envelope will give an approximation of the fissured strength of the soil.

#### 2.8 GENERAL COMPARISONS OF BORED AND DRIVEN PILES

It is reasonable to assume that the mechanisms causing alterations in the soil properties around and beneath a bored pile, and thereby controlling the behaviour of pile under load, are different from those associated with a driven pile. Design parameters for shaft friction valid for bored piles therefore may not be extended logically to driven piles.

In bored piles, it is usual to ignore the residual installation stresses since they are usually not significant

[Cooke (1979)]. However, in the case of a pile jacked or driven into the ground (that is, a displacement pile), relatively large soil movement is necessary to accommodate the pile. As a result, residual stresses are set up in the pile and surrounding soil. The state of stress and deformation of soil around a bored and driven pile have been discussed in Section 2.4.2 and shown in Fig. 2.6.

Considerable research has already been undertaken on piles driven into clay. A summary of various studies into the extent of disturbance around a pile during driving have been given by De Mello (1969) and Tomlinson (1977). Although some of the evidence is conflicting, it appears that the amount of initial remoulding varies from almost 100% at the pile-soil interface to almost zero at about 1.5 to 2 diameters from the pile surface.

On the basis of correlations between pile-soil adhesion,  $c_a$ , and undrained cohesion of soil,  $c_u$ , it would appear that the adhesion factor,  $c_a/c_u$ , can be as high as 1.5 for very soft clays and as low as 0.2 for stiff clays. Tomlinson (1970) has summarised the results of various load tests of driven piles in cohesive soils and related the adhesion factor to the undrained shear strength of the soil. One of the major conclusion was that the adhesion factors decrease with the increase in undrained strength. This relationship will be discussed further in the next chapter.

The load carrying capacity of driven piles in clay increases with time after driving, partly due to a recovery of strength of the remoulded clay around the pile and partly due to the dissipation of excess pore water pressure created by the pile driving operation. Hagerty and Garlanger (1972) showed that a significant part of reconsolidation (up to 50% of excess pore pressure) can occur within a few days.

## 2.9 A BRIEF REVIEW OF PILE GROUP BEHAVIOUR

In connection with ultimate load capacity and settlement, it is well known that a single pile is not representative of the behaviour of groups of piles. The mechanics of pile group behaviour and the effect of the placing of adjacent piles have not been investigated sufficiently in the field, in view of the large loads and high costs involved. In this respect, model tests have been widely used. Whitaker (1957), Cooke and Whitaker (1961), Sowers et al.(1961) and others investigated group behaviour of piles in clay while useful information of tests in sand can be found in Kedzi (1957), Hanna (1963) and Kishida and Meyerhof (1965).

A term commonly used in pile group behaviour is 'efficiency', which is defined as the ratio of ultimate load which can be supported by the group to the sum of ultimate loads of its members acting individually. Results from the above literature suggest that as pile spacing increase, the mode of failure changes, and efficiencies of unity are not reached in clays even at large spacing.

Piles as a group tend to settle more than individual piles under the same loading condition. Calculations of load distribution and settlement in groups of piles are complex and complete solutions require the use of computer techniques. Theoretical methods using elasticity theory have been proposed by D'Appolonia et al.(1971) and Poulos (1977).

Over the last few years, large diameter bored piles (i.e.  $D > 1200\text{mm}$ ) have been increasingly used to replace small groups of piles. Development of sophisticated drilling equipment in recent years and the ability of large diameter bored piles to carry very high loads on a single unit favour their use in the future.

TABLE 2.1 ADVANTAGES AND DISADVANTAGES IN THE USE OF BORED PILES

ADVANTAGES	COMMENTS
<ol style="list-style-type: none"> <li>1. Relatively noiseless and vibrationless.</li> <li>2. No significant ground heave or displacement.</li> <li>3. No storage space required.</li> <li>4. Can be cast to the level required.</li> <li>5. Light tripod rigs require minimum site preparation and relatively low cost.</li> <li>6. Allows inspection of soil before concreting.</li> <li>7. Large diameter piles can be formed.</li> <li>8. Can be used where presence of boulders and inclusions prevent use of driven piles.</li> </ol>	<p>} Important considerations in built-up areas.</p> <p>Economic savings.</p> <p>Useful if only small diameter piles required.</p> <p>Useful check for design assumptions.</p> <p>Provides increase in bearing capacity.</p> <p>-</p>
DISADVANTAGES	COMMENTS
<ol style="list-style-type: none"> <li>1. 'Necking' in soft soil.</li> <li>2. Adverse groundwater conditions affects structural integrity of piles.</li> <li>3. Spoil from boring operation require clearing.</li> <li>4. Integrity of constructed pile unknown.</li> <li>5. Failure of a bored pile can be expensive.</li> </ol>	<p>Affects carrying capacity.</p> <p>Require permanent casing which may increase costs.</p> <p>Can be expensive in major works.</p> <p>Serious defects may go undetected.</p> <p>Important when designed to carry large loads.</p>

TABLE 2.2 TYPICAL SIZES AND LOADS FOR BORED PILES

PILE TYPE			NORMAL RANGE OF SIZE AVAILABLE		NORMAL LOAD RANGE (kN)
			CROSS-SECTION (mm)	LENGTH (m)	
PERCUSSION BORED	Small diameter		300 to 600 (in steps of 50)	Up to 25	400 to 1200
	Large diameter		600 to 1500	Up to 40	2000 to 6500
ROTARY BORED	Small diameter		250 to 550 (in steps of 50)	Up to 45	Up to 1000
	Large diameter	Straight shaft	450 to 1500 (in steps of 150)	Up to 45	Up to 10000
		Under-reamed	Up to 3 times the shaft diameter above	Up to 36	Very high loads possible

TABLE 2.3 RECOMMENDED SLUMP FOR BORED CAST-IN-PLACE PILES  
[from ICE Piling - Model Procedures and Specifications (1978)]

PILING MIX WORKABILITY	SLUMP (mm)		TYPICAL CONDITIONS OF USE
	MINIMUM	MAXIMUM	
A	75	125	Placed into water-free unlined bore. Widely spaced reinforcement leaving ample room for free movement between bars.
B	100	175	Where reinforcement is not spaced widely enough to give free movement between bars. Where casting level of concrete is within the casing. Where pile diameter is less than 600mm.
C	150	-	Where concrete is to be placed by tremie under water or drilling fluid.

TABLE 2.4 WORKING STRESSES AND MAXIMUM WORKING LOADS IN COMPRESSION ON BORED-AND-CAST-IN-PLACE PILES. (after Tomlinson, 1977)

Country	Code	Tube	Structural core	Reinforcing steel	Concrete in shaft	Remarks																																																				
United Kingdom	CP 2004	—	—	—	0.25 $u_w$	Concrete not to be leaner than 1:2:4																																																				
USA	American Concrete Institute Recommendations	0.35 $f_c$ 87N/mm <sup>2</sup> (12 600lb/in <sup>2</sup> ) max	0.50 $f_c$ 172N/mm <sup>2</sup> (25 000lb/in <sup>2</sup> ) max	0.40 $f_c$ 206N/mm <sup>2</sup> (30 000lb/in <sup>2</sup> ) max	0.33 $u_w$ (unconfined) 0.40 $u_w$ (confined)*	* Steel shell confining the concrete to be not greater than 432mm (17in) in diameter. Shell to be 14g (us) or thicker. Seamless or spiral welded; $f_w \leq 206\text{N/mm}^2$ (30 000lb/in <sup>2</sup> ). Not exposed to corrosion and does not carry part of working load. Corrugated steel shells not considered as load bearing																																																				
	Chicago	—	—	—	0.25 $u_w$	Where permanent lining tube is provided, maximum allowable stress is 0.3 $u_w$ + 1.5 $t/f_t D$ but not greater than 0.4 $u_w$ (where $t$ is thickness and $D$ is diameter of tube)																																																				
	New York (1965)	0.35 $f_c$ ≥ 248N/mm <sup>2</sup> (36 000lb/in <sup>2</sup> )	0.50 $f_c$ ≥ 248N/mm <sup>2</sup> (36 000lb/in <sup>2</sup> )	0.40 $f_c$ ≥ 206N/mm <sup>2</sup> (30 000lb/in <sup>2</sup> )	0.25 $u_w$	Min thickness of tube to be 3mm (1/8in) before it can contribute to structure strength of pile. Max. working load not to exceed 1 500kN (150 tons) for piles bearing on medium to hard rock, 800kN (80 tons) for bearing on soft rock and 1 000kN (100 tons) for bearing on hardpan over rock. Max. loads can be exceeded if substantiated by load tests. No upper limit for caisson piles with structural steel core. Uncased piles permitted only when borehole can be kept free of water during placement of concrete and sides and bottom can be inspected before placement																																																				
W. Germany	DIN 4014					Min. cement content 350kg/m <sup>3</sup> (590lb/yd <sup>3</sup> ) [400kg/m <sup>3</sup> (675lb/yd <sup>3</sup> ) for concrete placed under water]. Min. 5 reinforcing bars 14mm (1/2in) diameter. Longitudinal steel to be 0.8% of gross cross-sectional area. Cover 30mm (1 1/8in) [50mm (2in) in aggressive ground].  Max. load on piles <table border="1" style="margin-left: auto; margin-right: auto;"> <thead> <tr> <th colspan="2">Without enlarged base</th> <th colspan="4">With enlarged base</th> </tr> <tr> <th>Diameter (mm) (in)</th> <th>Max. load (kN) (tons)</th> <th>Size of base (mm) (in)</th> <th>Max. load (kN) (tons)</th> <th>Size of base (mm) (in)</th> <th>Max. load (kN) (tons)</th> </tr> </thead> <tbody> <tr> <td>300</td> <td>12</td> <td>200</td> <td>20</td> <td>600</td> <td>24</td> <td>300</td> <td>30</td> </tr> <tr> <td>350</td> <td>14</td> <td>250</td> <td>25</td> <td>700</td> <td>28</td> <td>380</td> <td>38</td> </tr> <tr> <td>400</td> <td>16</td> <td>300</td> <td>30</td> <td>800</td> <td>32</td> <td>470</td> <td>47</td> </tr> <tr> <td>500</td> <td>20</td> <td>400</td> <td>40</td> <td>900</td> <td>36</td> <td>550</td> <td>55</td> </tr> <tr> <td></td> <td></td> <td></td> <td></td> <td>1 000</td> <td>40</td> <td>650</td> <td>65</td> </tr> </tbody> </table>	Without enlarged base		With enlarged base				Diameter (mm) (in)	Max. load (kN) (tons)	Size of base (mm) (in)	Max. load (kN) (tons)	Size of base (mm) (in)	Max. load (kN) (tons)	300	12	200	20	600	24	300	30	350	14	250	25	700	28	380	38	400	16	300	30	800	32	470	47	500	20	400	40	900	36	550	55					1 000	40	650	65
Without enlarged base		With enlarged base																																																								
Diameter (mm) (in)	Max. load (kN) (tons)	Size of base (mm) (in)	Max. load (kN) (tons)	Size of base (mm) (in)	Max. load (kN) (tons)																																																					
300	12	200	20	600	24	300	30																																																			
350	14	250	25	700	28	380	38																																																			
400	16	300	30	800	32	470	47																																																			
500	20	400	40	900	36	550	55																																																			
				1 000	40	650	65																																																			
France	DTU 13	—	—	Min. 5 bars not less than 12mm (1/2in). Steel to be not less than 0.5% cross-section. Helical reinforcement not less than 5mm (1/8in) diam. spaced not more than 12 × main bar diam.	5N/mm <sup>2</sup> (725lb/in <sup>2</sup> )	Unreinforced concrete placed in dry hole. Reinforced concrete placed in dry hole 5N/mm <sup>2</sup> (725lb/in <sup>2</sup> ) allowed if contractor demonstrates complete cover of steel after extracting casing. Unreinforced or reinforced concrete placed under water by tremie pipe. Unreinforced or reinforced concrete placed under water by bottom opening bucket. Casing left in place; concrete placed in dry and vibrated. Casing left in place; concrete placed under water. Concrete mix to be determined from considerations of working stress and conditions of placing.																																																				
					4N/mm <sup>2</sup> (580lb/in <sup>2</sup> )																																																					
					5N/mm <sup>2</sup> (725lb/in <sup>2</sup> )																																																					
					3N/mm <sup>2</sup> (435lb/in <sup>2</sup> )																																																					
					7N/mm <sup>2</sup> (1 015lb/in <sup>2</sup> ) 5N/mm <sup>2</sup> (725lb/in <sup>2</sup> )																																																					
Sweden	SBS—s26:3 (1968)	—	—	—	—	Concrete to have minimum crushing strength of 39N/mm <sup>2</sup> (5 700lb/in <sup>2</sup> ).																																																				

TABLE 2.5 SUMMARY OF FIELD STUDIES ON MOISTURE MIGRATION

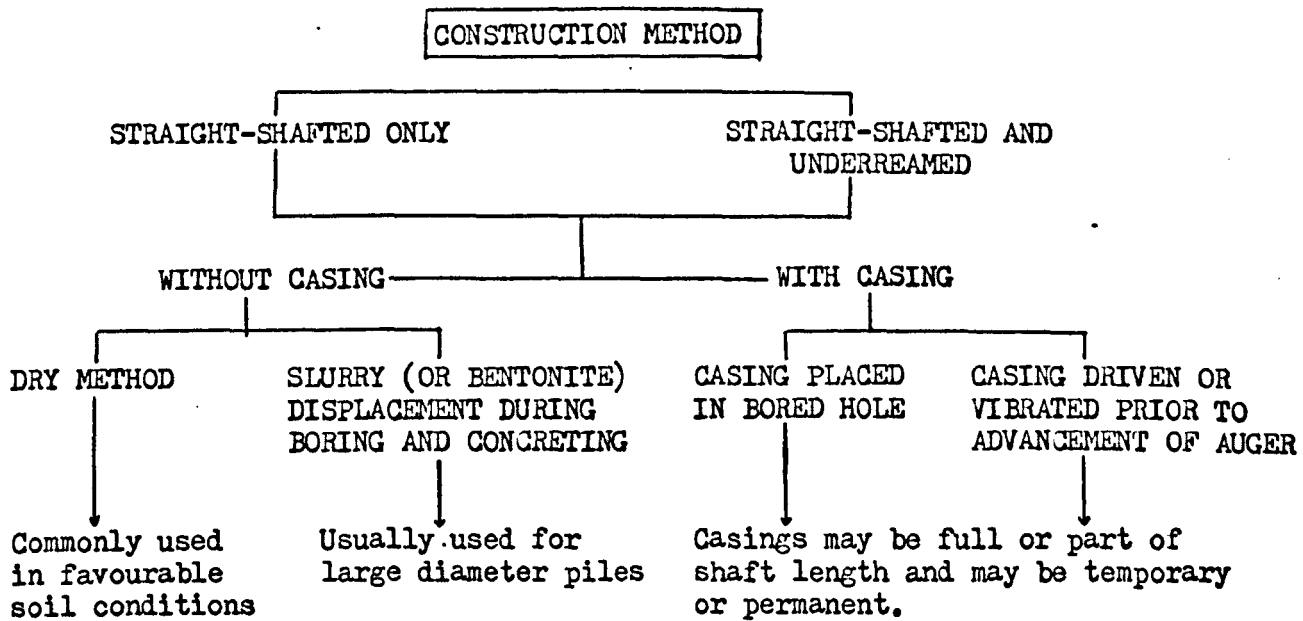
REFERENCE	SOIL TYPE	MOISTURE CONTENT %	NOTES ON CONSTRUCTION METHOD	INCREASE IN MOISTURE CONTENT % AT INTERFACE	THICKNESS OF AFFECTED ZONE mm	INCREASE IN MOISTURE CONTENT IN LAB. UNDER ZERO LOAD %	COMMENTS
Meyerhof and Murdock (1953)	London Clay	30	water-cement ratio=0.4 water-cement ratio=0.2 (Holes drilled by hand - 2/3 days)	3 at top to 7 at bottom 0	50	5-8	-
Burland (1963)	London Clay	27	no drilling mud with drilling mud	1.5 1.5 to 2.0	38 to 50	-	Decrease in moisture content more typical above GWL and incr.in m/c typical below GWL
Mohan and Chandra (1961)	Black Cotton clay	19.5	Dry	2 to 3	38	3.0	-
O'Neill and Reese (1972)	Beaumont clay	20	Dry	8	20	-	-
Chandler (1977)	London Clay	29	No mention	6	-	-	Increase of 6% for soil close to pile but at interface it self, seems to be a fall off in water content

TABLE 2.6 SUMMARY OF EXISTING LITERATURE ON ADHESION FACTORS OF BORED PILES IN CLAY

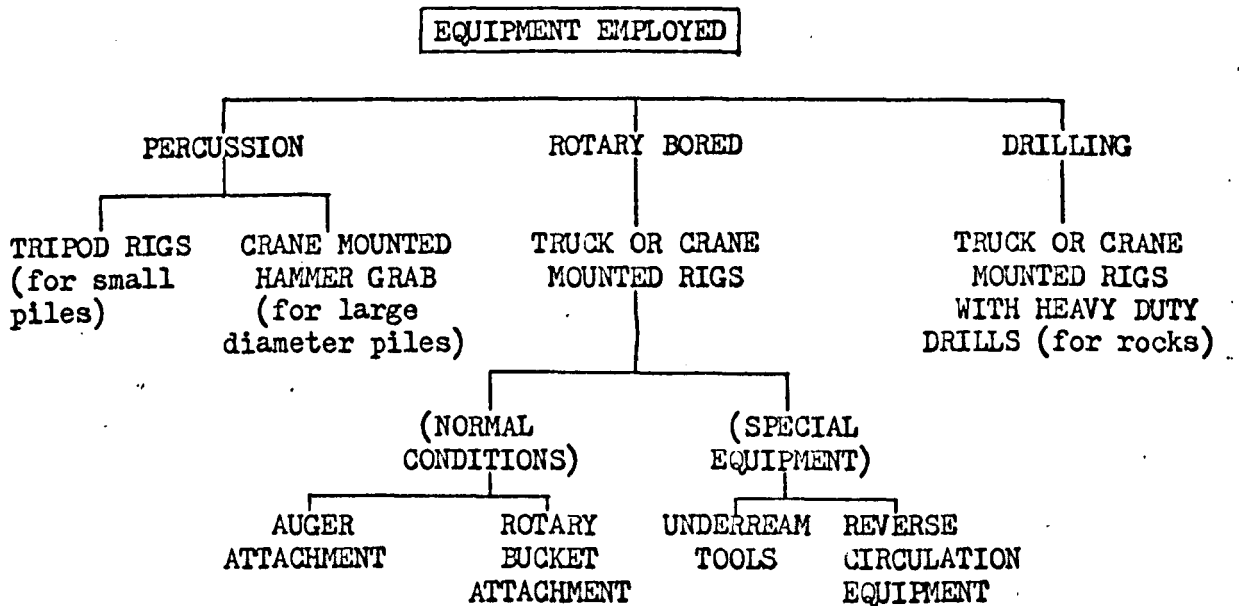
	REFERENCE	SOIL TYPE AND LOCATION	MEAN SHEAR STRENGTH $\bar{c}$ kN/m <sup>2</sup>	$\alpha$ ADHESION FACTORS		CONSTRUCTION NOTES
				RANGE	MEAN	
1	Meyerhof and Murdock (1953)	London Clay	168	0.6-1.0	0.80	Dry method
2	Golder and Leonard (1954)	London Clay	125	0.5-0.7	0.70*	Dry method *for piles > 9m
3	Skempton (1959)	London Clay	-	0.3-0.6*	0.45*	*based on numerous case histories of load tests.
4	Mohan and Chandra (1961)	Expansive Black Cotton Clay (various parts of India)	80-165	0.42-0.60	0.50	No mention of construction method
5	Woodward et al. (1961)	California Clay	95-120	0.49-0.52	0.50	-
6	Frischmann and Fleming (1962)	London Clay	117-177	-	0.45	Casing method with underream
7	Whitaker and Cooke (1966)	London Clay	130	-	0.44	Dry method
8	Matich and Kozicki (1967)	Glacial till, Nova Scotia	270	-	0.64*	*failure was not reached
9	O'Neill and Reese (1972)	Beaumont Clay, Houston	110	0.44-0.54	0.50	Dry method
10	Reese, O'Neill and Touma (1973)	Beaumont Clay, Houston	80-99	0.65-0.75	0.70	Slurry method
11	Reese, Touma and O'Neill (1976)	Beaumont Clay*, Houston	115	-	0.50 0.30	St. shafted Underreamed *with silt and sand.
12	Fearenside and Cooke (1977)	London Clay	140	0.26-0.46 0.27-0.43	- -	Bentonite method Dry method
13	Weltman and Healy (1978)	Glacial till, Hull Glacial till, Hartlepool	110 130	- 0.46-0.65	0.61 -	Dry method

TABLE 2.6 SUMMARY OF EXISTING LITERATURE ON ADHESION FACTORS OF BORED PILES IN CLAY

	REFERENCE	SOIL TYPE AND LOCATION	MEAN SHEAR STRENGTH $\bar{c}$ kN/m <sup>2</sup>	$\alpha$ ADHESION FACTORS		CONSTRUCTION NOTES
				RANGE	MEAN	
1	Meyerhof and Murdock (1953)	London Clay	168	0.6-1.0	0.80	Dry method
2	Golder and Leonard (1954)	London Clay	125	0.5-0.7	0.70*	Dry method *for piles > 9m
3	Skempton (1959)	London Clay	-	0.3-0.6*	0.45*	*based on numerous case histories of load tests.
4	Mohan and Chandra (1961)	Expansive Black Cotton Clay (various parts of India)	80-165	0.42-0.60	0.50	No mention of construction method
5	Woodward et al. (1961)	California Clay	95-120	0.49-0.52	0.50	-
6	Frischmann and Fleming (1962)	London Clay	117-177	-	0.45	Casing method with underream
7	Whitaker and Cooke (1966)	London Clay	130	-	0.44	Dry method
8	Matich and Kozicki (1967)	Glacial till, Nova Scotia	270	-	0.64*	*failure was not reached
9	O'Neill and Reese (1972)	Beaumont Clay, Houston	110	0.44-0.54	0.50	Dry method
10	Reese, O'Neill and Touma (1973)	Beaumont Clay, Houston	80-99	0.65-0.75	0.70	Slurry method
11	Reese, Touma and O'Neill (1976)	Beaumont Clay*, Houston	115	-	0.50 0.30	St. shafted Underreamed *with silt and sand.
12	Fearenside and Cooke (1977)	London Clay	140	0.26-0.46 0.27-0.43	- -	Bentonite method Dry method
13	Weltman and Healy (1978)	Glacial till, Hull Glacial till, Hartlepool	110 130	- 0.46-0.65	0.61 -	Dry method



(a) Classification according to method of construction



(b) Classification according to equipment employed

Fig. 2.1 CLASSIFICATION OF BORED CAST-IN-SITU PILES

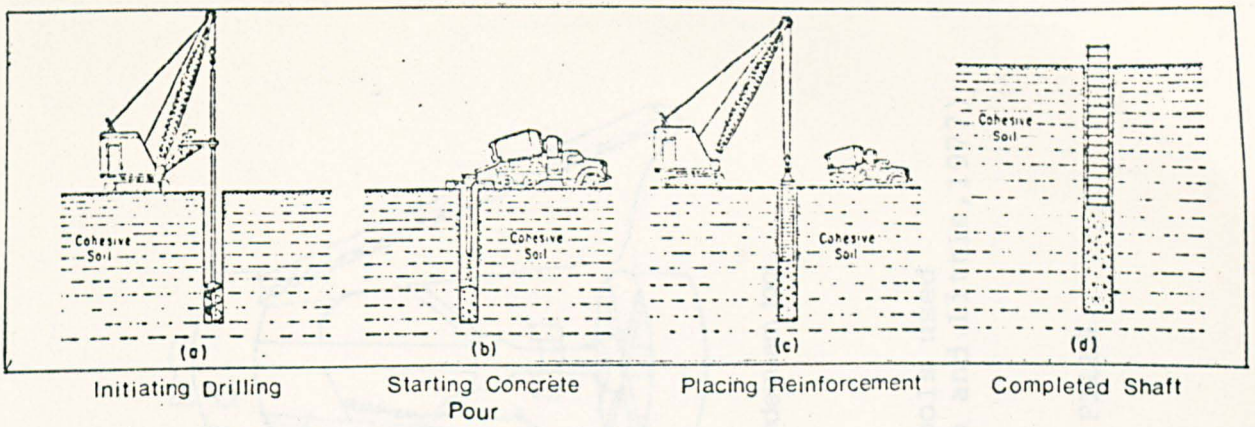


Fig. 2.2 DRY METHOD OF CONSTRUCTION

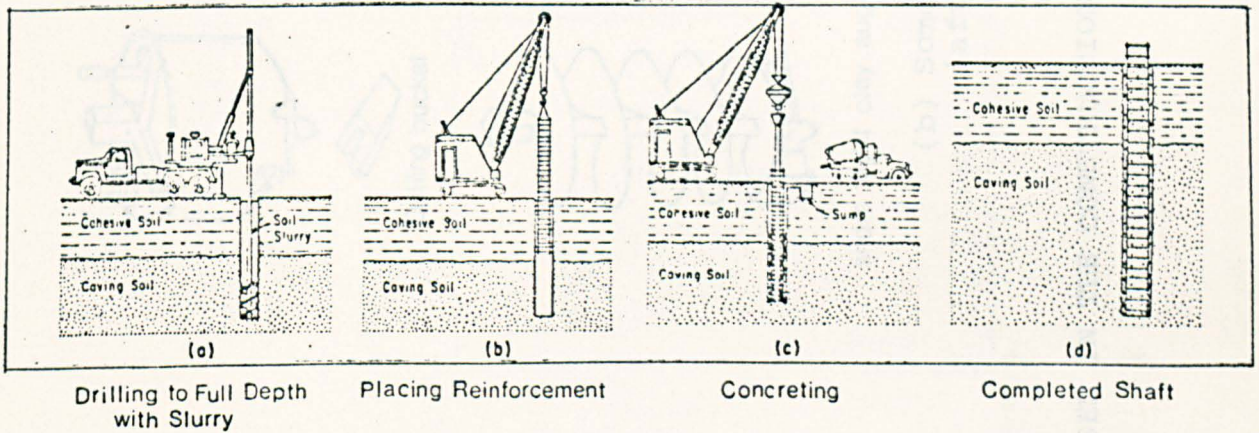


Fig. 2.3 SLURRY METHOD OF CONSTRUCTION

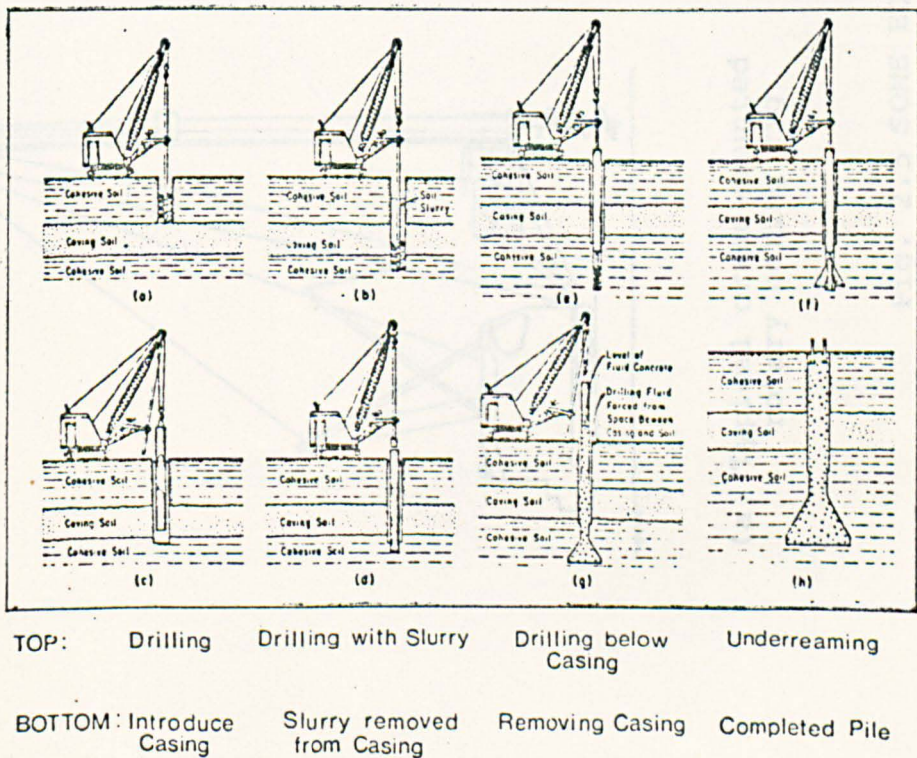
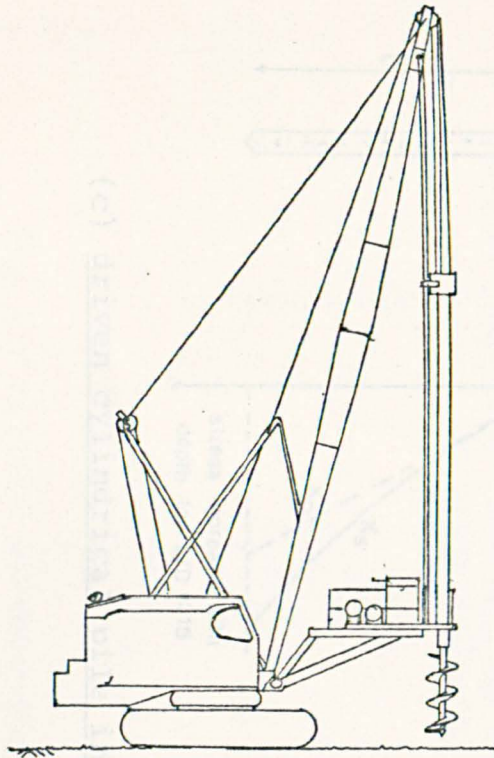
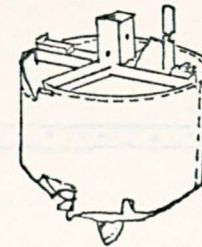


Fig. 2.4 CASING METHOD OF CONSTRUCTION



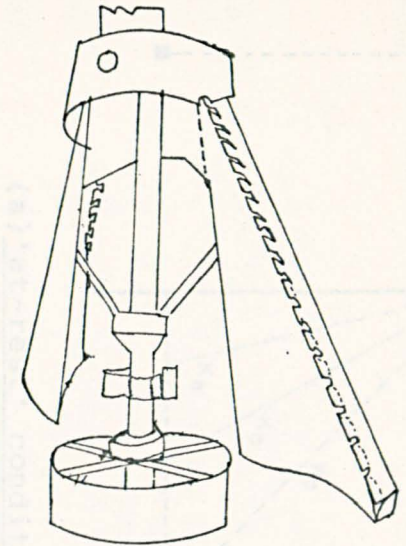
(a) Typical crane-mounted rotary boring rig



Drilling bucket



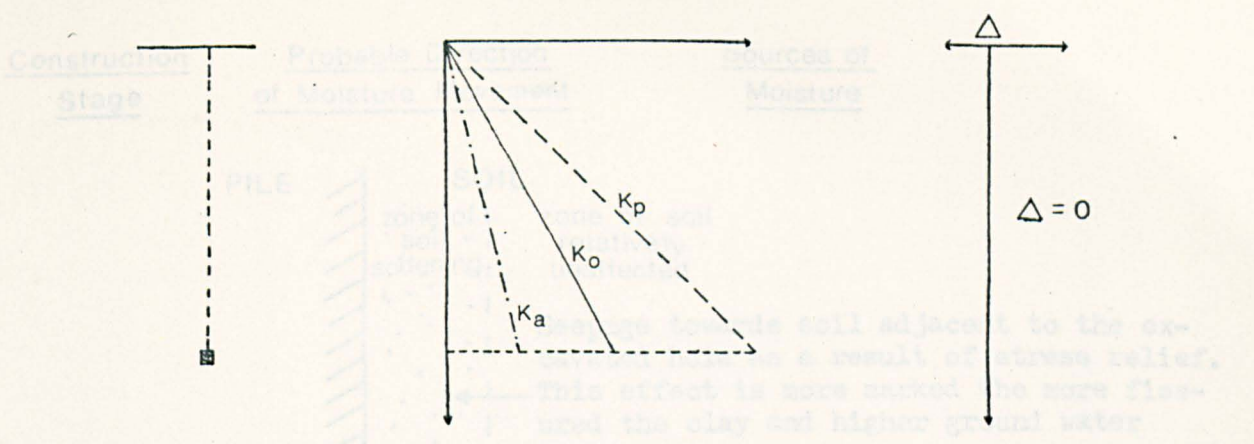
short flight clay auger



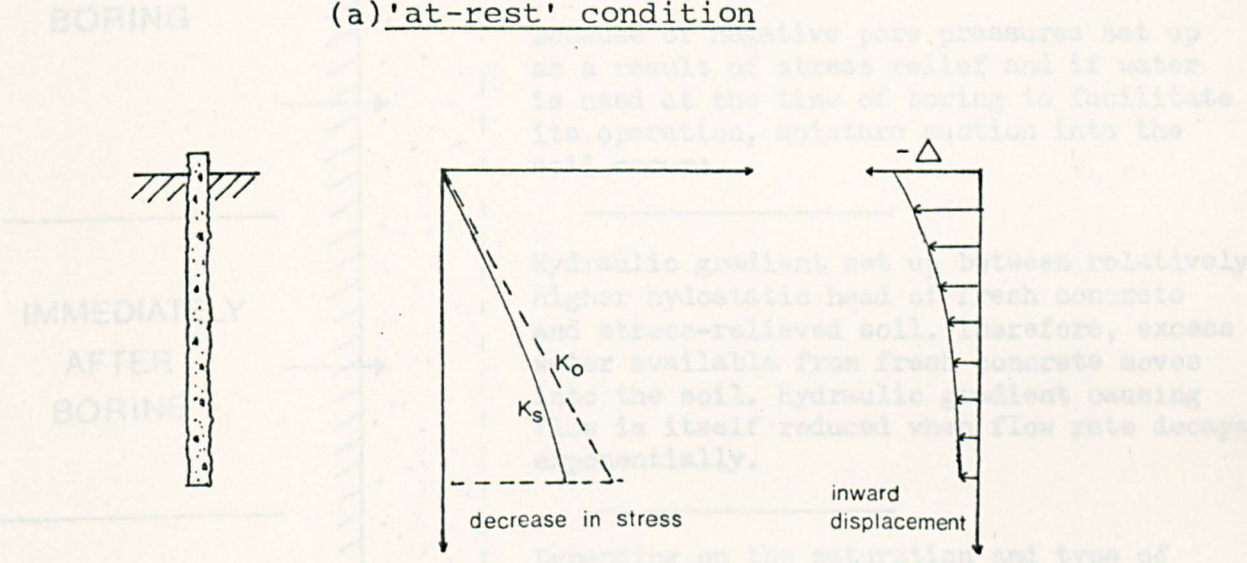
underream tool

(b) Some boring tools used  
(after Weltman and Little, 1977)

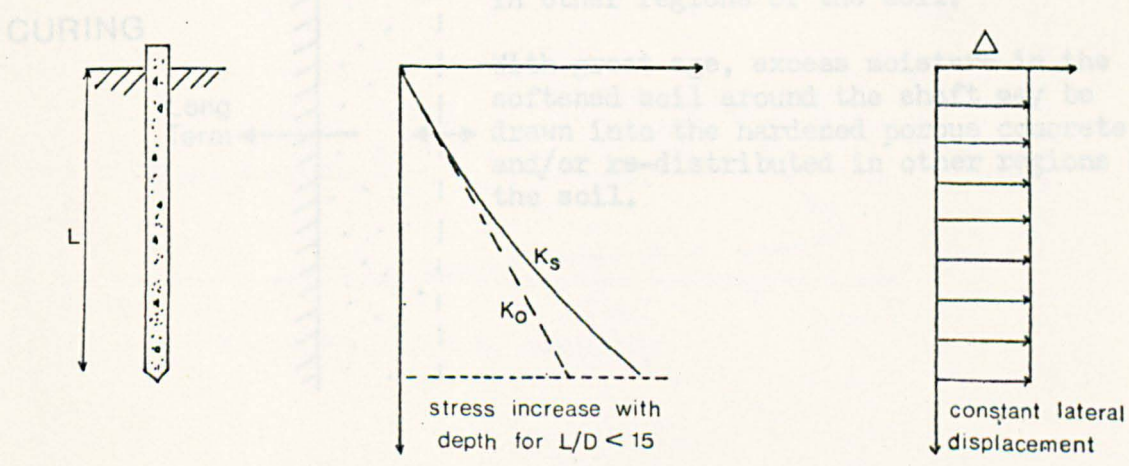
Fig. 2.5 SOME EQUIPMENT USED IN THE CONSTRUCTION OF BORED PILES.



(a) 'at-rest' condition



(b) bored pile in clay



(c) driven cylindrical pile in clay

Fig. 2.7 PATTERN OF MOISTURE MOVEMENT  
 Fig. 2.6 STATE OF STRESS AND DEFORMATION AROUND PILES (after Kedzi, 1975)

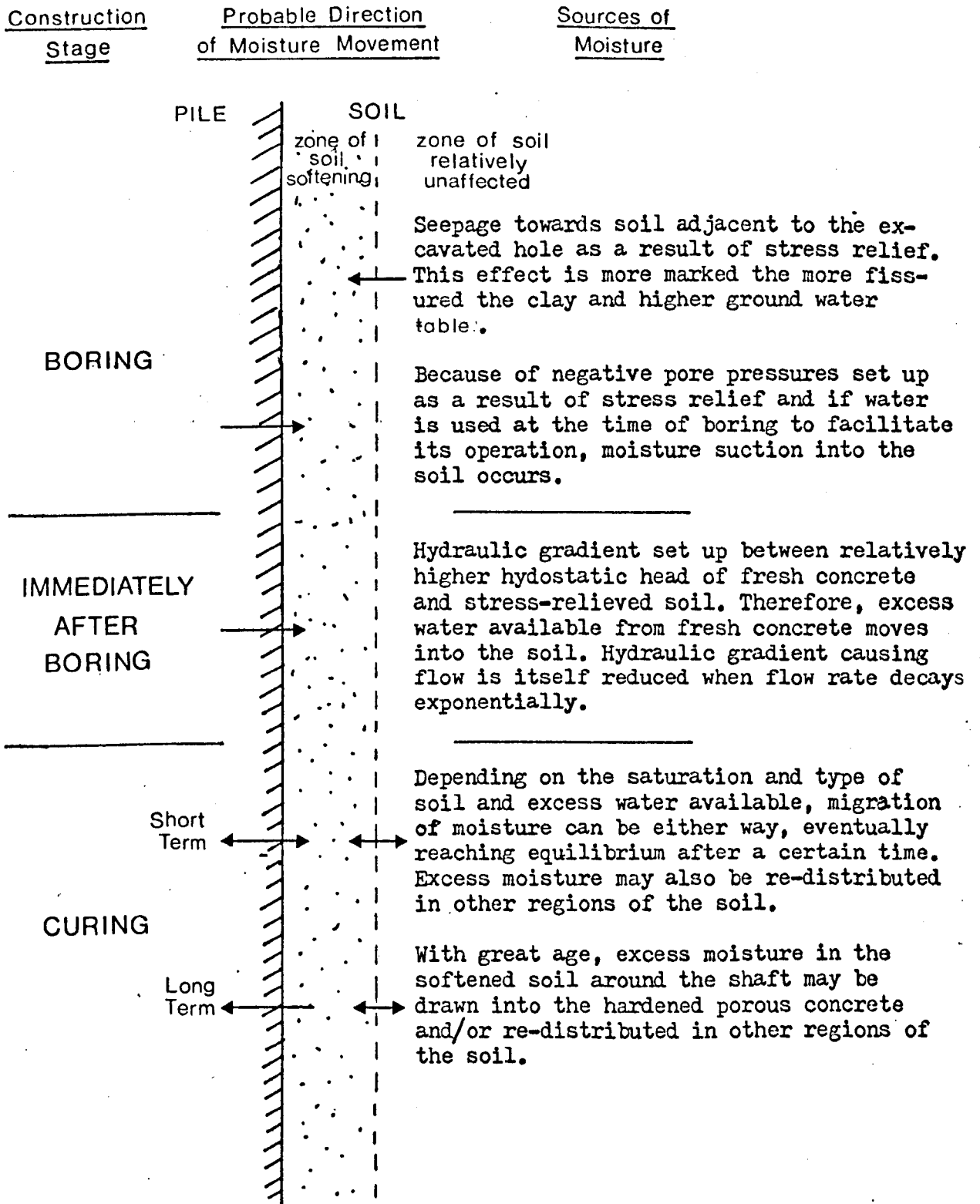


Fig.2.7 PATTERN OF MOISTURE MOVEMENT

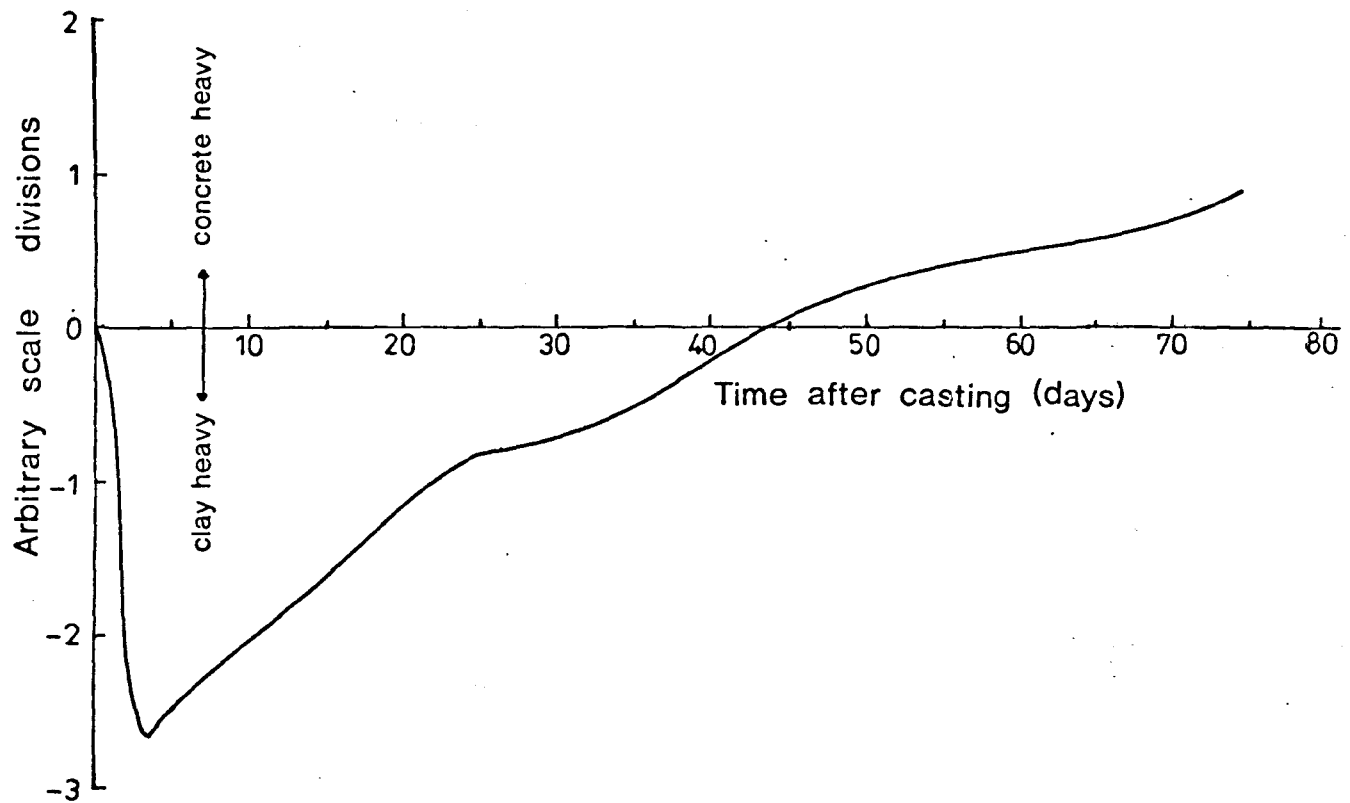
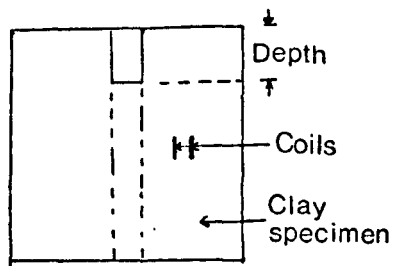
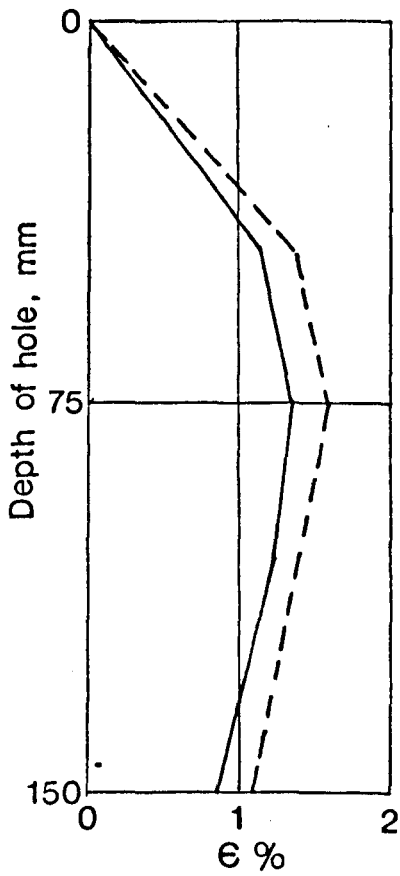


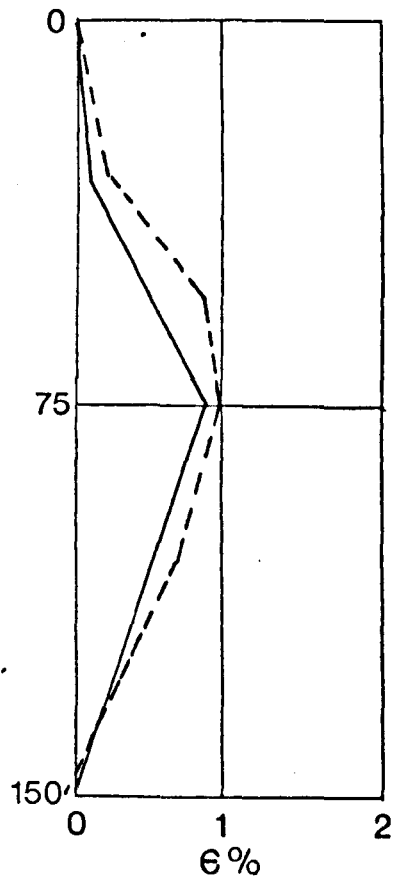
Fig.2.8 MOISTURE TRANSFER BETWEEN CONCRETE AND CLAY (after Taylor,1966)



— coils at 50 mm from centre  
 - - - coils at 25 mm from centre

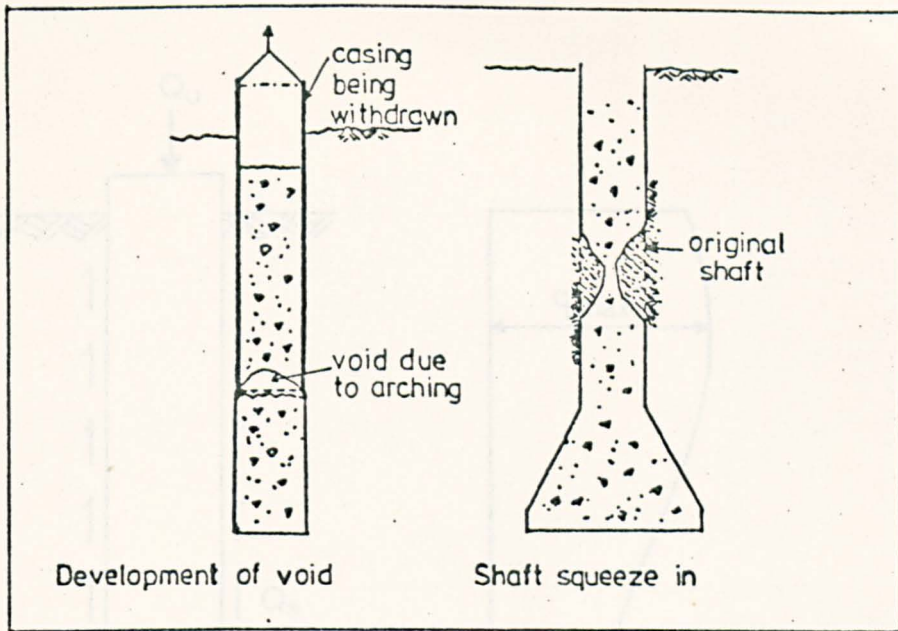


(a) Using polished brass tube

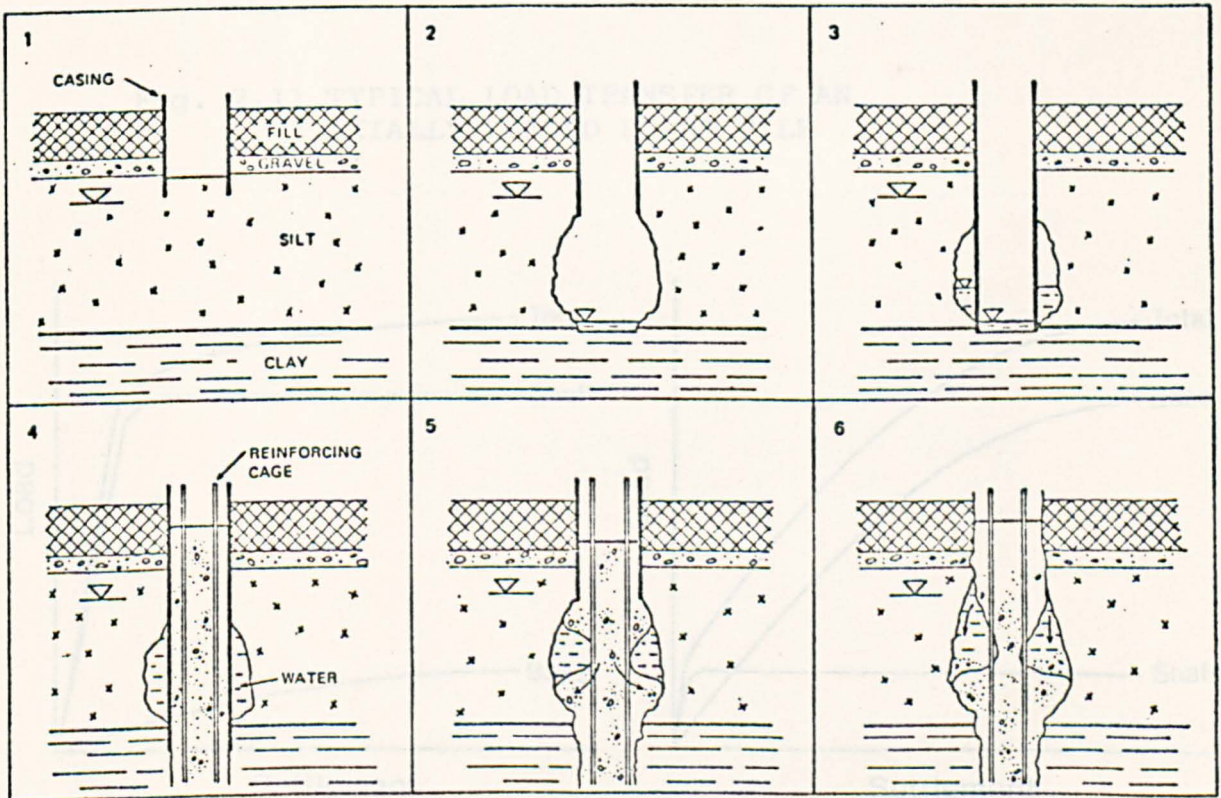


(b) Using auger

Fig.2.9 STRAIN CAUSED BY BORING A 25mm HOLE IN A KAOLIN SPECIMEN USING TWO DIFFERENT TECHNIQUES (after Eid,1978)



(a) after Baker and Khan (1971)



(b) after Thorburn and Thorburn (1977)

Fig. 2.10 FORMATION OF CAVITIES IN BORED PILE CONSTRUCTION

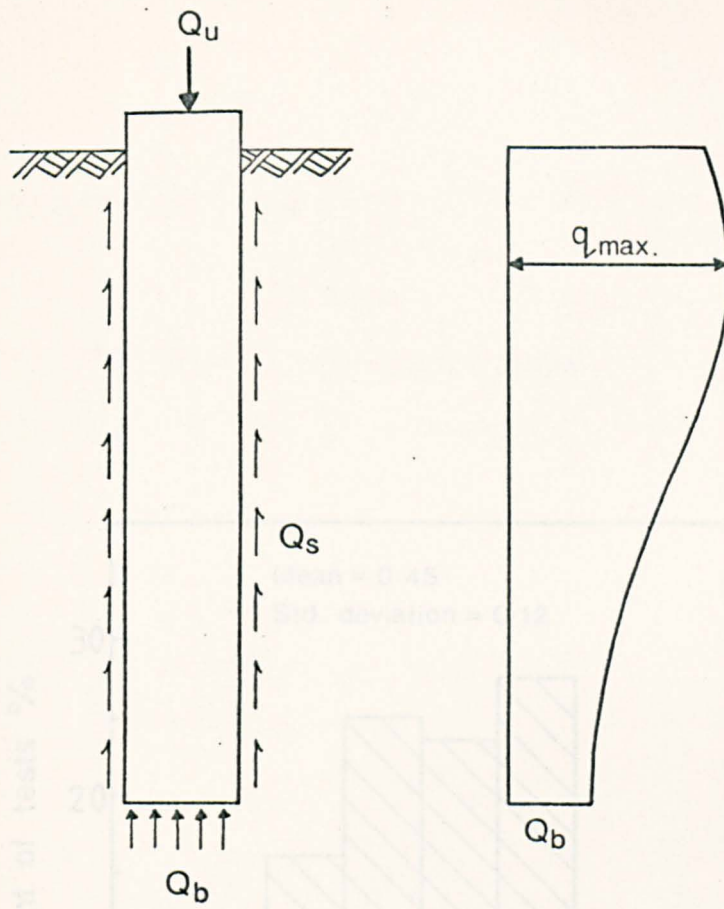


Fig. 2.11 TYPICAL LOAD TRANSFER OF AN AXIALLY LOADED BORED PILE

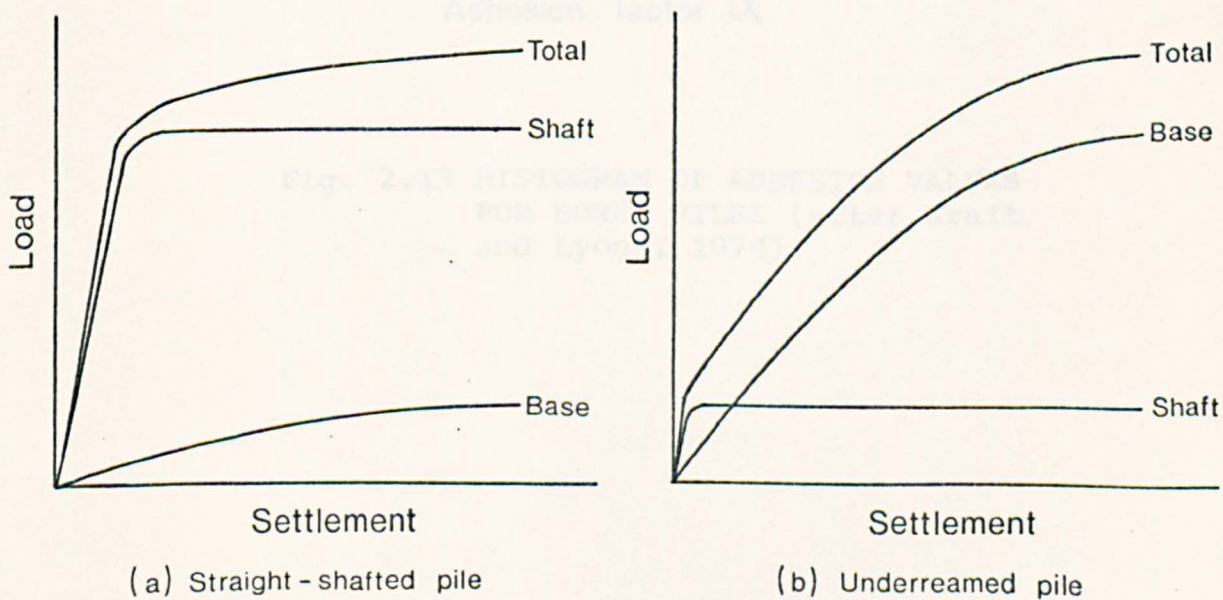


Fig. 2.12 DEVELOPMENT OF SHAFT AND BASE RESISTANCE (after Burland and Cooke, 1974)

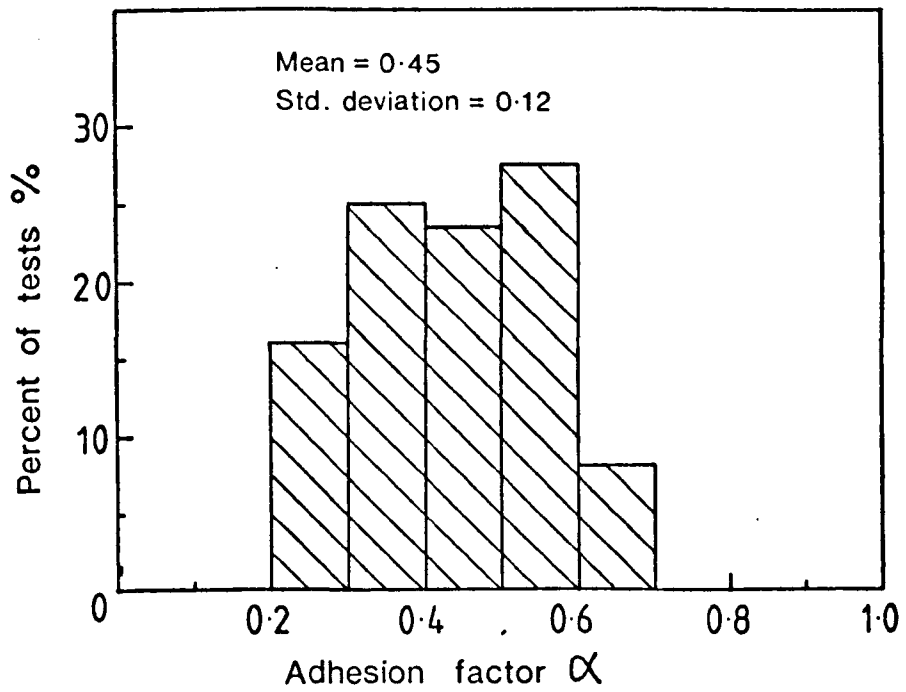
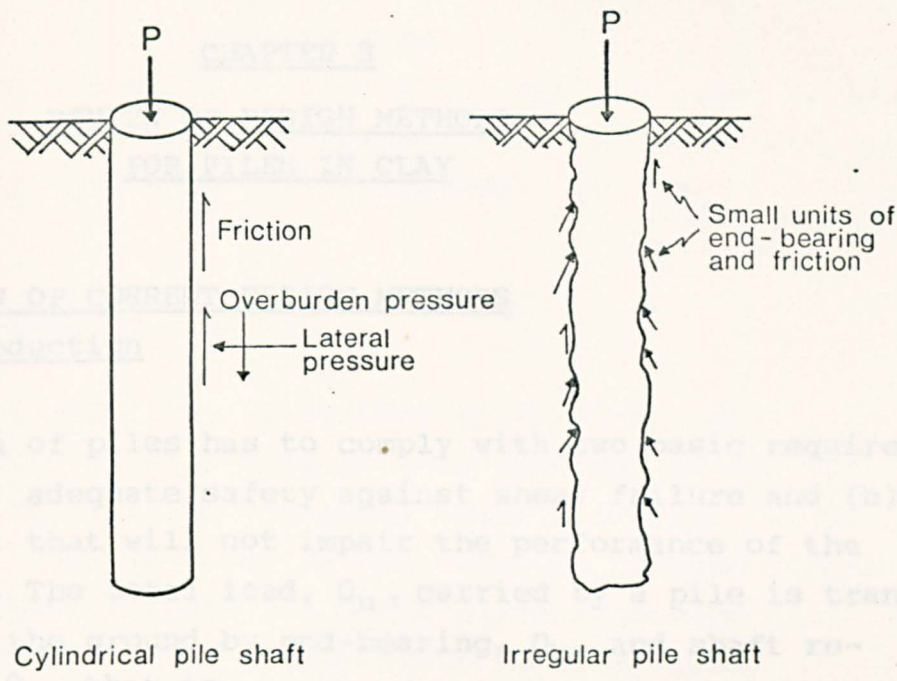


Fig. 2.13 HISTOGRAM OF ADHESION VALUES FOR BORED PILES (after Kraft and Lyons, 1974).



Cylindrical pile shaft

Irregular pile shaft

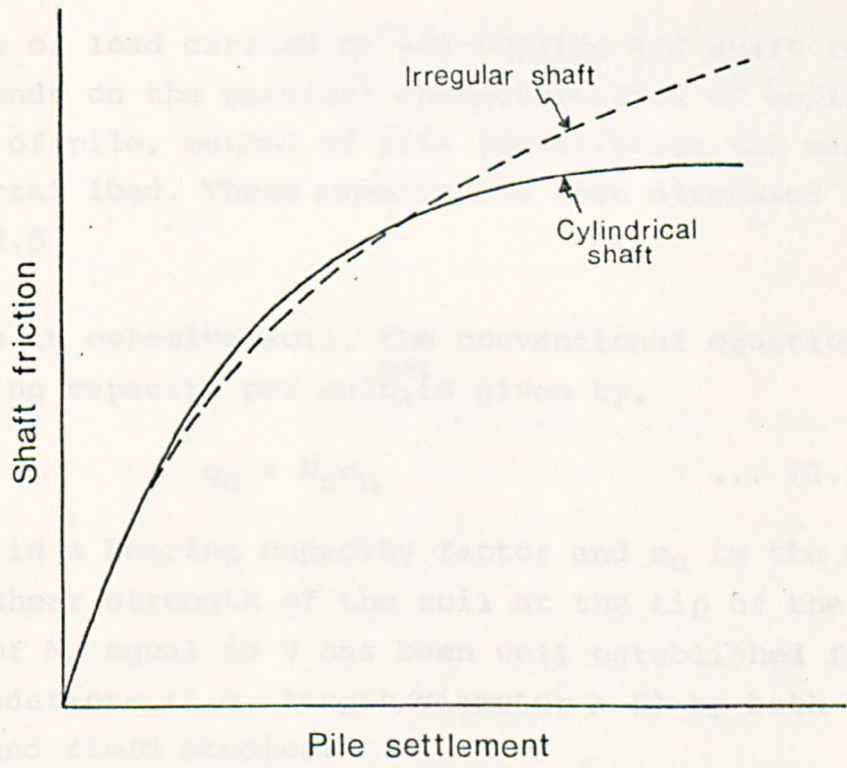


Fig. 2.14 DEVELOPMENT OF SHAFT FRICTION ON CYLINDRICAL AND IRREGULAR PILE SHAFTS (after Fleming and Sliwinski, 1977).

CHAPTER 3  
REVIEW OF DESIGN METHODS  
FOR PILES IN CLAY

3.1 REVIEW OF CURRENT DESIGN METHODS

3.1.1 Introduction

The design of piles has to comply with two basic requirements: (a) adequate safety against shear failure and (b) settlement that will not impair the performance of the structure. The total load,  $Q_u$ , carried by a pile is transferred to the ground by end-bearing,  $Q_b$ , and shaft resistance,  $Q_s$ , that is,

$$Q_u = Q_b + Q_s \quad \dots (3.1)$$

The ratio of load carried by end-bearing and shaft resistance depends on the physical characteristics of soil, dimensions of pile, method of pile installation and magnitude of the total load. These aspects have been discussed in Section 2.5

For piles in cohesive soil, the conventional equation for end-bearing capacity per unit <sup>area</sup> is given by,

$$q_b = N_c c_u \quad \dots (3.2)$$

where  $N_c$  is a bearing capacity factor and  $c_u$  is the undrained shear strength of the soil at the tip of the pile. A value of  $N_c$  equal to 9 has been well established for deep foundations (i.e. length/diameter  $\geq 5$ ) by both theoretical and field studies.

For shaft adhesion of piles in clay, a number of design methods are currently available, such as

- (a) adhesion factor or  $\alpha$ -method
- (b) API-method

(c)  $\lambda$ -method

(d) Effective stress methods.

These methods and their limitations are discussed briefly in the following sections and are applicable to both bored cast-in-place piles and driven piles.

### 3.1.2 Adhesion or $\alpha$ -method

This method was first introduced by Tomlinson (1957) in the form of a relationship between adhesion of driven piles in clay and the undrained shear strength. Later, Skempton (1959) applied the relationship between adhesion and undrained strength for bored piles in London Clay. The usual form of the relationship is given by,

$$q_s = \alpha \bar{c}_u \quad \dots (3.3)$$

where  $q_s$  is the unit shaft resistance,  $\alpha$  is the adhesion factor and  $\bar{c}_u$  is the average undrained shear strength of soil surrounding the pile shaft. The adhesion is a complex function of various factors such as the effects of installation and the variations in soil properties. A summary of existing literature on  $\alpha$ -values obtained from field tests on bored piles has been presented in Table 2.6.

For the design of bored piles, <sup>in London Clay</sup> Skempton (1959) recommended values of  $\alpha$  ranging from 0.3, where there is a high degree of remoulding and softening, to a value of 0.6 for piles constructed carefully under favourable conditions. Where there is no previous experience of adhesion factors in any particular type of clay,  $\alpha$  is usually taken as 0.45 with adequate load testing to confirm the design value. For this case, the maximum adhesion should not exceed 100 kN/m<sup>2</sup>. For piles with underreams, Reese et al. (1976) suggested an adhesion factor of 0.3 in view of the fact that a longer time is required for the underreaming operation and the clearing of debris. This may cause

appreciable softening due to soil swelling, and seepage of water may have occurred.

In general, for bored piles in normally and over-consolidated clay, values of  $\alpha$  vary between 0.5 to 1.0 and 0.3 to 0.5 respectively.

Design curves for adhesion factors for piles driven into clay soils have been presented by Tomlinson (1977) and are shown in Fig. 3.1. The adhesion factor depends partly on the cohesive strength of the soil and partly on the nature of soil above the bearing stratum of clay into which piles are driven.

The major limitation of this method of design is that all factors influencing the pile adhesion are combined into a single empirical correlation factor. Consequently, there is no basis for extrapolation of this factor when soil conditions, pile installation methods and loading conditions are different from those included in load test data from which the correlation or adhesion factor was derived. For example, the adhesion method of design works well for piles in London Clay and Beaumont Clay (Houston) where extensive field tests have been carried out to support the recommended  $\alpha$ -values. However, application of the method to other soil types is less well established. Another limitation of the method lies in the difficulty of choosing appropriate values of undrained shear strength. This is true especially for stiff fissured clay where there is usually a wide scatter in the results of undrained strength tests. Despite the above limitations, the method is widely used especially in the United Kingdom.

### 3.1.3 API-method

This method was developed by the American Petroleum Institute (1977) for predicting frictional pile capacity

according to the depth below the mudline and is used in connection with fixed offshore platforms. It is based on a total stress analysis similar to the adhesion method except that in the design recommendations,  $\alpha$  values of 1.0 and 0.33 are considered upper limits for depths up to 30m and depths greater than 30m respectively. Recommended values of  $\alpha$  reduce from 1.0 in soft clays where  $c_u < 25 \text{ kN/m}^2$  to 0.5 in stiff clays where  $c_u > 75 \text{ kN/m}^2$ .

#### 3.1.4 $\lambda$ -method

Developed by Vijayvergiya and Focht (1972), this method is a combination of total and effective stress analysis based on the theory that pile driving displaces sufficient soil to develop passive resistance. The shaft resistance is given by,

$$q_s = \lambda (\bar{\sigma}_v' + 2\bar{c}_u) \quad \dots (3.4)$$

where  $\lambda$  is the frictional coefficient and  $\bar{\sigma}_v'$  and  $\bar{c}_u$  are the mean values of the effective overburden pressure and the undrained shear strength of soil over the length of pile. The values of  $\lambda$  proposed by the authors are shown in Fig. 3.2. It can be seen that  $\lambda$ -values vary from 0.5 at the surface to about 0.15 at 30m depth and approaches a constant value of about 0.12 below this depth.

It is prudent to note that this method is suitable for long piles ( $L > 20\text{m}$ ). If used for short piles in stiff clay, it tends to give unsafe predictions (Tomlinson, 1977) since the method does not take into account the gap formation in stiff clay near the surface.

#### 3.1.5 Effective stress methods

At present, this approach is not widely used in pile design due to the difficulties in determining the design parameters.

However, because of its potential as a rational design method, there is increasing interest in its application. Recent studies by a number of authors indicate a promising future for the effective stress approach as a method for pile design. Therefore, it is of interest to review the various aspects of the effective stress approach in general, and the work of these authors in particular.

The principles and design approach discussed in the following sections are mainly related to bored piles in clay. Where applicable, variations in the approach for driven piles are mentioned.

### 3.1.6 Factors of Safety

The factor of safety is applied in pile design to cover against uncertainties in the design assumptions; to account for variation in the performance of individual piles forming a group; and to provide for the possible variation in soil properties within the site. The factor of safety is used with an over-riding condition that the absolute and differential settlement are within the tolerable limits specified in the Code of Practice. When the pile is predominately end-bearing, it is usual to maintain a factor of safety of 3.0 against base failure. For piles supported by end-bearing and shaft resistance, an overall factor of safety of 2.5 is commonly used. In cases where there is a comprehensive programme of testing and good site investigation, the overall factor of safety may be reduced to 2.0.

## 3.2 EFFECTIVE STRESS METHOD OF DESIGN

### 3.2.1 Concept of effective stress

Soil can be visualised as a compressible skeleton of solid particles enclosing voids. In saturated soils, these voids are filled with water. Since shear stress can only be

carried by the soil skeleton, it follows that the effective stress of a saturated soil is given by,

$$\sigma' = \sigma - u \quad \dots(3.5)$$

where  $\sigma'$  and  $\sigma$  are the effective and total stresses in the soil and  $u$  is the pore water pressure. This concept has made possible the rational understanding of many soil engineering problems. The important implication so far as strength is concerned is that a change in effective stress results in a change in strength.

### 3.2.2 Shaft resistance in terms of effective stress

In terms of fundamental soil mechanics theory, the ultimate shaft resistance per unit area of pile shaft,  $q_s$ , can be expressed by,

$$q_s = c' + \sigma_H' \tan \delta \quad \dots (3.6)$$

where  $c'$  is the effective cohesion of soil adjacent to the pile,

$\sigma_H'$  is the effective horizontal stress acting normal to the pile shaft, and

$\delta$  is the effective angle of shearing resistance between the soil and pile.

It is usual to assume that the effective cohesion of soil after pile installation is small and therefore can be neglected. Another simplifying assumption is made that  $\sigma_H'$  is related to the vertical effective overburden pressure,  $\sigma_V'$ , by the expression,

$$K_s = \frac{\sigma_H'}{\sigma_V'} \quad \dots (3.7)$$

where  $K_s$  is the coefficient of lateral stress at the pile shaft. Thus equation (3.6) becomes,

$$q_s = K_s \sigma_V' \tan \delta \quad \dots (3.8)$$

In an approximate analysis for the whole length of pile,

$$q_s = \bar{K}_s \bar{\sigma}_v' \tan \delta \quad \dots (3.9)$$

where  $\bar{K}_s$  and  $\bar{\sigma}_v'$  are average values over the length of pile.

The state of stress for a soil and pile element is shown in Fig. 3.3. For soil in the 'at-rest' condition (Fig. 3.3a), the coefficient of lateral earth pressure 'at-rest',  $K_0$ , is given by,

$$K_0 = \frac{\sigma_{Hc}'}{\sigma_{V0}'} \quad \dots (3.10)$$

where  $\sigma_{Hc}'$  and  $\sigma_{V0}'$  are the horizontal and vertical effective stresses of the soil in the undisturbed condition. The state of stress and deformation around a bored pile and a driven pile have been discussed in Section 2.4.2. As shown in Fig. 2.6, the coefficient of lateral stress,  $K_s$  is less than  $K_0$  for bored piles and greater than  $K_0$  for driven piles.

In the case of bored piles,  $K_s$  is low as a result of a decrease in total horizontal earth pressure after boring but will increase as concrete is placed in the shaft and the total horizontal earth pressure may re-establish itself. However, Chandler (1968) suggests that it is unlikely that the total horizontal earth pressure will ever reach the original value and attributes this to possible arching of concrete around the sides of the shaft. The effect of arching is to prevent full hydrostatic pressure of concrete developing against the soil (Sowa, 1970) and the phenomenon is more likely to occur in long rather short shafts. Tomlinson (1977) also suggests that radial shrinkage associated with curing will reduce the effective pressure on the shaft. For driven piles,  $K_s$  is greater than  $K_0$  because of the displacement of clay around the pile, with the coefficient of passive earth pressure,  $K_p$ , as the upper limit.



However, because of the difficulty in determining the coefficient of lateral stress after pile installation, it is usual to assume  $K_S$  to be equal to  $K_O$ . This assumption will give an upper limit to the ultimate shaft resistance for bored piles in clay and a lower limit for driven piles.

For soft clay, it is usual to assume  $\delta = \phi'$ , where  $\phi'$  is the effective angle of shearing resistance of the soil (see Fig. 3.3c). This assumption implies that failure takes place in the soil close to the pile surface when the shaft friction is fully developed. Thus, for piles in soft normally consolidated clay, equation (3.8) becomes,

$$q_s = K_O \sigma_v' \tan \phi' \quad \dots (3.11)$$

Equation (3.11) was initially proposed by Chandler(1968). Using the semi-empirical relationship for  $K_O$  for normally consolidated soil proposed by Jaky (1944), which is,

$$K_O = 1 - \sin \phi' \quad \dots (3.12)$$

the expression in equation (3.11) becomes,

$$q_s = \sigma_v' (1 - \sin \phi') \tan \phi' \quad \dots (3.13)$$

For the usual ranges of  $\phi'$  values between  $20^\circ$  and  $30^\circ$  for cohesive soil,  $q_s/\sigma_v'$  varies between 0.24 to 0.29.

For stiff overconsolidated clay where  $\sigma_H' > \sigma_v'$ , it can be seen from Fig. 3.3(d) that  $\delta < \phi'$ . In other words, the stress conditions are such that the effective angle of shearing resistance of the soil,  $\phi'$ , cannot be fully mobilized. Whether the value of  $\delta$  should be taken as the remoulded or the residual effective angle of shearing resistance of the soil remains uncertain at the present state of knowledge. However, various authors have suggested solutions to overcome this problem; these proposals are reviewed in Section 3.2.4.

Parry and Swain (1977a,1977b) also developed a number of expressions for shaft resistance based on effective stress, assuming that the soil immediately adjacent to the pile is failing in undrained shear. In order to consider various cases of soil conditions, the authors divided clays into two classes, A and B, where the stress conditions on the soil-pile interface are similar to those shown in Fig. 3.3(c) and (d) respectively. Some of the expressions derived by the Parry and Swain are slightly different from the effective stress expressions in this section. However, Burland (1978a) suggests that this difference is small and that the direct application of the simple Coulomb equation in (3.6) appears to offer a clearer insight than those obtained by Parry and Swain.

### 3.2.3 Potential of the Effective Stress Approach

The total stress method of pile design commonly used by engineers because of its apparent simplicity is actually an empirical procedure. However, it is effective stress rather than total stress that controls the fundamental behaviour of the soil in the consolidation and shearing processes. In view of the large variation in  $\alpha$ -values, Burland (1973) suggested that test results would be better understood if interpreted in terms of effective stresses.

The effective stress approach may also prove useful in assessing the long-term shaft resistance of piles in cohesive soil. Chandler (1968) suggests that since pile tests are usually carried out soon after casting when the total lateral stresses are not fully effective, the effective stress method generally gives results which are an upper limit to the recorded values. Tomlinson (1977) also pointed out that the shaft resistance of a pile in clay loaded very slowly may only be one-half of that which is measured under the rate at which load is normally applied during

a pile loading test. The slow rate of loading may correspond to that of a building under construction, yet the ability of a pile to carry its load is judged on its behaviour under a comparatively rapid loading test carried out only a few days after installation.

It is also important to note that the effective stress approach takes into account the stress history of the soil and the method of pile placement in its design parameters; factors which are not independently considered in the total stress method of design. Therefore, to put pile design on a more rational basis, Meyerhof (1976) in his 11th Terzaghi Lecture emphasized the need for continuing efforts to utilize effective stress concepts.

#### 3.2.4 Application of the Effective Stress Method in pile design

The effective stress approach for pile analysis was first suggested by Zeevaert (1959) and Eide et al. (1961) in connection with tests on driven piles in clay. However, it was Chandler (1968) who first applied the effective stress method in the analysis of load test results of bored piles in London Clay. He found that results of maintained load pile tests, in which the rate of penetration was slow enough to prevent pore pressure changes, were in reasonable agreement with the computed values using average values in equation (3.11).

Burland (1973) introduced a design method which avoids the direct application of  $K_s$  by using the relationship,

$$q_s = \beta \sigma_v' \quad \dots (3.14)$$

where  $K_s \tan \delta$  is replaced by  $\beta$ . He plotted the results of a large number of pile tests carried out on driven piles in a wide variety of soft clays (see Fig. 3.4) and found

that most of the results lie between  $\beta = 0.25$  and  $0.40$ . These values of  $\beta$  represent a smaller variation than the equivalent  $\alpha$  values for these tests. These  $\alpha$  values usually lie between  $0.5$  and  $1.6$ . On the basis of these results, Burland recommended that a value of  $0.3$  for  $\beta$  would be a reasonable design value for soft clay. Meyerhof (1976) also carried out an analysis of test results for a wide range of driven piles in soft clay published by a number of authors. He found that values of  $\beta$  lie mostly between  $0.22$  to  $0.40$  with an average  $\beta$  value slightly above  $0.30$ .

For stiff overconsolidated clay, Burland plotted the load test results of bored and driven piles in London Clay as shown in Fig. 3.5 and Fig. 3.6 respectively. On the basis of results in Fig. 3.5, he suggests that  $\beta$  equal to  $0.8$  could be used as a conservative preliminary design curve for London Clay. It is interesting to note that when equation 3.11 is plotted in both Figs. 3.5 and 3.6, the relationship appears to give a reasonable upper limit to shaft friction for bored piles and a lower limit to shaft friction for driven piles. Using Burland's approach, Weltman and Healy (1978) found that for shaft adhesion of bored piles in glacial till, values of  $\beta$  varied between  $0.50$  and  $0.63$  and exhibited a correlation with  $\alpha$  values.

Leach et al. (1976) compared measured values from field tests on bored piles in weathered Keuper marl with various design methods available and found that the effective stress approach to assessment of pile behaviour gave encouraging results. Flaate and Selnes (1977) also concluded from their study on friction piles in soft marine clays that the best estimate of shaft friction is obtained by an effective stress analysis.

The stages in the life of driven piles, from the initial state of stress to pile failure due to loading, have been described and modelled in terms of effective stress by

Esrig et al.(1977). The authors found that the effective stress approach gives explicit treatment of the events in the life of a pile so that uncertainties in the prediction of pile capacity can be recognised by the designer. A comparison between measured capacities based on pile load tests and predicted values showed promising results.

Searle (1979) introduced a residual shear strength concept into the effective stress equation by assuming that  $\delta$  is equal to the effective residual angle of friction,  $\phi_r'$ . This concept is based on the plastic flow of the soil rather than limit equilibrium state. Thus, equation (3.8) becomes,

$$q_s = K_S \sigma_v' \tan \phi_r' \quad \dots (3.15)$$

Searle found that published case histories of bored piles in overconsolidated clays showed consistent results when analysed by this method and that the approach is more predictable for longer piles than for short bored piles. The author also showed that the total stress method is theoretically related to the effective stress methods by the expression,

$$c_u \approx K_S \sigma_v' \frac{\sin \phi_p'}{1 - \sin \phi_p'} \quad \dots (3.16)$$

and

$$\alpha \approx \tan \phi_r' \frac{1 - \sin \phi_p'}{\sin \phi_p'} \quad \dots (3.17)$$

where  $\phi_p'$  is the peak effective angle of shearing resistance. Therefore, an approximate value of  $\alpha$  can be obtained from a knowledge of the peak and residual effective angle of shearing resistance.

### 3.3 ESTIMATION OF DESIGN PARAMETERS

#### 3.3.1 Introduction

Direct measurements of in-situ stresses in the field present serious difficulties due to disturbance of stress distribution resulting from the installation of the measuring devices. The State-of-the-Art report by Wroth (1975) focused attention on the uncertainty of laboratory measurements of  $K_0$  and the difficulty of making accurate measurements of stress in the field. However, improved techniques in field instrumentation have increased the accuracy and reliability of field measurements with the effect that design parameters can be used with a greater degree of confidence.

#### 3.3.2 Total and effective vertical stress

In practice, it is not usual to measure the total vertical pressure in the field. Instead, the total vertical stress is calculated from the weight of the overburden assuming that the ground surface is reasonably level. Therefore, to obtain a good estimation of the total vertical stress, the samples from which the unit weights are determined should be representative of the site.

To obtain the effective vertical stress, pore water pressure is estimated from the observed ground level or measured directly by piezometers installed in the soil. If the pore pressure is hydrostatic and water table is known, then the effective vertical stress at a depth,  $d$ , can be deduced from,

$$\sigma_v' = \sigma_v - u \quad \dots (3.18)$$

$$\text{or} \quad \sigma_v' = \gamma_s d - \gamma_w h \quad \dots (3.19)$$

where  $\gamma_s$  and  $\gamma_w$  are the bulk weights of the overlying soil strata and water respectively and  $h$  is the height of the

water table above the point considered. In estimating the pore water pressure, it is prudent to consider the seasonal fluctuation of the ground water table.

If piezometers are installed in the soil, excess pore pressure generated during the driving of the piezometer must be allowed to dissipate before any measurements can be made. Most of these piezometers are electrical devices available commercially and details of their operation can be found in Hanna (1973).

### 3.3.3 Total and effective horizontal stress

For the estimation of total and effective vertical stress, the problem seems to be one of sufficient accuracy. In the case of the total horizontal stress, it is more difficult to determine than the total vertical stress, and depends mainly on the stress history. However, the effective horizontal stress is related to the effective vertical stress by the coefficient of lateral stress given in equation (3.7). Wroth (1975) suggests that if  $\sigma_H$  can be measured and  $\sigma_H'$  deduced, then the importance of  $K_0$  and  $\sigma_v'$  declines. Increasing effort has been directed recently towards attempts to measure the total horizontal stress. At present, three methods are currently available: (a) direct measurement by total pressure cells, (b) measurements by pressuremeter instruments, and (c) measurement using the hydraulic fracturing method.

A number of pressure cells have been developed for measuring the lateral stresses in the field and the main problem with this method of measurement is the redistribution of stresses resulting from installation of the measuring devices. However, Massarsch (1975) developed a technique for measuring in-situ lateral stresses using a modified Glötzl pressure cell in which disturbance of the soil mass was relatively small.

The pressuremeter initially developed by Menard (1957) operates on the principle of expanding a cylinder in a pre-bored borehole. By observing the amount of expansion and pressure change, one may use the theory of an infinitely thick cylinder subjected to an internal pressure, to obtain the elasticity and strength of the soil around the pressuremeter.

Self-boring pressuremeter instruments have been developed independently in France by Banguelin et al. (1973) and in England by Wroth and Hughes (1974). These instruments have a good potential for providing engineers with useful information on the in-situ stress-strain behaviour. The advantages of these instruments are that they are suitable for both soft and stiff soil and they can be inserted into the soil with virtually no borehole disturbance and only minor borehole stress relief.

The Camkometer [Wroth and Hughes, (1974)], a self-boring pressuremeter, also incorporates lateral pressure cells and pressure transducers on the face of the expanding membrane. This enables an evaluation of the in-situ stress condition to be made in terms of effective stress.

The values of in-situ total horizontal stress are obtained from the self boring pressuremeter instruments by observing the pressure at which the membrane starts to expand radially. In assessing the results of pressuremeter tests, different methods of interpretation are possible and these methods have been summarized by McKinlay and Anderson (1975).

The use of the hydraulic fracturing method of determining in-situ stress was first reported by Bjerrum and Andersen (1972). A vertical crack is initiated in the soil around a piezometer tip. The water pressure at which the crack closes is measured and this pressure is assumed to be identical to the total horizontal stress across the crack. In order to achieve a vertical crack,  $\sigma_H'$  must be less than

$\sigma_v'$ ; therefore the application of the method is limited to normally or lightly-overconsolidated clays.

Once the total horizontal stress is determined from any of the above methods and the pore pressure estimated as in the previous section, the effective horizontal stress can then be deduced.

#### 3.3.4 Coefficient of lateral stress, $K_S$

The coefficient of lateral stress depends mainly on the initial ground condition, the method of pile placement and the pile shape and length. It has been stated in Section 3.2.2 that for bored piles,  $K_S$  is less than or equal to  $K_0$ , and for driven piles,  $K_S$  is generally greater than  $K_0$ , but because of the difficulty in determining the coefficient of lateral stress after pile installation, it is usually assumed that  $K_S$  equals  $K_0$ .

Values of  $K_0$  can be determined directly from measurements or indirectly from semi-empirical procedures. Studies by Brooker and Ireland (1965) and others showed that the coefficient of earth pressure at-rest is related to the effective angle of shearing resistance and plasticity index for various values of overconsolidation ratio. Therefore, if the overconsolidation ratio is approximately known from the stress history or from consolidation test results,  $K_0$  can be estimated.

The semi-empirical methods available for estimating  $K_0$  for normally and overconsolidated clays are summarized in Tables 3.1 and 3.2. However, it should be noted that the estimation of overconsolidation ratio from consolidation tests is often uncertain because of sample disturbance which tends to mask the undisturbed soil behaviour and makes the estimation of the maximum past pressure difficult. Therefore, to obtain a better estimate of the coefficient

of lateral stress, field instrumentation should be incorporated in the site investigation and pile testing programme.

### 3.3.5 Effective stress parameters

The effective stress parameters of the soil,  $c'$  and  $\phi'$ , are usually obtained from consolidated-undrained triaxial tests with pore pressure measurement or drained triaxial tests.

It is usual to ignore the effective cohesion in the calculation of the shaft resistance by the effective stress method. Chandler (1968) has shown that softening and remoulding reduces  $c'$  considerably without markedly influencing  $\phi'$ . To simulate the remoulding and softening that occur when bored piles are constructed, Chandler submerged four specimens remoulded at natural water content and wrapped with filter paper in distilled water for four days. Specimens were then reconsolidated and sheared under undrained conditions with pore pressure measurement. The effective stress parameters for the softened specimens were found to be  $c' = 8 \text{ kN/m}^2$  and  $\phi' = 21.5^\circ$ , whilst the effective stress parameters for the undisturbed specimens were  $c' = 30 \text{ kN/m}^2$  and  $\phi' = 22.5^\circ$ .

For driven piles in stiff clays, Tomlinson (1970) has shown that the effective cohesion reduced to zero from an initial value of between 20 to  $30 \text{ kN/m}^2$  with slight reduction in the effective angle of shearing resistance.

### 3.4 LIMITATIONS OF THE EFFECTIVE STRESS APPROACH

The principal limitation lies with the difficulty in measuring the effective stresses of the soil adjacent to the pile after installation. The effective stresses will vary radially and along the length of the pile. Thus selection

of the values for the design parameters become uncertain. However, these design parameters must be known if a rigorous calculation of shaft adhesion in terms of effective stress is to be made. Therefore, approximations are made on the magnitudes of the effective stresses and effective stress parameters. Hence, the accuracy of the prediction is limited by the approximations and assumptions made during the development of the effective stress method. The validity of these assumptions needs to be examined critically.

TABLE 3.1 EMPIRICAL RELATIONSHIPS FOR  $K_0$   
FOR NORMALLY CONSOLIDATED CLAYS.

NO	REFERENCES	FORMULAE FOR $K_0$	REMARKS
1	Terzaghi (1943)	$\frac{\nu}{1-\nu}$	rarely used
2	Jaky (1944)	$1-\sin\phi'$	most widely used method
3	Rowe (1957)	$\tan^2[45-\frac{1}{2}\phi_{em}]$	$\phi_{em}=1.15(\phi'-9^\circ)$
4	Brooker and Ireland (1965)	(a) $0.95-\sin\phi'$ (b) $0.40+0.007I_p$ (c) $0.68+0.001(I_p-40)$	for $I_p=0$ to 40% for $I_p=40$ to 80%
5	Alpan (1976)	$0.19+0.233 \log I_p$	

TABLE 3.2 EMPIRICAL RELATIONSHIPS FOR  $K_0$   
FOR OVERCONSOLIDATED CLAYS.

NO	REFERENCES	FORMULAE FOR $K_0$	REMARKS
1	Brooker and Ireland (1965)	Graphical form (see Fig.3.7)	most commonly used
2	Sherif and Koch (1970)	$0.70+0.10(OCR-1.2)$	based on results of 8 different clays
3	Schmertmann (1975)	$(1-\sin\phi') (OCR)^{0.42}$	
4	Wroth (1975)	$OCR \cdot K_{nc} - \frac{\nu'}{1-\nu'}(OCR-1)$	only for lightly overconsolidated clays. Values of $\nu'$ obtained from Fig. 3.8
5	Meyerhof (1976)	$(1-\sin\phi') (OCR)^{0.50}$	

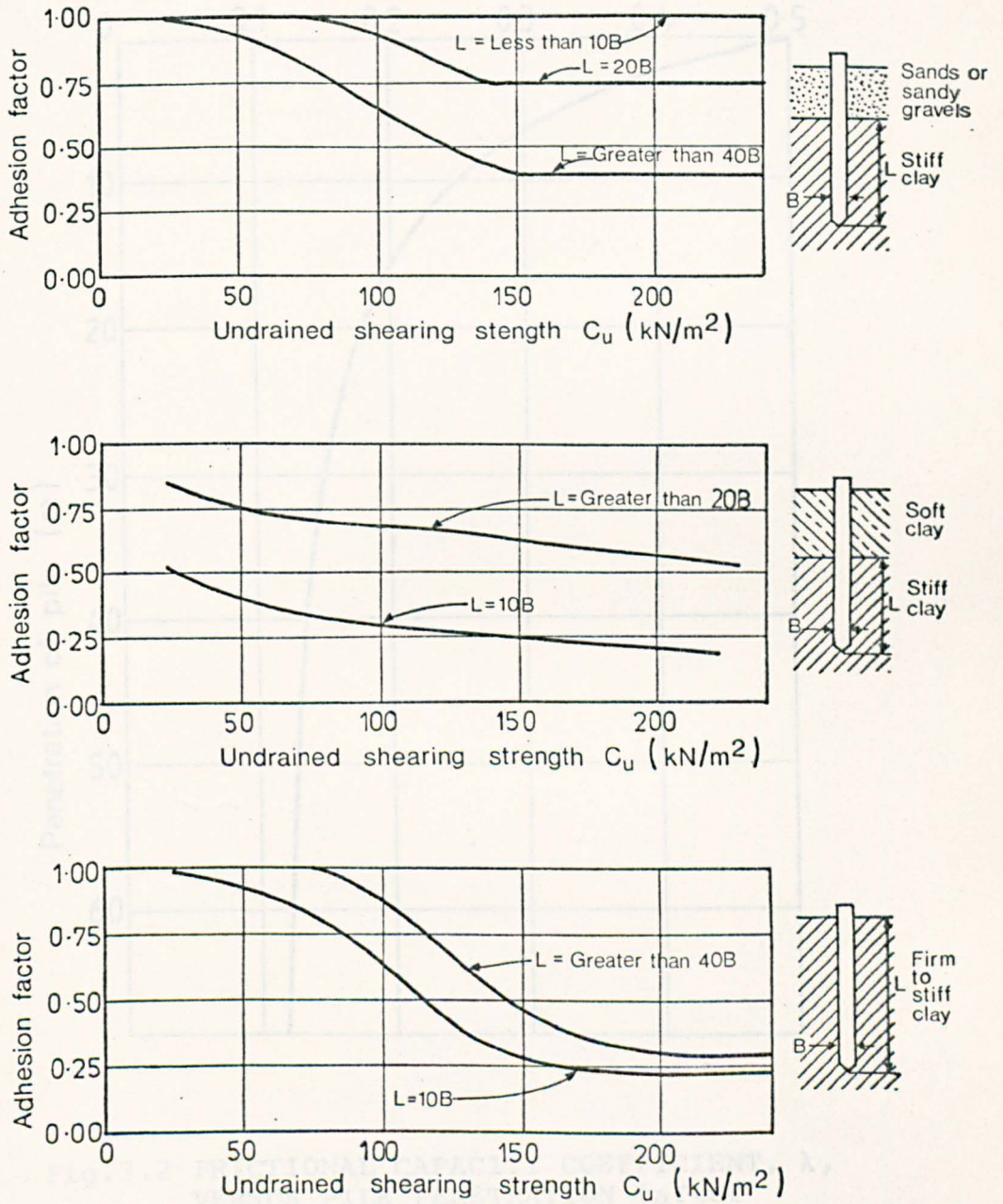


Fig. 3.1 DESIGN CURVES FOR ADHESION FACTORS FOR PILES DRIVEN INTO CLAY SOILS (after Tomlinson, 1977).

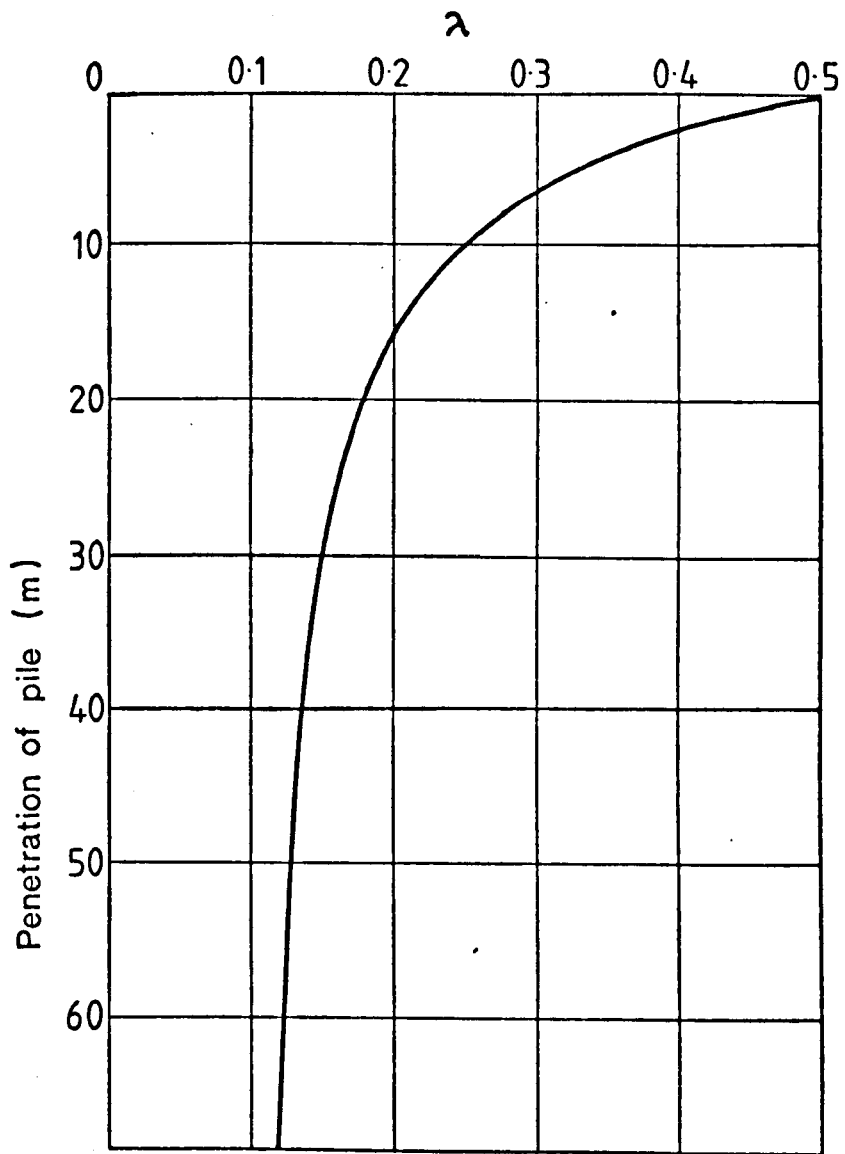
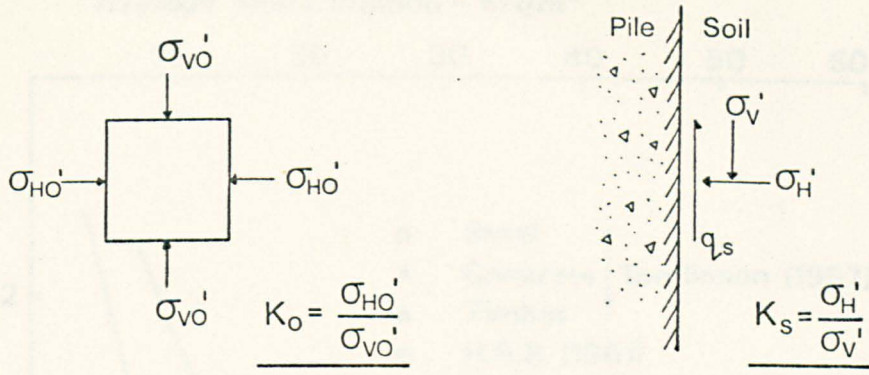


Fig.3.2 FRICTIONAL CAPACITY COEFFICIENT,  $\lambda$ ,  
 VERSUS PILE PENETRATION (after  
 Vijavergiya and Focht, 1972).



(a) 'at-rest' condition (b) pile-soil interface

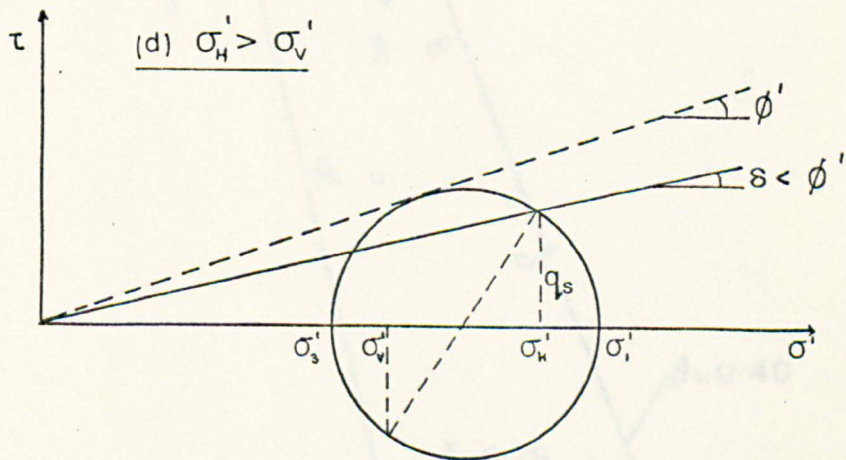
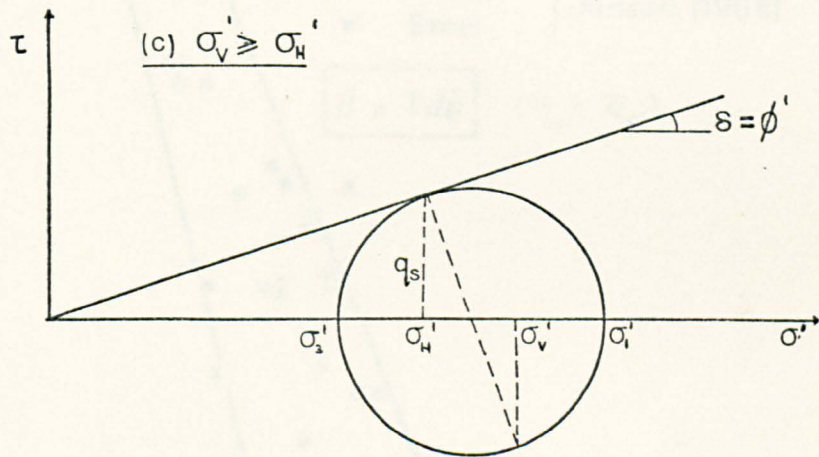


Fig. 3.3 STATE OF STRESS IN SOIL AND AT PILE-SOIL INTERFACE AT DEPTH, d.

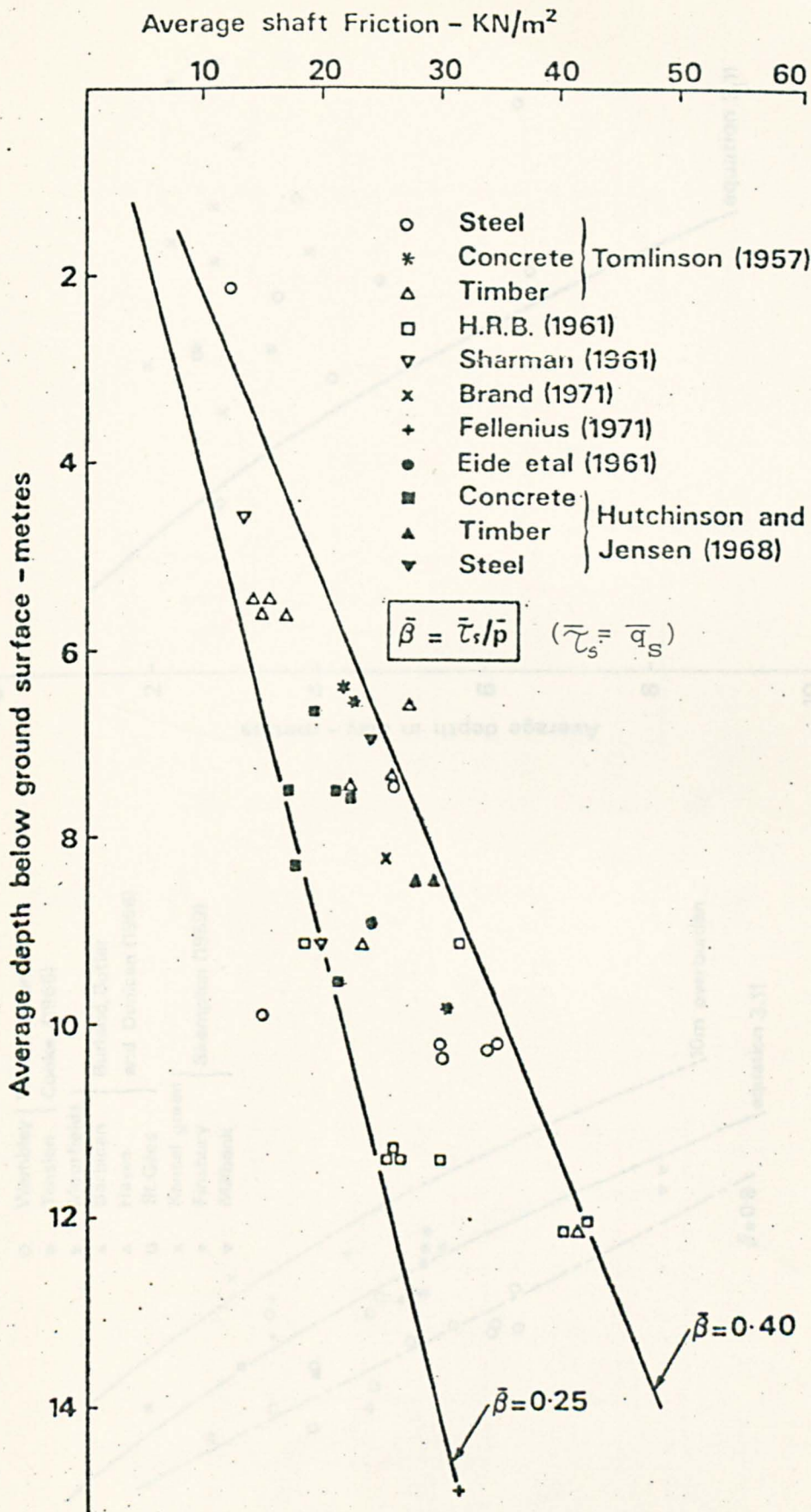


Fig. 3.4 RELATIONSHIP BETWEEN AVERAGE SHAFT FRICTION,  $\bar{q}_s$ , AND AVERAGE DEPTH FOR DRIVEN PILES IN SOFT CLAY (after Burland, 1973).

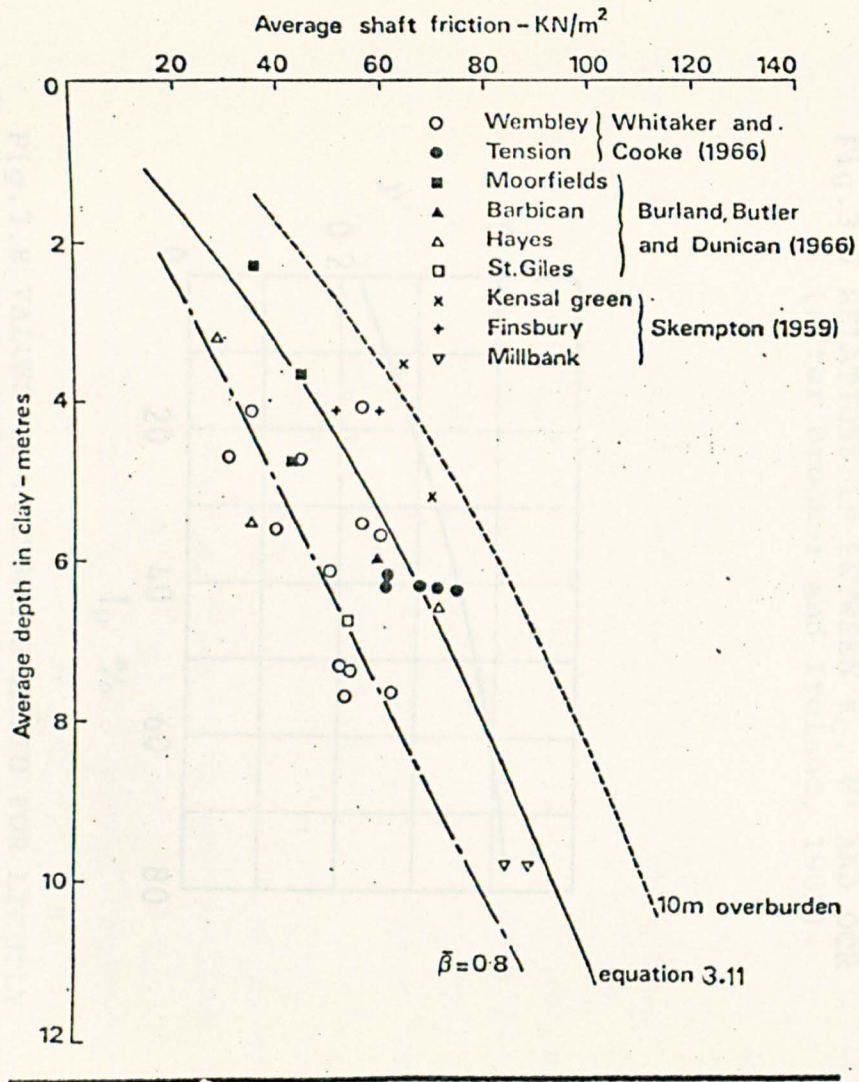


Fig. 3.5 RELATIONSHIP BETWEEN AVERAGE SHAFT FRICTION AND AVERAGE DEPTH IN CLAY FOR BORED PILES IN LONDON CLAY (after Burland, 1973).

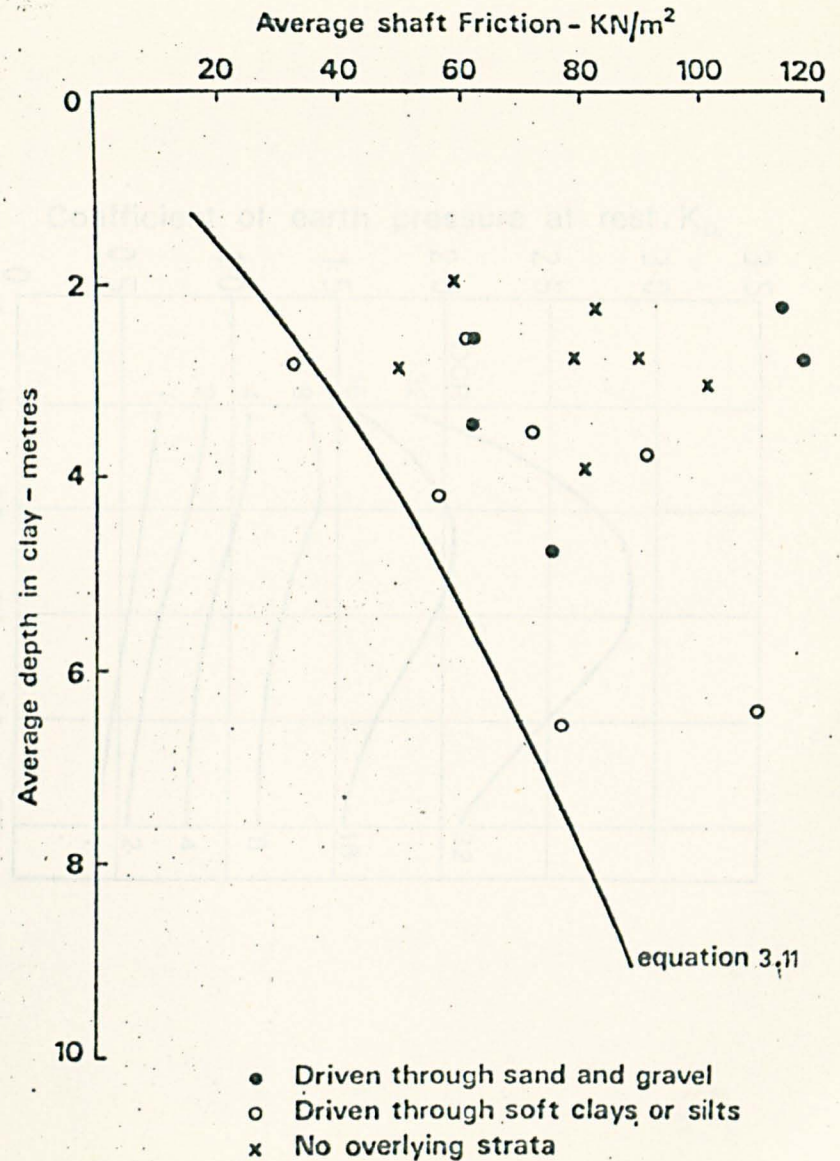


Fig. 3.6 RELATIONSHIP BETWEEN AVERAGE SHAFT FRICTION AND AVERAGE DEPTH IN CLAY FOR DRIVEN PILES IN LONDON CLAY (after Burland, 1973).

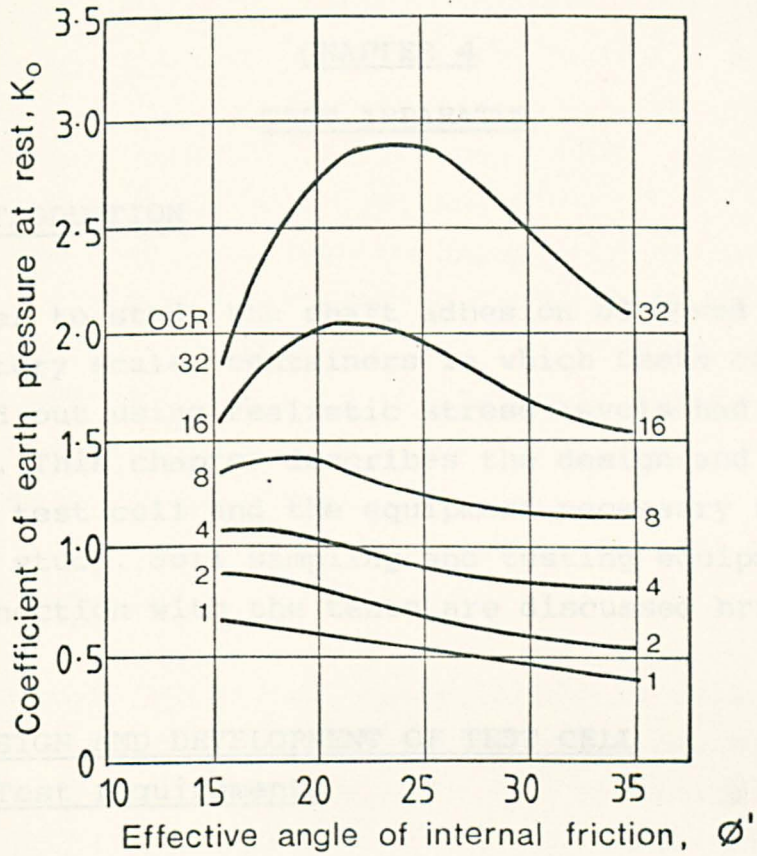


Fig.3.7 RELATIONSHIP BETWEEN  $K_0$ ,  $\phi'$  AND OCR (after Brooker and Ireland, 1965).

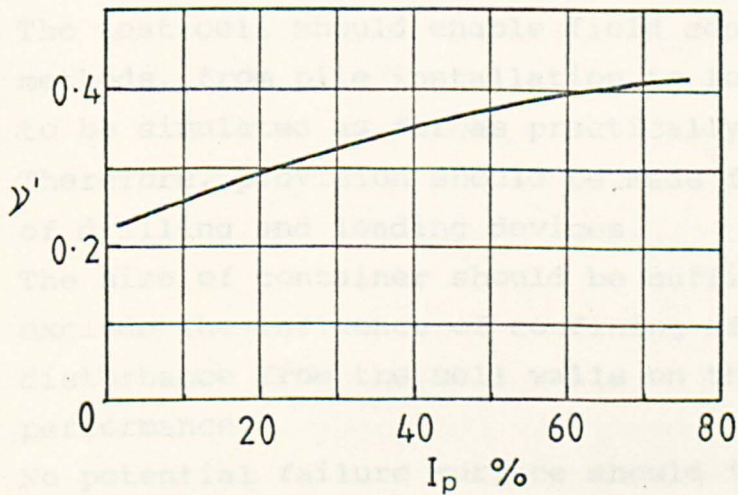


Fig.3.8 VALUES OF POISSON'S RATIO FOR LIGHTLY OVERCONSOLIDATED SOILS (after Wroth, 1975).

## CHAPTER 4

### TEST APPARATUS

#### 4.1 INTRODUCTION

In order to study the shaft adhesion of bored piles at laboratory scale, containers in which tests could be carried out using realistic stress levels had to be designed. This chapter describes the design and development of the test cell and the equipment necessary to conduct such a study. Soil sampling and testing equipment used in connection with the tests are discussed briefly.

#### 4.2 DESIGN AND DEVELOPMENT OF TEST CELL

##### 4.2.1 Test requirements

The main requirement of the study was a container in which homogeneous samples of kaolin prepared to a known stress history could be reproduced consistently and in which 'model' piles could be installed in the clay beds.

The design requirements of the container, or test cell, included the following considerations:

1. The test cell should enable field construction methods, from pile installation to load testing, to be simulated as far as practically possible. Therefore, provision should be made for attachment of drilling and loading devices.
2. The size of container should be sufficient to exclude the influence of confining effects or disturbance from the cell walls on the test performance.
3. No potential failure surface should intersect the boundary walls.
4. The size of container should be sufficiently

small to obviate the difficulty of preparing large quantities of uniform samples, i.e. consolidation time or time for excess pore water pressure to dissipate fully must be within reasonable limits.

5. The test cell must be capable of withstanding a maximum consolidation pressure of  $560 \text{ kN/m}^2$ .
6. Provision should be made for the installation of instrumentation in the soil and pile.
7. The ease of handling and operation should also be borne in mind.

The implications of some of the above design criteria are reviewed.

For a semi-infinite half space, there is no lateral or vertical strain in the 'at-rest' condition. Similarly, a stiff unyielding wall will give a condition of no lateral strain as well. However, the stress-strain response of the cell wall is not the same as that for soil. Therefore, ideally, the container size should be such that the stresses at the boundary do not affect the installation or testing of the pile.

For end-bearing, a comparatively large mass of clay is involved in the shearing process when the base of the pile is forced into the clay. In contrast, the shearing process which develops in the soil alongside the shaft of a bored pile is probably restricted to a narrow zone of soil surrounding the pile. As reported in Section 2.4.3, this zone does not usually exceed 50mm in the field tests.

Preliminary tests on a test cell of internal diameter 540mm and internal height 450mm used by Eid (1978) indicated that the procedure for the preparation of clay beds was time consuming and laborious. To enable the completion of an extensive test programme and the evaluation of results within the time available, a smaller

test cell which satisfies the design requirements was required. The test cell should be easy to handle and the time involved in the preparation should be kept to a minimum.

#### 4.2.2 Design of test cell

The design of test cell was based on BS1500:1958:Part I (and Amendments) for "Pressure vessels for general purposes" and BS4504:1969:Part I (and Amendments) for "Specifications for flanges and boltings". The basic structure of the cell is similar to that of a typical Rowe cell although several modifications were incorporated.

At the outset of design, two assumptions were made concerning stresses in the soil at the cell walls. It was assumed that as long as these stresses remained in the 'elastic' range throughout the test, their influence at any stage of the test could be considered negligible. Therefore, it was essential to reduce the friction between the soil and the cell wall so that stresses would not exceed the 'elastic' range. The method used was to apply silicone grease at the wall surfaces. It was also assumed that deformation of the cell walls was negligible and that the 'no lateral strain' condition of the soil 'at-rest' existed. The validity of these assumptions is discussed in Section 8.3.3.

The design calculations and technical details of the test cell are given in Appendix I.

#### 4.2.3 Construction details

A schematic diagram of the test cell designed is shown in Fig. 4.1. The test cell consists of three basic parts: (a) the cylindrical cell body, (b) the instrumentation

cell cover, modified to accommodate test requirements and instrumentation, and (c) the pressure application cover, used for the control of pressure supply into the test cell.

The cell body was made by cutting cylindrical tubes of carbon steel into 400mm lengths while the flange and cell covers were cut from a 20mm thick carbon steel plate. These parts were then machined and appropriate modifications made. The instrumentation cell cover incorporates a number of holes for a drilling rig and loading frame to be fixed, and instrumentation to be installed. There is also a central hole of nominal diameter 38mm to allow the 'model' pile to be formed. During consolidation, a removable porous stone 20mm thick and 38mm in diameter was placed in the central hole and covered with a cell cap as shown in Fig. 4.1. The pressure application cover has three holes for pressure supply, air relief valve and for the measurement of the consolidation pressure supplied. The details of the two types of covers are shown in Fig. 4.2 and the completed cell is shown in Fig. 4.3.

For this test cell, only single drainage in the vertical direction was used. The drainage layer consists of a thin porous plastic sandwiched between filter papers. Initially, there were plans to have double or radial drainage to reduce consolidation time. However, there were a number of problems associated with these systems of drainage. For double drainage, it would mean having an outlet through the rubber jack. This introduced the possibility of leaks if the outlet was not competently constructed. Rowe and Barden (1966) also established that the stiffness of an outlet in a flexible membrane will cause appreciable error in the actual pressure acting on the soil sample. For the case of radial drainage, preliminary tests showed that when filters were

installed at the wall of the test cell, the friction between the wall and the soil was significant enough to affect the test performance.

The pressure was applied to the clay by means of a convoluted rubber jack. Bolts and O-rings were used to seal and connect the various sections of the cell. To accommodate instrumentation and facilitate its installation, the cell was mounted on three strong legs.

Altogether, eight test cells of the type described were constructed. These cells were used to conduct tests on 25mm and 38mm diameter piles. A bigger cell with internal dimensions of 340mm diameter and 400mm height was used to conduct tests on 50mm diameter piles. This cell shown at the bottom right-hand corner of Fig. 4.4, was used by Eid (1978) and modified for the present investigation.

### 4.3 ANCILLARY EQUIPMENT

#### 4.3.1 Augering Devices

The apparatus required for forming holes in the clay bed is shown in Fig. 4.5. Three sizes of steel augers with nominal diameters of 25mm, 38mm and 50mm were used in the tests. When required, the auger 'a' was screwed into the end of a drilling rod 'b' and a handle 'c' was provided for the manual operation. A drilling frame 'd', centred over the test cell, was used to ensure verticality during the boring process and a spirit bubble was used to level the two circular plates. The threaded rods of the frame allowed rigid attachment on to the test cell.

To avoid any disturbance to the base of the borehole, the central tip of each drill was machined to level with the sides of the drills.

#### 4.3.2 Loading System

The apparatus for applying known static vertical loads is shown in Fig. 4.6. Details of the loading system are illustrated in Fig. 4.7. Known dead weights were placed on the loading platform 'a' supported directly by the pile. Loads were transmitted via a piston 'd' onto a loading platen with a central seating. This ensured that the load was applied centrally. The piston was guided by a device which was similar to the top part of a triaxial cell and was slotted into a beam system 'b' which was centred over the test cell.

The whole frame was designed to prevent any development of lateral forces during the load placement. To reduce any possible friction between the piston and the guide, silicone grease was applied prior to each load test.

#### 4.3.3 Void forming device

In the test programme, a 'soft toe' or 'void' was formed at the base of all the piles so that shaft resistance alone could be assessed. The use of 'voids' have been successfully applied in field studies by a number of authors such as Watt et al.(1969), Leach et al.(1976) and Fearenside and Cooke (1978). This method avoids the need for a load cell to be placed at the base of the pile to measure the end bearing component of the total pile capacity in order to deduce the shaft friction component.

The 'void' used in this study was formed as shown in Fig. 4.8 using two aluminium plates suspended from an incompressible nylon tube. The materials for making the 'void' are shown in Fig. 4.9. The two plates 'c' of diameter slightly less than the borehole were connected

together by a rubber membrane 'd'. Epoxy resin 'e' and surgical tape were used to fasten the membrane onto the plates and to seal the entire device. The completed device was then filled with water and a small pressure applied to check for any sign of leakage.

After insertion in the bored hole the membrane wall could be expanded to the diameter of the borehole by filling the soft toe with water and closing the clip valve 'f'. Full contact with the base and sides of the 'void' was achieved by the elasticity of the membrane, thus preventing deterioration of the clay around the sides of the 'void'.

During casting, water in the 'void' supported the hydrostatic head of the concrete and by opening the clip valve during pile loading, the water in the soft toe was allowed to escape freely for the pile to settle.

#### 4.3.4 Convoluting Rubber Jack

The consolidation or overburden pressure was applied to the soil by means of an air-water pressure system acting through a convoluted rubber membrane. This method has three advantages: (i) the relatively thin, flexible rubber membrane produced a uniform stress distribution across the sample, (ii) the soil was not subjected to vibration effects, and (iii) the convolution allowed the extension of the membrane as the soil sample decreased in volume. However, the thickness of the rubber membrane must be such that it is impermeable to pressurised water, have a low resistance to expansion and yet capable of transmitting the applied pressure directly to the soil sample.

The materials required for the manufacture of rubber jacks are shown in Fig. 4.10. The mould 'd' for the

rubber jacks was designed in conjunction with the test cells. A completed membrane 'e' with holes punched for bolts to pass through is also shown. Basically the procedure consisted of painting a number of coatings of rubber latex 'b' onto the mould and allowing each film of latex to dry in the air at room temperature. The details of the manufacturing process are given in Appendix II.

When the rubber jacks were completed, they were removed from the mould and subjected to an air pressure of between 50 to 100 kN/m<sup>2</sup> under water to check for leaks and defects. The rubber jacks were also subjected to stress relaxation by loading and unloading the membrane. Out of ten membranes manufactured and used, none developed any leaks during the entire study.

#### 4.3.5 Borehole measuring device

To allow measurement of the diameter of the borehole, a caliper was modified for the purpose as shown in Fig. 4.11. By turning the screw at 'C', the footing which was free to move about a pivot was brought into contact with the wall of the borehole. By measuring the distance 'AB' of the pre-calibrated rod with a vernier caliper, the diameter of the hole was deduced to an accuracy of  $\pm 0.1\text{mm}$ .

### 4.4 SOIL SAMPLING AND TESTING EQUIPMENT

#### 4.4.1 General

Basic properties of the soil, including liquid limit, plastic limit and the specific gravity were determined using standard laboratory equipment. Consolidation characteristics were also determined by monitoring the volume of water discharged from the clay sample with time. At the end of consolidation, moisture content and

shear strength of the soil were determined for various stress histories. In particular, a large number of determinations on moisture content and changes in undrained shear strength were carried out during the study of the effects of installation.

Preliminary tests showed that using a spatula to obtain samples for moisture content determination was unsatisfactory. This is due to the requirements of the test study in which the moisture content of the soil at a specified location and depth was required. Therefore, an alternative method which enabled samples to be obtained at the required location was developed.

The method employs a small brass tube having an internal diameter of 11mm and an area ratio of 13.5%. The working principle is similar to the triaxial sampling procedure. At one end of the tube is a cutting edge to minimise disturbance when the tube is pushed into the soil. An extruder was also fabricated to remove the samples for moisture content determination. This method allows a large number of samples to be obtained rapidly from specified locations. The sampling tube and extruder are shown in Fig. 4.12.

Undrained shear strength of the soil was determined using two methods.: (a) a laboratory vane shear apparatus and (b) standard triaxial test apparatus.

#### 4.4.2 Vane Shear Apparatus

This device is useful for the rapid determination of shear strength in soft to firm clay. The working principle of the laboratory vane shear apparatus is similar to the field version in that the shear strength is related to the angle through which the known torque is applied. This torque is very nearly equal to the moment developed by

the shear strength of clay acting over the surface of a cylinder with a radius and height equal to that of the vane.

The laboratory vane shear apparatus used in this study is available commercially under the trade name 'Pilcon'. The vane has a standard size of 19mm diameter by 28.8mm in length. To measure the shear strength of the soil, the device was pushed into the sample and rotated at about a rate of 1 revolution per minute until shear failure occurred. Since the device was precalibrated, the shear strength was then read directly from the vane tester. The influence of disturbance in evaluating the results of vane shear tests in clays has been examined by Flaate (1966).

#### 4.4.3 Triaxial test apparatus

Triaxial samples were obtained using thin-walled standard sampling tubes with internal diameter of 38mm. A guiding frame was provided to ensure that the tube remained vertical when pushed into the soil. The specimens were then sealed with wax and stored in a constant humidity room until required.

Soil specimens, 38mm diameter and 76mm high, were then extruded from the sampling tubes and tested in a conventional triaxial test apparatus. Two types of triaxial tests were carried out: (i) the unconsolidated-undrained or quick tests, and (ii) the consolidated-undrained tests with pore water pressure measurements. Details of the procedures for both types of triaxial tests can be found in Bishop and Henkel (1962).

The unconsolidated-undrained tests were carried out at a strain rate of 1.5mm/min on at least three samples for

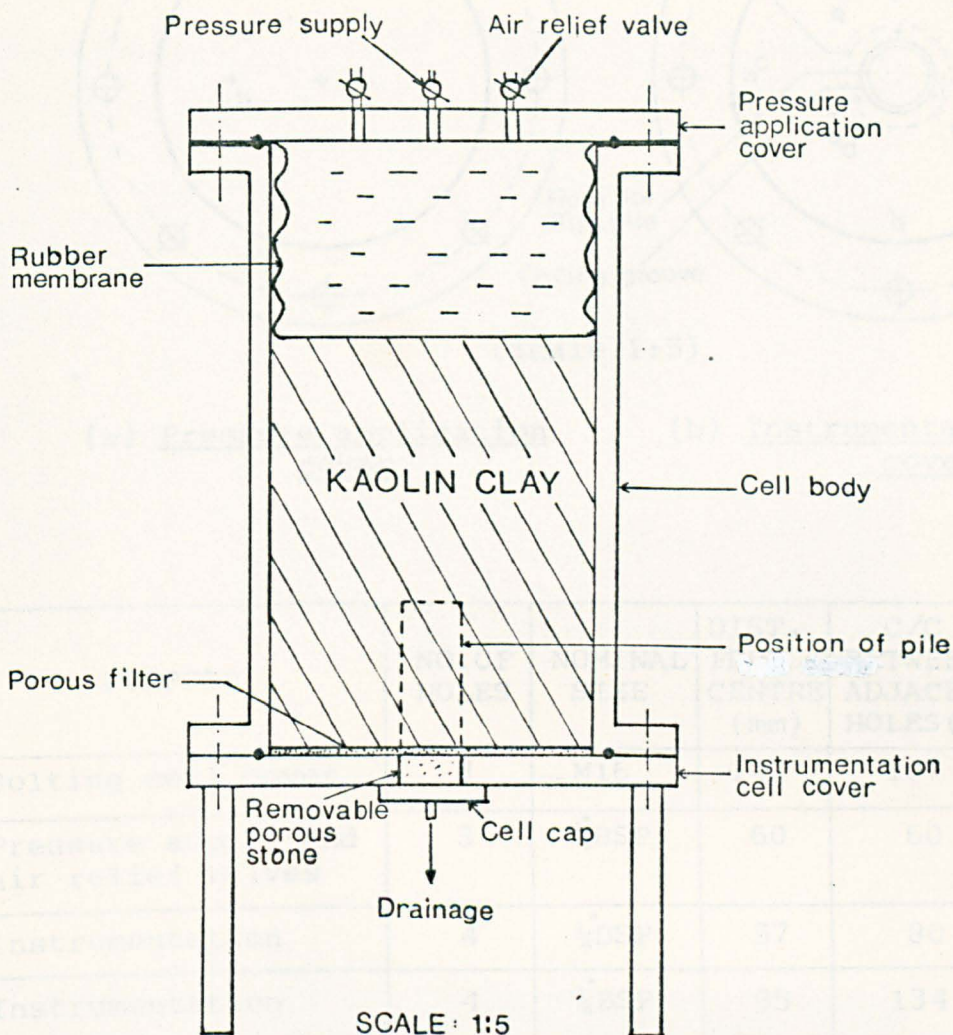
a particular stress history. The three samples were tested at different cell pressures, usually 100, 200 and 400 kN/m<sup>2</sup>, and the shear strength for each specimen was taken as one-half the peak deviator total stress as the soil was essentially saturated.

For the consolidated-undrained tests, the specimens were first consolidated under various cell pressures until the consolidation pore pressures were dissipated, and then the specimens were sheared. At least one of the specimens was consolidated under a mean stress equal to that existing before sampling, given by,

$$\sigma_m = \frac{1}{3}(1 + 2K_0)\sigma_{v0} \quad \dots \quad (4.1)$$

where  $\sigma_{v0}$  is the total vertical consolidation pressure and  $K_0$  is the coefficient of lateral pressure at rest. The value of  $K_0$  was based on direct measurements of the effective vertical and horizontal stress of the clay bed at the end of consolidation. According to Raymond et al. (1971) and Berre and Bjerrum (1973), consolidation of the sample using the mean stress approximates to the undisturbed stress condition.

To obtain satisfactory results, the rate of strain during shearing of the reconsolidated sample was kept to a low rate of 0.015mm/min. to ensure uniform distribution of the pore pressure within the sample. This strain rate was calculated from the method recommended by Bishop and Henkel (1962) for specimens with end and radial drainage.



#### SPECIFICATIONS

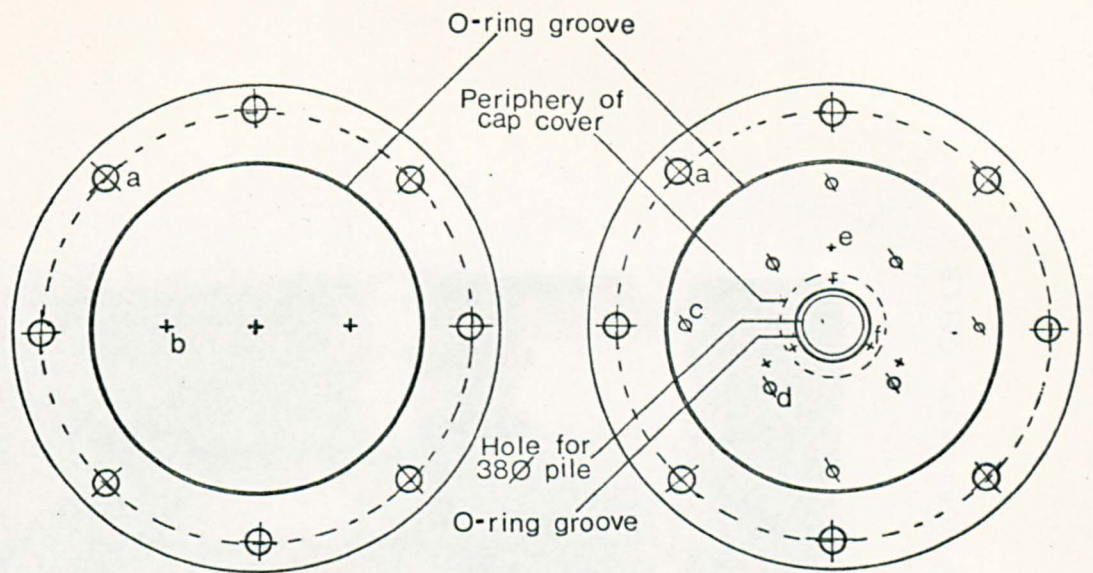
MAXIMUM PRESSURE =  $560 \text{ kN/m}^2$

INTERNAL DIAMETER = 200 mm

INTERNAL HEIGHT = 400 mm

MAX. SIZE OF PILE = 38 mm  $\varnothing$

Fig.4.1 SCHEMATIC DIAGRAM OF TEST CELL



(a) Pressure application cover

(b) Instrumentation cell cover

REF.	PURPOSE	NO. OF HOLES	NOMINAL SIZE	DIST. FROM CENTRE (mm)	C/C BETWEEN ADJACENT HOLES (mm)	REMARKS
a	Bolting cell cover	8	M16	140	107	-
b	Pressure supply and air relief valves	3	$\frac{1}{4}$ "BSP	60	60	-
c	Instrumentation	4	$\frac{1}{4}$ "BSP	57	80	-
d	Instrumentation	4	$\frac{1}{4}$ "BSP	95	134	-
e	Drilling frame	3	M8	52	90	Blind holes
f	Bolting cap cover	3	M8	30	52	Blind holes

Note: Precision of location important for Ref. a, e and f.

Fig. 4.2 DETAILS OF CELL COVERS

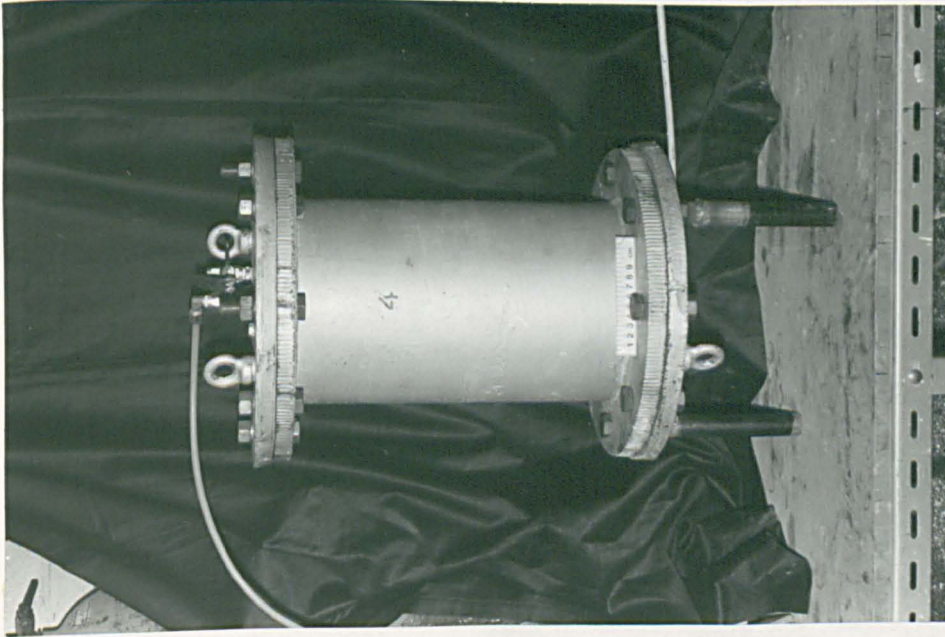


Fig. 4-3 TYPICAL TEST CELL

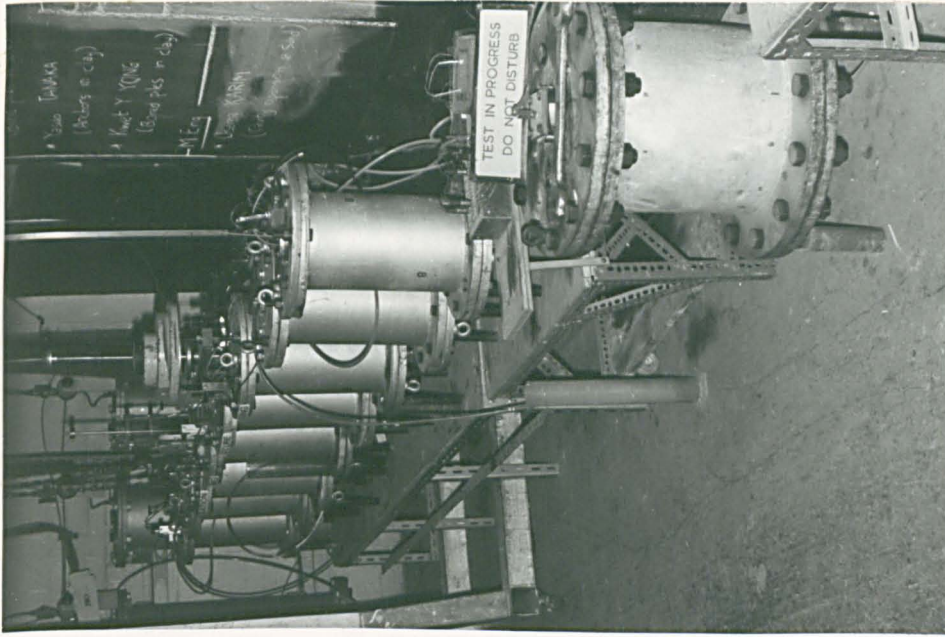


Fig. 4-4 ARRANGEMENT OF TEST CELLS

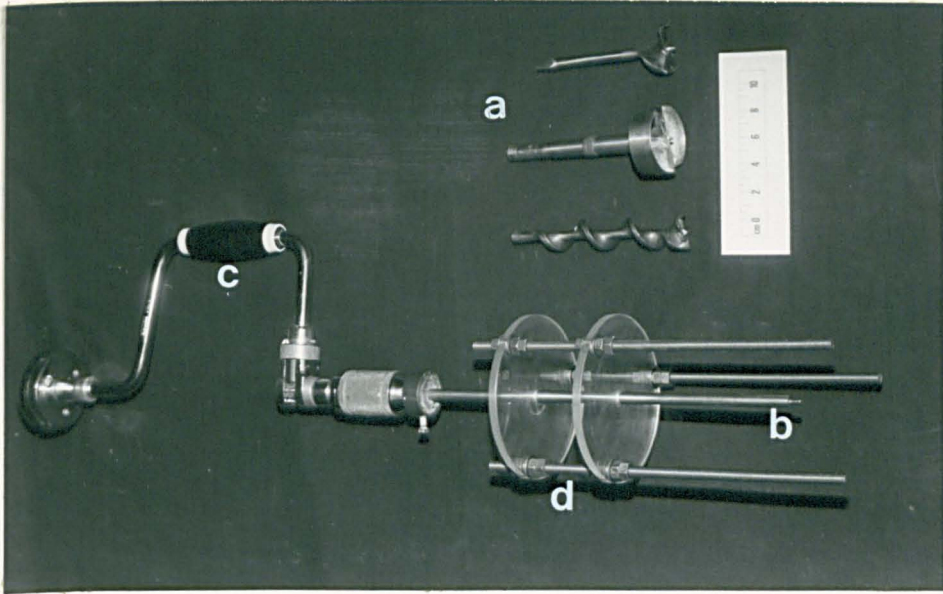


Fig. 4-5 AUGERING DEVICES

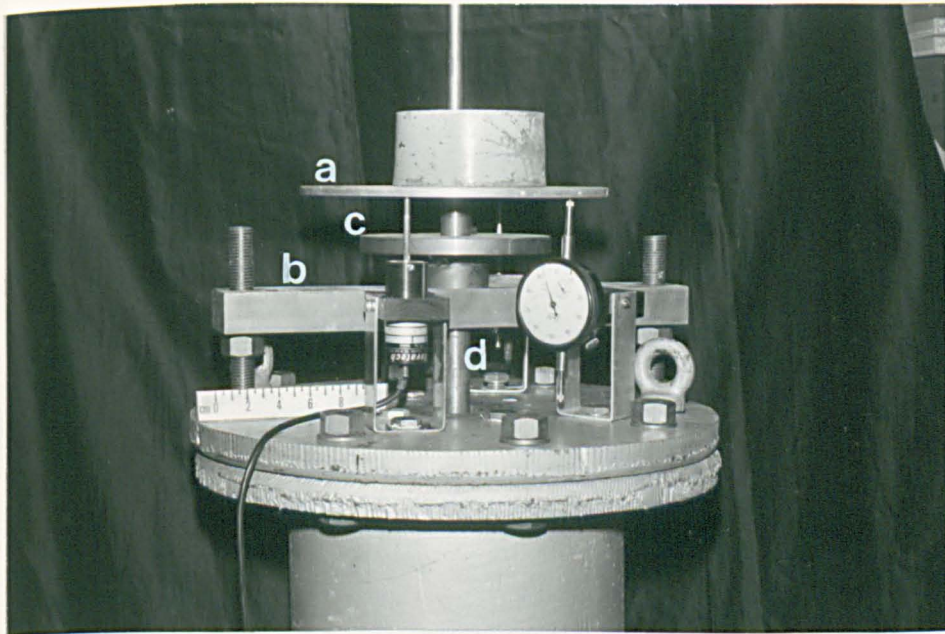


Fig. 4-6 LOADING SYSTEM

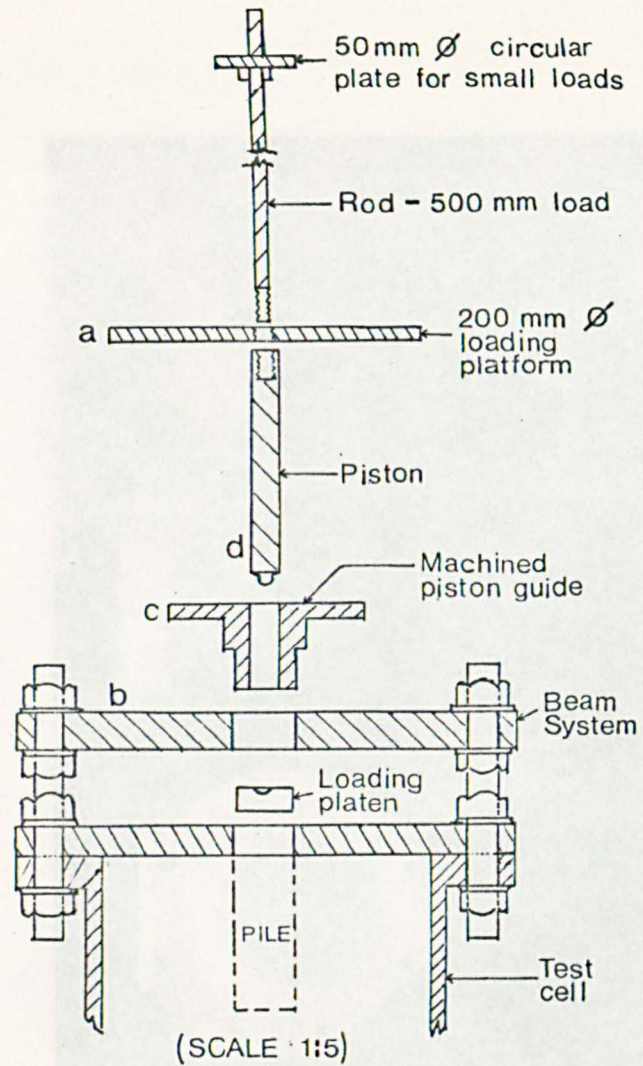


Fig.4.7 DETAILS OF LOADING ARRANGEMENT

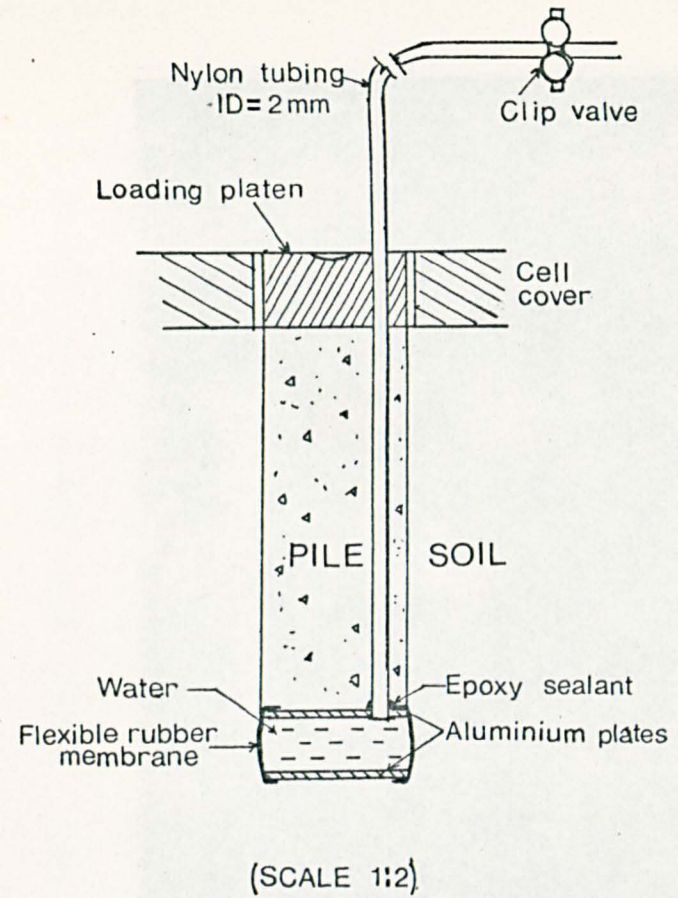


Fig.4.8 VOID-FORMING DEVICE

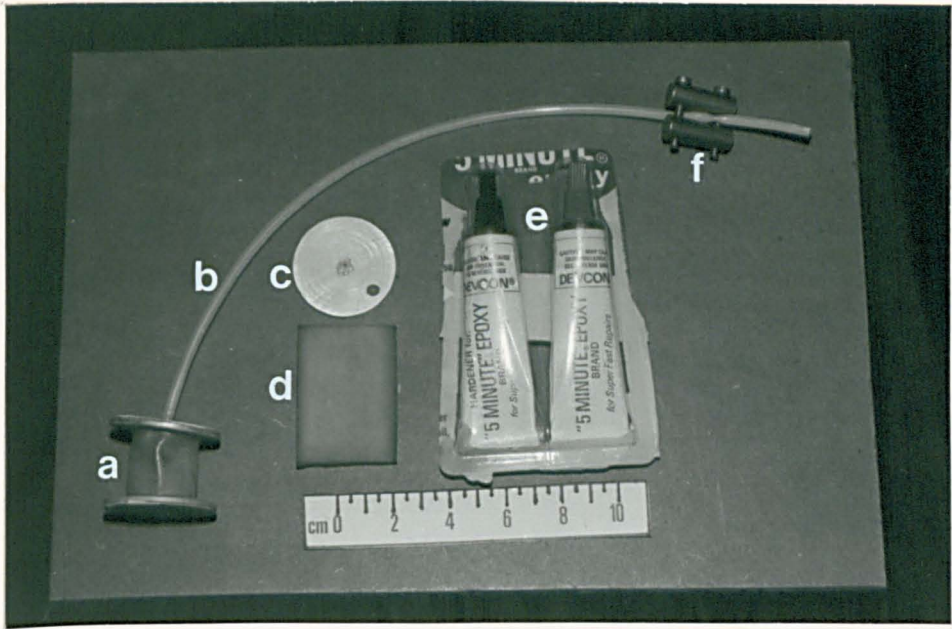


Fig. 4.9 MATERIALS FOR MAKING 'VOID'

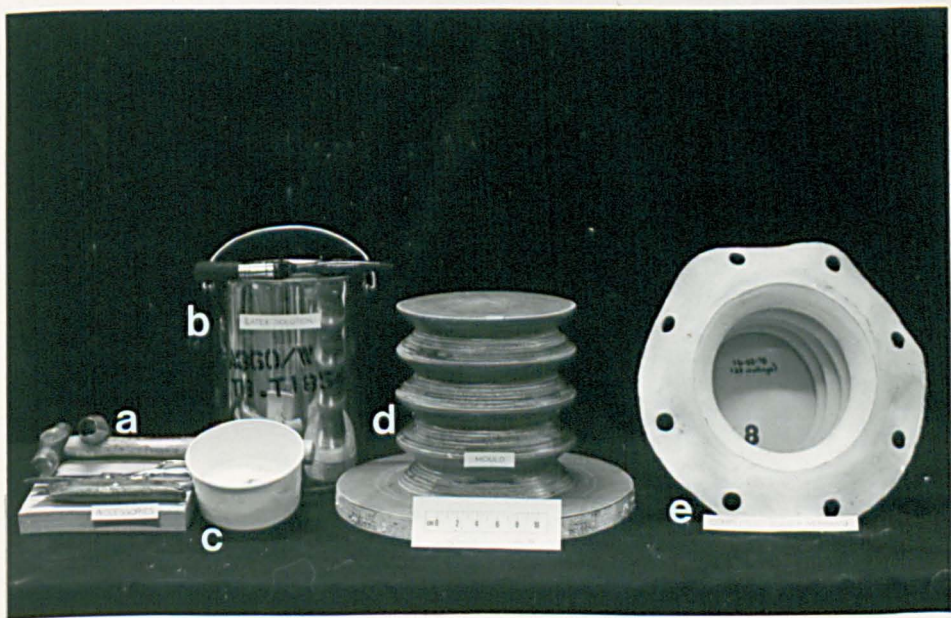


Fig. 4.10 EQUIPMENT FOR MANUFACTURE OF RUBBER JACKS

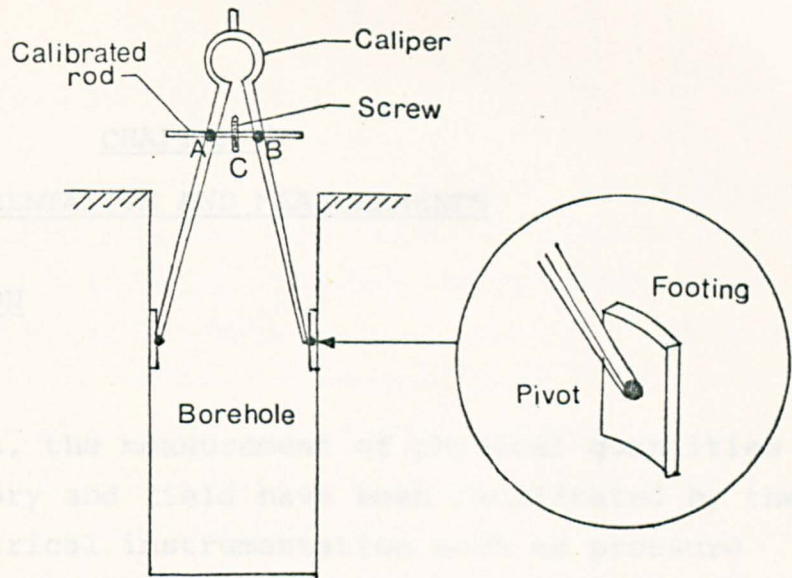
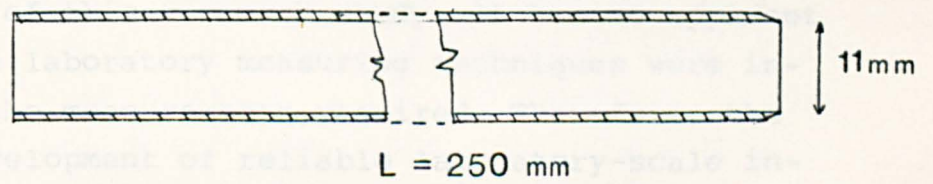
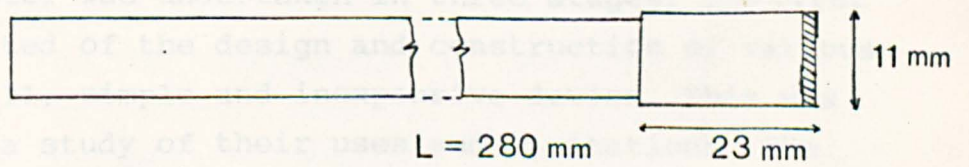


Fig.4.11 BOREHOLE MEASURING DEVICE



(a) SAMPLING TUBE



(b) EXTRUDER

Fig.4.12 MOISTURE CONTENT SAMPLING EQUIPMENT (not to scale)

## CHAPTER 5

### INSTRUMENTATION AND MEASUREMENTS

#### 5.1 INTRODUCTION

##### 5.1.1 General

In recent years, the measurement of physical quantities in the laboratory and field have been facilitated by the advent of electrical instrumentation such as pressure and displacement transducers and electronic techniques for data acquisition. Although instrumentation can provide useful information in understanding soil-structure interaction and stresses in the soil mass, the measurements obtained have always been plagued with uncertainty attached to their veracity.

At the outset of this research study, it became apparent that available laboratory measuring techniques were inadequate for the measurements required. Therefore, the design and development of reliable laboratory-scale instrumentation formed an important part of this investigation. Of primary importance was the instrumentation to measure stresses in the soil.

The design and development of instrumentation described in this chapter was undertaken in three stages. The first stage consisted of the design and construction of various types of small, simple and inexpensive device. This was followed by a study of their uses and limitations. The third stage involved the application of the most appropriate instrumentation for the research study.

### 5.1.2 Fundamentals of Instrumentation

An important consideration in the design of instrumentation is the ability of the instrument to measure the required quantity reliably, without its presence significantly influencing the behaviour of the soil. Hanna (1973), Arman et al.(1975) and Burland (1977) have summarised the essential features of instrumentation. The measuring devices should be: (a) simple in principle and operation, (b) easy to install with minimum disturbance, (c) sensitive and reliable, (d) stable over the period of measurement, (e) convenient to calibrate, and (f) inexpensive.

However, it should be noted that it is not possible for measuring devices to have all these features and that most instruments have drawbacks and limitations. In most cases, the design of instrumentation is essentially a compromise between all the requirements of an ideal cell. As Hanna (1973) has stressed "...in the research for the best possible measurement, the importance of accuracy must not obscure the importance of applicability."

### 5.2 MEASUREMENTS REQUIRED FOR TEST STUDY

In a typical test, measurements were required during (a) slurry consolidation, (b) the 'at-rest' condition of the soil, (c) the construction of the pile, (d) the loading test. In general, five different quantities were monitored to document the complete stress history of the soil sample: total vertical stress, total horizontal stress, pore water pressure, deformation and time.

The types of measurements and the method of instrumentation used are shown in Table 5.1. The total vertical and

horizontal stress in the soil, and the total horizontal stress at the pile interface were measured using strain gauged, diaphragm-type pressure cells. The pore water pressures in the soil and at the pile interface were measured using probes connected to pressure transducers. Tell tale devices were used to monitor any information in the soil during the loading test. Details of these measuring devices are discussed in the following sections.

One of the major causes of inaccurate measurements is inadequate compaction of the soil in the vicinity of the measuring instrument, as well as the disturbance inherent with installation. To overcome this problem in the laboratory, all soil instruments were installed prior to consolidation of the clay bed. The procedure for installation is described in the next chapter.

The approximate location of the measuring devices is shown in Fig. 5.1. It can be seen that most of the instrumentation is placed at about the level of the mid-height of the pile. It should be appreciated that not all the devices shown were used in any one test. In view of the size of the clay bed, care was taken not to install too many devices which could influence the behaviour of the soil.

### 5.3 DESIGN AND DEVELOPMENT OF PRESSURE CELLS

#### 5.3.1 Introduction

The idea of using pressure cells to measure stresses in the soil mass appears simple, but the actual application involves numerous difficulties and uncertainties. To obtain reliable results, it is necessary that details of design, development, calibration, installation and recording be carefully controlled.

Two types of pressure cells were developed using strain-gauged diaphragm principles. One type was used to measure the vertical or horizontal total earth pressure, depending on its orientation with soil mass, and the other to measure the horizontal total pressure at the soil-pile interface. These cells are designated 'EP' and 'IF' pressure cells respectively.

### 5.3.2 Review of pertinent literature

Early studies by the Waterways Experimental Station (1944) on flat cells embedded in soil provided useful guidelines. Many excellent studies of the soil pressure cells followed, such as the work by Redshaw (1954), Kallstenius and Bergau (1956), Trollope and Lee (1961), Dunn and Billam (1966), Tory and Sparrow (1967), Krizek et al. (1974) and Tavenas (1975). Interfacial devices for measuring normal and shear stresses simultaneously have also been developed by Arthur and Roscoe (1961), Agarwal and Venkatesan (1965) and Thorley et al. (1970). All these reported studies have advanced the understanding of the behaviour of instrumentation embedded in the soil.

Installation of resistance strain gauges along the shaft and at the bottom of piles have now become normal features of many pile-testing programmes. However, apart from the work carried out by Reese et al. (1968) and Reese, Touma and O'Neill (1976), there appears to be no published work on the design and development of a device to measure stress changes at the soil-pile interface of a bored cast-in-situ pile. The paucity of studies is related to the difficulty in installing the device in the shaft of a bored pile. The periphery of the pile-soil interface is not well defined for a bored pile in the field and depends on various factors such as soil conditions and hydrostatic head of

fresh concrete. However, in the laboratory, this uncertainty can be controlled

### 5.3.3 Factors influencing the performance of pressure cells

The presence of a pressure cell can appreciably alter the stress distribution of the soil in the vicinity of the device and as a result the cell may not register the true pressure. The phenomenon of 'cell action' which is generally defined as the ratio of pressure cell output and the true stress in the soil, has been investigated by Taylor (1947), Peattie and Sparrow (1954), Selig (1964) and Tory and Sparrow (1967) and others. Mackey (1966), Dunn and Billam (1966), and Calder and Krawczyk (1975) have shown that a cell action factor can be obtained by (i) calibrating the device directly under hydrostatic pressure in a fluid medium, assumed as the 'true stress', and (ii) re-calibrating the device by applying pressure on it via a soil medium, the soil being similar to that used in the tests.

To perform satisfactorily, the pressure cell must be insensitive to stresses other than those normal to the active diaphragm. Krizek et al. (1974), Peaker (1965) and Øien (1958) found that the normal stress acting on a diaphragm cell is almost independent of other components of stress in the region. These results were based on finite element analysis and experimental studies. Nevertheless, the problem of cross-sensitivity is of particular importance when measuring normal stresses in the presence of large shear stresses.

Calder and Krawczyk (1975) studied the effects of repeated loading on cell performance and found that the magnitude of hysteresis decreased on repeated loading. This is attributed to the increase in density and stiffness of the soil adjacent to the cell face as a result of repeated deflection.

The reloading cycles are therefore of value in assessing the accuracy of pressure cell measurements in situations where large fluctuations in soil pressure are expected.

#### 5.3.4 Design considerations

Based on various studies quoted in previous sections, design guidelines were established for static measurements. These guidelines provided the framework governing the design of EP and IF pressure cells and are presented in Table 5.2. Of these guidelines, the main criteria is that the ratio of the maximum deflection of the diaphragm and the diameter of the diaphragm must be less than or equal to 1:2000 for the EP devices and 1:1000 for the IF devices. The former requirement is for pressure cells embedded in the soil while the latter is for pressure cells installed at a rigid boundary (i.e. pile shaft). Once this main criteria is satisfied, the rest of the requirements can be satisfied by proper selection of cell and diaphragm dimensions.

The size of the cell is limited by the necessity of providing a means of measuring the deflection of the cell diaphragm. The diaphragm movement is in turn restricted by a design requirement. Unless movement is kept within the limits specified in Table 5.2, severe stress concentrations can develop in the diaphragm material and continual redistribution of these stresses can lead to gross errors in the recorded soil pressures. Therefore, cell-soil interaction is a complex function of cell geometry and cell-soil stiffness.

In view of the large number of pressure cells required, simplicity and reliability, without sacrificing accuracy, were principal considerations in the design. These features also kept the cost of the devices relatively low.

### 5.3.5 Design of pressure cells

The calculations for the design of EP and IF pressure cells are given in Appendices III and IV. Based on these calculations a relationship between the diaphragm thickness and normal pressure acting on the diaphragm was derived and is shown in Fig. 5.2. A trial and error process made it possible to select the dimensions of diaphragm and cell which would best fit the criteria listed in the design guidelines.

For the EP pressure cells, instead of choosing a constant diaphragm thickness to cover all the different pressure ranges, it was decided to vary the thickness to suit the particular range of pressure likely to be encountered in the test. Hence, sensitivity of the cell would be consistent with the stress level to be measured.

In the case of IF pressure cells, the diaphragm thickness was limited by the machining requirements. The minimum thickness to which the diaphragm could be accurately machined was 0.5mm, and this thickness was used for all the IF pressure cells. The length of the casing depended on the diameter of the 'model' pile to be installed and the diameter/projection ratio.

Details of the dimensions for EP and IF pressure cells are given in Fig. 5.3. It should be mentioned that the design of EP cells for measuring the soil pressure was straight-forward because of the amount of published material on this topic. However, this was not true for the IF pressure cells where research studies are very limited. Therefore, four different types of IF cells were developed and their performance under test conditions were examined. The advantages and disadvantages of these cells are summarized in Table 5.3. The type of IF cell used in

the research study described in this chapter was selected mainly on the basis of simplicity in fabrication and its response under test conditions.

### 5.3.6 Construction details

The cross-section and plan of the EP and IF cells are shown in Fig. 5.3 while Fig. 5.4 shows the completed cells. Each unit consists essentially of a sensing diaphragm protected by a rigid cover or casing. Pressure is transmitted through the diaphragm mounted with a strain rosette on the underside. The thickness of the diaphragm depends on the range of pressure to be measured.

Generally, the procedure for fabricating the pressure cells consisted of cementing a strain rosette onto the diaphragm, soldering electrical lead wire connections and enclosing the functional parts with a rigid cover. The materials used are shown in Fig. 5.5.

The diaphragms were machined from a high grade aluminium alloy bar (BS1470/HS-30TF) to the required thickness. Aluminium was chosen as the diaphragm material because of its high modulus of elasticity and its resistance to corrosion during long periods of contact with moist soil. The casings of the IF cells were also machined from this aluminium bar. The hard plastic covers of the EP cells were fabricated from a sheet of perspex. The advantage of using perspex was its transparency, so that any defects such as damage to solder and lead wire connections or any moisture penetration into the cell could be observed.

Mounting the strain rosette at the centre of diaphragm had the advantage of enhancing the sensitivity. The bonding of gauges is discussed in the next section. Since the

device employed electrical circuits, it was susceptible to damage if moisture was present. Therefore, the strain rosette, terminals and exposed leads were sealed with a 'Scotch' electrical sealer, while the cell was made watertight by adhering the diaphragm to the cover with epoxy and finally encasing the periphery of the cell with surgical tape.

The completed cells were then checked electrically for continuity and insulation resistance using a pocket digital voltmeter (DVM). Stability checks were then carried out over a period of 3 to 4 weeks, this being the typical duration of a short term test. Before calibration, the cells were subjected to repeated loading and unloading cycles at half the design pressure to ensure that remaining 'locked-up' stresses in the element and bonding were relieved. Finally, a label was attached to each cell bearing the cell reference number.

### 5.3.7 Strain Gauge Technique

The method of bonding strain gauges is not new and the procedure applied in this study was based on the experience of a number of authors such as Coutts and Coombs (1969) and Procter (1977).

The procedure for bonding the strain gauges onto the diaphragm is shown in Fig. 5.6 and numbers in the figure refer to the steps to be followed:

1. The surface of the diaphragm was cleaned thoroughly with acetone after the position of the strain gauge had been marked on it.
2. A tiny drop of 'CN' adhesive was then applied onto the back of the gauge held by a pair of clean forceps and the gauge was immediately mounted on the diaphragm. A gentle thumb pressure was applied via

- a silicone paper to ensure proper bonding.
3. Similarly, adhesive was applied on two tabs (terminals) and mounted next to the gauge.
  4. The gauge leads and connecting leads were then soldered at the tabs and the whole electrical circuit was sprayed with a waterproof-sealing compound. The continuity of the electrical circuit was checked before encasing the strain gauge.

The manufacturer's specifications for the strain rosettes used are given in Table 5.4. Each rosette has two arms arranged at right angles. Two active arms were connected to two dummy arms to form a four-arm bridge circuit with temperature compensation. The pressure cells contained the two active arms whilst the dummy arms were mounted on a compensating strip of the same material. The dummy gauges, shown in Fig. 5.7, were placed in an aluminium tube, sealed and embedded in a small container of clay to give a compatible environment to the active gauges. The principles of strain gauging and the bridge circuit used are given in Appendix V. The completed bridge circuits were then tested for electrical continuity, insulation resistance and zero drift as described in the previous section.

Limitations of resistance strain gauge measurements are now well appreciated especially the effects of temperature and the long term stability. Both affect the performance of the strain gauge device and must be considered in the evaluation of the recorded results. Peekel (1972) considered errors occurring in strain gauge measurements and suggested solutions to minimise their influence. Pople (1978) drew attention to the factors affecting the long term stability of strain measurements using metal foil gauges, while Chalmers (1972) provided some thoughts on making reliable strain gauge measurements. The performance of the pressure cells under long term condition and variations of temperature will be discussed later in Chapter 8.

### 5.3.8 Calibration

From the calibration point of view, it is essential to estimate as closely as possible the divergence of any cell pressure measurement from the in-situ pressure; the latter is defined as the pressure that would exist if the cell was absent. Carder and Krawczyk (1975) found that a suitable correction can be made for errors in cell registration provided laboratory calibrations of pressure cells have been carried out in conditions which closely simulate situations in which the instruments are to be employed.

To correct for soil-cell interaction (discussed in Section 5.3.3), pressure cells were calibrated in water and in clay under known pressures. The cell action factor was then derived,

$$C_A = \frac{\text{pressure cell output}}{\text{true stress}}$$

where true stress is represented by values obtained from hydrostatic calibration in which the cell-soil interaction is absent.

For the calibration of pressure cells, a standard 150mm Rowe cell, shown in Fig. 5.8, was modified to permit continuity of electrical wiring. For the EP and IF pressure cells developed, the Rowe cell satisfies the suggested criterion that the diameter of the testing cell must be at least 6 times the diameter of the device [Triandafilidis (1974)]. Calibration output in microvolts was monitored on both the digital voltmeter and data logger. Input voltage of 3 volts was from a Kingshill Constant Voltage Power Supply and the voltage selected was a compromise between the need to have a high supply voltage to increase the sensitivity and the need to avoid over-heating the strain gauges and test specimens.

The following precautions were taken during the calibration test:

1. The Rowe cell was smeared with silicone grease to reduce any possible friction between the soil and the wall of the container.
2. Prior to calibration, the strain gauges were allowed to 'warm-up' by a constant supply of voltage.
3. During the test, the cell diaphragm was placed face upwards and exposed to direct soil pressure.
4. Cells were first subjected to load and unload cycles to stress-relax the gauge and diaphragm before commencement of calibration.
5. Each pressure cell was calibrated over at least two cycles of loading and unloading.
6. A uniform technique of placing devices in the clay was essential to obtain consistent results.

For the hydrostatic calibration, the cell was immersed in water and subjected to external hydrostatic pressure via a rubber jack. For calibration in clay, the state of stress acting on the devices under actual test conditions was simulated. The cell was first embedded in clay with an initial moisture content equal to the liquid limit. A small pressure of  $50 \text{ kN/m}^2$  was then applied and the clay allowed to consolidate around the device. After 24 hours, the drainage valve was closed and calibration proper commenced. The cover of soil was usually between 20mm and 30mm. Since the pressure on top of the clay specimen was hydrostatic and since the layer of the soil was thin, the vertical stress distribution in the soil was assumed to be equal to the applied pressure.

Cell response was measured for different pressure increments up to the design pressure. Typical results obtained for EP10 and IF38 pressure cells are shown in Fig. 5.9. The

response was linear within limits of experimental error and a slight hysteresis on unloading was observed for the calibration curves in clay. From these curves, the sensitivities of the pressure cells and the cell action factors were derived.

Reproducibility of the calibration results was checked by repeating calibration on some of the pressure cells. Individual calibration of these cells were found to be within  $5 \text{ kN/m}^2$  of the mean determined from three tests.

#### 5.3.9 Summary

Typical characteristics of the pressure cells developed are summarised in Table 5.5. The maximum skin friction calculated at the diaphragm centre was based on the equation in Appendix IV. The cell action factor was obtained from the calibration constants in clay and in water. The test performance of these cells will be reviewed in Section 8.4.

It should be noted that the values shown in the table are only typical for each type of pressure cell and that it is wrong to assume that cells with the same diaphragm thickness will have the same calibration constant. The cell response depends not only on the diaphragm thickness but also on the strain gauging technique. Therefore, each cell fabricated was calibrated individually.

### 5.4 PORE WATER PRESSURE PIEZOMETERS

#### 5.4.1 Introduction

A knowledge of pore pressure existing in the soil is essential for a proper determination of effective stresses as well as for the understanding of soil behaviour.

Electrical resistance transducers with their low flexibility and small volume change are largely replacing older instruments such as null indicators used in conjunction with manometers and Bourdon pressure gauges. In the laboratory, pore water pressure measurements can be measured by two methods: with miniature transducers or with probes connected to an external recording device by a fluid-filled pressure transfer system.

#### 5.4.2 Factors affecting pore water pressure measurement

A number of factors influence the response of the measuring devices, such as flexibility of the system, presence of air or gas bubbles, clogging of the probe, leakage through joints or instruments.

The operation of a piezometer is simple in principle but it has one serious drawback: a flow of water from soil into the measuring device is required to give a reading. This is important with a low permeability soil such as clay. An appreciable time is required for flow to achieve equilibrium, and this time lag depends on the soil properties and the flexibility of the piezometer system. The stiffer the system, the shorter is the response time. The effects of time lag and suggestions to reduce system flexibility can be found in studies by Hvorslev (1951), Penman (1960), Whitman et al. (1961), Gibson (1963) and Hughes and Townsend (1966).

The time lag is also influenced by the presence of air bubbles. Minute air bubbles can become inadvertently trapped in the piezometer system. Also, air initially entrapped in the pores of the soil, or dissolved in the pore water, may be released into the system. If these bubbles are not removed, they contribute to a reduction in overall stiffness of the system and can lead to errors

in the measured pore pressures. Lee and Black (1972) conducted tests to determine the time taken to dissolve air bubbles in a drainage line and found that for soft soils such as normally consolidated or compacted clays at low consolidation pressures, a few small air bubbles in the system may not have a serious effect. However, for stiff soils, the presence of a few small air bubbles may reduce pore pressure response to unacceptable values. If this is the case, and if air bubbles cannot be flushed out, then it is necessary to dissolve bubbles under an elevated back pressure.

Baracos (1976) examined the clogging of filter discs under an electron microscope and found that partial blockage reduces the permeability. This will inevitably influence the response of the piezometer system.

When piezometers are driven into the soil, sufficient time must be allowed for the excess pore water pressure, due to driving to be dissipated. When they have to be installed in boreholes, leakage may occur along the boreholes. Leakage may also occur in the joints of the piezometer system. Any such leakage will result in erroneous readings.

The effect of temperature is a major consideration especially in long term testing. Since the sample and pore pressure apparatus form a sealed system, any increase in temperature will lead to a corresponding increase in the recorded pressure. Rowe and Barden (1966) reported that variations in room temperature by  $1^{\circ}\text{C}$  can cause differential pressure changes in a closed pore pressure system of the order of  $3 \text{ kN/m}^2$ . Therefore, for accurate measurements, either the temperature fluctuation is kept to a minimum or else correction factors are applied to recorded readings. In cold climates, the system is filled with alcohol rather than water to prevent freezing.

### 5.4.3 Development of piezometers

Hanna (1973) listed the primary requirements of a piezometer as accuracy, minimum disturbance to the soil, good response to changes in water pressure, durable and stable over long periods of time. Because of the size of soil sample, it was essential to have a probe as small as possible but sensitive enough to pick up the pore pressure changes accurately. As with the pressure cells, simplicity in design was an important criteria in view of the number of measuring devices required.

An essential part of development of the piezometers was the estimation of the time lag. A method of calculating time lag based on the work of Hvorslev (1951) and Penman (1960) is given in Appendix VI. From this theoretical relationship, it can be derived that time lag can be minimised by reducing the volume of flow required for pressure equalisation and by making the intake area as large as possible.

Most of the errors associated with time lag can be eliminated by constructing the sensing device into the probe so that the whole unit is embedded in the soil. Such miniature piezometer systems, which are available commercially, consist of a silicon semiconductor element mounted on a very thin sensitive diaphragm and encased in a stainless steel case. One of these miniature pressure transducers is shown in Fig. 5.10(a) and is about three times more sensitive in response than the 'Bell and Howell' pressure transducer shown in Fig. 5.11. The negligible time lag makes it ideal for measuring rapid pore water pressure changes. However, as with most instruments, it has its disadvantages as well. It is expensive, delicate and easily susceptible to damage if handled roughly. Moreover, its gauge drift cannot be cancelled out and therefore long term stability becomes a

problem. For this study, the miniature piezometer was used only as a control device to check the response time of the piezometer systems developed.

After studying various potential methods of pore water pressure measurement, an external measuring device with a piezometer system was chosen because it was better suited for use with the available instrumentation system. After a number of trials to develop a reliable system, three types of probes were selected. These probes are shown in Fig. 5.10 (b), (c) and (d) and designated drive-in probe, soil probe and interface probe respectively. The materials for fabricating the probes are shown in Fig. 5.11.

The drive-in probe was the easiest to fabricate. Rigid nylon tubes were cut to the required length and at one end, brass fittings were connected. At the other end, filter paper was inserted into the tube followed by porous plastic trimmed to the internal dimension of the tube. However, the drive-in probes were used only when the soil probes embedded in the soil failed to respond to pressure changes at some stage of the test.

For the soil and interface probes, brass sections were first fabricated. Nylon tubes were cut to 300mm length, and at one end of each tube a flange was made by inserting a cone-shaped pre-heated rod into the tube. This procedure enabled the tube to 'seat' firmly at the base of the brass section. Epoxy was then applied to seal the joint. For the soil probe, the brass casing was then inserted with filter paper, well graded sand and a thin porous filter was used to seal the brass section. In the case of the interface probe, a porous stone was cut and placed snugly in the brass connector.

The details of the probes and the piezometer arrangement is shown in Figs. 5.12 and 5.13 respectively. Basically, the system consists of a piezometer (probe, tubing and brass fittings), a de-airing block (Type A) with three openings, a valve for de-airing and a pressure transducer. These parts were designed for easy assembly, high permeability across the probe and minimum overall elasticity in the tubing. According to Beard (1974), overall elasticity of piezometer tubing can be minimised by choosing a semi-rigid plastic tubing with an outer to inner diameter ratio of 2. The nylon tubing used has an outer and inner diameter of 4mm and 2mm respectively. The transparency of the nylon tubing ensured that the de-airing operations were carried out completely with a continuous visual check being made.

#### 5.4.4 De-airing of piezometer system

For accurate pore water pressure measurements, it is necessary to achieve complete saturation of the measuring system through the test, since the presence of air bubbles or voids will increase the elasticity of the system resulting in a longer response time for equalisation.

Before installation into the test apparatus, the piezometer systems were first assembled under water. The active part of the pressure transducer was de-aired by injecting water into the cavity by means of a hypodermic needle and small syringe. The transducer was then connected to the de-airing block under water and the whole system was flushed with freshly de-aired water from a burette, through the de-airing block and out of the probe. The system was then kept saturated for about 24 hours prior to its use. If the presence of air bubbles was suspected in the system, a small pressure was applied to allow the air to go into the solution. When the piezometer was installed in the test apparatus, the water level in the burette was kept slightly above the level

of the probe to keep the latter saturated. When the slurry poured into the test cell had reached the level of the probe, the de-airing valve was closed and readings were recorded immediately.

The second type of de-airing block, Type B, (shown in Fig. 5.13) was supplied together with some of the pressure transducers. This was particularly useful when the pressure transducer was connected directly to the test apparatus to measure pore pressure at the boundary. By removing the air bleed valve at the side of the block, de-aired water could be flushed through the transducer without the need to disconnect it from the cell.

#### 5.4.5 Calibration

Twenty-five 'Bell and Howell' type pressure transducers capable of recording up to  $700 \text{ kN/m}^2$  were used for the experiments. Calibration checks on the linearity and repeatability of these transducers were carried out using a standard triaxial test cell.

Three transducers were first de-aired by the method described in the previous section. They were then connected under de-aired water to the triaxial cell. The screws of the cell were tightened and de-aired water was used to top-up the triaxial cell. Pressure was then applied to the triaxial cell in increments and the change in pressure was immediately recorded by the transducers connected to the data logger. A power supply provided excitation voltage of 10 volts to the transducers throughout the calibration test. The whole procedure was then repeated for the rest of the transducers.

The results concurred with the values quoted by the manufacturer. Linearity of the response was good with hysteresis

of less than  $\pm 0.3\%$  of the full range output. Sensitivities of the transducers ranged between 6.0 to 6.5  $\mu\text{V}/\text{V}/\text{kN}/\text{m}^2$  and a typical calibration curve is shown in Fig. 5.14.

## 5.5 SETTLEMENT MEASUREMENTS

### 5.5.1 Introduction

Two types of settlement measurements were required from the tests: soil settlement and pile settlement. Soil settlement was obtained by a mechanical 'tell-tale' device installed in the soil and a footing at the surface to record any relative movement during a pile loading test. These movements were registered by springless linear variable displacement transducers (LVDT) mounted on metal brackets.

For pile settlement, two spring-type displacement transducers were placed at opposite sides of the loading frame to measure movements relative to the test cell cover. This arrangement has been shown in Figs. 4.6 and 4.7 in Section 4.3.2. A dial gauge indicator was also installed for visual checking. Both these devices were capable of recording the settlement to the nearest 0.01mm.

### 5.5.2 Tell-Tale Arrangement

Tell-tale devices are widely used by various investigations in the field and laboratory for measuring axial deformation of a pile or movement in soil. Details of the assembly used in this study are shown in Fig. 5.15. The outer sleeve provided protection for the inner unstrained rod which transmitted movement of footing to the LVDT. Tell-tales of various lengths were used for the experiments. A small rubber padding at the footing prevented soil from entering the space between the rod and tube. As a further protection,

as well as reducing friction, the space was filled with silicon grease. Finally, for attachment to the test cell, a  $\frac{1}{4}$ BSP plug was incorporated into the arrangement.

### 5.5.3 Calibration of displacement transducers (LVDT)

The spring and springless transducers used were manufactured by Novatech and have a maximum travel of 25mm. Typical responses of these transducers are shown in Fig. 5.16.

The transducers were calibrated by an apparatus shown in Fig. 5.17(a). By turning the screw on the left of the apparatus, a corresponding movement was induced in the dial gauge and displacement transducer. This movement was then recorded by a digital voltmeter and data logger.

## 5.6 DATA ACQUISITION

The instrumentation process covers not only the design and selection of measuring devices but also the method of acquiring the data output effectively. The use of electrical transducers in this study enabled automatic recordings of the soil stresses, pore pressures and settlement. This was achieved by connecting the output leads of the measuring devices to a scanner unit of a data logging system. At pre-selected times, the devices were scanned, the readings registered by a digital voltmeter and recorded on a teletype printer or on punched tape. This arrangement was ideal for overnight readings. However, during a test, it was often more convenient to record the readings by the manual mode with a visual display on the digital voltmeter. The rapid readout permitted a near simultaneous recordings of stresses, pore pressure and displacement.

After installation in the test cell, the instrument leads were connected to a terminal box (see Fig. 5.18) adjacent to the test cell. Each type of measuring device was independently supplied by an excitation voltage from a Kingshill Constant Voltage Power Supply (Fig. 5.19 a). A portable Solartron A200 digital voltmeter (Fig. 5.19 b) was used to check the supply voltage to each terminal box. Six boxes were fabricated and wired to meet the requirements of the different types of instrumentation. Four boxes contained 20 channels each, while the other two boxes had 10 channels each. Altogether, 10 channels were allocated for each of the nine test cells with the remainder being used as spare channels.

The instrumentation terminal boxes were all wired to a junction control box (Fig. 5.19 c) which was connected to the data logger by way of screened 25-way cables. It is essential to 'screen' the cables and circuiting because d.c. electrical signals are prone to pick up electrical noises.

The data logger used is a Solartron Compact 33 machine capable of monitoring up to 1000 analogue channels. Basically the data logger shown in Fig. 5.20 consists of an analogue scanner 'a' comprising 100 channels to convert analogue to digital units; a control unit 'b' for the selection of various modes of operation; a Solartron A200 digital voltmeter 'c' with automatic voltage range selection and a sensitivity of 1 microvolt; and the output unit 'd' with teletype and tape printout facilities.

To facilitate the computation of the huge amount of raw data and the plotting of results, a number of computer programmes were written. Calibration constants of all measuring devices used, together with their reference number

were stored in the computer and recalled when required. Readings were fed in either by tape or more often by cards. When graphs were required, the University Computer Centre's 'GHOST' graph plotting technique was employed. A flow diagram of a typical programme to calculate test results is shown in Fig. 5.21.

A summary of the procedure for data acquisition is shown in Fig. 5.22.

TABLE 5.1 MEASUREMENTS AND INSTRUMENTATION

TYPE	LOCATION	METHOD OF MEASUREMENT
Load	Pile Top	Dead weights
Stresses	Soil Mass	Earth Pressure cells (Strain Gauge - diaphragm)
	Soil-pile Interface	Interface Pressure cells (Strain Gauge - diaphragm)
Pore Water Pressure	Soil Mass	Miniature piezometers } ceramic probes } Pressure Transducers
	Soil-pile Interface	
Settlement	Soil Settlement	'Tell-tale' rods and displacement transducers
	Pile Settlement	Displacement transducers and dial gauges
Miscellaneous 1. Temperature 2. Consolidation pressure	Ambient	Thermometer
	Test Cell	Pressure gauge and Pressure transducers

TABLE 5.2 DESIGN GUIDELINES FOR PRESSURE CELLS

NO	TYPE	DESIGN REQUIREMENTS	PURPOSE
1a	EP	$\frac{\delta}{d} \leq \frac{1}{2000}$	To eliminate the possibility of arching over the diaphragm and to reduce cell-soil interaction.
b	IF	$\frac{\delta}{d} \leq \frac{1}{1000}$	
2	EP	$\frac{D}{T} \geq 5$	To reduce the effect of differential stiffness of the cell and soil, and to prevent build-up of stress on the instrument
3	IF	$D/P > 30$	To enable stress to be registered with minimum disturbance
4	EP/IF	$A_a / A_d < 0.50$	To eliminate registration of edge stresses
5	EP/IF	$f_c / f_a < 1$	Structural consideration ( $f_a = 59 \times 10^3 \text{ kN/m}^2$ )
6	EP/IF	$d > (50 \times \text{max. particle size})$	For results to be representative
7	EP/IF	Flexibility factor, $F = \frac{E_s d^3}{E_c t^3}$	Should be as small as possible for consistent results, i.e. cell should be as rigid as possible

**LEGEND :**

- $\delta$  maximum deflection
- $d, t$  diaphragm diameter and thickness
- $D, T$  cell diameter and thickness
- $P$  projection of IF cell
- $A_a, A_d$  Active and overall diaphragm area
- $f_c, f_a$  Maximum and allowable skin stress in diaphragm
- $E_s, E_c$  Modulus of soil and cell

TABLE 5.3 TYPES OF IF PRESSURE CELLS DEVELOPED

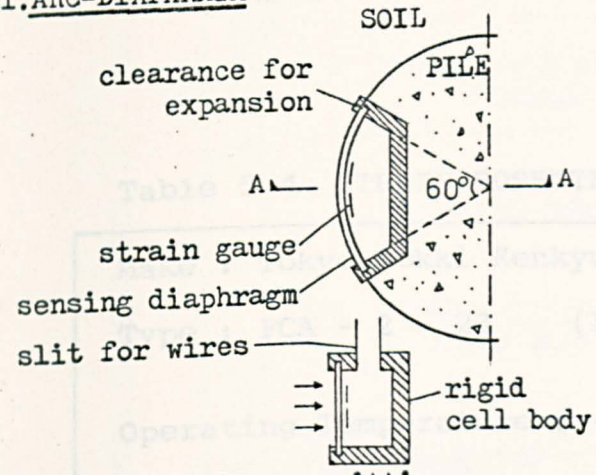
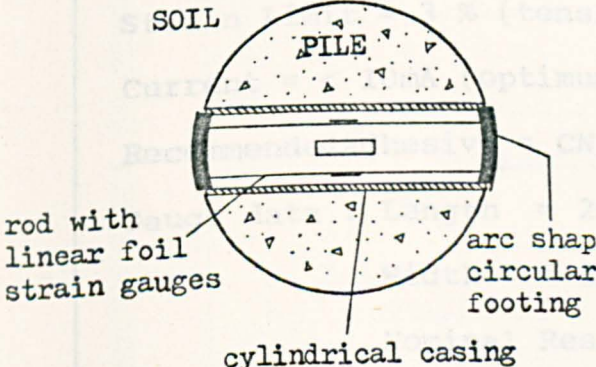
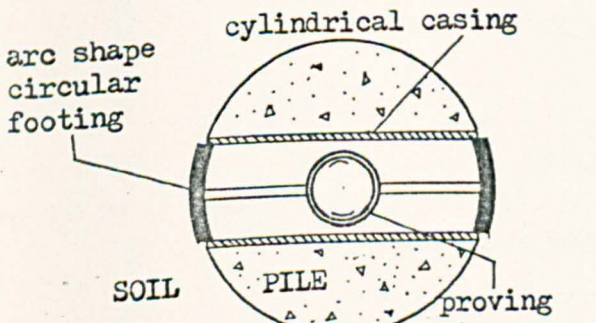
TYPES OF IF CELL	MAIN ADVANTAGES	DISADVANTAGES
<p><u>1. ARC-DIAPHRAGM</u></p>  <p>Scale: Full size.</p>	<ul style="list-style-type: none"> <li>(a) 'flush' with pile; no projection into soil, thereby minimising soil disturbance</li> <li>(b) useful for high stresses in soil (<math>p &gt; 500 \text{ kN/m}^2</math>)</li> </ul>	<ul style="list-style-type: none"> <li>(a) difficult to fabricate</li> <li>(b) high initial stress on strain gauge may damage gauge bonding</li> <li>(c) not sensitive to low stress</li> <li>(d) difficult to waterproof</li> </ul>
<p><u>2. STRAIN ROD TYPE</u></p>  <p>Scale: Full size.</p>	<ul style="list-style-type: none"> <li>(a) Linear response</li> <li>(b) Footing 'flush' with pile</li> <li>(c) Easy to fabricate and install strain gauges</li> <li>(d) Thin membrane over footing ensures reasonable waterproofing</li> </ul>	<ul style="list-style-type: none"> <li>(a) Not very sensitive to low stress</li> </ul>
<p><u>3. PROVING RING TYPE</u></p>  <p>Scale: Full size</p>	<ul style="list-style-type: none"> <li>(a) Very sensitive even at low stress</li> <li>(b) Linear response</li> <li>(c) footing 'flush' with pile</li> <li>(d) Reasonable waterproofing</li> </ul>	<ul style="list-style-type: none"> <li>(a) difficult to fabricate</li> <li>(b) Because of size of proving ring, installation of strain gauges is a very skilled operation</li> </ul>
<p><u>CIRCULAR DIAPHRAGM TYPE</u> (discussed in the text and selected for the research study)</p>	<ul style="list-style-type: none"> <li>(a) Reasonable sensitivity; linear response</li> <li>(b) Easy to fabricate</li> <li>(c) Good waterproofing</li> </ul>	<ul style="list-style-type: none"> <li>(a) diaphragm thickness has to be varied so that sensitivity is consistent with stress level</li> </ul>

Table 5.4 STRAIN ROSETTES (MANUFACTURER'S SPECIFICATIONS)

Make : Tokyo Sokki Kenkyujo Co. Ltd

Type : FCA - 2 - 23 (Foil Series)

Operating Temperature :  $-20^{\circ}\text{C}$  to  $80^{\circ}\text{C}$

Accuracy of temperature compensation  $\approx \pm 1.8 \times 10^{-6}/^{\circ}\text{C}$

Coefficient of expansion,  $\alpha = 23 \times 10^{-6}/^{\circ}\text{C}$

Strain Limit = 3 % (tension) ; 2 % (compression)

Current = < 10mA (optimum) ; 25mA (maximum)

Recommended adhesive = CN or P2

Gauge data : Length = 2mm, Base = 7mm dia.

Width = 1mm, Gauge Factor = 2.07

Nominal Resistance =  $120 \pm 0.5 \Omega$

TABLE 5.5 TYPICAL CHARACTERISTICS OF PRESSURE CELLS DEVELOPED

PRESSURE CELL DESIGNATION	MAXIMUM PRESSURE RANGE (KN/M <sup>2</sup> )	OVERALL CELL			DIAPHRAGM			CHARACTERISTIC RATIOS					CALIBRATION				
		DIAMETER, D (mm)	THICKNESS, T (mm)	LENGTH OF CASING, L (mm)	DIAMETER, d (mm)	THICKNESS, t (mm)	MAX. SKIN FRICTION F <sub>0</sub> (x 10 <sup>3</sup> KN/M <sup>2</sup> )	σ <sub>1/2</sub> (nominal)	φ	DIAMETER PROJECTION RATIO	ACTIVE DIAPHRAGM AREA	OVERALL DIAPHRAGM AREA	MAX. SKIN FRICTION ALLOWABLE STRESS (t/σ <sub>1/2</sub> )	NOMINAL SENSITIVITY μV / V / (KN/M <sup>2</sup> )	CLAY	HYSTERESIS (% OF MAX. OUTPUT)	NOMINAL SENSITIVITY μV / V / (KN/M <sup>2</sup> )
EP6	100	25	5	-	20	0.6	20.8	2000	5	-	0.16	0.35	3.24	0.6	3.05	0.94	
EP7	140	25	5	-	20	0.7	21.4	2000	5	-	0.16	0.36	2.40	0.5	2.21	0.92	
EP9	280	25	5	-	20	0.9	25.9	2000	5	-	0.16	0.44	1.54	0.9	1.34	0.87	
EP10	420	25	5	-	20	1.0	31.5	2000	5	-	0.16	0.53	1.28	1.5	1.09	0.85	
EP11	560	25	5	-	20	1.1	34.7	2000	5	-	0.16	0.59	1.14	1.1	0.91	0.80	
IF25	450	14	-	26	12	0.5	48.6	1000	-	56	0.44	0.82	1.67	1.9	1.50	0.90	
IF38	450	14	-	38.5	12	0.5	48.6	1000	-	31	0.44	0.82	1.68	1.2	1.50	0.89	
IF50	450	14	-	51.5	12	0.5	48.6	1000	-	40	0.44	0.82	1.72	1.0	1.50	0.87	

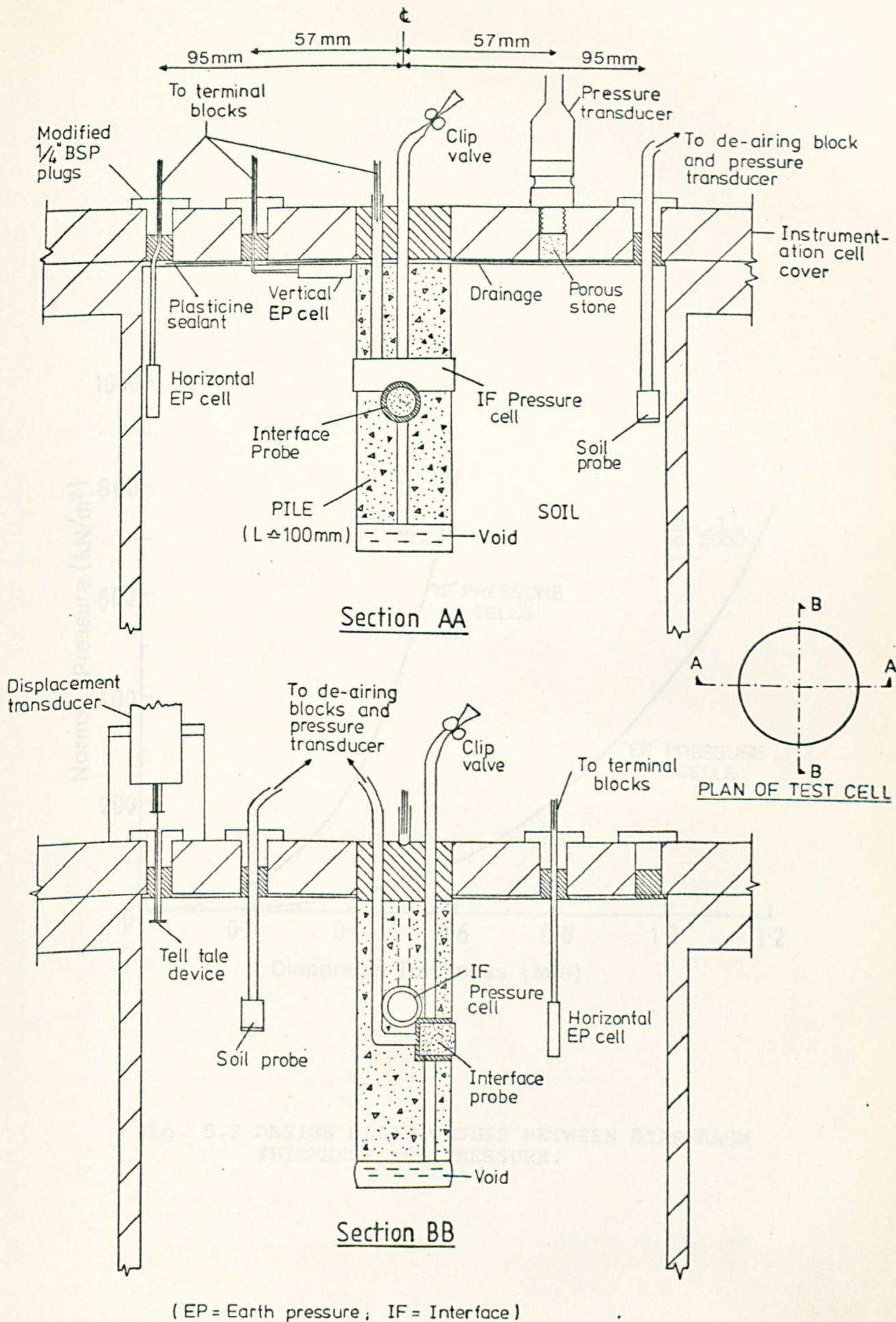


Fig. 5.1 APPROXIMATE LOCATION OF INSTRUMENTATION USED

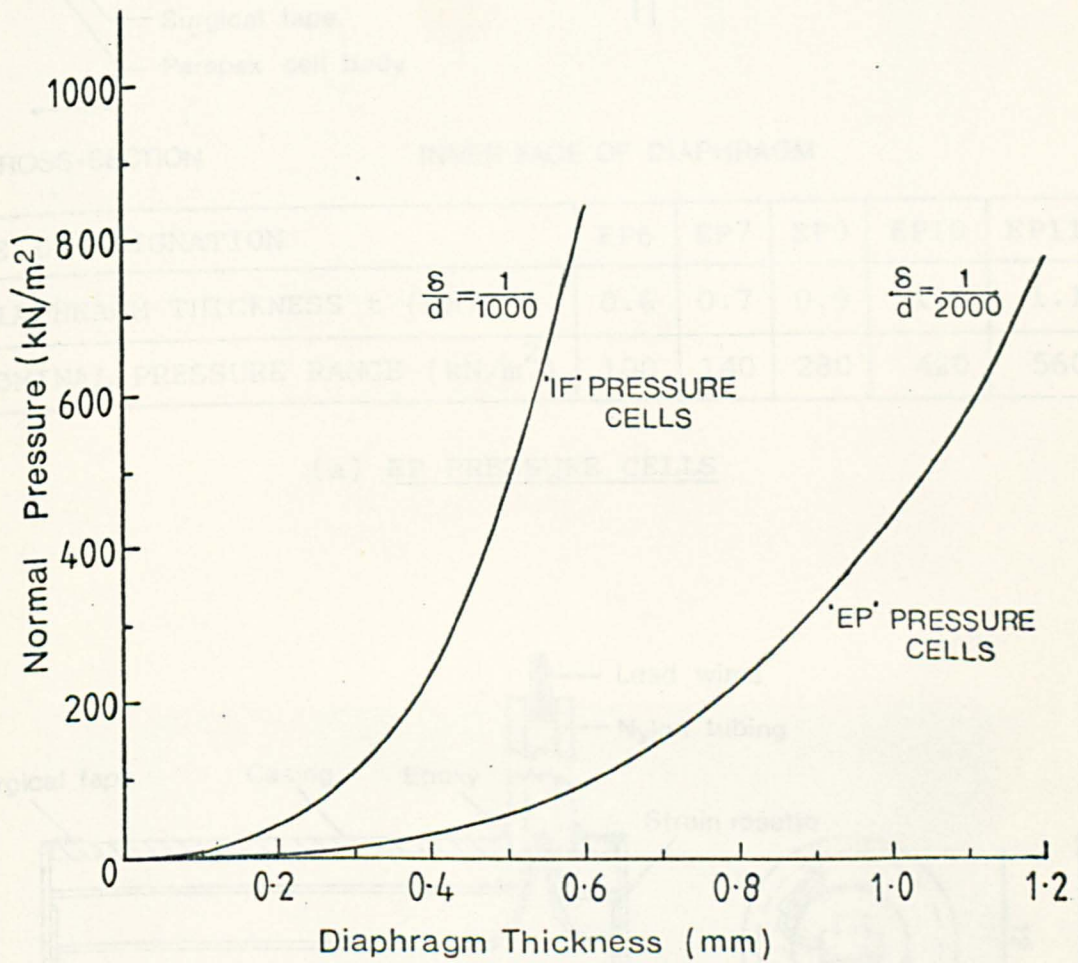
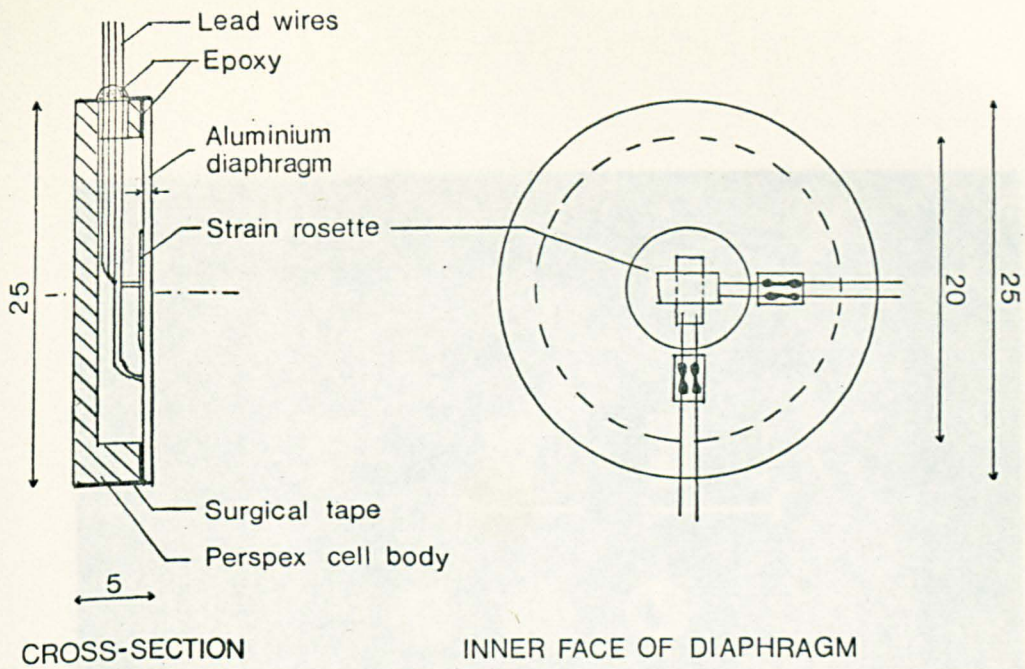


Fig. 5.2 DESIGN RELATIONSHIP BETWEEN DIAPHRAGM THICKNESS AND PRESSURE.

LENGTH OF CASING, L (mm)	26	38.3	51.5
MAXIMUM PRESSURE RANGE (kN/m <sup>2</sup> )	450	450	450

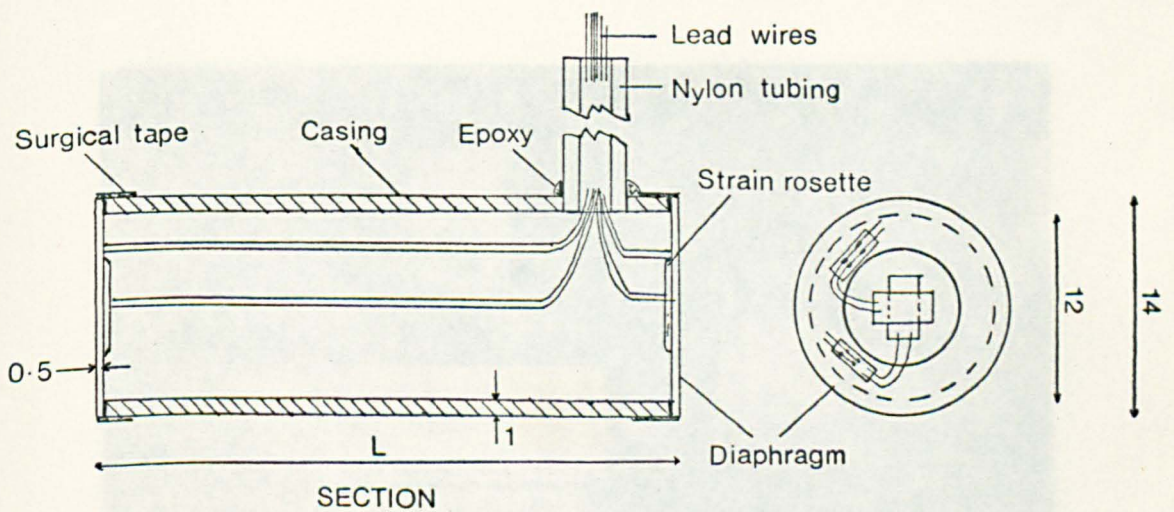
(b) IF PRESSURE CELLS

Fig. 5.3 DETAILS OF PRESSURE CELLS



CELL DESIGNATION	EP6	EP7	EP9	EP10	EP11
DIAPHRAGM THICKNESS $t$ (mm)	0.6	0.7	0.9	1.0	1.1
NOMINAL PRESSURE RANGE ( $\text{kN/m}^2$ )	100	140	280	420	560

(a) EP PRESSURE CELLS



CELL DESIGNATION	IF25	IF38	IF50
LENGTH OF CASING, $L$ (mm)	26	38.5	51.5
MAXIMUM PRESSURE RANGE ( $\text{kN/m}^2$ )	450	450	450

(b) IF PRESSURE CELLS

Fig.5.3 DETAILS OF PRESSURE CELLS

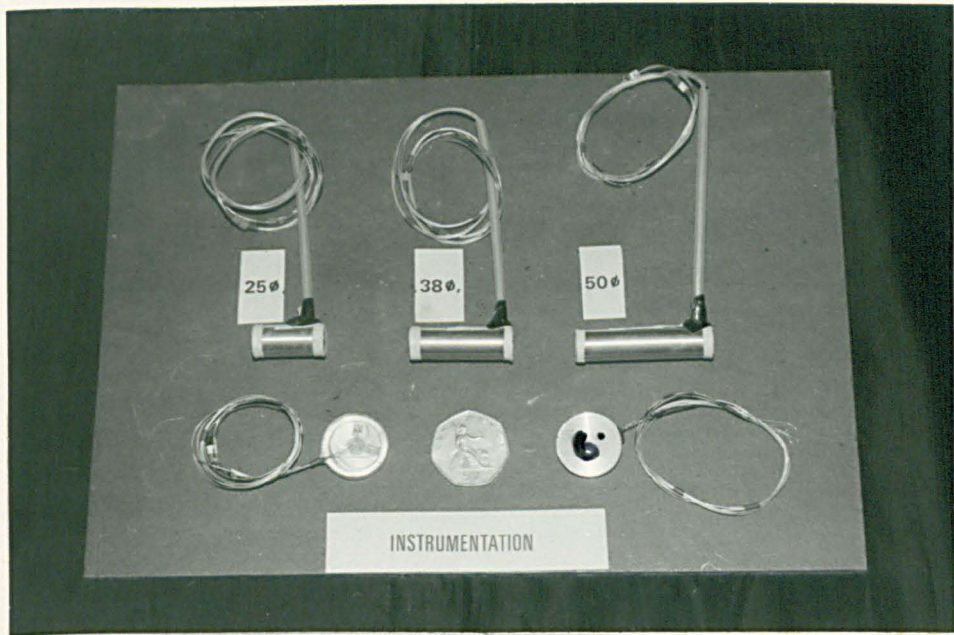


Fig. 5-4 PRESSURE CELLS



Fig. 5 5 MATERIALS FOR FABRICATING PRESSURE CELLS

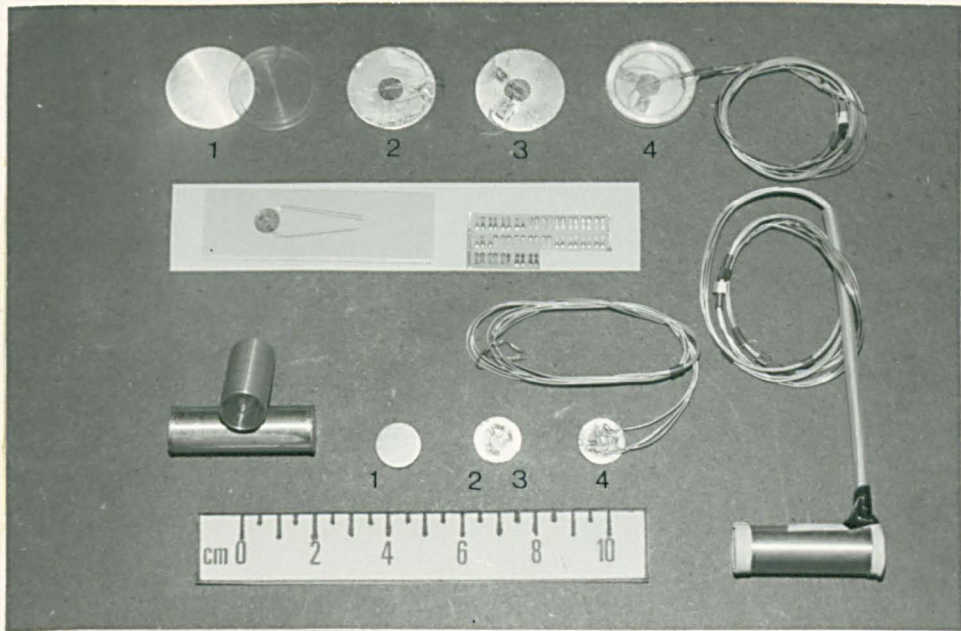


Fig. 5-6 BONDING OF STRAIN GAUGES

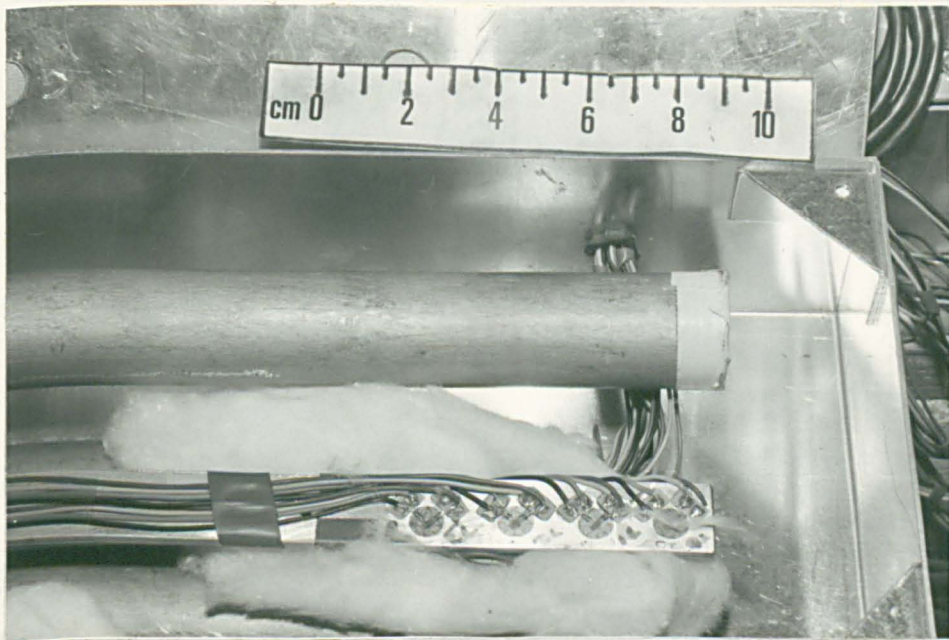


Fig. 5-7 DUMMY GAUGES

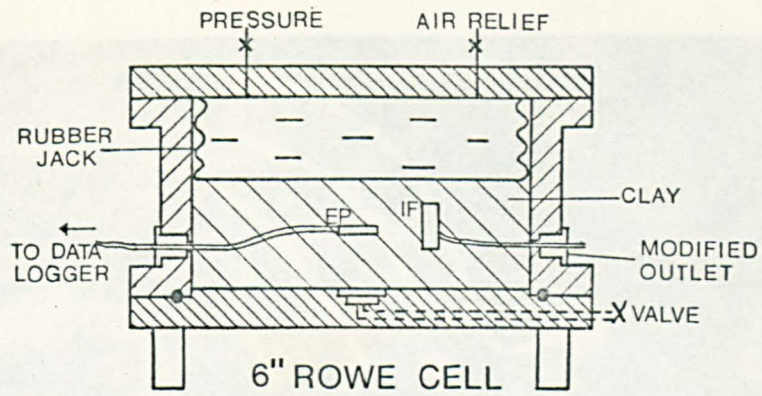


Fig.5.8 CALIBRATION OF PRESSURE CELLS

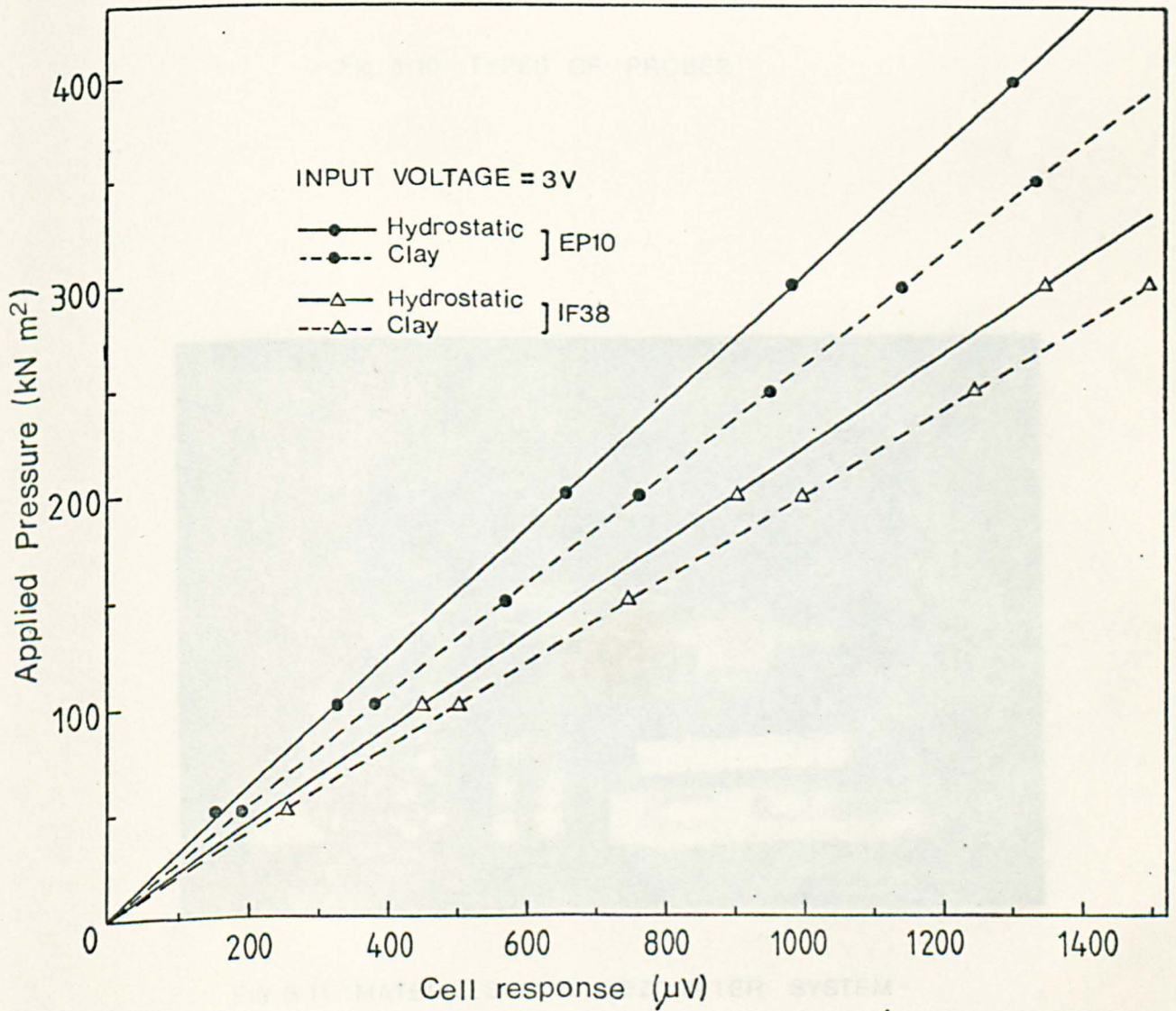


Fig.5.9 TYPICAL CALIBRATION CURVES FOR PRESSURE CELLS

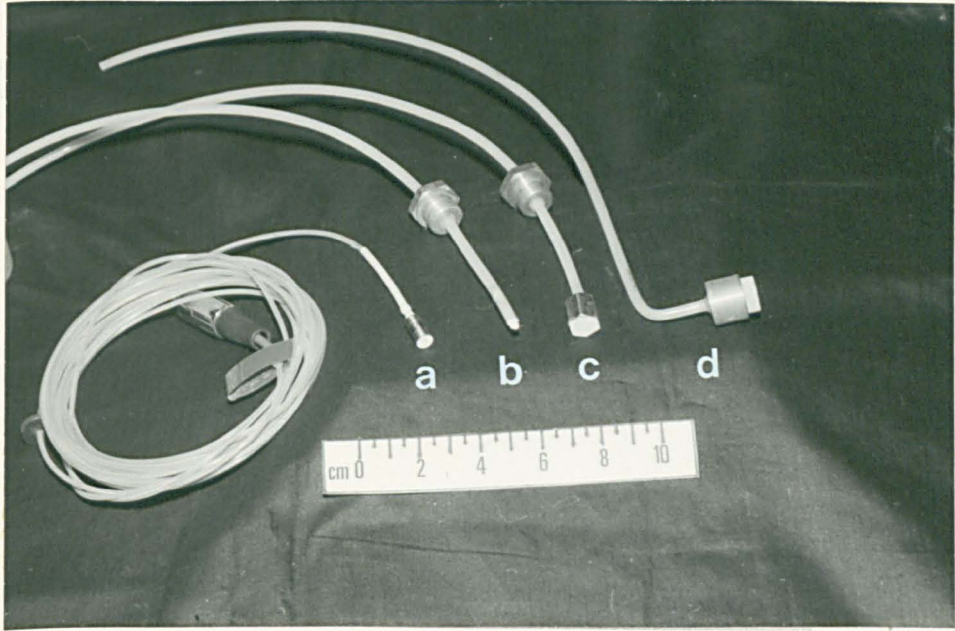


Fig. 5-10 TYPES OF PROBES

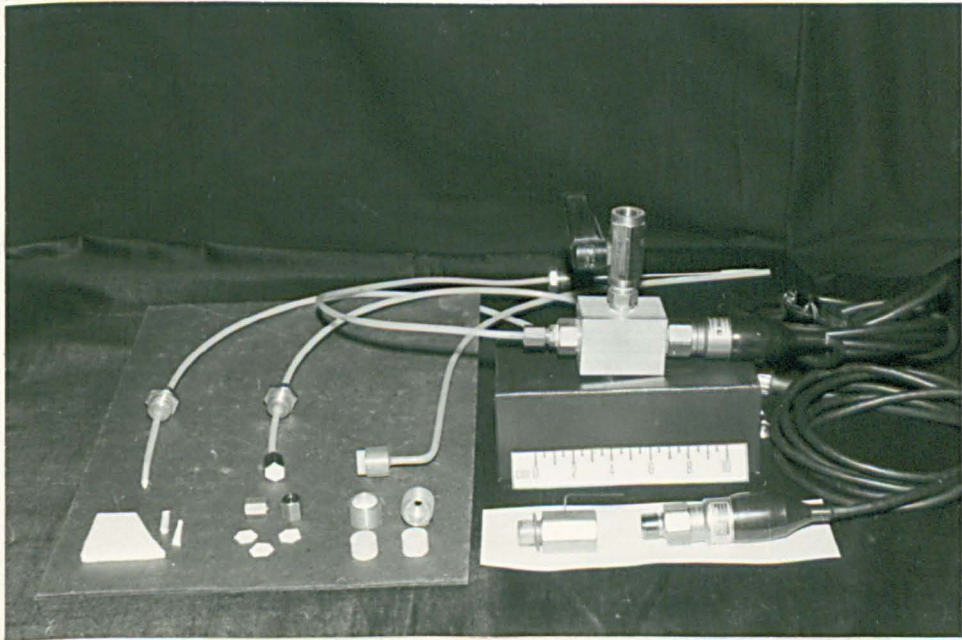


Fig. 5-11 MATERIALS FOR PIEZOMETER SYSTEM

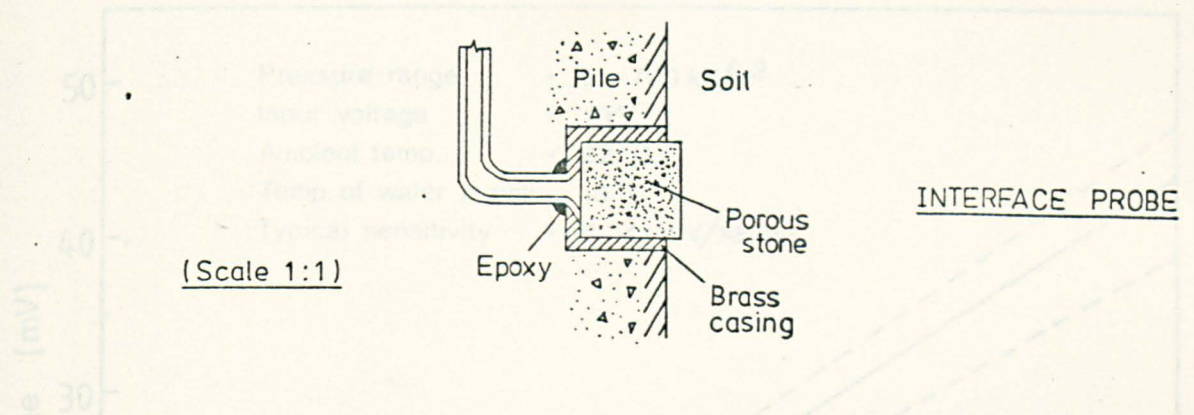
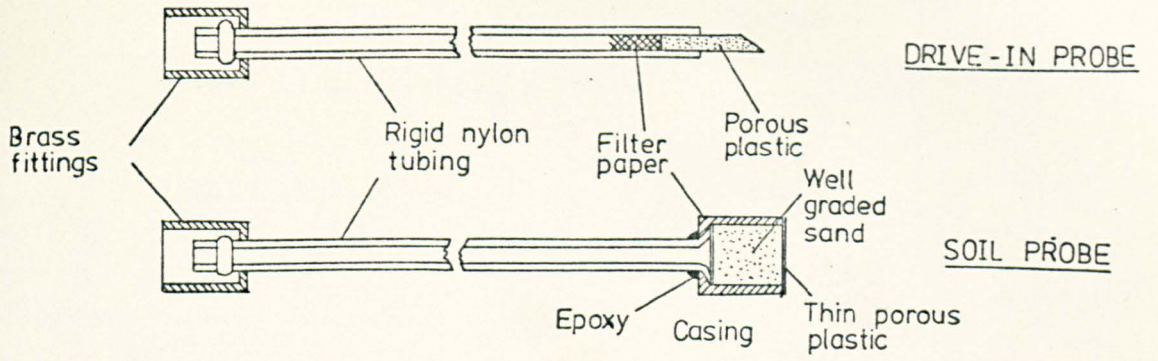


Fig.5.12 DETAILS OF PROBES

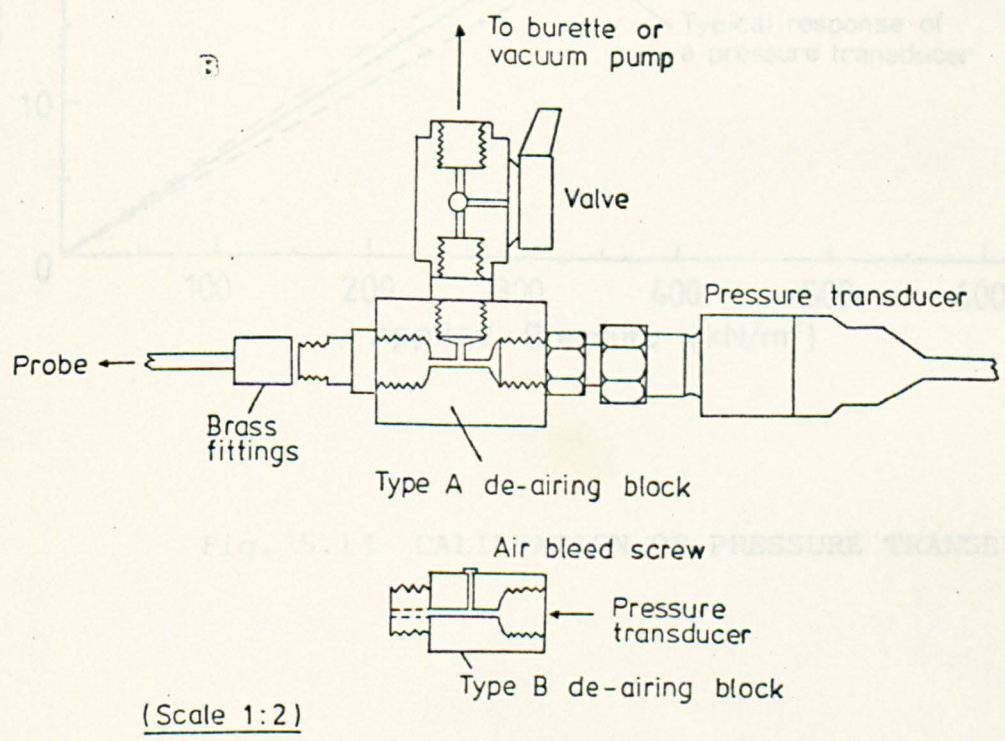


Fig.5.13 PIEZOMETER ARRANGEMENT

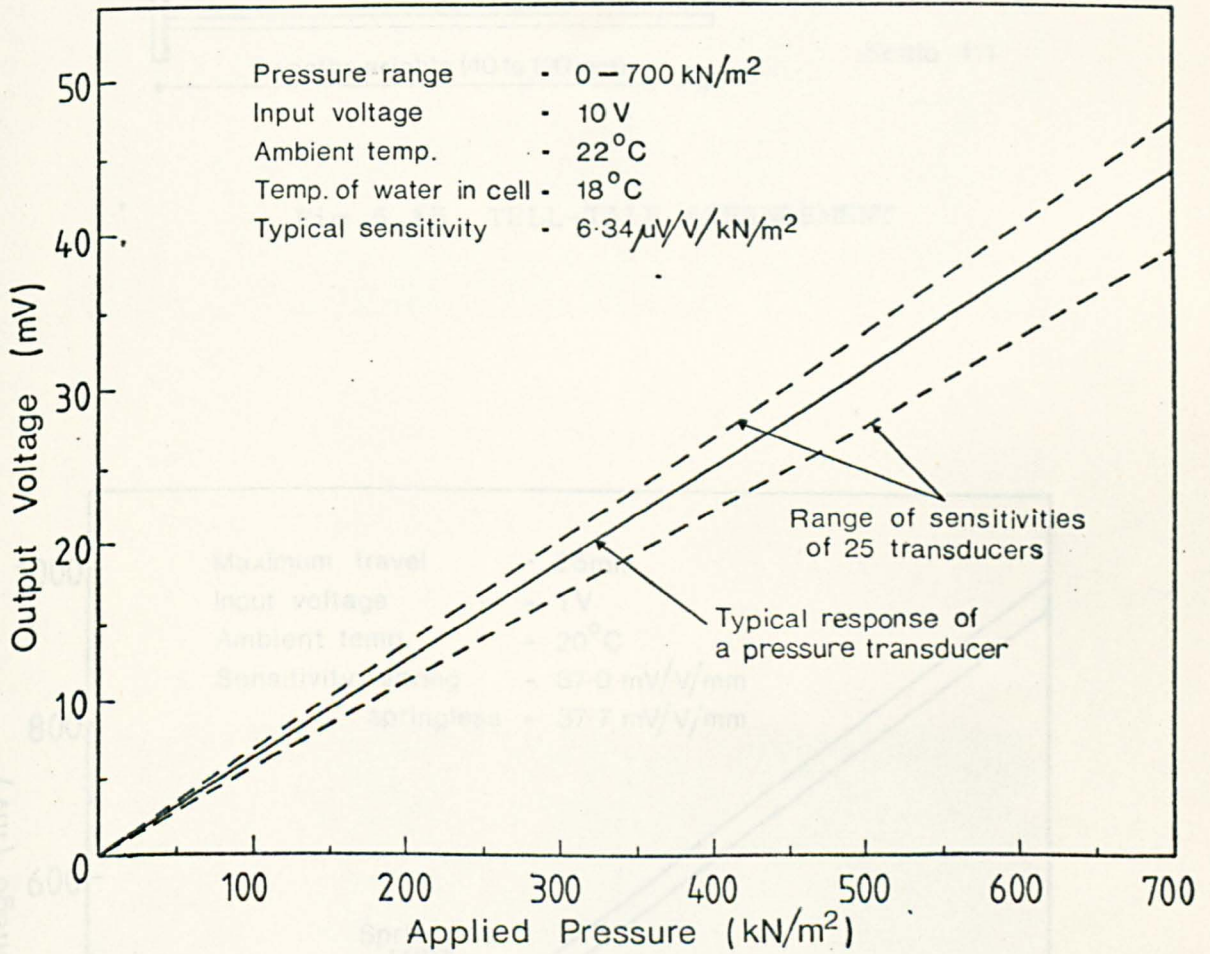


Fig. 5.14 CALIBRATION OF PRESSURE TRANSDUCERS

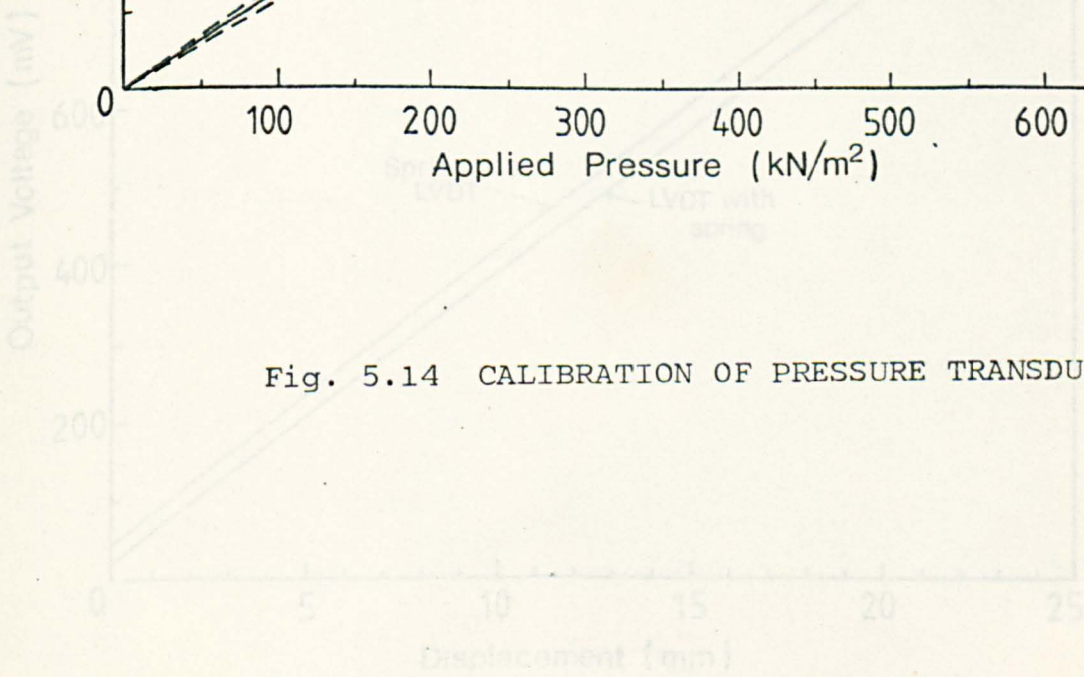


Fig. 5.16 CALIBRATION OF LINEAR VARIABLE DISPLACEMENT TRANSDUCERS

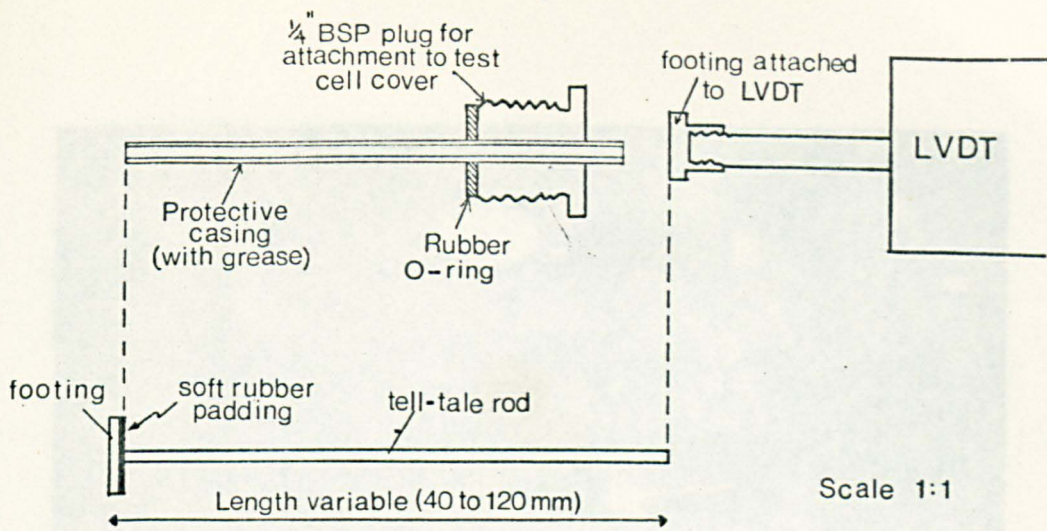


Fig.5.15 TELL-TALE ARRANGEMENT

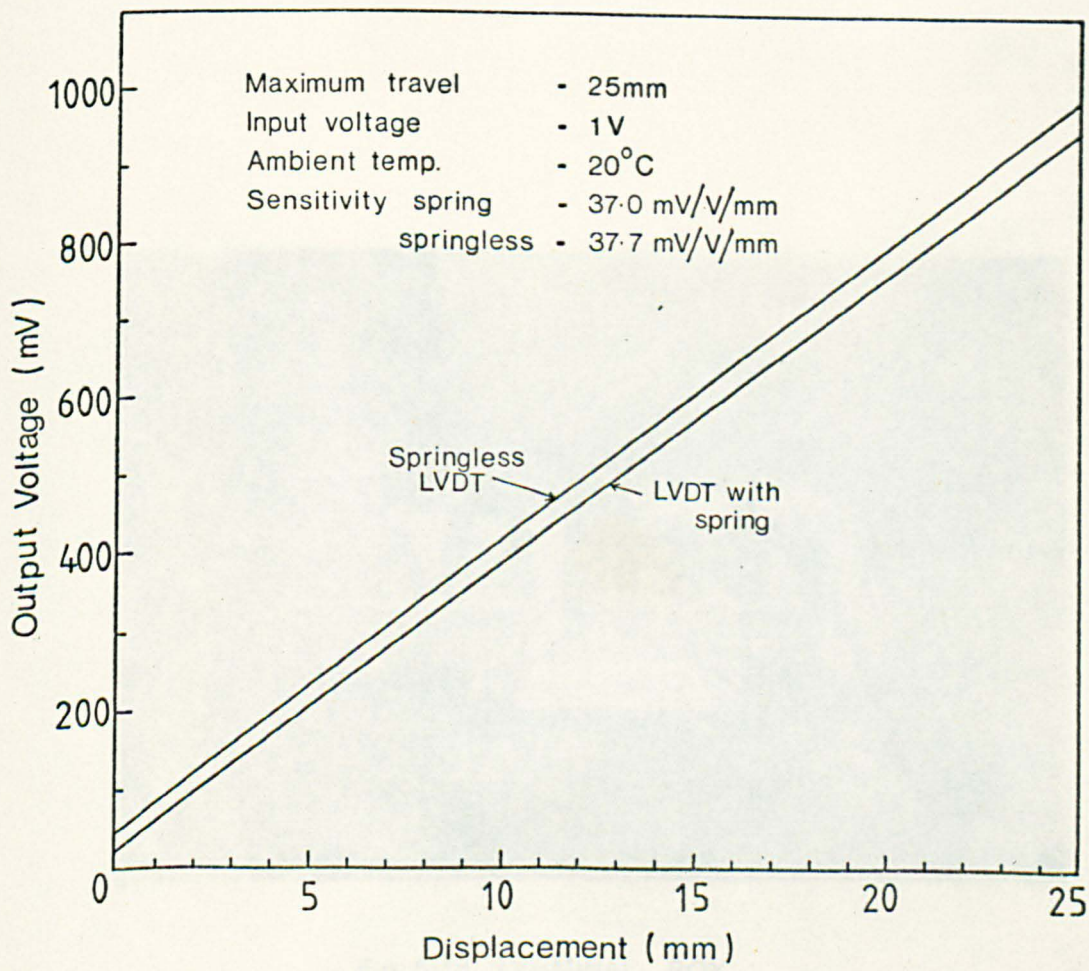


Fig.5.16 CALIBRATION OF LINEAR VARIABLE DISPLACEMENT TRANSDUCER(LVDT)

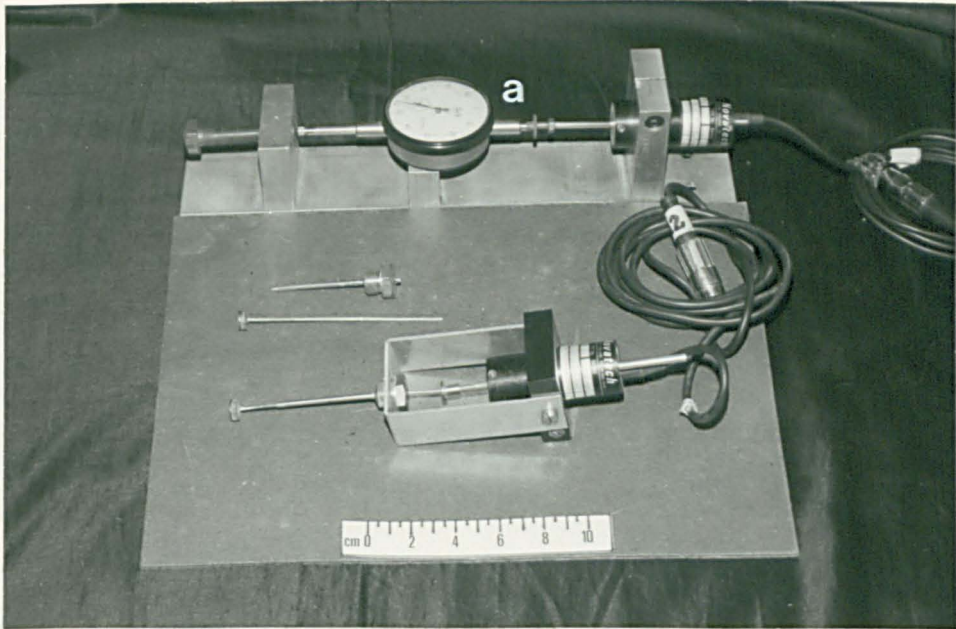


Fig. 5-17 TELL-TALE DEVICE AND LVDT  
CALIBRATING APPARATUS

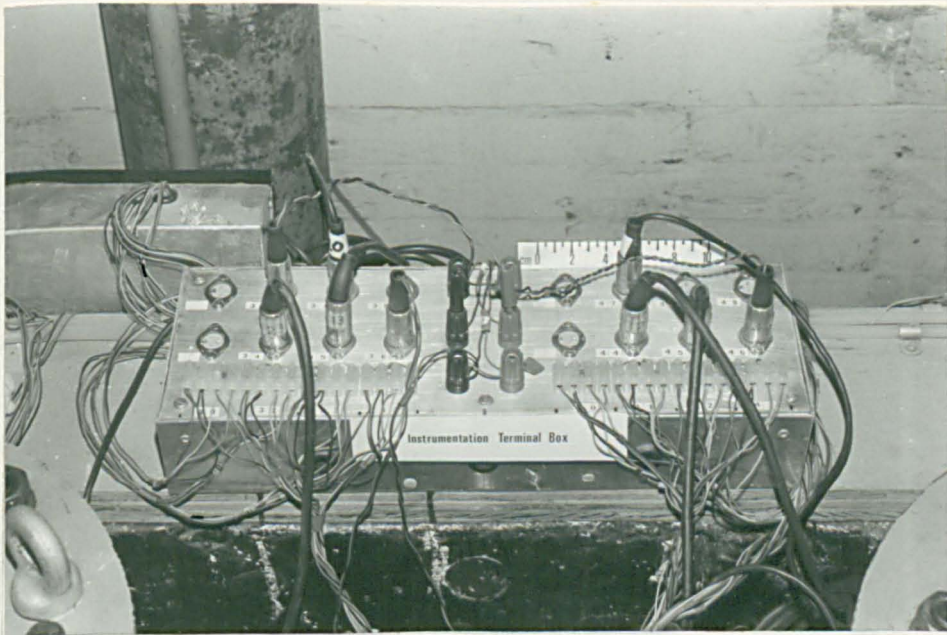


Fig. 5-18 TERMINAL BOX

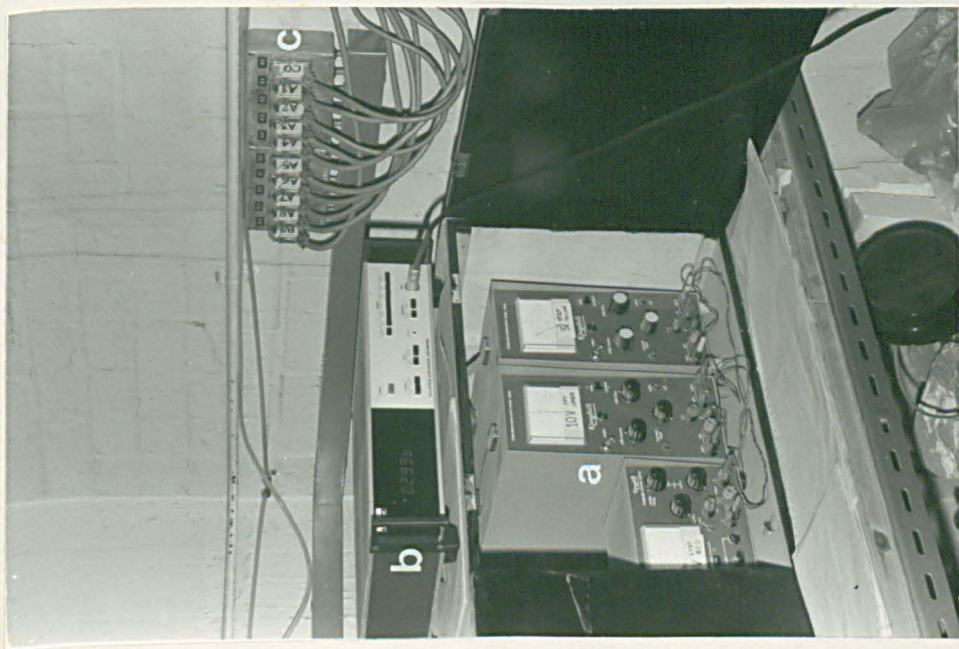


Fig. 5-19 (a) POWER SUPPLY (b) PORTABLE DVM (c) JUNCTION BOX

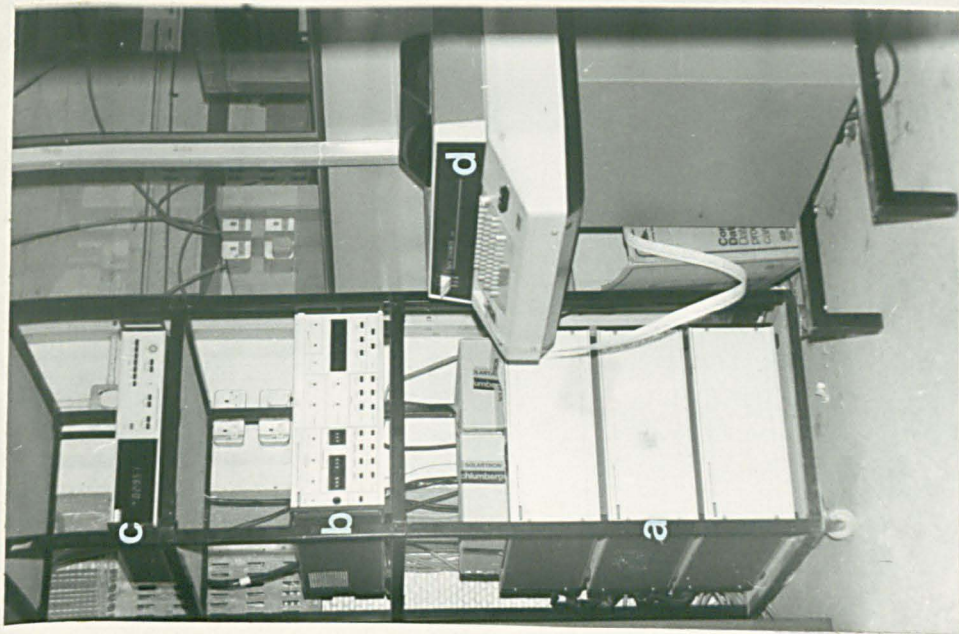


Fig. 5-20 DATA LOGGER

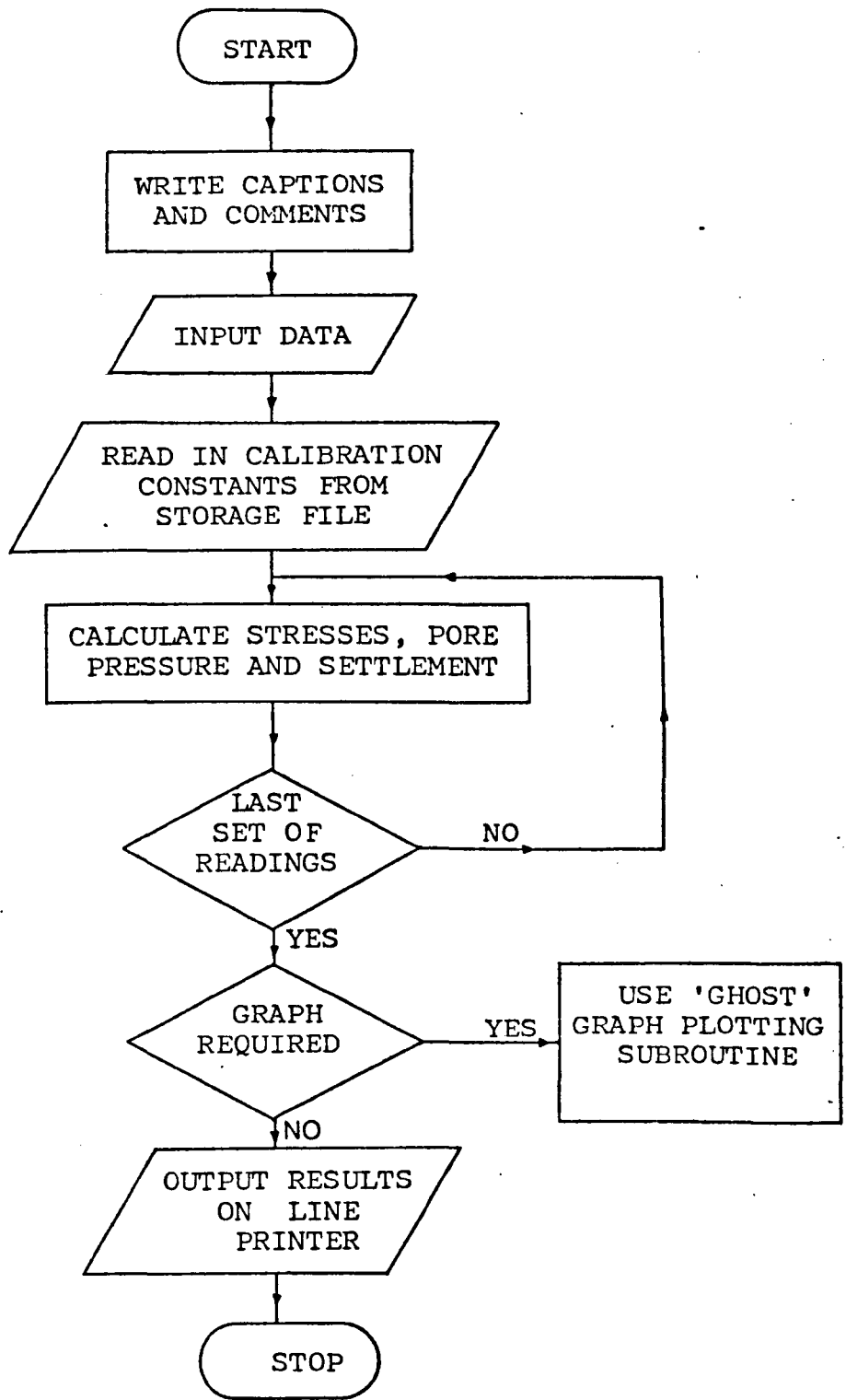


Fig. 5.21 FLOW DIAGRAM FOR COMPUTATION OF RESULTS

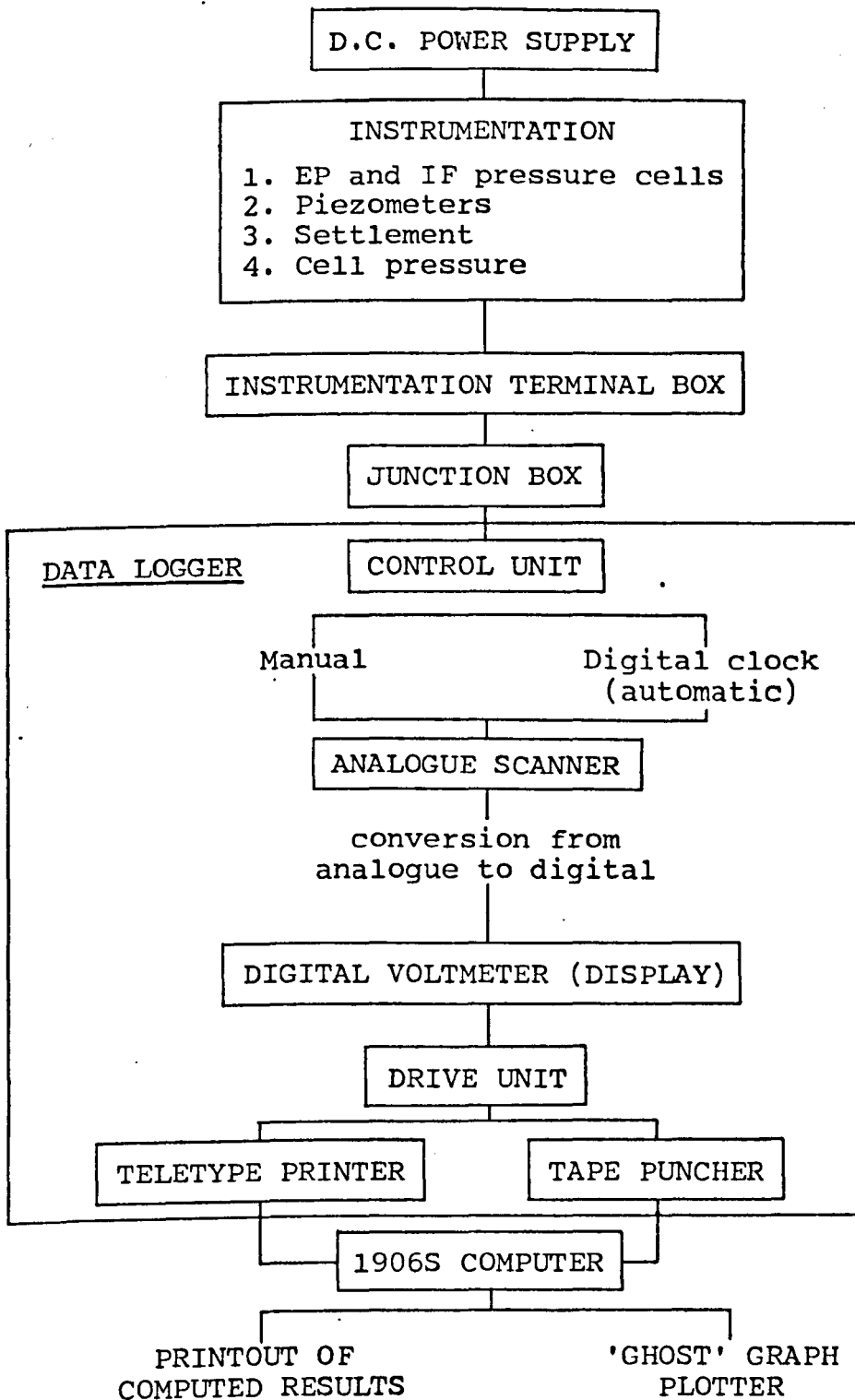


Fig. 5.22 FLOW DIAGRAM FOR DATA ACQUISITION

## CHAPTER 6

### TEST PROGRAMME AND EXPERIMENTAL PROCEDURES

#### 6.1 TEST PROGRAMME

The main test programme, shown in Table 6.1, was arranged in three series to investigate the short term and long term effects of several variables affecting the behaviour of bored piles. This programme was complemented by separate but related investigations on soil properties and factors influencing the test performance (Table 6.2).

A short term test (denoted by 'ST' in the Test Reference) refers to one in which piles were tested 7 days after casting while a long term test (denoted by 'LT') refers to one in which piles were tested after a curing time greater than 7 days.

However, no loading tests were conducted on the piles in Test Series ST5 and LT1 after the specified curing period. Instead, vane shear tests were carried out at various radii from the pile centre and at various depths. Samples were also taken at various positions for moisture content determinations to map out the distribution of moisture in the clay bed.

Altogether, 48 tests were carried out, of which four were of a preliminary nature to determine the practicality of the test apparatus and techniques, and the suitability of the various instruments. With the exception of the long term series, at least one test in each series was repeated to examine the reproducibility of results.

Details of all the tests carried out in the main programme are given in Table 6.3.

## 6.2 GENERAL PROCEDURE

The test procedure generally involved the following stages:

1. Installation of soil instrumentation and cell accessories on to the test cell
2. Preparation of clay beds by anisotropic consolidation.
3. Construction of a pile with measuring devices installed in it.
4. Load testing of the piles after a defined curing period, and
5. Studies to determine relevant soil properties for analysis.

The arrangement of equipment for the different stages of test is shown in Fig. 6.1 and illustrated in Fig. 6.2. Reference should be made to these figures during the discussion of the various stages of the test procedure. Throughout the test, regular measurements of the physical quantities described in Section 5.2 were recorded on the data logger.

A standard or control test was one in which a 38mm diameter microconcrete pile with a water-cement ratio of 0.6 was installed in a normally consolidated clay prepared at a consolidation pressure of  $420 \text{ kN/m}^2$  and tested 7 days after casting by a Quick Maintained Load procedure.

## 6.3 PREPARATION OF CLAY BEDS

### 6.3.1 Introduction

Homogeneous clay beds were prepared by anisotropically consolidating a slurry mix to a known stress history. The procedure for the preparation of clay beds was simple and reproducible. It was drawn from the experience of previous investigators in this Department such as Rice (1975) and Eid (1978), and from the work of Sheeran and Krizek (1971).

A good account of the general philosophy of slurry preparation is given by Sheeran and Krizek. They suggested that a high initial water content between 1.5 to 2.0 times the liquid limit for the slurry, allows de-airing and placement to be carried out with little difficulty. Berry (1965) has also shown that by mixing clay to twice the liquid limit the viscosity of soil is considerably reduced and any entrapped air could be easily removed during mixing. Yong and Warkentin (1966) and Mitchell (1976) provide useful information on the clay-water interaction and colloidal behaviour of soil for a better understanding of the slurry preparation technique.

### 6.3.2 Cell and Soil Instrumentation

To document the stress history of the clay bed, measuring devices described in the previous chapter were installed. These devices were installed prior to the preparation of the clay bed. This procedure reduced the problem of soil disturbance inherent with instruments forced into the soil. Instead, the method allowed compaction of clay around the devices during consolidation, thus ensuring a continuity of stress.

The cell pressure applied to the soil specimen was measured either by a pore pressure transducer (for data logging) or by a Bourdon gauge (for visual checking) attached directly on top of the pressure application cover. For the pressure transducer, a Type B de-airing block (see Fig.5.13) was incorporated so that the transducer could be de-aired prior to application of the consolidation pressure.

The soil measuring devices installed on the instrumentation cell cover is shown in Fig.6.3 and consists of (a) and (b) EP pressure cells; (c) piezometer system; (d) tell tale device with displacement transducer; (e) pressure transducer connected directly to the cover; and (f) the terminal block. The locations of these measuring devices in the test cell have been shown in Fig. 5.1. It should be mentioned that the test cell in Fig. 6.3 has been inverted for the purpose of photographing and that normally the instruments would have been at the bottom end of the test cell prior to the preparation of the clay bed.

In general, one EP pressure cell was placed horizontally in the clay bed to check whether the stress level in the soil sample was the same as the stress in the consolidation pressure system. Another EP pressure cell was positioned vertically at about 50mm from the cover (i.e. at about the mid-height of the pile) to measure the horizontal earth pressure. The positions of the EP cells were fixed by the nylon tubing through which the electrical wires were conducted out of the test cell to be connected to the terminal block.

For pore pressure measurements, two soil piezometers were installed at about the same level as the EP pressure cell, but at different radii from the pile shaft. The use of at least two piezometers was a precaution in case clogging of one of them occurred. This safeguard was found to be

satisfactory and the drive-in piezometer developed as a replacement when both soil piezometers were not working was rarely used. The success of the soil piezometer depended on the complete de-airing of the piezometer system. The valve which allowed water to be flushed through the system and out of the probe was turned off as soon as the slurry reached the level of the soil probe. The de-airing technique has been described in Section 5.4.4.

It can be seen in Figs.5.1 and 6.3 that the measuring devices are attached on to the cell cover by  $\frac{1}{4}$ " BSP brass plugs modified to suit each type of instrument. As a precaution against leakage, the gap left between the bottom of each plug and the inside surface of the cell cover was sealed with a plasticine sealant which could be removed after a test. It should be noted that all the electrical measuring devices were allowed to 'warm-up' by supplying the selected excitation voltages for at least twenty-four hours before using them.

During the later stages of the test programme, the number of measuring devices used were reduced when improved techniques and experience enabled measurements to be obtained with confidence.

### 6.3.3 Preparation procedure

The kaolin used for the preparation of the clay beds is available commercially under the trade name 'Speswhite'. Its physical and chemical properties are given in Table 6.4. To avoid any chemical interaction between the water and kaolin during the slurry preparation, and to ensure the saturation of the soil sample, it was necessary to use de-ionised and de-aired water.

The slurry was prepared by mixing the kaolin powder and the de-ionised and de-aired water to an initial moisture content of about the twice the liquid limit. The mix was then agitated in a motor-driven rotary mixer for about 40 minutes. During this period, the cell and soil instruments were installed on to the test cell as described in the previous section, and initial readings were taken. The drainage filter consisting of a porous plastic sandwiched between filter papers was placed at the base of the test cell to provide one-dimensional vertical drainage. The wall of the test cell was then smeared with silicone grease.

Studies by Rowe and Barden (1966) and Burland (1967) showed that side friction could almost be eliminated by smearing the wall of the consolidation cell with silicone grease. In this study, it was found that the use of silicone grease also inhibited rusting in the carbon steel cell wall and facilitated the removal of the clay bed from the cell after a test.

When the preliminary preparation of the test cell was completed, the slurry was spooned into the cell under about 100mm of water to avoid trapping any pockets of air during placement. The height of the slurry in the test cell varied between 370 and 380mm. Excess water from the top of the slurry was removed with a soft sponge. The rubber jack was then placed over the slurry and the pressure application cover was bolted onto the cell body. Another set of readings from the measuring devices was then recorded.

The space between the rubber jack and the cell cover was filled with water and an initial pressure of  $70\text{kN/m}^2$  was applied. The pressure was supplied from an air-water pressure cylinder connected to an air-compressor. The flexible convoluted rubber jack then transmitted a uniform

distribution of vertical stress on to the soil specimen. To ensure uniform conditions throughout a sample before the start of pore pressure dissipation, the increment of pressure was applied with the drainage valve closed. An immediate response of the <sup>pore</sup> pressure transducers confirmed the degree of saturation. When the drainage valve was opened, the volume of water discharged and the response of the instruments were measured at pre-selected times.

Complete consolidation could be detected by monitoring the dissipation of pore pressure or by plotting the consolidation curve of volume of water discharged against the logarithm of time. Various pressure increments were applied depending on the stress history required. In general, for the normally consolidated clays, the following pressure increments were adopted:

0 → 70 → 140 → 280 → 420 → 560 kN/m<sup>2</sup>

Overconsolidated specimens were prepared by allowing samples consolidated at a higher pressure to swell under a lower pressure, i.e. samples were allowed access to water as load was removed.

Starting from an initial slurry height of about 370 to 380mm; a relatively homogeneous bed of clay, 200mm diameter and 180 to 200mm thick, was obtained at the end of the final consolidation stage. The homogeneity was determined by preliminary experiments using a laboratory vane shear apparatus and moisture content measurements on various positions in the clay beds. The final water content of the clay bed ranged between 40% and 55% depending on the stress history, giving a consistency varying from soft to firm.

At the end of the final stage of consolidation (or swelling), usually between 14 to 30 days depending on the stress

history, the test cell was inverted whilst maintaining the overburden pressure. The test cell was now ready for the construction of the laboratory pile.

## 6.4 INSTALLATION OF 'MODEL' CONCRETE PILE

### 6.4.1 Introduction

The 'model pile' constructed in the laboratory was intended to simulate a small segment of a pile shaft as shown in Fig. 6.4. The tests were conducted in such a manner that the effect of depth on the behaviour of pile element could be simulated. This was achieved by using various consolidation pressures from 140 to 560 kN/m<sup>2</sup> in the preparation of the clay beds and maintaining a vertical stress on the soil during the tests. The test piles were then installed in stages similar to the field procedure of constructing bored piles by the dry method. The procedure involved boring a hole, placing fresh concrete in it, applying a head on the concrete to simulate hydrostatic pressure of the fresh concrete and then allowing the pile to cure before load testing.

In this study, measuring devices were installed in the shaft to observe stress changes at the soil-pile interface. The pile instrumentation shown in Fig. 6.5 consisted of an IF pressure cell 'a' and an interface probe 'b'. A device for forming a void 'c' and the aluminium loading platen 'd' are also shown in the figure.

Technically, the procedure was not difficult, but it had to be done with the utmost care and efficiency, especially in the placement of the instrumentation and concrete.

#### 6.4.2 Use of microconcrete for 'model' piles

Microconcrete, which is a mixture of Ordinary Portland Cement, graded fine aggregates and water, was used to form the 'model' piles for two principal reasons: (i) the ease of placement into the relatively small borehole and (ii) to avoid exaggeration of the pile surface roughness which would occur if coarse aggregates had been used.

The microconcrete used was a scaled model, one-eighth size of the prototype mixture. The details and method of obtaining the desired gradations of aggregate are given by Johnson (1962) and Aldridge and Breen (1968). The latter authors showed that provided stress in the concrete is less than  $10 \text{ N/mm}^2$ , the stress-strain characteristics are the same for both the microconcrete and normal concrete (see Fig. 6.6). British Standard CP2004 recommends that the average working stress in cast-in-situ piles should not exceed  $5 \text{ N/mm}^2$  of the total cross-sectional area. With a specified cube strength of at least  $14 \text{ N/mm}^2$  at 7 days and  $20 \text{ N/mm}^2$ , this gives a factor of safety of 4.

Assuming that the maximum load on a 38mm diameter 'model' pile is 1000N, and assuming a factor of safety of 2, the maximum stress in the microconcrete is  $1.8 \text{ N/mm}^2$ . Therefore, this value is well below the maximum stress suggested by Aldridge and Breen.

Based on the design method given in the above references, and the recommendation of ICE Piling Model Procedure and Specifications (1978), the following design mix was obtained after a trial and error process to achieve the required slump of 150mm and the required strength:

$$\text{WATER/AGGREGATE/CEMENT} = 0.6:2.4:1.0$$

Details of this concrete mix are given in Table 6.5. The

properties of the microconcrete are determined from standard laboratory tests including slump cone tests and strength tests on cube and cylindrical concrete specimens. Results of these tests are given in Table 6.6

To study the effects of mix design on the moisture migration at the pile-soil interface, microconcrete with water-cement ratios of 0.4, 0.5 and 0.7 were also investigated in Test ST5.5 to ST5.7.

#### 6.4.3 Boring

At the end of consolidation, the test cell was inverted and the boring device set-up. However, before the boring operation was commenced, one important experimental precaution was taken. The pressure supplied to the test cell is a constant air-water pressure system. In order to maintain this constant pressure in the test cell when the soil is excavated, the rubber jack will expand upwards causing movement of the soil to fill up the excavated hole. Hence, it was essential to close the valve supplying the cell pressure for about 30 minutes during the boring and concreting process. Continuous measurements of the actual pressure in the test cell showed a slight drop in pressure during this short duration.

After the pressure supply valve was closed, the cell cap covering a 40mm central hole of the cell cover was removed. In some experiments, a vane shear test was carried out in the centre of the sample at the location where the hole was to be bored. The value was then used to predict the shaft resistance which would develop along the pile element.

The hole was then bored to a depth of about 120mm using a 38mm diameter auger attached to the drilling rod. In

Test Series ST3, the 25mm and 50mm diameter augers were also used. Since the boring process was a manual operation, a boring rate of about 50mm/min. was adopted to standardize the procedure. The drilling frame ensured that the hole bored was vertical and central with respect to the test cell. Since computation of the shaft resistance assumed a constant area, every effort was made to ensure a uniform cylindrical borehole.

Immediately after boring, a slight heave was observed at the base of the borehole. The spoil from the boring process was taken for moisture content determination and any debris in the borehole was removed with the aid of a thin rod. The void forming device was then placed in the hole and the borehole dimensions were measured with a ruler and a borehole measuring device (Fig. 4.11).

#### 6.4.4 Casting and curing

In view of the small quantity required, the microconcrete used was hand-mixed. The concrete was placed into the borehole immediately after boring and after the 'void' was in position. Initially, the microconcrete was placed to about one-third to one-half depth of the pile with the aid of a funnel. The IF pressure cell and the interface probe were then placed into the hole and it was essential that these devices had a slight projection of 0.5mm and 1.0mm respectively, into the soil to ensure intimate facial contact. This delicate operation was done with the help of a pair of long forceps.

It should be noted that prior to its installation, the non-functional parts of the pile instrumentation and the loading platen which were exposed to the concrete were coated with lubricating oil. The aim was to facilitate their recovery from the concrete pile after a test.

Apart from the loading platen and the 'void', the other devices were difficult to retrieve after a test.

The remainder of the microconcrete was then placed in the borehole. In practice, the fall of the concrete is considered adequate for self-compaction of concrete. However, in this study, the fall was less than 100mm. Therefore, concrete was tamped gently with a 6mm diameter rod during placement to promote intimate contact with the soil wall and to prevent concrete arching around the pile instrumentation. During tamping, care was taken to avoid changing the position of the pile instrumentation.

The loading platen was then placed on top of the pile and wire and nylon tubing were led out of the cell. The concrete was then pressurised to simulate the hydrostatic head of fresh concrete. Unset concrete can usually be regarded as a fluid with horizontal and vertical pressure being equal. However, in practice, actual lateral pressure caused by the fresh concrete is likely to be less than fully hydrostatic. This can be attributed either due to the arching of fresh concrete within the bored hole or if placement is undertaken in batches as in the case of long piles, concrete in the lower part of the pile begins to set up and inhibits full hydrostatic pressure. The method for calculating the actual lateral pressure of the concrete in this study is based on the work of Peurifoy (1965). Calculations are given in Appendix VII and are found to be a function of the rate of placement.

The pile was then left to cure for 7 days or a longer curing period, after which time the load tests were conducted. During the construction of the pile and, in particular, the curing stage, readings of the measuring devices were recorded at regular intervals to observe the total stress and pore water pressure changes at the pile-soil interface.

## 6.5 PILE TESTING PROCEDURE

### 6.5.1 Introduction

Testing a pile to failure provides useful information to design engineers and researchers. Unless piles are tested to failure, test results are of limited value. As Burland (1978) correctly pointed out,

"A splendidly stable pile indicates conservative design, rather than good design, and leaves much valuable information unrevealed. Much more information is revealed by a trial pile which fails or is near to failure, under test loading..."

For the short term tests, piles were tested 7 days after casting. Throughout this period, measurements of pore pressures and stresses in the soil were obtained to determine the stresses existing before load testing commenced. For the long term tests, the loading of piles were delayed for various periods between 14 days to 300 days after casting to allow some restoration of soil conditions. The state of stress of soil surrounding the 'model' pile during a load test is shown in Fig. 6.7.

### 6.5.2 Loading procedure

The Quick Maintained Load (ML) procedure in which small increments of load were applied for short intervals of time was adopted for testing the laboratory-scale piles. In the interest of saving time, increments were larger during early stages of the test and in the interest of accuracy, increments were made smaller as the total load increased.

Load increments of 50 N were placed during the first 75% of the predicted ultimate shaft load and thereafter 10 N increments were used. In order not to miss the peak value of ultimate load due to sudden failure, increments were

kept to 5N when failure was imminent as observed by a relatively large movement. Each increment was applied when settlement was less than 0.01mm per 5 minutes or until 15 minutes had elapsed, whichever occurred first. Load was increased until failure was achieved, failure load being defined as the load at which the bored pile continued to settle excessively without additional load being applied. A typical test lasted between 4 to 6 hours. After completion of the test, the load was removed and the pile permitted to rebound. Most of the rebound generally took place within the first 10 minutes.

The loading apparatus has been discussed in Section 4.3.2 and shown in Figs. 4.6 and 4.7. General lay-out with the test cell is shown in Figs. 6.2 and 6.3. The loads were applied by dead weights while settlement was continuously monitored by two displacement transducers arranged diagonally opposite each other. A dial gauge was also employed as a visual check. Readings were taken before and after each load increment and at sufficient intermediate intervals in order to allow load-settlement curves to be drawn. Care was taken to ensure that no lateral or impact forces were induced on the pile during load placement.

The Quick Maintained Load procedure was employed because it produces essentially undrained shear failure in the soil, which is consistent with the type of failure encountered in laboratory strength tests. The short duration of the test also minimised the time and temperature variations in the instrumentation and soil. The simplicity of the test procedure ensured the standardisation of the test and the ease of interpretation of the results.

## 6.6 SUMMARY OF EXPERIMENTAL PROCEDURES

A summary of the experimental procedures followed is shown in Fig. 6.8. In general, the duration of a complete short term test varied between 20 and 36 days depending on the stress history of the clay bed, while duration of a long term test depended on the curing period.

## 6.7 OBSERVATIONS AFTER PILE TESTS

### 6.7.1 Introduction

At the termination of each test, the test cell body was removed exposing the clay bed and the top of the pile. The ease of removal suggests that the side friction between the wall and the clay was small and therefore negligible. Vane shear tests were immediately conducted at various locations as a quality control check while samples were taken for moisture content determination and triaxial testing.

When soil sampling and testing were completed, the clay was partly removed with a cheese wire to expose the pile shaft on one side. The aim was to ascertain: (i) the effects of construction technique on the integrity and geometry of the pile, (ii) any soil contamination in the concrete or vice versa, (iii) the actual position of the soil and pile instrumentation, and (iv) the actual dimensions of the pile.

After a complete inspection of the pile and soil, the instrumentation in the soil and pile was recovered for further use. The pile instrumentation was retrieved by chipping away the microconcrete. Although the external casings of the instruments were initially oiled, removal was fairly difficult, and in some cases the chipping

process damaged the sensitive parts of the measuring devices. For the pressure cells, these were re-calibrated and checked. In the case of the piezometers, the probes and porous stones were replaced with new ones.

#### 6.7.2 General observations

A general examination of the soil and pile instruments showed that they were located in the positions predicted. The EP pressure cells were reasonably horizontal or vertical and showed no inclination. Typical views of instruments' position are shown in Figs. 6.9, 6.10 and 6.11. Soil piezometers are not shown because in view of their construction, they had to be removed before the cell cover could be lifted.

No penetration of microconcrete into the clay was observed. Instead, a close examination of the surface of the pile showed that minute quantities of clay were lodged within the small pores of the concrete. No overbreaks or voids were observed in the shafts except the pile in Test No. ST5.5. In this test, a water-cement ratio of 0.4 was used and the workability was inadequate to form an integral pile.

After general observations, the pile was extracted and the dimensions were measured with a vernier caliper. Typically, the length varied between 90 to 100mm and the average diameter measured was within  $\pm 5\%$  of the assumed diameter of 38mm measured in the borehole. The difference is relatively small and the assumption that the borehole diameter represents the pile diameter appears reasonable.

## 6.8 EXPERIMENTS ON FACTORS AFFECTING TEST PERFORMANCE

### 6.8.1 Introduction

A number of factors influence the test performance and hence the results. Most of these factors will be discussed in Chapter 8. However, two factors which have a major influence require a closer examination: (i) the effect of side friction between the cell walls and the soil on the behaviour of piles, and (ii) the stability of the instrumentation employed. Therefore, experiments were conducted to examine the significant of these factors.

### 6.8.2 Boundary Effects

A separate investigation was carried out to study the boundary effects on the test performance and results by measuring the distribution of total stress and pore pressure across the wall and the cover of the cell. The procedures from consolidation of clay bed to load testing were similar to those described in the previous sections. The difference is in the positions of the soil instruments.

At the clay-cell cover boundary, EP pressure cells and soil piezometers were placed at radii of 57mm and 95mm from the pile shaft. For the cell wall, measuring devices were placed at depths of 20mm and 100mm from the cell cover. These devices were also installed prior to consolidation of the slurry. Results and observations of these tests are discussed in Section 8.3.3

### 6.8.3 Stability of Instrumentation

When strain gauges are used in the measuring devices, the data recorded by the instrumentation can be influenced by temperature and time. Therefore, there was a need to

examine the stability of the instrumentation at zero load over a period of time. The strain gauges used in the pressure cells, although compensated, could be affected if temperature variations were large. With a view to recording the zero drift due to temperature and time, a concrete mould was set up as shown in Fig. 6.12. EP and IF pressure cells were embedded in the remoulded clay and concrete respectively and the mould was sealed with wax and a layer of plastic sheet. Readings were taken at regular intervals for the duration of the test programme, usually daily at a time approximately 1200 hours.

In the case of the piezometers, strain readings for zero load of a pressure transducer were taken over similar intervals of time as the pressure cells. This transducer was not installed on to any test cell but was left under ambient conditions and continuously supplied with an input voltage.

Results and observations on the stability of the electrical devices are discussed in Section 8.4.

TABLE 6.1 MAIN TEST PROGRAMME

SERIES NO.	TEST SERIES	TEST REF. NO.	TEST OBJECTIVE
I	STRESS HISTORY	ST1	Behaviour of bored piles in normally consolidated clay
		ST2	Effect of overconsolidation
II	INSTALLATION EFFECTS	ST3	Effect of pile dimensions
		ST4	Installation Technique
		ST5	Moisture migration and shear strength study
III	LONG TERM TESTS	LT1	Long term effects of installation on soil-pile behaviour
		LT2	Effect of curing time on shaft resistance of bored piles.

TABLE 6.2 COMPLEMENTARY TEST PROGRAMME

SERIES NO.	TEST SERIES	TEST REF. NO.	TEST OBJECTIVES
IV	STUDY OF SOIL PROPERTIES	SE1	Basic Properties
		SE2	Consolidation and Compression data
		SE3	Triaxial tests
		SE4	Experimental study of $K_0$
V	AFFILIATED EXPERIMENTS (ON FACTORS INFLUENCING TEST RESULTS AND PERFORMANCE)	AE1	Effect of wall friction and boundary effects
		AE2	Time lag study - theoretical and experimental
		AE3	Material Properties (Concrete, Aluminium)
		AE4	Stability experiments on instrumentation

Legend: ST - short term; SE - Soil Experiments;  
 LT - long term; AE - Affiliated Expts..

TABLE 6.3 DETAILS OF MAIN TEST PROGRAMME

SERIES NO	TEST REF. NO.	CONSOL PRESSURE (kN/m <sup>2</sup> )	NOMINAL PILE DIAMETER (mm)	WATER-CEMENT RATIO	CURING TIME (days)	REMARKS
I	ST1.1	420	38	0.6	7	} CONTROL TESTS (ST1.2 without instrumentation)
	ST1.2	420				
	ST1.3	140				
	ST1.4	280				
	ST1.5	420				
	ST1.6	560				
	ST2.1	140→140	38	0.6	7	OCR=1;2;3;4
	ST2.2	280→140				
ST2.3	420→140					
ST2.4	560→140					
II	ST3.1	420	25	0.6	7	
	ST3.2		38			
	ST3.3		50			
	ST4.1	420	38	( 2hrs)*	7	* Delay time between boring and casting
	ST4.2			0.6(12hrs)		
	ST4.3			(24 hrs)		
	ST5.1	140	38	0.6	7	} Influence of initial moisture content (stress history)  } Influence of water-cement ratio
	ST5.2	280		0.6		
	ST5.3	420		0.6		
	ST5.4	560		0.6		
	ST5.5	420		0.4		
ST5.6	420	0.5				
ST5.7	420	0.7				
III	LT1.1	420	38	0.6	14	
	LT1.2				30	
	LT1.3				60	
	LT1.4				100	
	LT1.5				200	
	LT1.6				300	
	LT2.1	420	38	0.6	14	
	LT2.2				30	
	LT2.3				60	
	LT2.4				100	
	LT2.5				200	
	LT2.6				300	

TABLE 6.4 BASIC PROPERTIES OF KAOLIN

(a) General Description

TYPE	Speswhite fine china clay
VISUAL FEATURES	White and floury in dried form
USUAL CLASSIFICATION	'CH'- inorganic clay of high plasticity

(b) Physical Properties

PROPERTIES	SYMBOL	VALUE
Liquid limit	$W_L$	72%
plastic limit	$W_p$	36%
plasticity index	$I_p$	36%
Specific gravity	$G_s$	2.60
Percent finer than $2\mu$	-	82%
Activity	A	0.44

(c) Chemical Analysis  
(from Manufacturer)

pH	5.0
	%
SiO <sub>2</sub>	46.2
Al <sub>2</sub> O <sub>3</sub>	38.7
Fe <sub>2</sub> O <sub>3</sub>	0.56
TiO <sub>2</sub>	0.09
CaO	0.2
MgO	0.2
K <sub>2</sub> O	1.01
Na <sub>2</sub> O	0.07
Loss on ignition	13.14

TABLE 6.5 MICROCONCRETE MIX DESIGN

DESIGN MIX	WEIGHT RATIO
1.Cement (Ordinary Portland Cement)	1.0
2.Water	0.6
3.Fine aggregates :	2.4
<u>B.S sieve sizes</u> .	
<u>pass through - retained</u>	<u>Percentage</u>
7 - 14	15
14 - 25	35
25 - 52	30
52 - 100	20

TABLE 6.6 PROPERTIES OF MICROCONCRETE

PROPERTIES	VALUE	REMARKS
Water-cement ratio	0.6	-
Slump	150mm	average of three slump tests
Cement content	530 kg/m <sup>3</sup>	based on mix design
Density	2.13 Mg/m <sup>3</sup>	average of 12 samples
Cube strength (7 days)	25.0 N/mm <sup>2</sup>	average of 9 tests
Cube strength (28 days)	32.5 N/mm <sup>2</sup>	average of 3 tests
Modulus of elasticity	35.5 kN/mm <sup>2</sup>	average of 3 tests

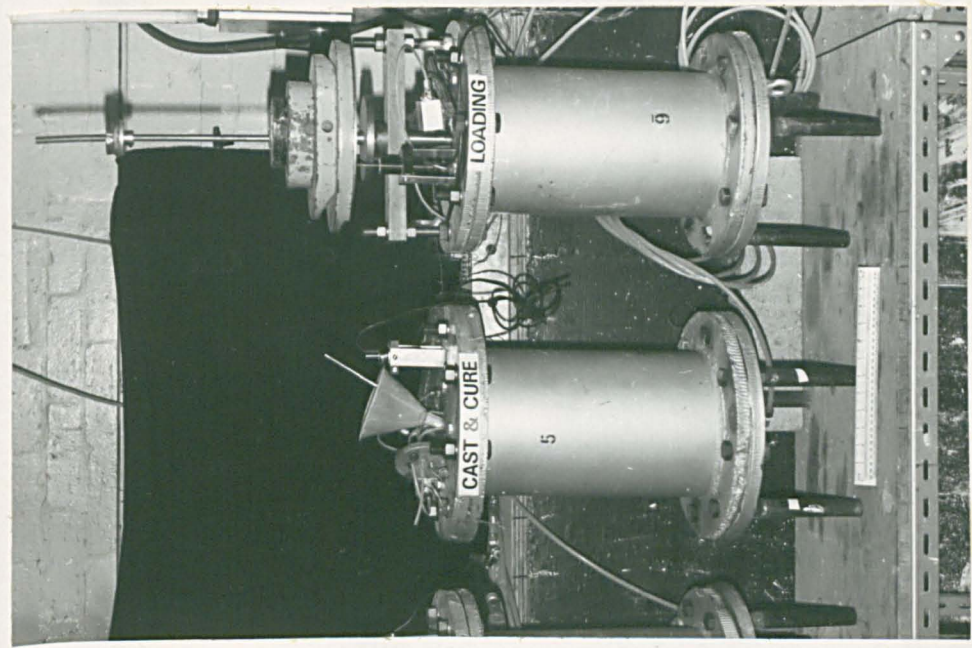
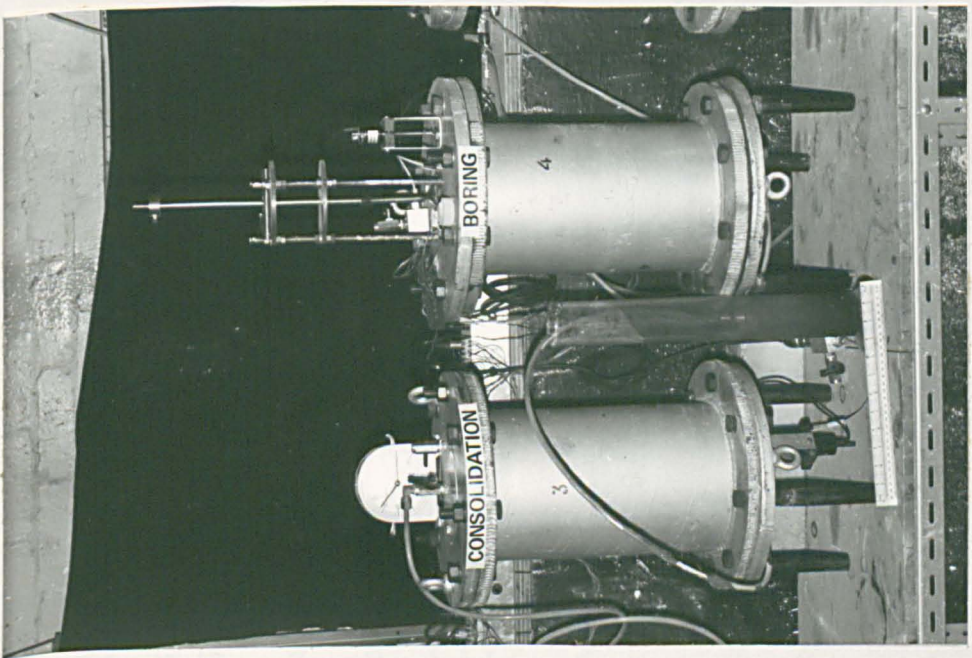


Fig. 6.1 TEST ARRANGEMENT

Internal cell dimensions

$\phi = 200\text{ mm}$   $H = 400\text{ mm}$

Pile dimensions

$\phi = 25, 38, 50\text{ mm}$ ,  $L = 100\text{ mm}$

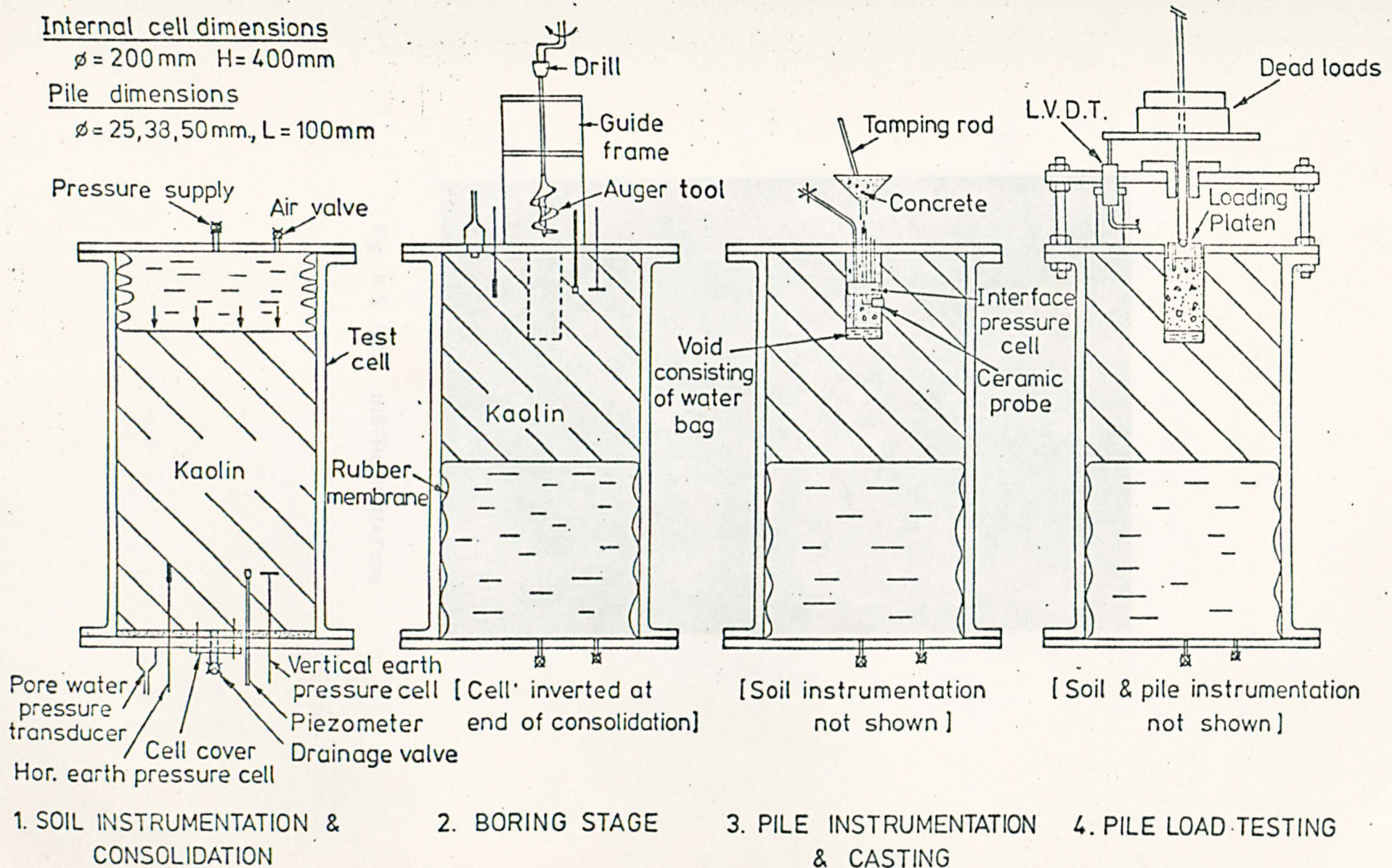


Fig. 6.2 SCHEMATIC DIAGRAM OF TEST ARRANGEMENT.

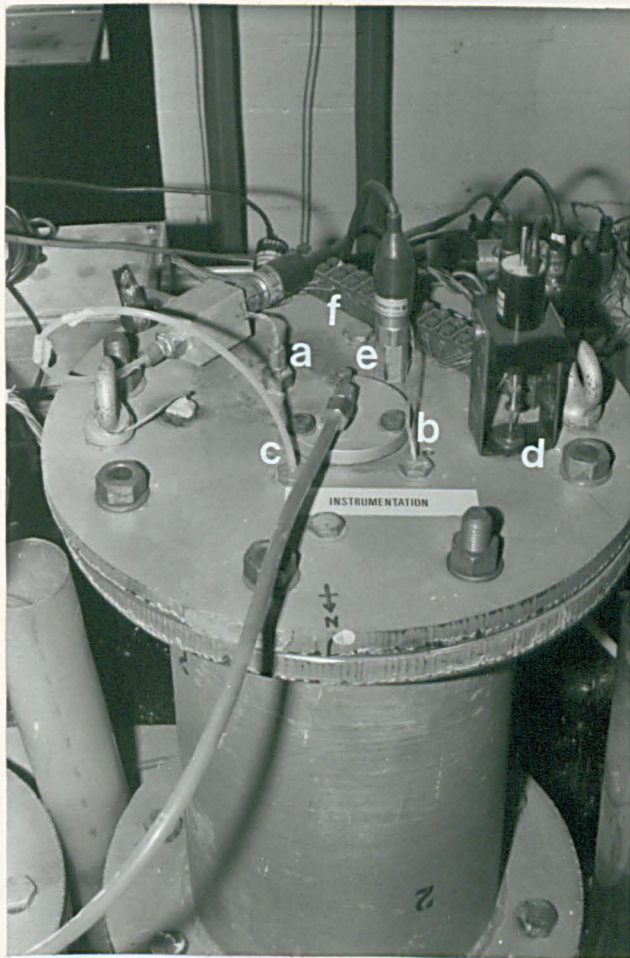


Fig. 6-3 SOIL INSTRUMENTATION

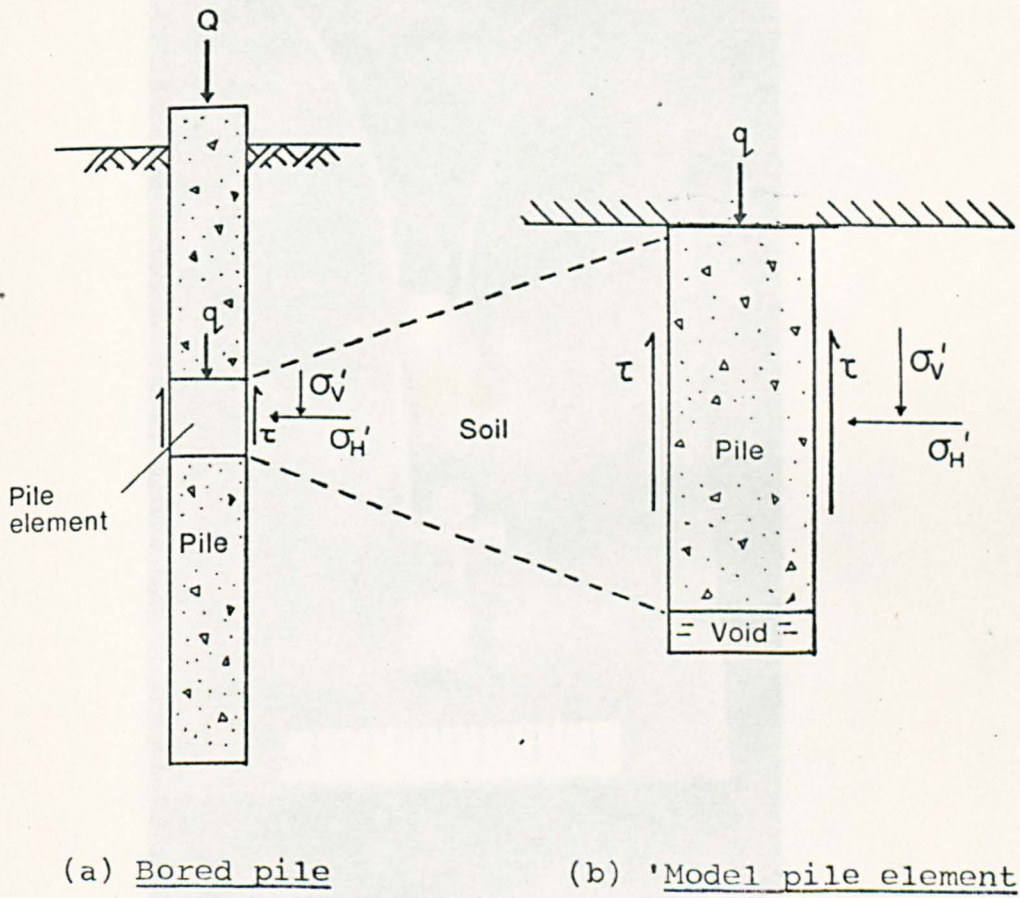


Fig. 6.4 SIMULATION OF SHAFT RESISTANCE ON PILE ELEMENT

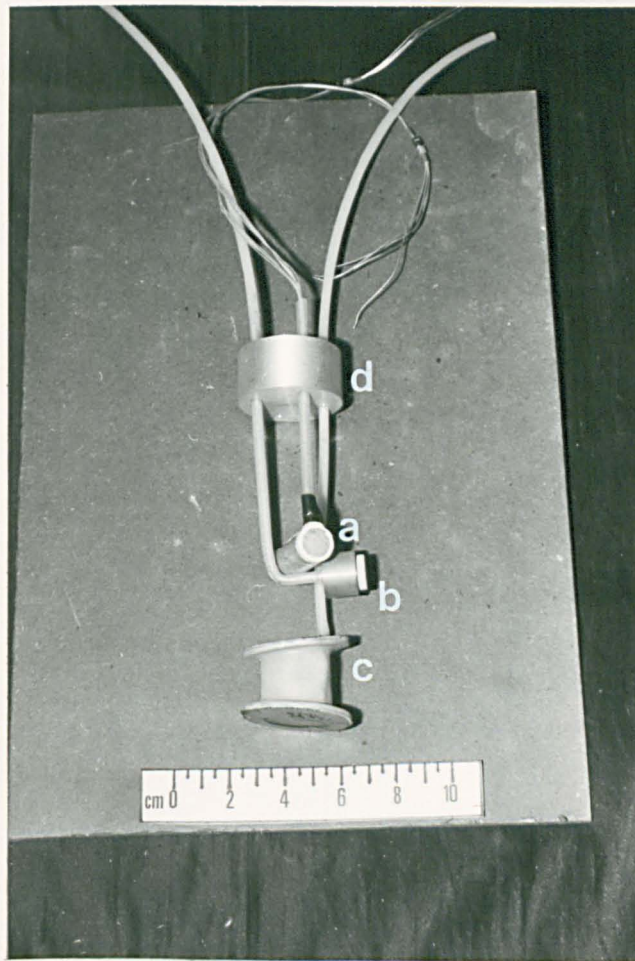


Fig. 6-5 PILE INSTRUMENTATION

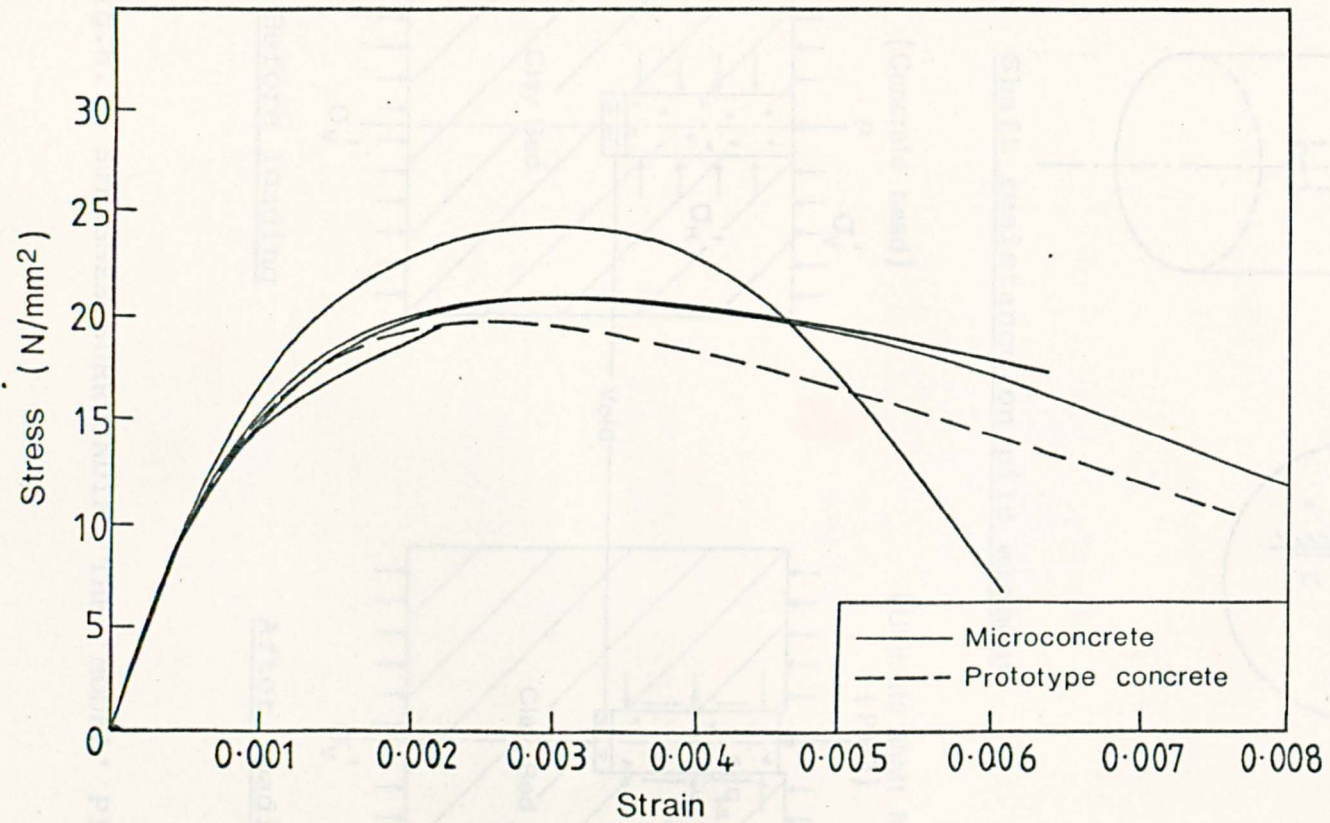
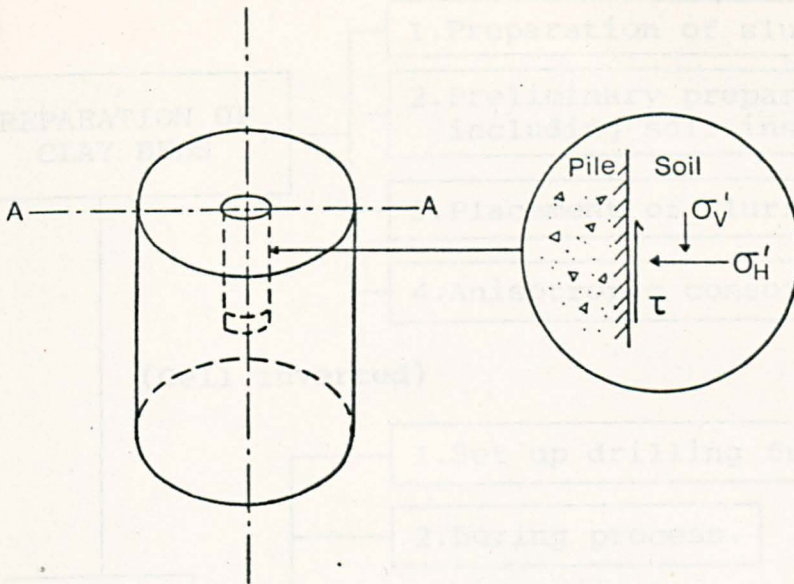


Fig.6.6 STRESS-STRAIN CURVES FOR PROTOTYPE AND MICROCONCRETE  
(after Aldridge and Breen, 1968)



Shaft resistance on pile element

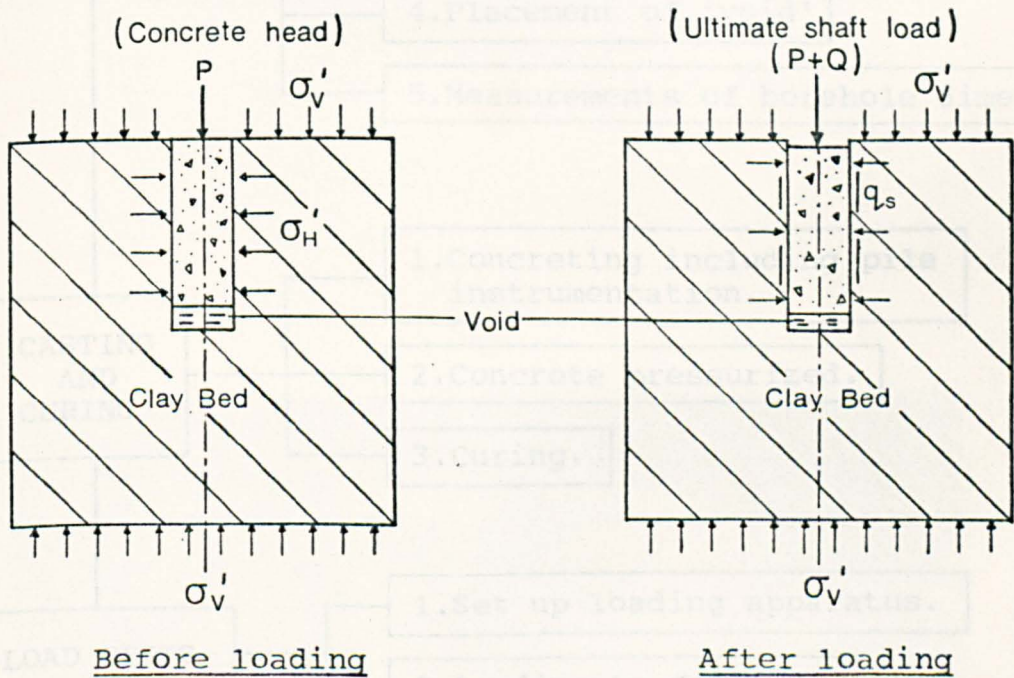


Fig.6.7 STRESSES SURROUNDING THE 'MODEL' PILE

Fig. 6-8 SUMMARY OF EXPERIMENTAL PROCEDURES

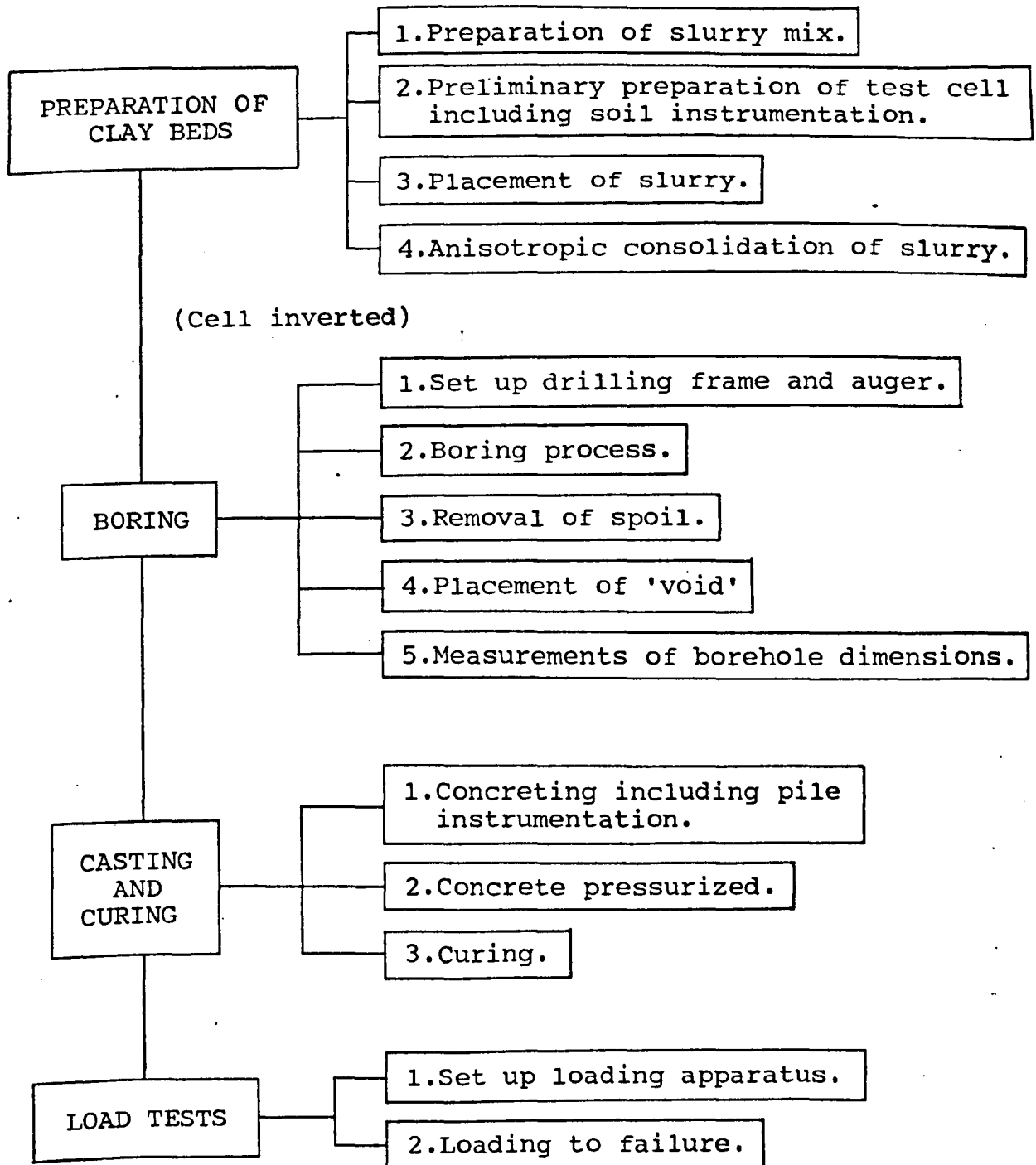


Fig. 6.8 SUMMARY OF EXPERIMENTAL PROCEDURES

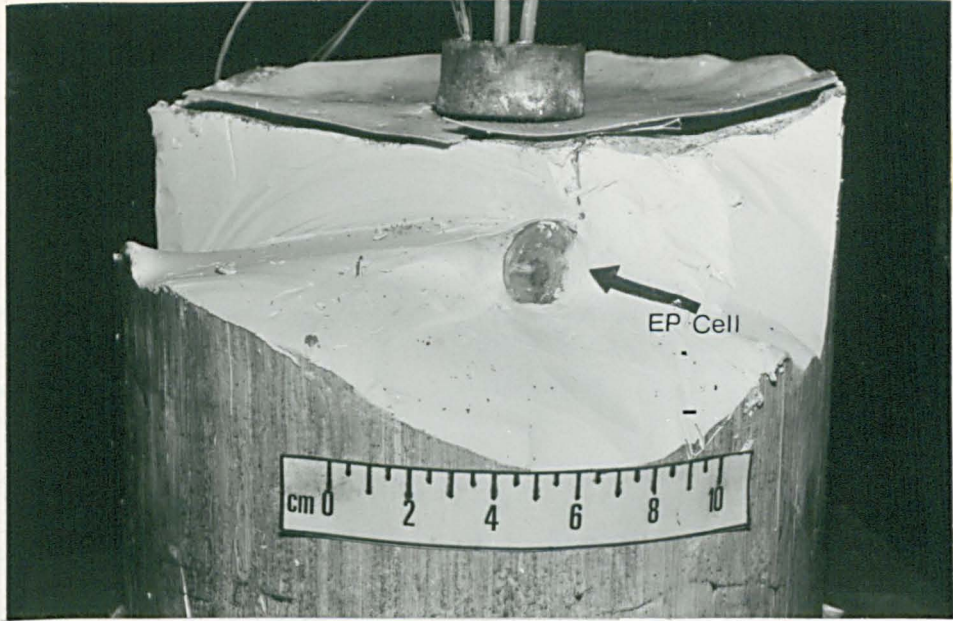


Fig. 6-9 (HORIZONTAL) EP PRESSURE CELL

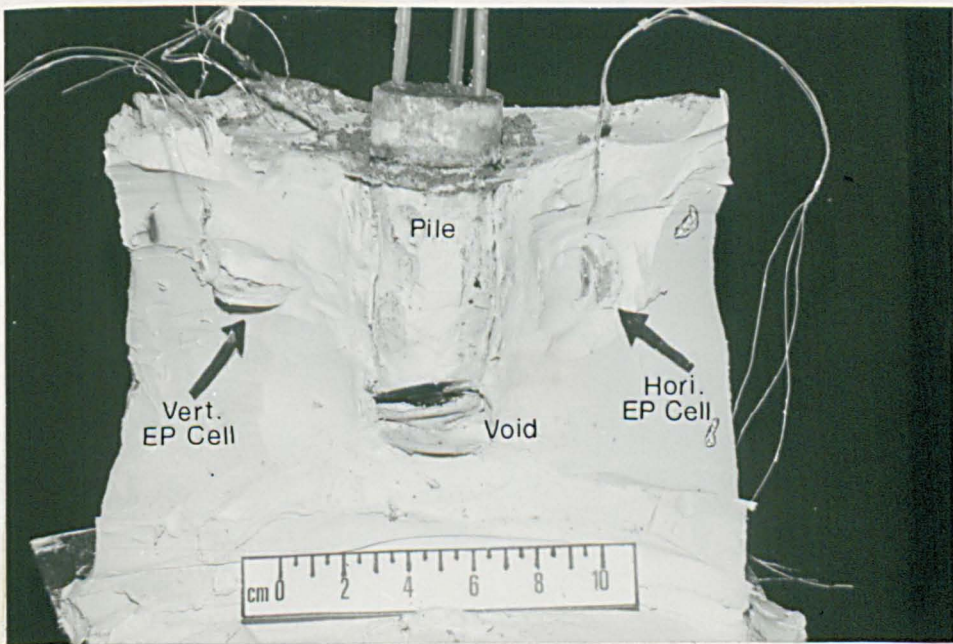
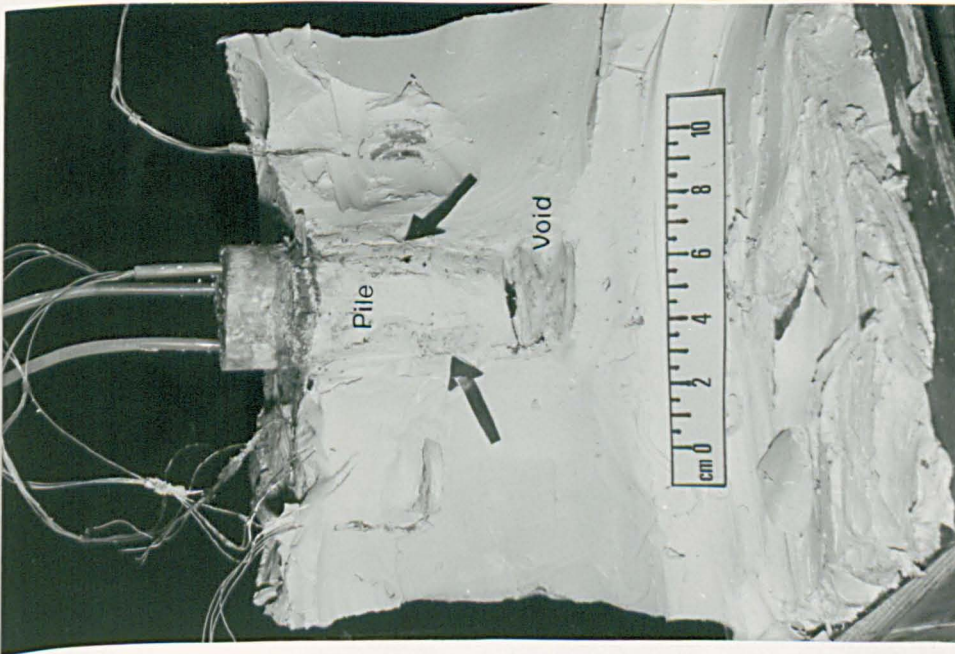
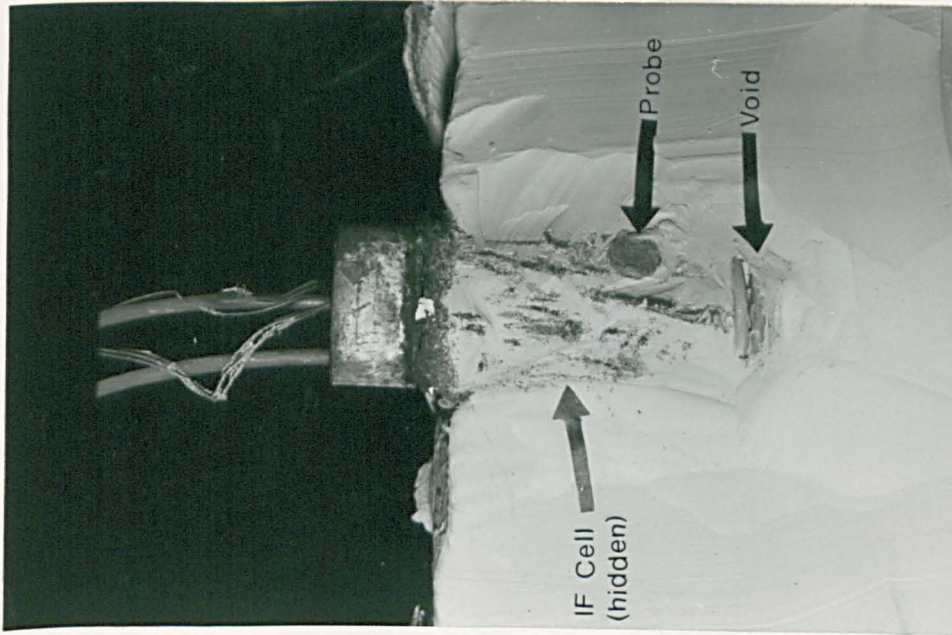


Fig. 6-10 LOCATION OF SOIL INSTRUMENTATION



(a)



(b)

Fig. 6.11 EXPOSED PILE SHAFT & LOCATION OF INSTRUMENTATION

CHAPTER 7  
PRESENTATION AND INTERPRETATION  
OF TEST RESULTS

7.1 INTRODUCTION

All the experiments carried out under the main and complementary test programs yielded a substantial quantity of data. These results were analyzed and compiled into various tables and are presented in this chapter. In tests where the results are not typical, typical results are given to illustrate significant features of all these tests.

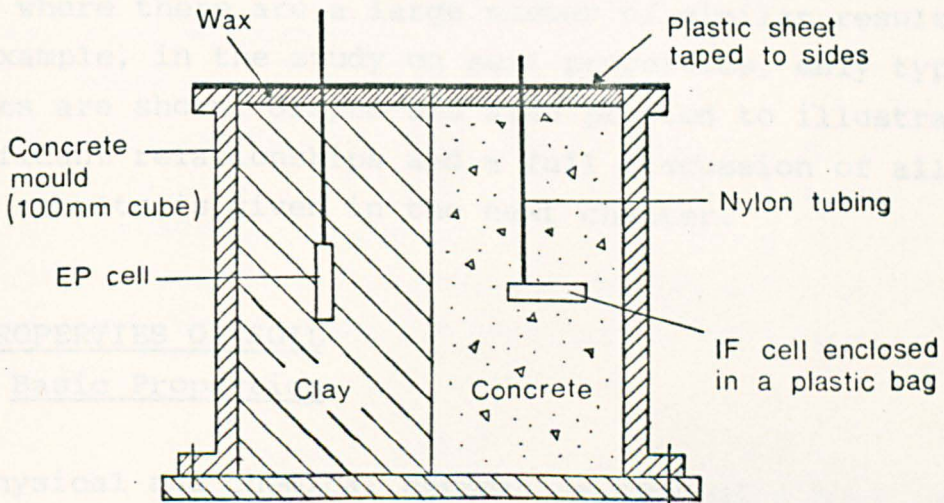


Fig.6.12 SET-UP FOR STABILITY TEST

From an initial slurry water content of 55% (based on the dry weight of the solids) the liquid limit, clay beds at water content of 55%, depending on the consolidation stress, the results obtained at the end of consolidation. The relationship between water content and consolidation stress is shown in Fig. 7.1. Bulk density data for the samples varied between 1.94 and 2.00 g/cm<sup>3</sup> for the range of consolidation stresses used in the tests.

The degree of saturation,  $S_v$  of the samples prepared ranged from 0.97 to 1.00. These values were based on (1) measurements of liquid limit and plastic limit.

## CHAPTER 7

### PRESENTATION AND INTERPRETATION OF TEST RESULTS

#### 7.1 INTRODUCTION

All the experiments carried out under the main and complementary test programme yielded a substantial quantity of data. These results were analysed and compiled into various tables and are presented in this chapter. In tests where there are a large number of similar results, for example, in the study on soil properties, only typical results are shown. Graphs are also plotted to illustrate significant relationships and a full discussion of all these results is given in the next chapter.

#### 7.2 PROPERTIES OF SOIL

##### 7.2.1 Basic Properties

The physical and chemical properties of kaolin used have been given in Table 6.4 (Section 6.3). Of relevance to this study are the Index properties. For the type of kaolin used, the liquid limit and plasticity index were found to be 72% and 36% respectively.

From an initial slurry water content of 140% (two times, the liquid limit), clay beds at water content of 41% to 55%, depending on the consolidation stress histories, were obtained at the end of consolidation. The relationship between water content and consolidation pressure is given in Fig. 7.1. Bulk density determined from triaxial test samples varied between  $1.69 \text{ Mg/m}^3$  to  $1.72 \text{ Mg/m}^3$  for the range of consolidation pressures used in the tests.

The degree of saturation,  $S_r$  of the clay bed prepared ranged from 0.97 to 1.00. These values were based on (i) the measurements of immediate response of piezometers

in the soil mass to the applied stress at the start of consolidation, and (ii) the pore pressure parameter B determined from consolidated-undrained triaxial tests with pore water pressure measurements. According to the work of Lowe and Johnson (1960), specimens with a degree of saturation within the range given could be considered to be fully saturated.

### 7.2.2 Consolidation and swelling characteristics

During the consolidation of the clay bed in the test cell, water expelled was measured at predetermined time intervals. A typical anisotropic consolidation curve given in Fig. 7.2 shows the relationship between the average degree of primary consolidation, U, and the logarithm of time for a pressure increment from 280 kN/m<sup>2</sup> to 420 kN/m<sup>2</sup>. The coefficient of consolidation, c<sub>v</sub>, was determined from the consolidation curve using the Casagrande 'Logarithm of time' method,

$$c_v = \frac{0.197H^2}{t_{50}} \quad \dots (7.1)$$

Values of c<sub>v</sub> measured over different pressure ranges are given in Table 7.1

To obtain the coefficient of volume compressibility, m<sub>v</sub>, results of consolidation data are plotted as void ratio versus consolidation pressure as shown in Fig. 7.3. The values of m<sub>v</sub> were determined from the equation,

$$m_v = - \frac{1}{(1+e_0)} \frac{\Delta e}{\Delta p} \quad \dots (7.2)$$

where  $\frac{\Delta e}{\Delta p}$  represents the slope of the curve over the specified pressure range and e<sub>0</sub> is the initial void ratio. Values of m<sub>v</sub> obtained varied between 0.76 m<sup>2</sup>/MN depending on the pressure range.

By plotting the void ratio versus consolidation pressure using a logarithm scale, the relationship yields straight lines as shown in Fig. 7.4. The compression index  $C_c$  which is the slope of the virgin consolidation line was found to be 0.600. When the sample was allowed access to water as load was removed, a change in void ratio occurred. The swelling indices, which are the slopes of the rebound curves, were found to be 0.066, 0.084 and 0.100 corresponding to overconsolidation ratios of 2, 3 and 4 respectively.

The coefficient of permeability,  $k$ , was obtained indirectly from the relationship,

$$k = c_v m_v \gamma_w \dots (7.3)$$

The values of  $k$  were of the order of  $10^{-9}$  m/s, which are typical of soil with low permeability. Values of  $k$  calculated for different pressure ranges are also shown in Table 7.1.

It should be stressed that the consolidation characteristics shown in Table 7.1 are measured over the pressure range indicated in the table. These pressure increments represent the stages in which the clay samples were consolidated to arrive at the maximum consolidation pressure required.

### 7.2.3 Strength properties

Within the range of stress histories considered, the consistency of clay beds varied from soft to firm. For the soft clay, it could easily be remoulded with the fingers, whereas for the firm clay, the soil could only be remoulded by strong pressure of the fingers. Values of undrained shear strength were determined by three methods: (i) laboratory vane shear tests, (ii) unconsolidated-

undrained triaxial tests and (iii) consolidated-undrained triaxial tests. Details of these tests have been given in Sections 4.4.2 and 4.4.3.

Typical deviator stress-strain curves for normally consolidated clay obtained from unconsolidated-undrained and consolidated-undrained triaxial tests are shown in Fig. 7.5. Failure stress is defined either by a peak in the stress-strain curves or by an asymptotic value as the curve approaches a horizontal straight line. For the unconsolidated-undrained test, the undrained shear strength was taken as one-half of the failure deviator stress. For the consolidated-undrained tests, the undrained shear strength was taken as one-half of the deviator stress obtained from the sample reconsolidated at a mean stress existing before sampling,  $\frac{(1+2K_0)}{3} p$ , where  $p$  is the vertical consolidation pressure. For the vane shear tests, the shear strength was read directly from the vane shear apparatus.

The average shear strength obtained using these three test methods are shown in Table 7.2. The results from the vane shear tests and unconsolidated-undrained triaxial tests gave approximately similar values whereas results obtained from consolidated-undrained triaxial tests are about twice those obtained from the other two methods. For normally consolidated clay,

$$\frac{c_1}{p} = 0.10 \quad \text{and} \quad \frac{c_2}{p} = 0.20$$

where  $c_1$  is the average of vane shear and unconsolidated-undrained tests,  
 $c_2$  is the mean value from consolidated-undrained tests, and  
 $p$  is the  $\Delta$  consolidation (overburden) pressure.

Similar differences in undrained shear strength obtained by different methods have also been observed by various authors. Berre and Bjerrum (1973) reported an increase

of 60% in the shear strength of Drammen Clay when samples were reconsolidated in the triaxial cell. Eid (1978), using the same soil type and sampling procedure as in this study, also found that reconsolidated-undrained tests gave approximately twice the values from undrained tests without reconsolidation. Arman et al. (1975) found that field vane shear tests yielded shear strength values which were twice those obtained using the laboratory vane shear test, using unconfined compression tests and using unconsolidated-undrained triaxial tests. These conclusions were based on results of about 500 tests carried out on soft normally consolidated clays.

The low values from the laboratory vane shear and unconsolidated-undrained tests are probably due to swelling and disturbance inherent in the sampling and testing procedure. To conduct tests by the laboratory vane shear apparatus or to obtain triaxial samples, the test cell had to be dismantled to gain access to the clay beds. This inevitably led to a relief of overburden pressure. Although there were no measurable water content changes during triaxial sampling or vane shear testing, the strain resulting from the stress relief might influence the strength of clay [Skempton and Sowa (1963)]. Effective stresses were therefore lower than they would have been had the test represented 'in-situ' conditions.

On the other hand, samples reconsolidated under stresses applied during the consolidation of soil samples may simulate the effective stress condition of the undisturbed soil. Since reduction in water content resulting from reconsolidation was small (< 1%), then according to Berre and Bjerrum (1973), the results of consolidated-undrained tests can be considered to be representative of the 'in-situ' strength. However, Bishop and Henkel (1962) suggest that reconsolidation affects the value of pore pressure parameter  $A_f$  which is sensitive to resulting

modification in soil structure. This in turn leads to undrained shear strength much higher than the 'in-situ' value.

The actual undrained strength probably lies somewhere between the two sets of values, that is  $\frac{c}{p}1 = 0.10$  and  $\frac{c}{p}2 = 0.20$ . However, based on the observation of significant swelling when the clay bed was removed from the test cell and the effects of sampling, it would be reasonable to assume that values from consolidated-undrained tests represent a better estimation of the shear strength. In fact, consolidated-undrained test results for normally consolidated clay appear to be closer to the value of  $\frac{c}{p} = 0.24$ , obtained from the empirical relationship given by Skempton (1954),

$$\frac{c}{p} = 0.11 + 0.0037 I_p \quad \dots (7.5)$$

Despite the difference in the two sets of experimental values for  $c/p$ , it is interesting to note that each of the three methods gave consistent values of undrained shear strength, although unconsolidated-undrained triaxial tests showed some slight scatter. In the analysis of pile load tests, undrained shear strength obtained from consolidated-undrained tests were used, while results from vane shear tests were used as a quick quality control check on the homogeneity of the clay beds as well as in the study of installation effects. A plot of the undrained shear strength obtained from vane shear tests and from consolidated-undrained triaxial tests is shown in Fig. 7.6.

The variation of undrained shear strength (obtained from consolidated-undrained triaxial tests) with stress history is shown in Fig. 7.7. As can be seen, the values of undrained shear strength increase with an increase in consolidation pressure and overconsolidation ratio.

Pore pressure parameters obtained from consolidated-undrained tests are given in Table 7.3. Values of  $B$  for both normally and overconsolidated clay varied between 0.97 to 1.00 implying that the samples were essentially saturated. Values of  $A_f$  were plotted against the logarithm of overconsolidation ratio in Fig. 7.8(a) and found to be in good comparison with Skempton (1954). If plotted in an alternative form as shown in Fig. 7.8(b),  $A_f$  is found to be inversely proportional to the overconsolidation ratio.

#### 7.2.4 Effective stress parameters

Since pore water pressures were measured during the undrained stage of the consolidated-undrained triaxial tests, results can be expressed in terms of effective stress. For normally consolidated clay, the effective stress parameters  $c'$  and  $\phi'$  were found to be zero and  $20^\circ$  respectively. For overconsolidated clay at an overconsolidation ratio of 4, the effective stress parameters  $c'$  and  $\phi'$  are  $7 \text{ kN/m}^2$  and  $21^\circ$  respectively. Mohr stress circles for the consolidated-undrained triaxial tests are plotted in Fig. 7.9 for both normally and overconsolidated clays.

#### 7.2.5 $K_0$ studies

By installing earth pressure cells and piezometers in the clay beds as discussed in the previous chapter, the total soil stresses,  $\sigma_H$  and  $\sigma_V$ , and the pore water pressure,  $u$ , were measured during the entire process of anisotropic slurry consolidation. Hence, values of  $\sigma_H'$  and  $\sigma_V'$  and finally  $K_0$  were deduced.

Typical variation of  $\sigma_V'$ ,  $\sigma_H'$  and  $u$  during two different stages of consolidation are shown in Fig. 7.10 (pressure increment from 0 to  $70 \text{ kN/m}^2$ ) and Fig. 7.11 (pressure

increment from 280 to 420 kN/m<sup>2</sup>). For both cases the measured total vertical stress was fairly constant. However, readings of the total horizontal stress in the first stage of consolidation, that is from 0 to 70 kN/m<sup>2</sup> showed considerable scatter during the early part of consolidation (Fig. 7.10). This was thought to be due to the movement of water in the soil as a result of rapid dissipation of excess pore pressure. Any moisture movement in the soil will affect the sensitivity of the pressure cell. During the later part of consolidation, when the rate of dissipation decreased and when the soil system was near equilibrium, the readings of  $\sigma_H$  were fairly consistent. Hence the  $\sigma_H'$  curve is plotted only towards the end of the consolidation. For the other stages of consolidation, the trend of the effective horizontal stress is as shown in Fig. 7.11. At the end of primary consolidation, a small residual positive pore pressure of between 5 to 15 kN/m<sup>2</sup> was registered in all the samples prepared. This implies that there may be a threshold value of hydraulic gradient required to cause flow.

The relationship between horizontal and vertical effective stresses measured at the end of primary consolidation is shown in Fig. 7.12. The scatter is reasonably small and it is evident that a linear relationship exists between  $\sigma_H'$  and  $\sigma_V'$  for the entire range of virgin loading. Therefore, for normally consolidated clay,  $K_0$  is a constant at 0.64. During unloading,  $K_0$  values exceed 0.64 and increase as the overconsolidation ratio increases and eventually exceed unity. This behaviour can be explained in terms of the fabric orientation of the samples and the associated swelling potential in the unloading stage. Results of fabric studies by Abdelhamid and Krizek (1976) have shown that normals to the particle surfaces are parallel to the direction of the major principal consolidation stress. This observation suggests that the vertical swelling pressure is larger than the horizontal one.

The variation of measured values of  $K_0$  with stress history is shown in Fig. 7.13, together with the results of Parry and Nadarajah(1974)who obtained  $K_0$  values using an instrumented oedometer. The slight difference in results may be attributed to the different techniques used in determining the values of  $K_0$ . In general, the results indicate that the stress history of the soil governs the coefficient of earth pressure at rest. From this graph, it can be seen that  $K_0$  is greater than unity at an overconsolidation ratio (OCR) of about 2.75. Values of  $K_0$  measured are summarised in Table 7.4.

Reported measurements of  $K_0$  for kaolinite clay by other authors are given in Table 7.5 as a basis of comparison with the measured values in Table 7.4. It can be seen that the  $K_0$  value found in this study for normally consolidated kaolin is of the same order as that reported by other authors. For overconsolidated clay,  $K_0$  is greater than unity at an overconsolidation ratio of about 2 to 2.7, which is slightly less than the value obtained from this study.

Values of  $K_0$  can also be obtained from any of the semi-empirical methods listed in Tables 3.1 and 3.2 (Section 3.3). Taking  $\phi' = 20^\circ$  as determined from consolidated-undrained triaxial tests and  $I_p = 36\%$ , the values of  $K_0$  for normally and over-consolidated kaolin clay were calculated and are tabulated in Table 7.6. For normally consolidated clay, the measured values were reasonably close to all the empirical values except that obtained using Alpan's method (1967). For overconsolidated clay, the best estimates of  $K_0$  are those predicted by Schmertmann (1975) and Wroth (1975) which lie within 5% of the measured values.

In general, the results have shown that reliable estimates of  $K_0$  for normally and overconsolidated clays can be obtained from the semi-empirical methods available.

## 7.3 SHORT TERM EFFECTS OF INSTALLATION ON SOIL PROPERTIES

### 7.3.1 General

The effects of installation on moisture migration and changes in soil strength were studied to complement the understanding of the soil-pile interaction. Results presented in this section are based on Test Series ST5. In these tests, samples for moisture content determination were taken at various positions in the clay bed 7 days after casting of pile using a special sampling tube described in Section 4.4.1. Soil shear strength was also determined at various positions using a laboratory vane shear apparatus. Procedures for the preparation of clay beds and the installation of piles were the same as those described for other tests, except that in this Test Series, the piles were not loaded. It should also be noted that during sampling and testing, the cell cover was removed to gain access to the clay beds.

Results of the study of moisture migration and the study of soil strength changes are first presented in separate sections and then compared in Section 7.3.4. These results are then used to correlate with the load test results since they provide an indication of the condition of the soil adjacent to the pile prior to loading.

### 7.3.2 Moisture Migration Study

Predominant factors affecting moisture migration were investigated. These include the influence of initial water content (i.e. consolidation pressure) and the water-cement ratio of microconcrete. Results obtained from the study are given in Tables 7.7 and 7.8. The moisture contents shown are the average of at least 5 samples. The initial moisture content was obtained from the material taken out of the borehole when the pile was installed.

Results given in the tables were based on samples obtained at the level of about the mid-height of the pile. The average increase in moisture content in the first 20mm from the interface is denoted by  $\Delta w\%$ . This symbol indicates the degree of moisture migration in the soil close to the pile. The constants for the tests are shown in the last column of the tables. Test ST5.5 which was to investigate the effect of using a water-cement ratio of 0.4 was not carried out because of the difficulty in forming an integral pile as a result of the low workability and inadequate self compaction of the concrete.

Results from the tables are plotted in the form of graphs to show the trend. The influence of the initial moisture content on moisture migration in the soil surrounding the pile is plotted in Fig.7.14. In all the tests, there is a distinct increase of moisture content towards the interface (Fig. 7.14a). This observation appears to be in general agreement with observations by various authors reported in Section 2.4.3. Since the greatest change in moisture content occurred in the soil within a radial distance of 20mm from the interface, it is reasonable to assume that the degree of softening was highest within this region. It is also interesting to note that beyond 60mm the moisture content of the soil is relatively unaffected by the pile installation. This observation again agrees with the experimental and field data reported in Table 2.5 (Section 2.4.3) where the thickness of affected zone was generally reported to be about 50mm.

Results in Fig.7.14(b) also showed that the higher the initial moisture, the lower is the average increase  $\Delta w\%$ . The possible explanation for this observation lies with the fact that the movement of water in the ground depends on the gradient of the pore water pressure; the water moving to areas where absolute pressure is lowest. The lower initial moisture content corresponds to a greater

consolidation pressure. Therefore, the greater the magnitude of stress relief after boring, the greater will be the negative pore pressure set up at the soil interface. Since negative pore pressure sets up a differential pressure gradient, excess moisture flows from the concrete into the soil. It therefore follows that the higher the consolidation pressure, the higher will be the average increase  $\Delta w$ .

The influence of water-cement ratio on moisture migration is shown in Fig.7.15. From the figure, it is apparent that the higher the water-cement ratio, the higher is the average increase in moisture content in the first 20mm from the interface. This is probably due to the greater amount of excess water available in concrete with a higher water-cement ratio. The graph in Fig.7.15(b) shows a linear relationship between the water-cement ratio and  $\Delta w\%$ . For an increase of 0.1 in water-cement ratio, there is a possible increase of  $\Delta w$  of approximately 2.0%. It is interesting to note that the theoretical value of water-cement ratio required for complete hydration of cement is 0.38 (Neville, 1973). If water-cement ratio lower than 0.38 was used, then it is more likely that the excess water causing the increase in  $\Delta w$  would come from the soil away from the pile, thus giving a hypothetical graph indicated by the broken line . However in practice, it is unlikely that a water-cement ratio of less than 0.45 is used since the construction of bored piles requires a concrete mix of adequate workability as discussed in Section 2.3.6.

### 7.3.3 Changes in undrained shear strength

Part of the scope of investigation was to study the consequence of pile installation on the undrained shear strength properties of the soil. The change in undrained shear strength with respect to the undisturbed undrained

strength will be termed the remoulding factor, ' $\alpha_r$ '. This factor will indicate the degree of softening that has occurred as a result of pile installation.

It has been discussed in Section 7.2.3 that laboratory vane shear apparatus gives low values of undrained strength. However, in this study, the absolute value is not of primary importance; only the relative values are of interest to indicate the trend in the changes of strength. The laboratory vane shear apparatus provides a quick and consistent method of determining the relative shear strength of the soil. In a similar manner to the moisture migration study, the shear strength of the clay was measured at various distances from the pile interface, at a depth equal to the mid-height of the pile. Because of the obvious difficulty in measuring the soil strength at the interface, the strength which was measured at a distance of about 20mm from the pile shaft was assumed to be the strength value of soil close to the interface.

Tables 7.9 and 7.10 show the influence of consolidation stress history and the water-cement ratio on the remoulding factor. Values of undrained shear strength are quoted to the nearest  $0.5 \text{ kN/m}^2$  and are based on the average of at least 5 measurements. Results from the tables are plotted in Figs. 7.16 and 7.17.

In Fig.7.16, it can be seen that the higher the consolidation pressure, the lower is the remoulding factor. When the results in Fig.7.16 are compared with those in Fig.7.14, it can be seen that the greater the increase in water content, the greater is the degree of softening. Although, the effect of overconsolidation was not investigated, it appears reasonable to assume that the higher the overconsolidation ratio, the lower is the remoulding factor. This can be attributed to the fact that as overconsolidation ratio increases, the initial water content decreases (Fig.7.1), leading to an increase in the value of  $\Delta w\%$

after pile installation. This implies a greater degree of softening and hence a lower remoulding factor. This effect is discussed further in the next section. It can also be seen from Fig. 7.16 that for a distance greater than 60mm from the pile shaft, the undrained shear strength remains relatively unaffected and significant changes appear to be confined to a narrow zone of soil 20mm from the pile shaft.

In Fig. 7.17, the graph shows a linear relationship between water-cement ratio and the remoulding factor. An increase in water-cement ratio of 0.1 appears to cause a strength reduction of about 15%. Again, if the graph is extrapolated, when  $\alpha_r = 1$ , i.e. no loss in strength, the water-cement ratio is 0.32. However, this conclusion is hypothetical, since a number of factors are involved in the remoulding of soil. Furthermore, for reasons given in Section 2.3.6 as regards the need for good workability, it is unlikely that this water-cement ratio will be used in practice. Nevertheless, it is of interest to compare this deduction with the work of Meyerhof and Murdock (1953). These authors reported that no softening or moisture increase was observed in the soil adjacent to the pile when a water-cement ratio of 0.2 was used for a bored pile constructed in London Clay. However, in view of the very low workability of the concrete, the structural integrity of the bored pile constructed is in question.

#### 7.3.4 General relationship between moisture migration and changes in soil strength

From results presented in the previous sections, there appears to be a direct relationship between the increase in moisture content and the changes in undrained strength of the soil. Generally, the reduction in shear strength of the soil after concreting the borehole is found to be influenced by the initial moisture content of the soil

and the water-cement ratio of the concrete mix.

The relationship between the remoulding factor and the initial moisture content of the soil is shown in Fig. 7.18. It can be seen that the lower the initial moisture content, the lower is the remoulding factor. It has been shown in Fig. 7.1 that the stress history is related to the water content of the soil. The higher the consolidation pressure or overconsolidation ratio, the lower is the initial moisture content of the soil. Therefore, after boring, the magnitude of stress relief is greater for soil consolidated at higher pressure and overconsolidation ratio. Excess water from the concrete will flow into the soil until the excess negative pore pressure equalises. The amount of water flowing into the soil depends on the magnitude of the negative pore pressure.

The relationship between the remoulding factor and the average increase in moisture content of soil within 20mm from the pile face is shown in Fig. 7.19. It can be seen that for the range of stress history and water-cement ratio considered, an increase of 1% in moisture content of soil close to the pile reduces the undrained shear strength by 7%.

However, it should be appreciated that all the measurements for moisture content and shear strength presented were taken 7 days after casting. The main aim was to correlate these results with the pile load test results conducted after a 7-day curing period. Therefore, moisture content may have increased significantly in the first few days and then started to decrease as observed by Taylor (1966). This observation has been shown in Fig. 2.8. In other words, measurements of moisture content at 7 days after casting may be less than those during the first few days after casting. Similarly, shear strength at 7 days may be higher than the value soon after casting of pile.

Nevertheless, all the graphs presented show important trends which are consistent with field behaviour. In this study, the increase in moisture content of the soil close to the pile varied between 2% to 6% and the thickness of the affected zone was about 60mm from the pile shaft. Both these results compare well with field studies reported in Table 2.5 (Section 2.4.3) in which the corresponding values observed were 2% to 8% and 50mm respectively.

#### 7.4 LONG TERM INSTALLATION EFFECTS ON SOIL PROPERTIES

##### 7.4.1 General

For bored piles, the mutual migration of water between concrete and the surrounding soil goes on for a certain length of time. Since the load carrying capacity of the shaft is directly related to the shear strength at the time of loading, it was necessary to study the effect of moisture migration on changes in the shear strength of the soil.

For the long term tests, piles were constructed in two separate test cells containing clay beds consolidated at  $420 \text{ kN/m}^2$ , both to be as similar as practically possible. One test pile was loaded while the other was used for the purpose of studying moisture migration and changes in soil strength. Moisture content was taken at various distance from the interface while the shear strength was measured for soil within the zone of soil at a distance of 20mm from the pile shaft. This zone of soil is referred to as the zone of soil close to the pile in the subsequent discussions. All measurements were taken at a level equal to the mid-length of the pile. Results shown are the average of at least five measurements.

#### 7.4.2 Influence of curing time on moisture migration

Results of moisture content determinations after a specified curing time are given in Table 7.11 and the relationship between moisture content and curing time is shown in Fig. 7.20. It can be seen from this graph that changes in moisture content are significant for soil within 20mm from the pile interface and relatively unaffected for soil at a distance greater than 60mm from the interface. With increase in time after concreting, the moisture content of soil close to the pile decreases until it reaches its original value in about 60 days.

The decrease in moisture content in the soil close to the pile is due to the migration of water to the soil away from the pile (soil between a distance of 20 to 60mm shows some increase in moisture content as can be seen in Fig. 7.20) and movement of water into the porous hardened concrete. The latter reason was deduced from the work of Taylor (1966), shown in Fig. 2.8, in which the author demonstrated the presence of water in the concrete about 40 days after casting under laboratory conditions. This is attributed to the affinity of the porous concrete to water. It may also be due to the difference in pore pressure gradient between the soil adjacent to the pile and the hardened concrete.

At great age, between 60 and 300 days, the moisture content of the soil close to the pile is slightly below its original moisture content. This observation can be similarly explained by the reasons given in the previous paragraph.

Since there was no environmental source of moisture as in the field, the only source of excess water causing the changes in moisture content was from the microconcrete mix. It is not possible that moisture was gained from or lost to the atmosphere since the test cell is essentially a sealed system.

### 7.4.3 Influence of curing time on shear strength

Shear strength measurements were taken at a distance of about 20mm from the pile shaft with a laboratory vane shear apparatus after a specified curing time. Results are shown in Table 7.12. Values of shear strength in the table are based on the average of at least 5 measurements.

The relationship between changes in soil strength, expressed as the remoulding factor,  $\alpha_r$ , and the curing time is shown in Fig. 7.21. From the graph plotted, the shear strength appears to regain its initial undrained strength after about 60 days and in fact shows a slight increase thereafter. This observation has important implications for load tests carried out on piles after a short curing time. Since insufficient time was available for equilibrium conditions to be established in the soil around the test pile, load test results would be an underestimation of the actual long term value.

The average increase in moisture content of the soil close to the pile is also plotted in Fig. 7.21 to illustrate the relationship between the remoulding factor and increase (or decrease) in moisture content. The comparisons again indicate the direct correlation between the moisture content and undrained shear strength of the soil.

The implications of the effects of time on moisture migration and changes in soil strength are discussed in greater detail in the next chapter.

## 7.5 RESULTS OF LOAD TESTS ON PILES

Compression load tests were performed in accordance with the procedure described in Section 6.5. For the short term (ST) series, piles were tested 7 days after casting, whereas

in the long term (LT) series, six similar piles were tested at ages varying from 14 days to 300 days. All piles were tested until 'plunging' failure occurred; this is defined as the load at which the piles continue to settle excessively without additional application of load.

Results of load tests on piles are given in Table 7.13. The failure loads ranged from 260 N to 845 N depending on the stress history and variables and the values are quoted to the nearest 5 N. The shaft resistance,  $q_s$ , was obtained by dividing the failure load by the surface area of the pile shaft. The area of the shaft was based on actual pile measurements with average pile diameter varying between 37.6 and 38.2 mm and length varying between 80 and 100 mm.

In general, the shaft resistance mobilized increased with higher consolidation pressure and overconsolidation ratio. There is also an increase in shaft resistance with piles tested at great age. Results of load tests will be analysed in greater detail in the next chapter in terms of total and effective stress and correlated with the results of soil properties and the effects of pile installation. Only typical features of the load tests are discussed in this section.

A typical load-settlement-time relationship is shown in Fig. 7.22. The load-time plot shows the time for which each increment of load was applied. The load test to pile failure usually took between 4 to 6 hours. The load-settlement curve indicates a quick build-up of resistance. On removal of the load, there is a rebound. In general, rebound was of the order of 15 to 30% of total settlement for all the piles tested. Since the pile is short and the load is small, elastic compression of concrete shaft is negligible. Therefore, rebound is due either to the expansion of soil or to the release of stress along the shaft.

For comparison of results, it is sometimes convenient to plot some of the curves using dimensionless parameters. A typical plot of shaft resistance divided by the maximum consolidation pressure versus settlement ratio is shown in Fig. 7.23. Settlement ratio is defined as the ratio between the settlement and pile diameter. For the piles tested, the settlement just before plunging was generally between 0.4 and 1.5% of the pile diameter and was assumed to be the value in which the shaft resistance was fully mobilized. The range in values are in reasonable agreement with reported laboratory and field studies that shaft resistance of bored pile in clay is mobilized at very low settlement, of the order of 0.5 to 1.0% of the shaft diameter (Section 2.5.1). Since settlement is relatively small, the results suggest that it is unlikely to be a major criterion in the design of the shaft resistance of bored piles.

The mobilization of shaft resistance appears to follow a parabolic law as shown in Fig. 7.24. It is interesting to note that the pile begins to settle only when 25% of the maximum shaft resistance is mobilized. This is typical for most tests. Full mobilization of shaft resistance occurs after a settlement of about 0.9% of the pile diameter. The deviator stress-strain curve obtained from a consolidated-undrained triaxial test on the kaolin is also plotted as a broken line in Fig. 7.24. Despite the fact that the soil in the triaxial test was subjected to triaxial stresses as opposed to the shear stresses of the soil at the pile interface, there is a similarity in stress-strain behaviour. However, it should be noted that the degree of agreement between the two sets of curves is a function of the scale chosen for the axes of the graph.

TABLE 7.1 CONSOLIDATION CHARACTERISTICS OF KAOLIN

COEFFICIENTS	SYMBOL	UNIT	PRESSURE RANGE OVER WHICH COEFFICIENTS ARE MEASURED (kN/m <sup>2</sup> )			
			70 → 140	140 → 280	280 → 420	420 → 560
COEFFICIENT OF CONSOLIDATION	c <sub>v</sub>	m <sup>2</sup> /yr	8.0	9.8	11.5	13.5
COEFFICIENT OF VOLUME COMPRESSIBILITY	m <sub>v</sub>	m <sup>2</sup> /MN	0.76	0.41	0.28	0.22
COEFFICIENT OF PERMEABILITY (x10 <sup>-9</sup> )	k	m/s	1.92	1.27	1.02	0.92

TABLE 7.2 STRENGTH PROPERTIES

MAX. CONSOL. PRESSURE p kN/m <sup>2</sup>	OCR	MEAN SHEAR STRENGTH (kN/m <sup>2</sup> )			$\frac{c_1}{p}$	$\frac{c_2}{p}$
		VANE SHEAR	UU TRIAXIAL	CU TRIAXIAL		
140	1	13.5	15	29	0.10	0.21
280	1	26	29	56	0.10	0.20
420	1	39	44	84	0.10	0.20
560	1	52	58	110	0.10	0.20
280	2	24	28	53	0.19	0.38
420	3	36	39	74	0.27	0.53
560	4	48	50	95	0.35	0.68

TABLE 7.3 PORE PRESSURE PARAMETERS

OCR	CU TRIAXIAL TESTS	
	A <sub>f</sub> (average)	B (average)
1	0.96	0.99
2	0.38	0.98
3	0.18	1.00
4	0.07	0.99

TABLE 7.4 MEASURED VALUES OF  $K_0$

METHOD OF DETERMINATION	NORMALLY CONSOLIDATED	OVERCONSOLIDATION RATIO			COMMENTS
		2	3	4	
Direct measurement by horizontal and vertical soil pressure cells and pore pressure piezometers in the test cell.	$0.64 \pm 0.01$	0.82	1.06	1.21	$I_p = 36\%$ $\phi' = 20^\circ$

TABLE 7.5 SUMMARY OF REPORTED  $K_0$  MEASUREMENTS FOR KAOLINITE CLAY

	REFERENCES	METHOD OF DETERMINATION	$K_0$ VALUES			COMMENTS
			CONSOLIDATED	OVERCONSOL. OJR VALUE		
1.	Bishop (1958)	By triaxial tests	0.64 - 0.70	-	-	$I_p=23\%$ ; $\phi'=20.2^\circ$
2.	Burland(1967)	Zero lateral strain tests in oedometer	0.70			Spestone kaolin $I_p = 32\%$
3.	Parry and Nadarajah (1974)	Instrumented oedometer.	0.66	2.7	1	see Graph 7.13
4.	Abdelhamid and Krizek (1976)	Direct measurements from triaxial tests	0.68	2 8	1 $K_p$	Georgia kaolin-ite, $I_p=28\%$ $\phi'=18^\circ$
5.	Moore and Cole (1977)	(a)direct measurement by pressure transducer in consolidation cell	0.57	-	-	$I_p = 40\%$
		(b)direct measurement in triaxial apparatus.	0.55	-	-	
6.	Eid (1978)	Cavity expansion tests	0.66	1.5	0.82	Speswhite kaolin $I_p = 32\%$

TABLE 7.6 VALUES OF  $K_0$  CALCULATED  
FROM EMPIRICAL RELATIONSHIPS

(a) Normally consolidated clay

	REFERENCE		VALUE
1	Jaky (1944)		0.66
2	Rowe (1957)		0.64
3	Brooker and Ireland (1965)	(i) $\phi'$ method	0.61
		(ii) $I_p$ method	0.65
4	Alpan (1967)		0.55

(b) Overconsolidated clay

	REFERENCE	OVERCONSOLIDATION RATIO			
		1	2	3	4
1	Brooker and Ireland (1965)	0.61	0.79	0.92	1.04
2	Sherif and Koch (1970)	0.68	0.78	0.88	0.98
3	Schmertmann (1975)	0.66	0.88	1.04	1.18
4	Wroth (1975)	0.66	0.83	0.99	1.16
5	Meyerhof (1976)	0.66	0.93	1.14	1.32

TABLE 7.7 INFLUENCE OF INITIAL MOISTURE CONTENT ON MOISTURE MIGRATION

TEST NO	INITIAL MOISTURE CONTENT %	Average moisture content (%) at various distances from interface (mm)				$\Delta w$ (%)	CONSTANTS
		0-20	20-40	40-60	60-80		
ST5.1	54.8	57.5	56.2	55.3	54.9	2.7	Water-cement ratio = 0.6 Curing time = 7 days Diameter, D = 38mm
ST5.2	47.5	51.0	49.0	47.8	47.4	3.5	
ST5.3	44.3	48.5	45.6	44.6	44.1	4.2	
ST5.4	41.0	47.0	42.9	41.4	41.1	6.0	

( $\Delta w$  = average increase in moisture content of soil within 20mm from the pile interface)

TABLE 7.8 INFLUENCE OF WATER-CEMENT RATIO ON MOISTURE MIGRATION

TEST NO	WATER-CEMENT RATIO	Average moisture content (%) at various distance from interface (mm)				$\Delta w$ (%)	CONSTANTS
		0-20	20-40	40-60	60-80		
ST5.6	0.5	46.6	45.3	44.5	44.3	2.3	Initial moisture content 44.3% Curing time = 7 days Diameter, D = 38mm
ST5.3	0.6	48.5	45.6	44.6	44.1	4.2	
ST5.7	0.7	50.7	46.5	44.8	44.2	6.4	

TABLE 7.9 INFLUENCE OF STRESS HISTORY ON THE REMOULDING FACTOR,  $\alpha_r$

TEST NO.	MAX. CONSOLIDATION PRESSURE kN/m <sup>2</sup>	INITIAL VANE SHEAR STRENGTH $c_u$ (kN/m <sup>2</sup> )	VANE SHEAR STRENGTH $c$ (kN/m <sup>2</sup> ) TESTED AT VARIOUS DISTANCES FROM INTERFACE.				VALUES OF $\alpha_r = \frac{c}{c_u}$				CONSTANTS
			mm 20	40	60	80 mm.	$\alpha_1$	$\alpha_2$	$\alpha_3$	$\alpha_4$	
ST5.1	140	13.5	11	12.5	13.5	13.5	0.81	0.93	1.00	1.00	Water-cement ratio=0.6 Curing time = 7 days Diameter, D =38 mm
ST5.2	280	26	20	24	26.5	26.5	0.74	0.92	1.02	1.02	
ST5.3	420	39	25.5	32	39	39	0.65	0.82	1.00	1.00	
ST5.4	560	52	29.5	40	50	51.5	0.57	0.77	0.96	0.99	

Legend:  $\alpha_1, \alpha_2, \alpha_3, \alpha_4$  represents strength reduction at approximate distance of 20, 40, 60 and 80 mm from the pile face respectively.

TABLE 7.10 INFLUENCE OF WATER-CEMENT RATIO ON THE REMOULDING FACTOR,  $\alpha_r$

TEST NO.	WATER-CEMENT RATIO	INITIAL VANE SHEAR STRENGTH $c_u$ (kN/m <sup>2</sup> )	VANE SHEAR STRENGTH AFTER CASTING AND CURING, $c$ (kN/m <sup>2</sup> )	$\alpha_r = \frac{c}{c_u}$	CONSTANTS
ST5.6	0.5	39	30	0.77	Consolidation pres. =420 kN/m <sup>2</sup>
ST5.3	0.6	39	25.5	0.65	Curing time = 7 days
ST5.7	0.7	39	20.5	0.53	Diameter = 38 mm

TABLE 7.11 INFLUENCE OF CURING TIME ON MOISTURE MIGRATION

TEST NO		ST5.3	LT1.1	LT1.2	LT1.3	LT1.4	LT1.5	LT1.6
CURING TIME (days)		7	14	30	60	100	200	300
Average moisture content (%) at various distances from inter-face (mm)	0-20 mm	48.5	47.3	45.8	44.2	43.7	43.1	43.1
	20-40 mm	45.6	46.1	45.4	44.8	44.2	43.5	43.3
	40-60 mm	44.6	45.2	44.8	44.4	44.4	44.0	43.9
	60-80 mm	44.1	44.5	44.3	44.5	44.3	44.4	44.3

TABLE 7.12 INFLUENCE OF CURING TIME ON SHEAR STRENGTH

TEST NO	CURING TIME (days)	INITIAL SHEAR STRENGTH (VANE) $C_u$ (kN/m <sup>2</sup> )	SHEAR STRENGTH AFTER CASTING AND CURING $C$ (kN/m <sup>2</sup> )	$\alpha_r = \frac{C}{C_u}$	$\Delta w\%$
ST5.3	7	39 (average)	25.5	0.65	4.2
LT1.1	14		27.5	0.71	3.0
LT1.2	30		31	0.79	1.5
LT1.3	60		39.5	1.01	-0.1
LT1.4	100		40	1.03	-0.6
LT1.5	200		42	1.08	-1.2
LT1.6	300		41	1.05	-1.2

Constants for Table 7.11 and Table 7.12: water-cement ratio = 0.6  
 initial moisture content = 44.3%  
 consolidation pressure = 420 kN/m<sup>2</sup>  
 diameter, D = 38 mm

TABLE 7.13 RESULTS OF LOAD TESTS

TEST NO	MAXIMUM CONSOLIDATION PRESSURE p kN/m <sup>2</sup>	FAILURE LOAD N	MAXIMUM SHAFT RESISTANCE q kN/m <sup>2</sup>	SETTLEMENT PRIOR TO FAILURE Δ mm	RATIO OF SETTLEMENT TO PILE DIA. (Δ/D) %	VARIABLES
ST1.1	420	590	55.0	0.49	1.3	Normally consolidated
ST1.2	420	595	55.4	0.48	1.3	
ST1.3	140	260	22.0	0.30	0.8	
ST1.4	280	510	39.8	0.45	1.2	
ST1.5	420	585	54.6	0.36	0.9	
ST1.6	560	685	63.8	0.40	1.1	
ST2.1	140	265	22.2	0.34	0.9	OCR=1
ST2.2	280	355	29.7	0.26	0.7	2
ST2.3	420	440	36.9	0.19	0.5	3
ST2.4	560	510	42.7	0.15	0.4	4
ST3.1	420	385	52.4	0.30	0.8	File Dia. 25(mm)
ST3.2		600	54.8	0.38	1.0	38
ST3.3		845	60.0	0.60	1.2	50
ST4.1	420	570	52.9	0.48	1.3	Delay time 2(hrs)
ST4.2		520	48.7	0.44	1.2	12
ST4.3		465	43.7	0.34	0.9	24
LT2.1	420	635	59.2	0.39	1.0	Curing time 14 (days)
LT2.2		685	63.8	0.42	1.1	30
LT2.3		705	65.6	0.47	1.2	60
LT2.4		720	67.0	0.55	1.4	100
LT2.5		730	68.0	0.49	1.3	200
LT2.6		725	67.5	0.54	1.4	300

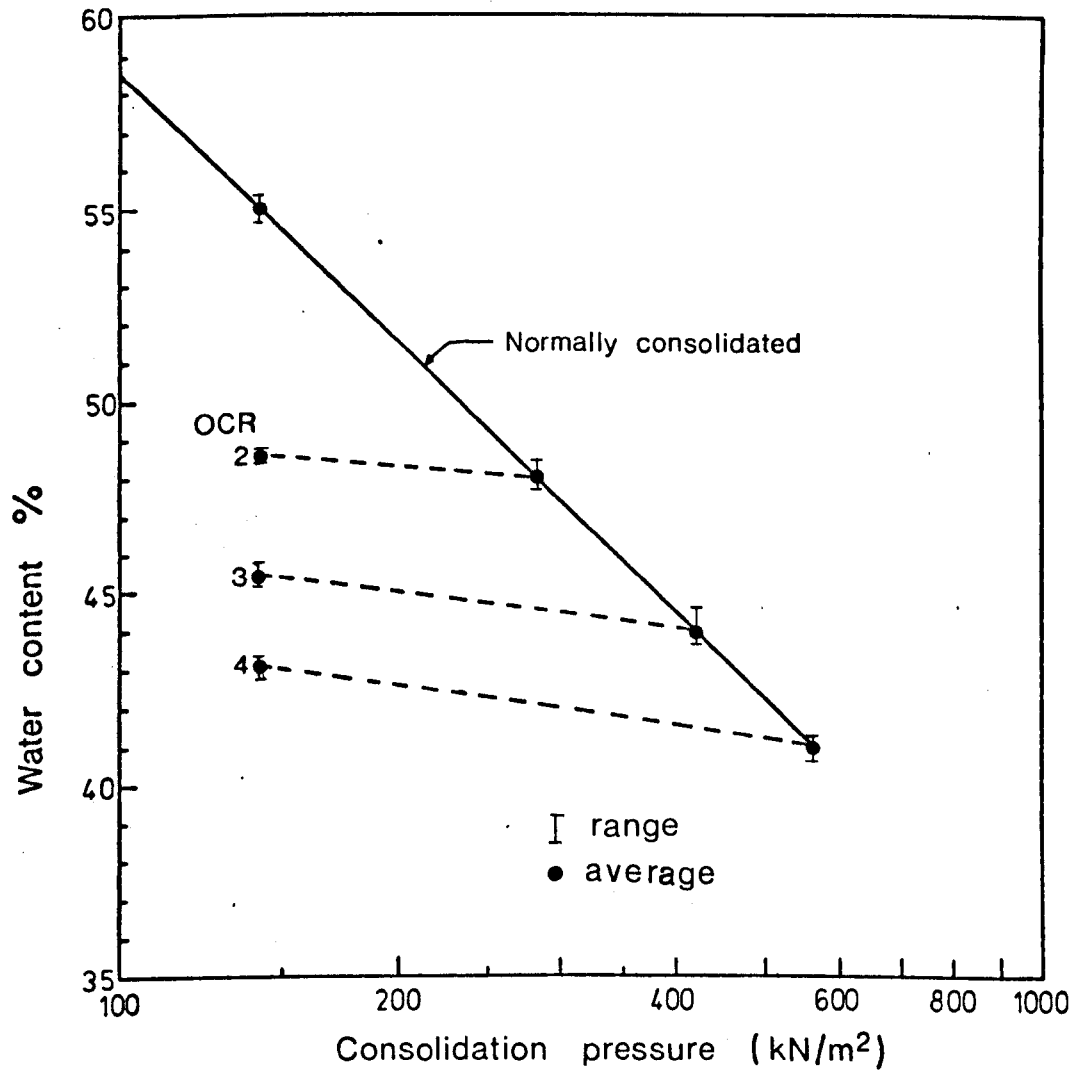


Fig.7.1 RELATIONSHIP BETWEEN WATER CONTENT AND CONSOLIDATION PRESSURE (LOGARITHM SCALE)

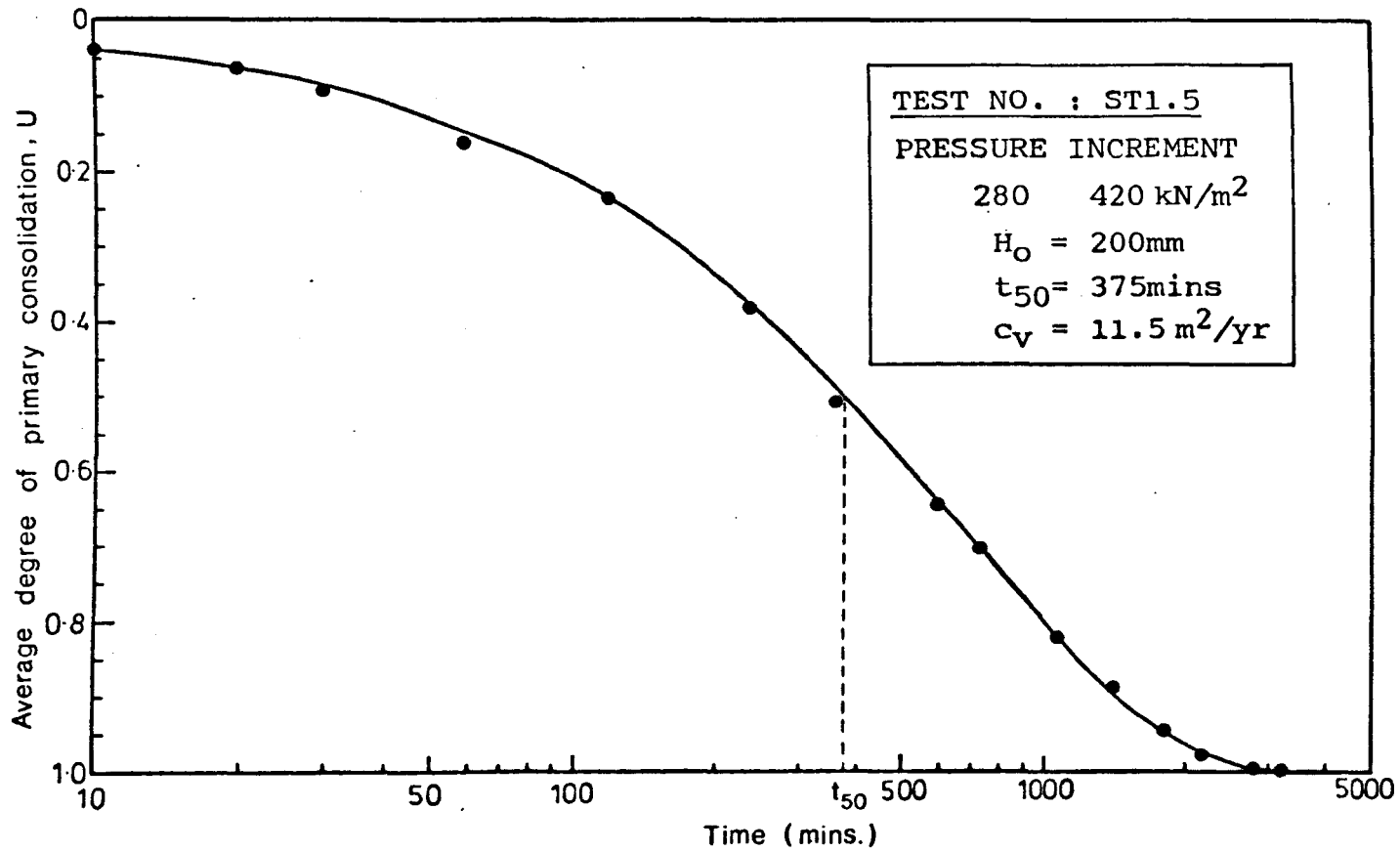


Fig. 7.2 TYPICAL CONSOLIDATION CURVE

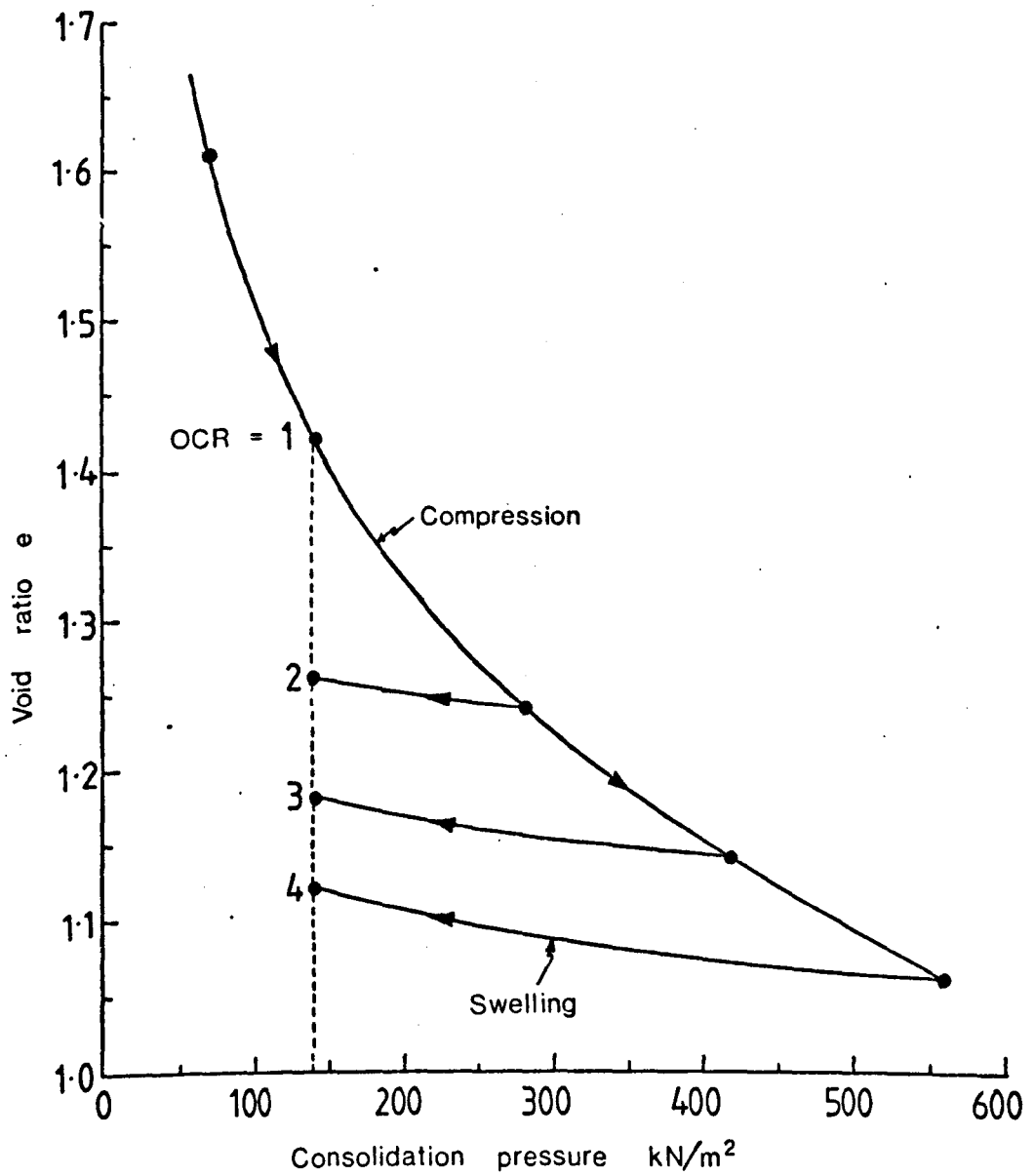


Fig.7.3 RELATIONSHIP BETWEEN VOID RATIO AND CONSOLIDATION PRESSURE

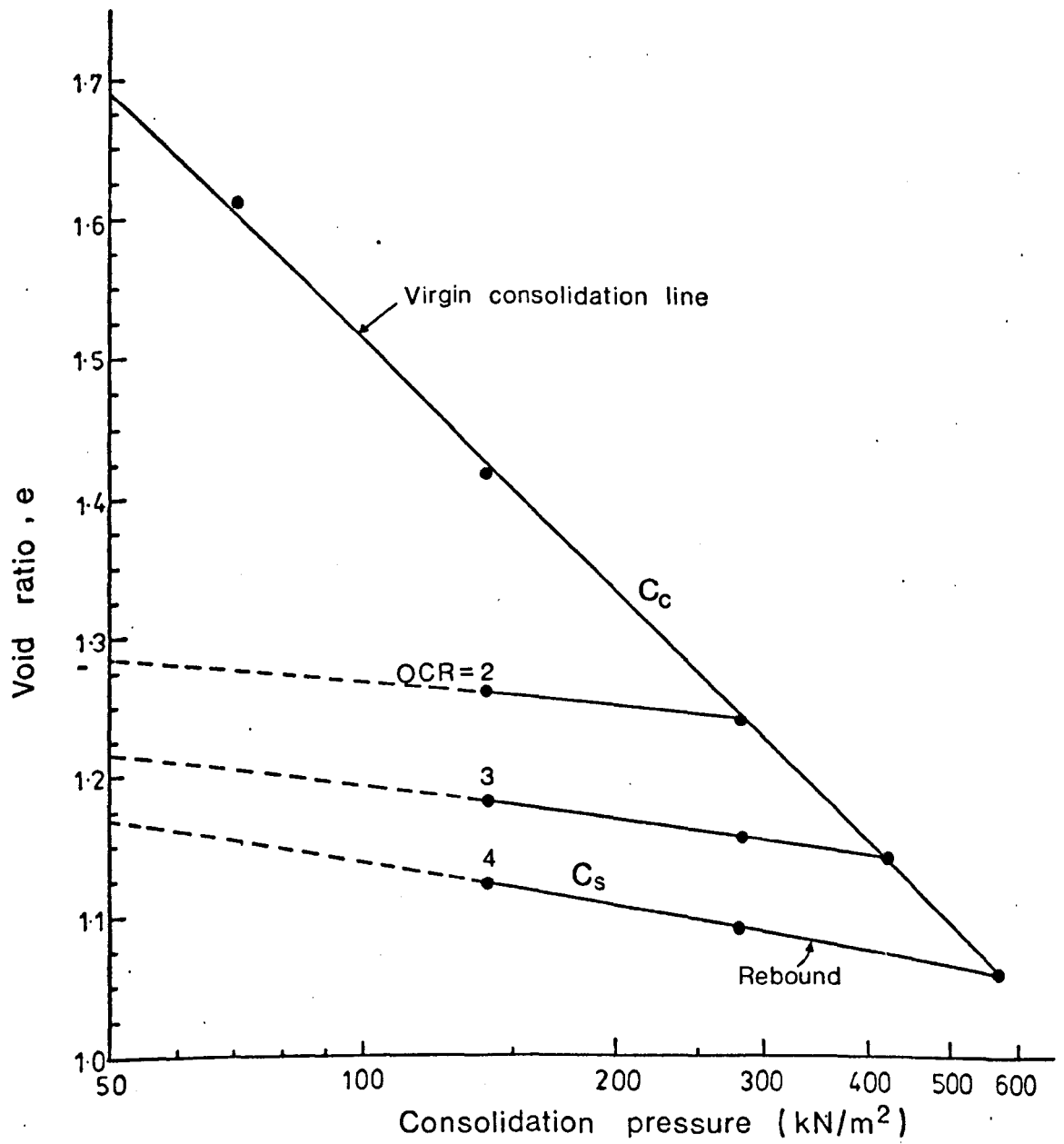


Fig.7.4 PLOT OF VOID RATIO VERSUS CONSOLIDATION PRESSURE (LOGARITHM SCALE)

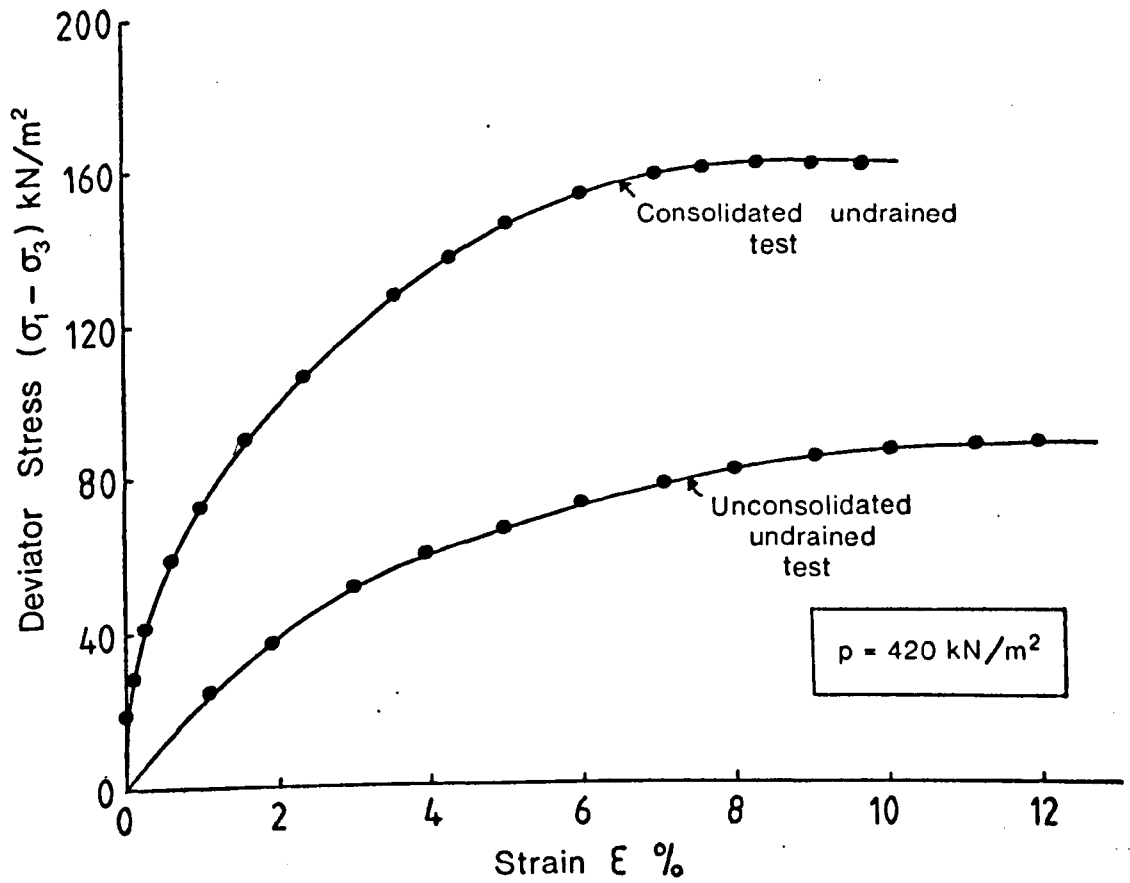


Fig.7.5 TYPICAL STRESS-STRAIN RELATIONSHIP

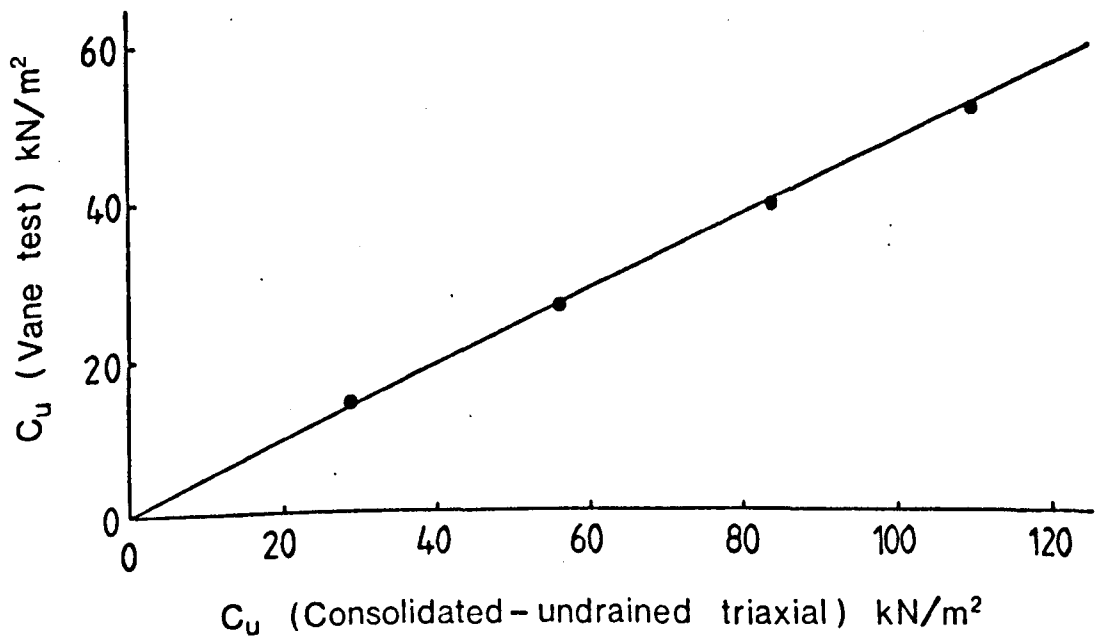
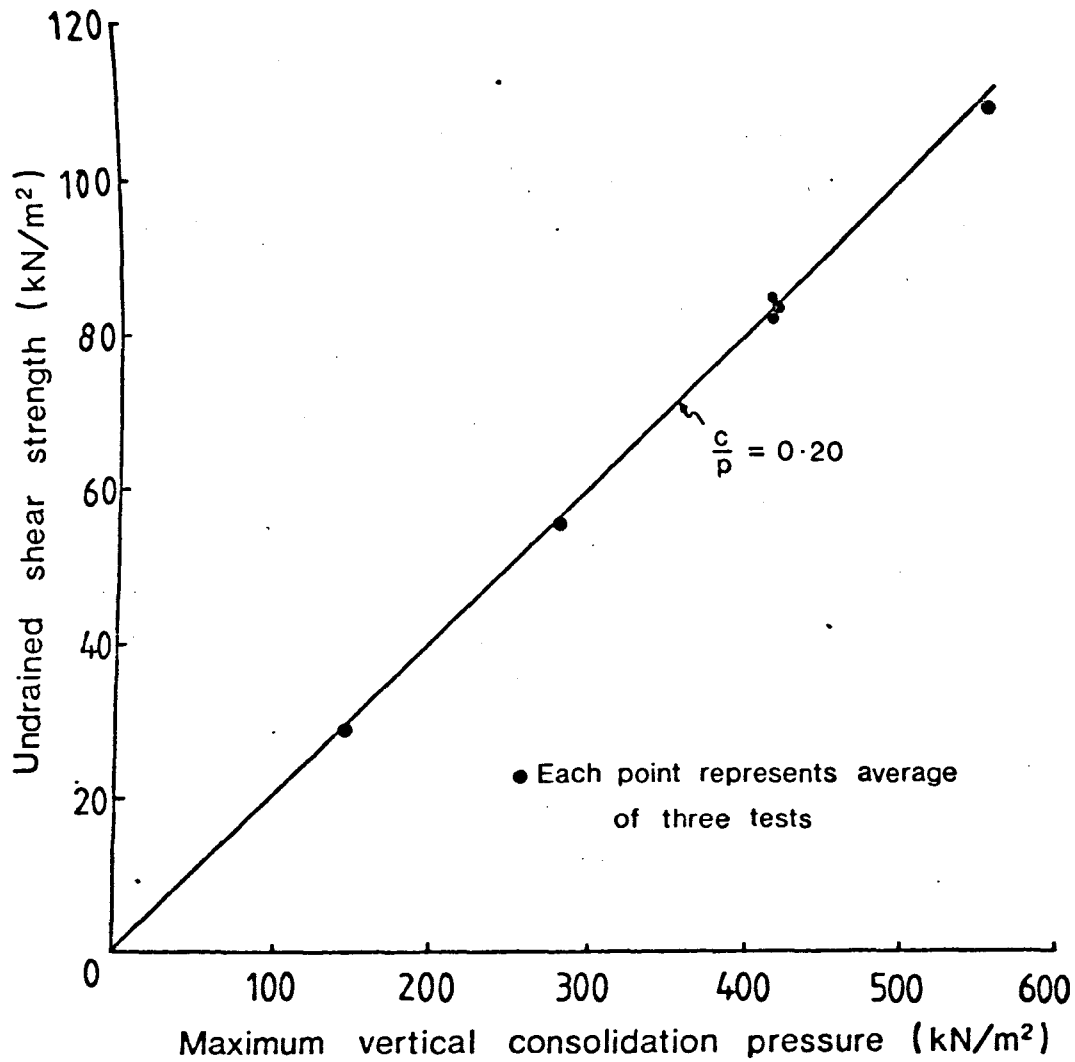
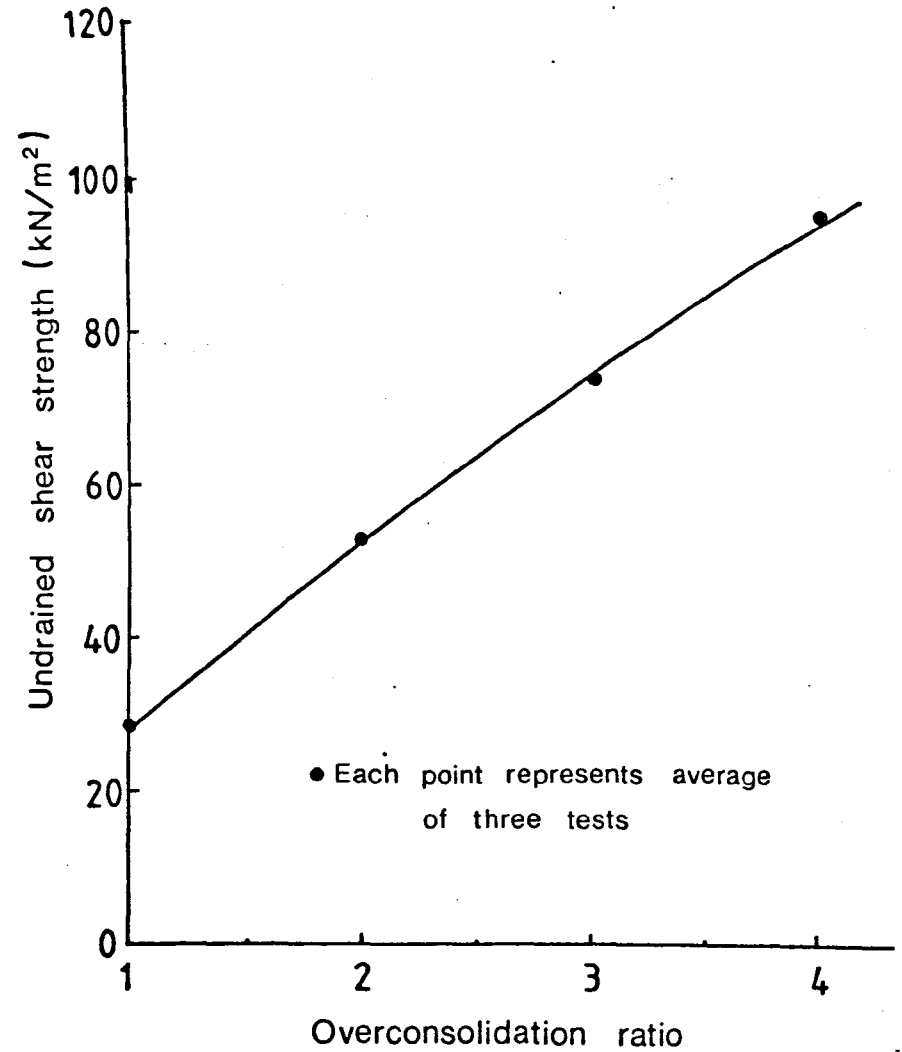


Fig.7.6 PLOT OF UNDRAINED SHEAR STRENGTH OBTAINED FROM VANE SHEAR TESTS AND FROM CONSOLIDATED UNDRAINED TRIAXIAL TESTS

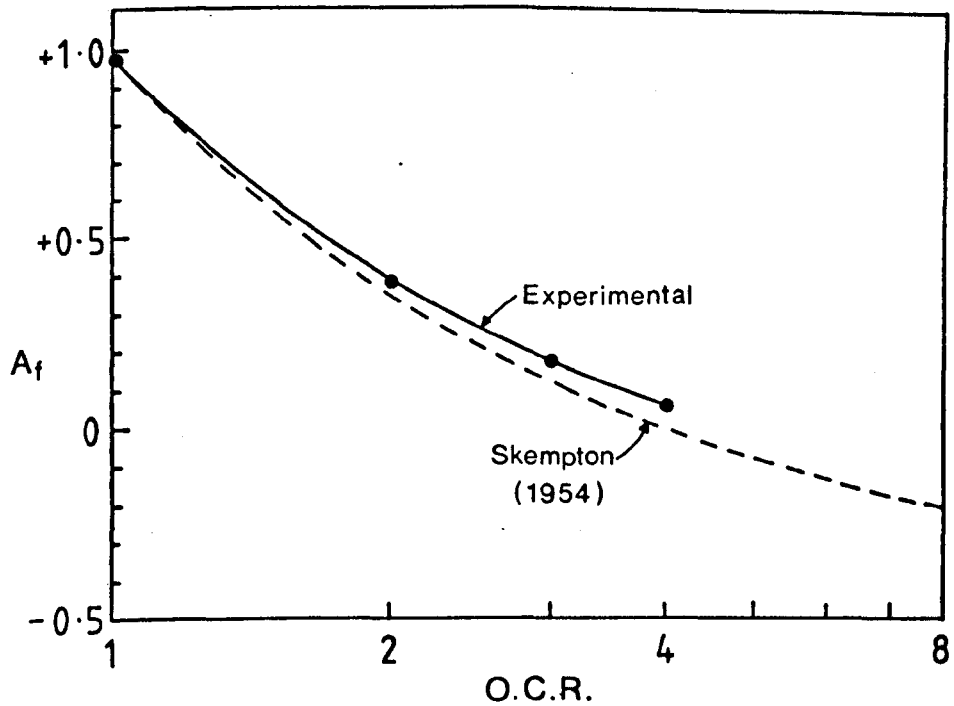


(a) Normally consolidated clay

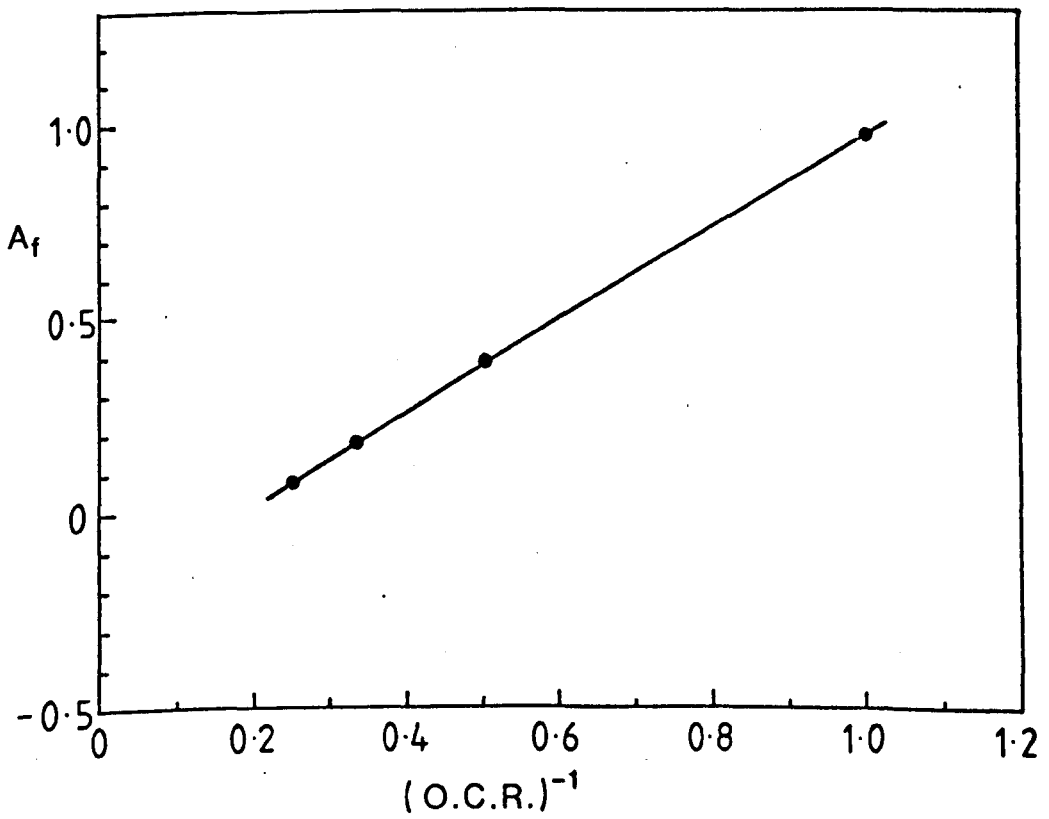


(b) Overconsolidated clay ( $p_o = 140 \text{ kN/m}^2$ )

Fig.7.7 VARIATION OF UNDRAINED SHEAR STRENGTH (FROM CONSOLIDATED UNDRAINED TRIAXIAL TEST) WITH STRESS HISTORY.

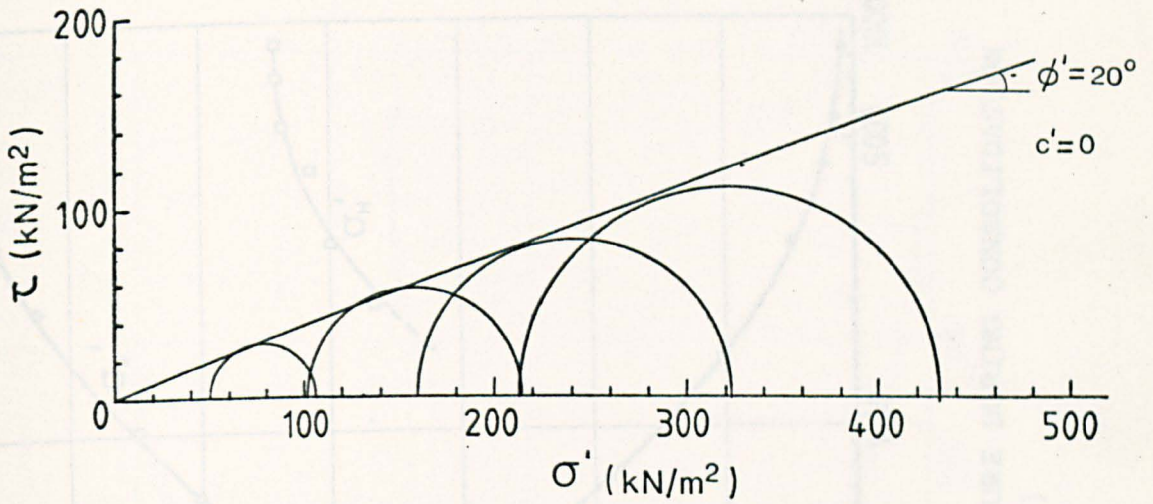


(a)

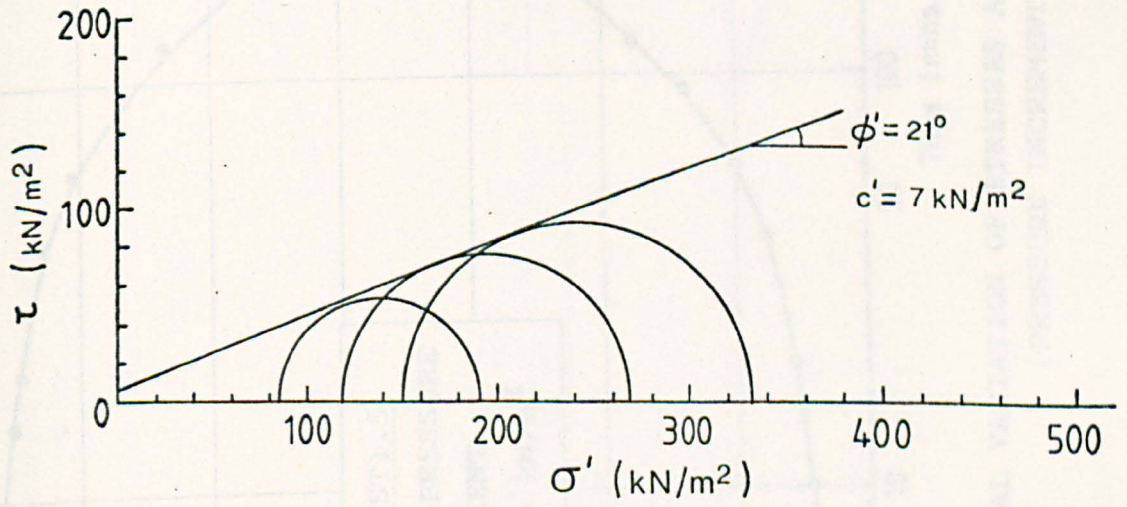


(b)

Fig.7.8 PLOTS OF PORE PRESSURE PARAMETER  $A_f$  VERSUS OVERCONSOLIDATION RATIO (OCR) ON (a) LOGARITHM SCALE, AND (b) INVERSE SCALE



(a) Normally consolidated clay



(b) Overconsolidated clay

Fig.7.9 MOHR'S STRESS CIRCLES FOR CONSOLIDATED-UNDRAINED TRIAXIAL TEST

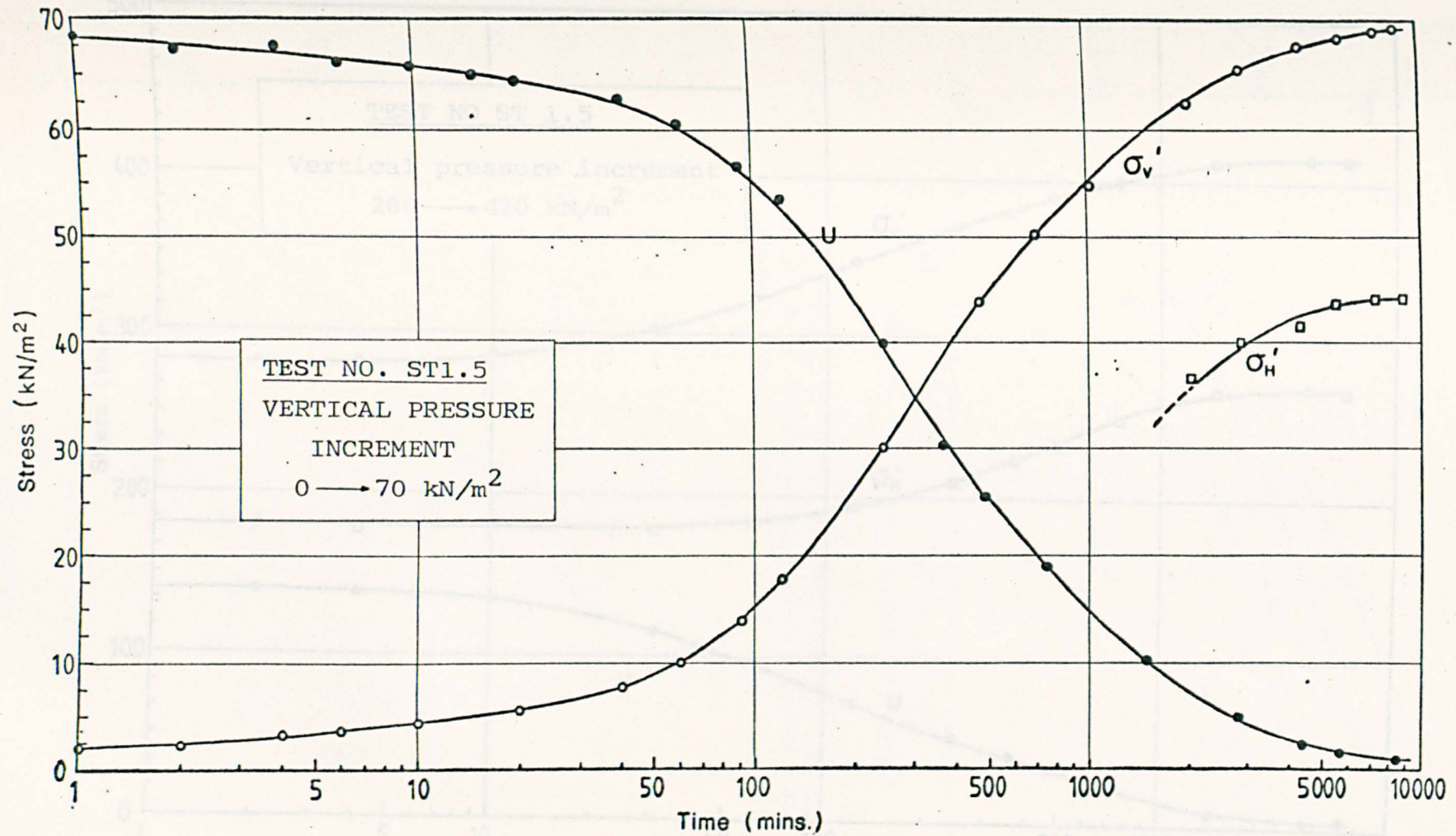


Fig. 7.10 TYPICAL VARIATION OF STRESSES AND PORE PRESSURE DURING CONSOLIDATION  
 (PRESSURE INCREMENT 0 → 70 kN/m<sup>2</sup>)

Fig. 7.11 TYPICAL VARIATION OF STRESS AND PORE PRESSURE DURING  
 CONSOLIDATION (PRESSURE INCREMENT 220 → 420 kN/m<sup>2</sup>)

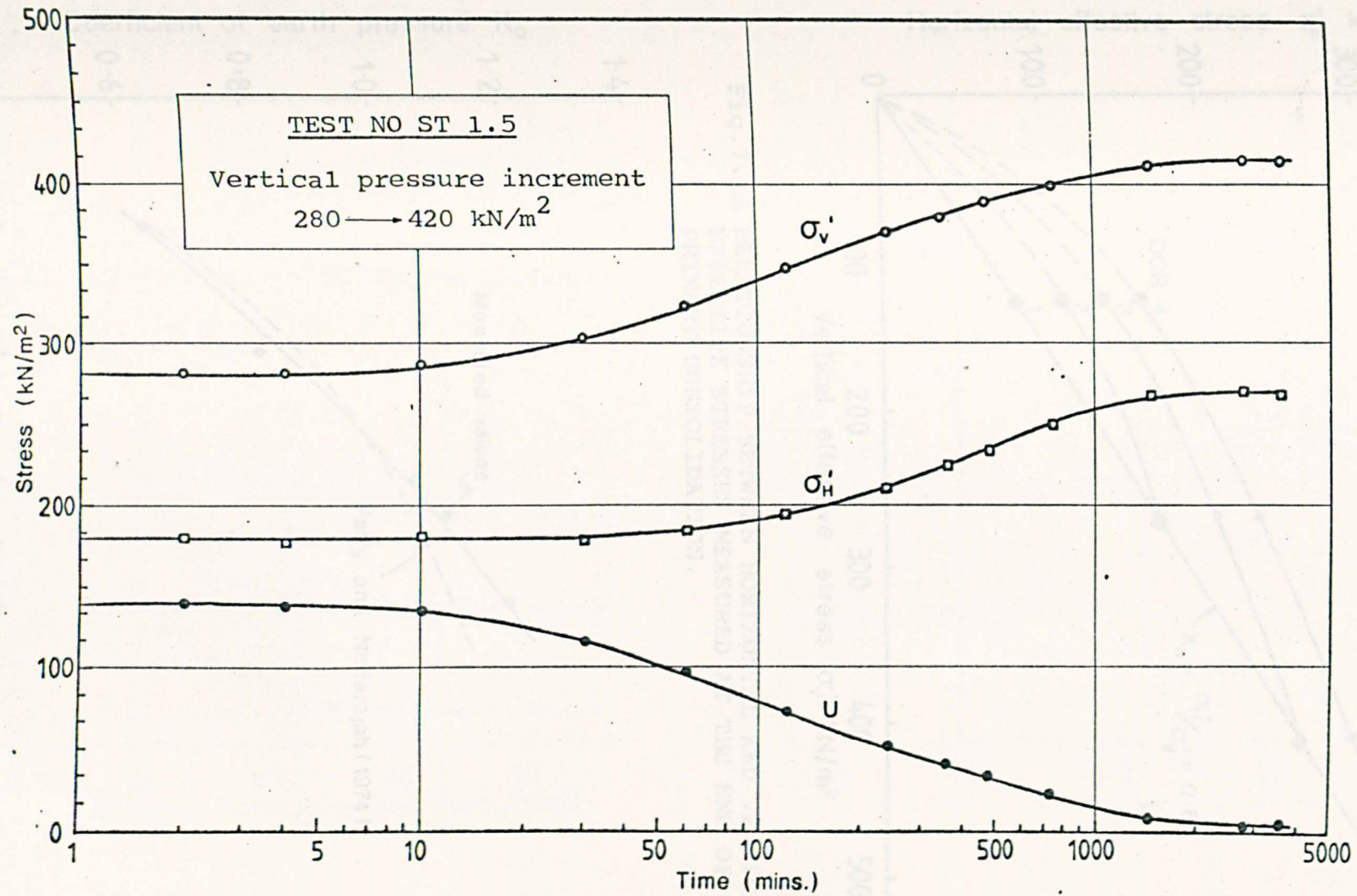


Fig.7.11 TYPICAL VARIATION OF STRESS AND PORE PRESSURE DURING CONSOLIDATION ( PRESSURE INCREMENT 280 → 420 kN/m<sup>2</sup>)

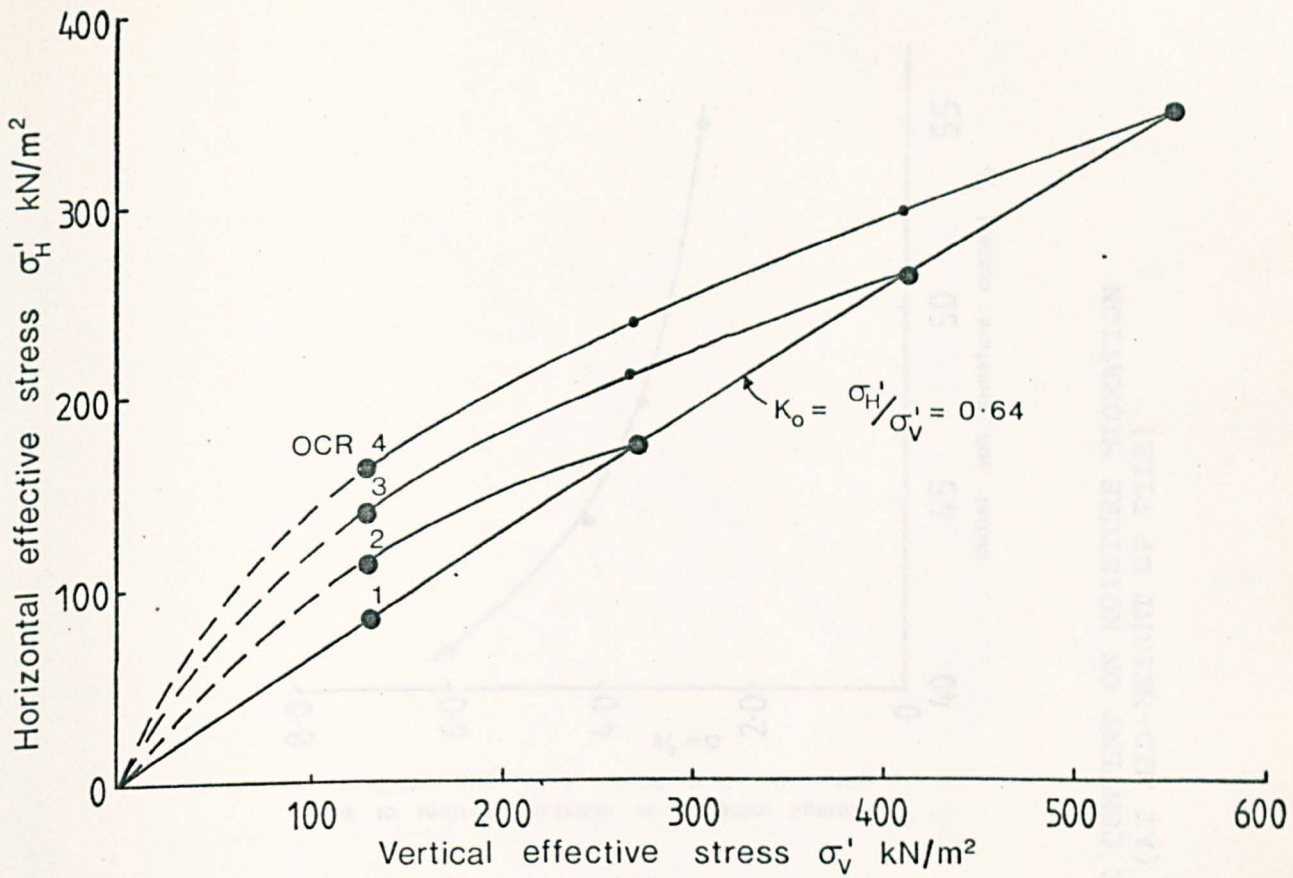


Fig.7.12 RELATIONSHIP BETWEEN HORIZONTAL AND VERTICAL EFFECTIVE STRESSES MEASURED AT THE END OF PRIMARY CONSOLIDATION.

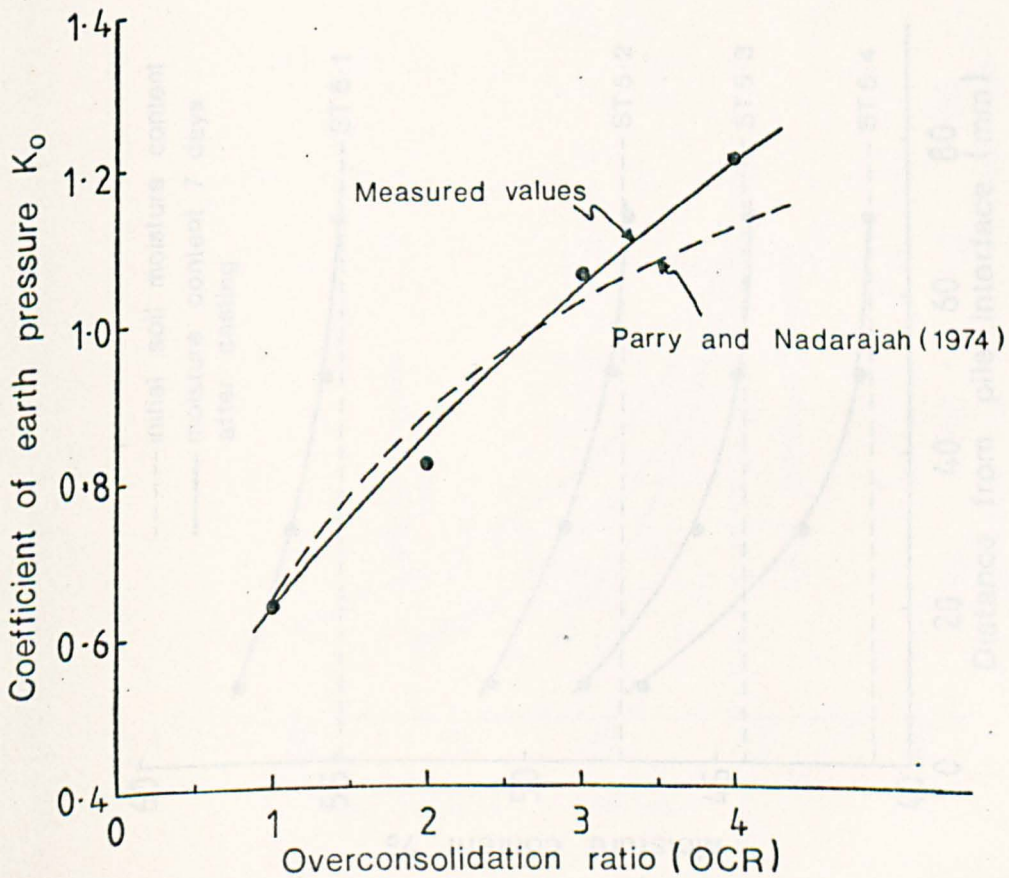


Fig.7.13 VARIATION OF  $K_o$  WITH STRESS HISTORY FOR KAOLIN CLAY

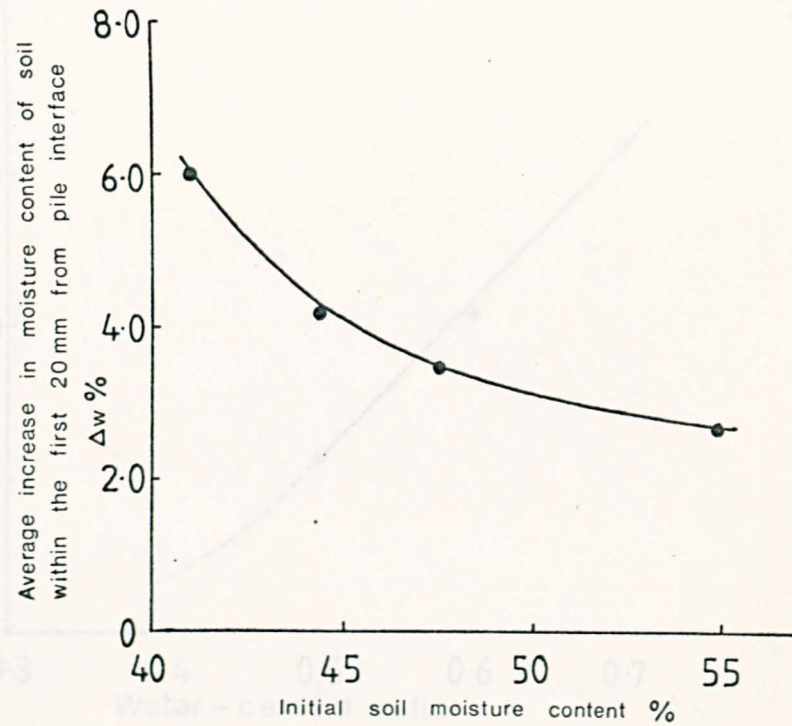
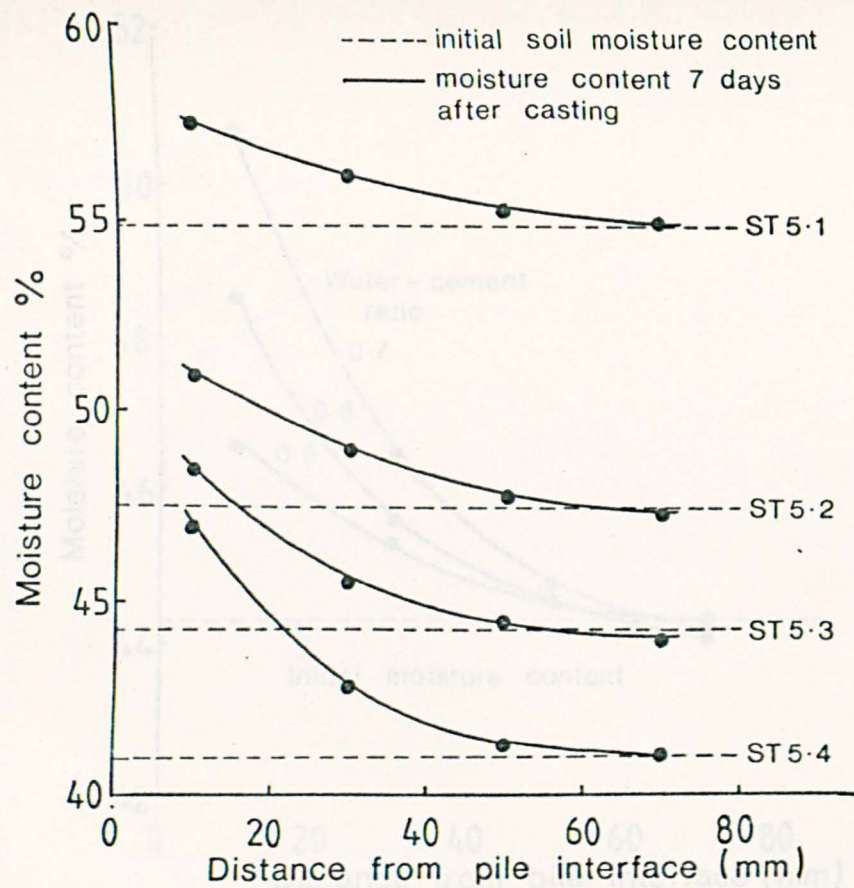


Fig.7.14 INFLUENCE OF INITIAL MOISTURE CONTENT ON MOISTURE MIGRATION IN SOIL SURROUNDING THE PILE (AT MID-HEIGHT OF PILE)

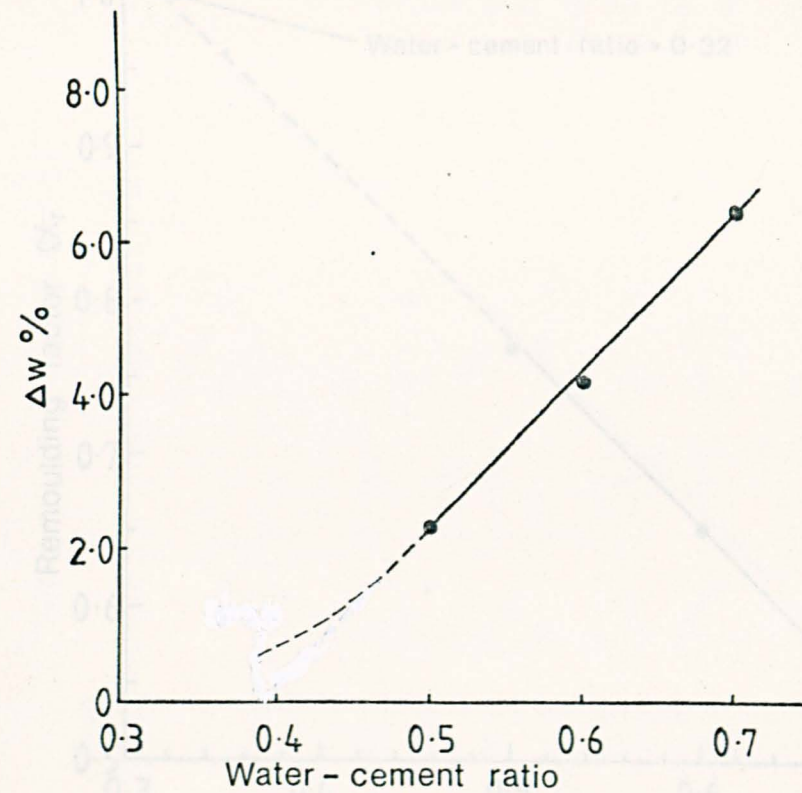
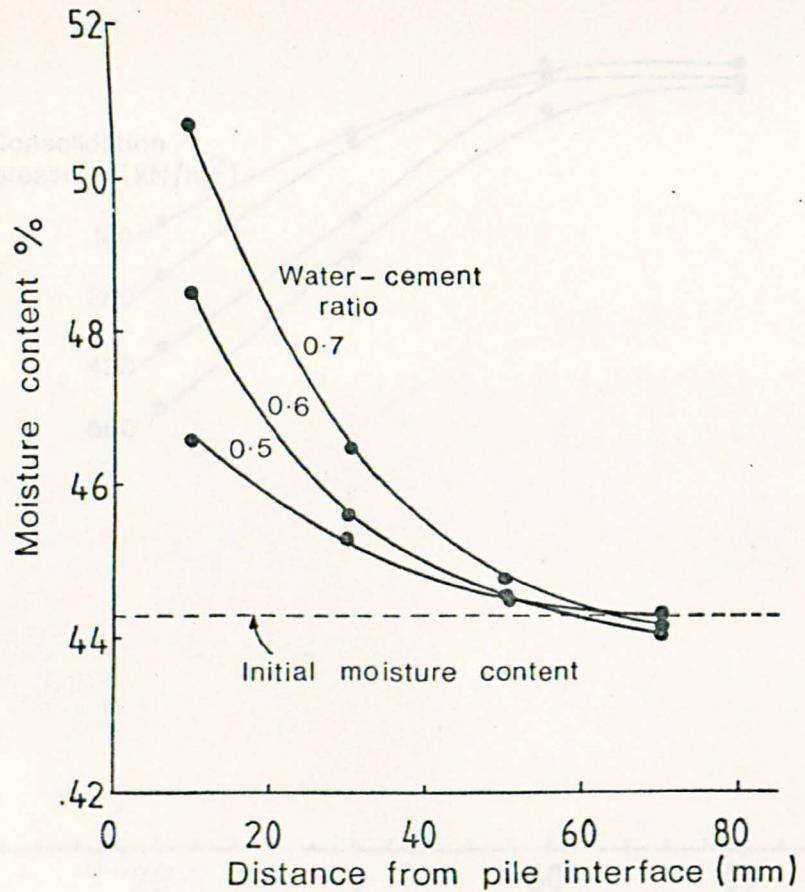


Fig.7.15 INFLUENCE OF WATER-CEMENT RATIO ON MOISTURE MIGRATION IN SOIL SURROUNDING THE PILE (AT MID-HEIGHT OF PILE)

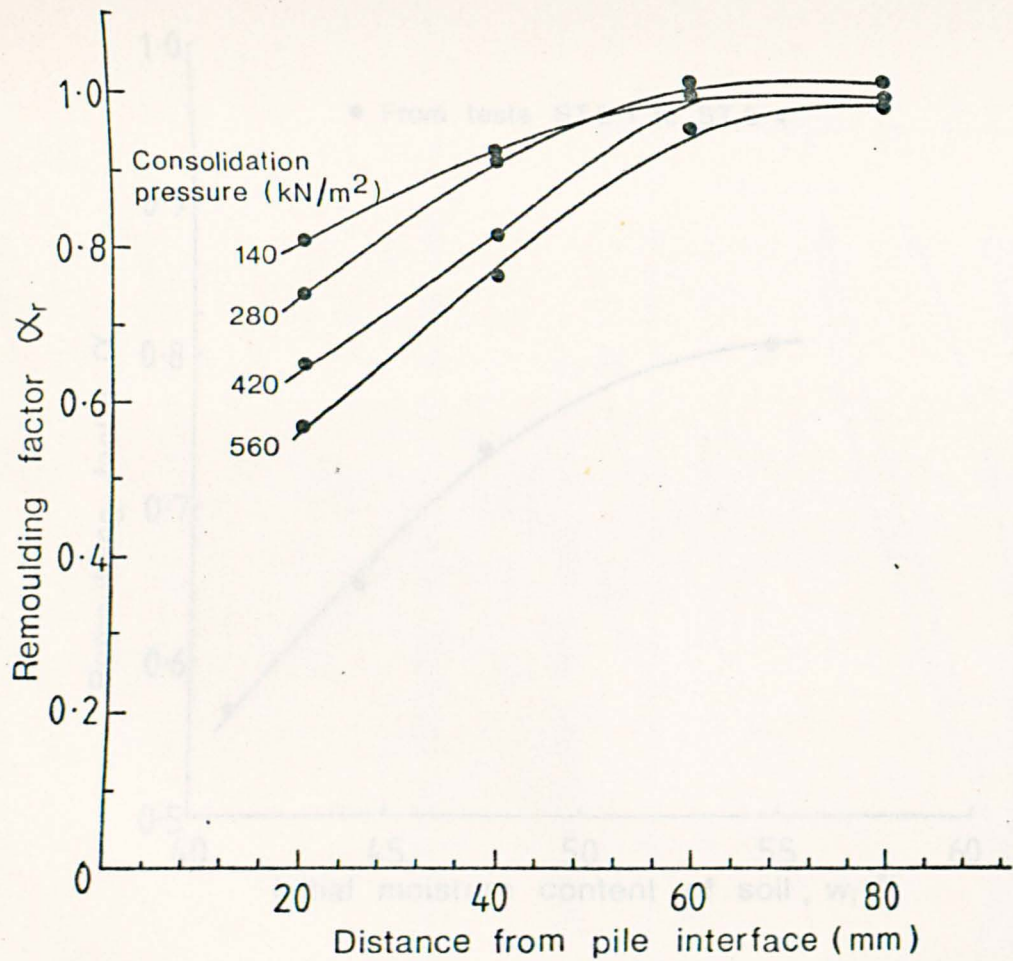


Fig.7.16 INFLUENCE OF STRESS HISTORY ON THE REMOULDING FACTOR IN SOIL SURROUNDING THE PILE

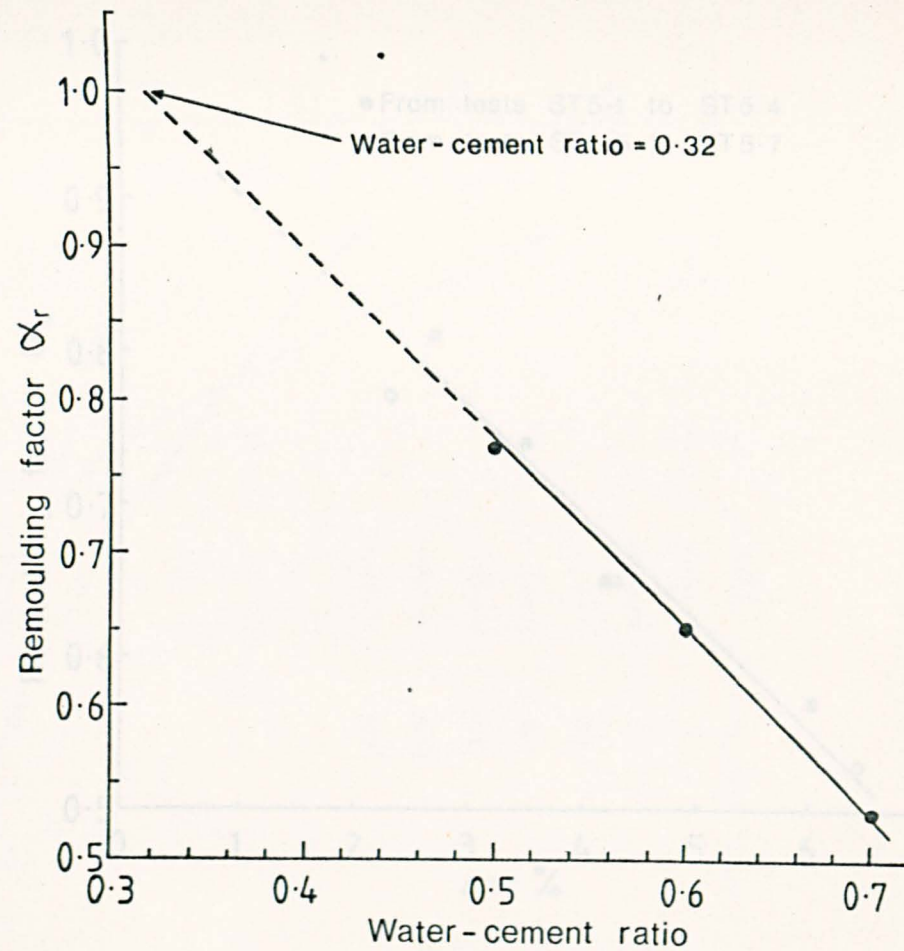


Fig.7.17 INFLUENCE OF WATER-CEMENT RATIO ON THE REMOULDING FACTOR IN SOIL ADJACENT TO THE PILE.

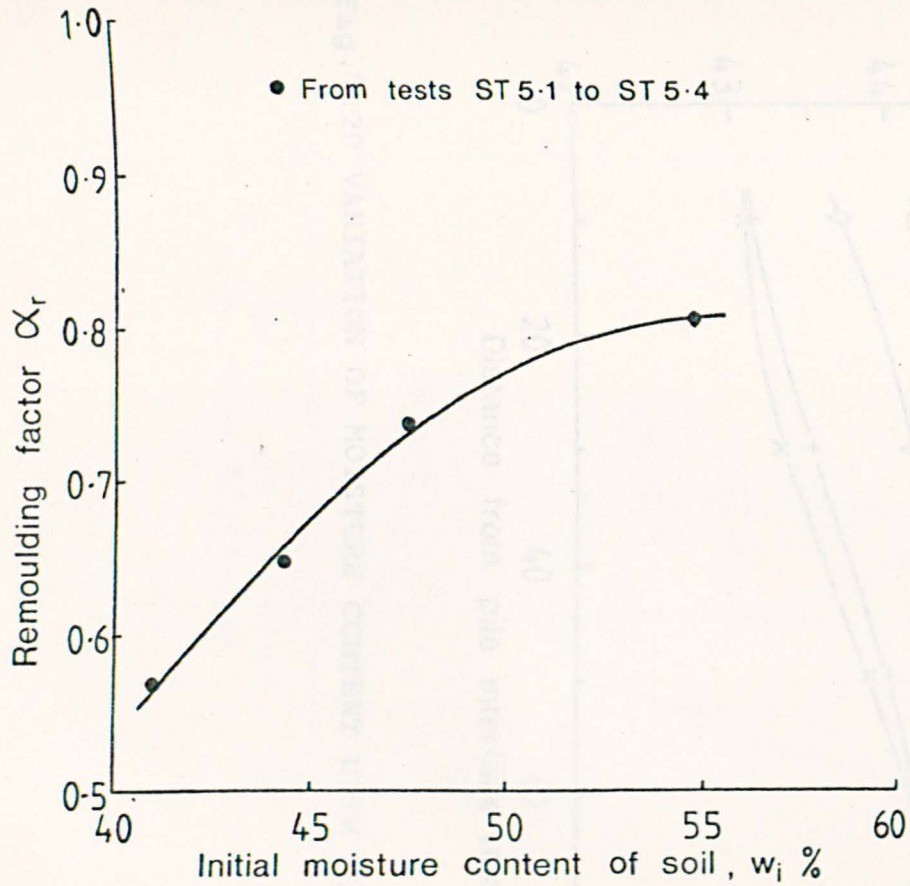


Fig.7.18 RELATIONSHIP BETWEEN REMOULDING FACTOR AND INITIAL MOISTURE CONTENT OF SOIL

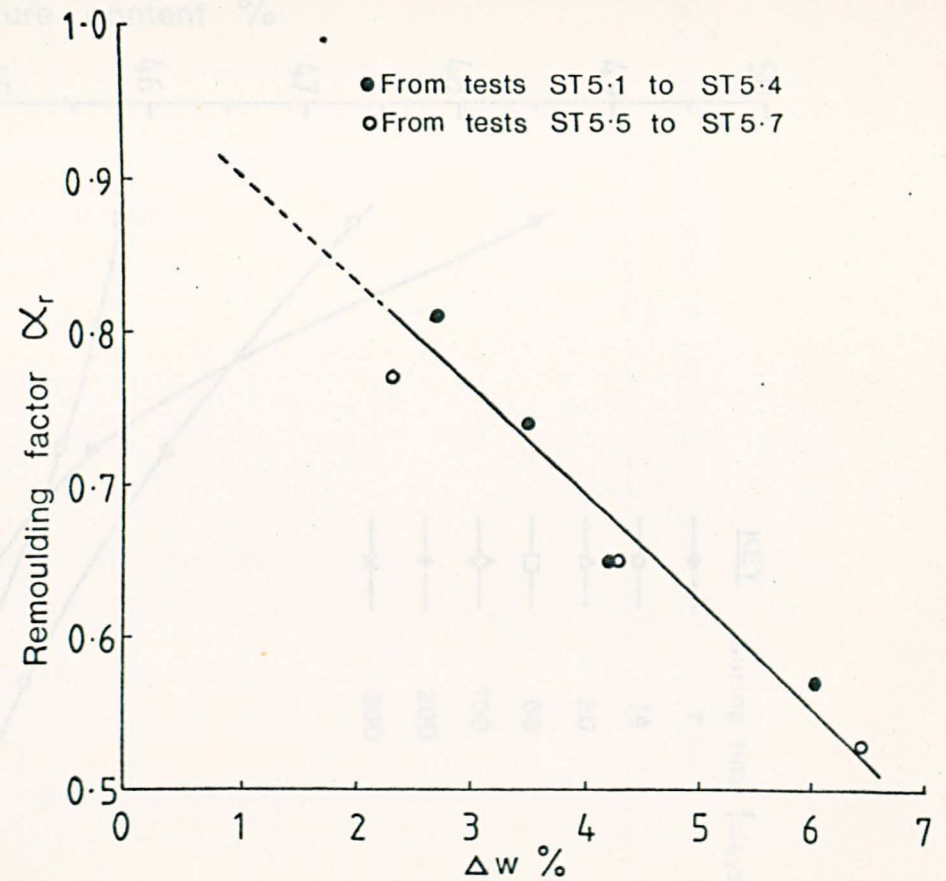


Fig.7.19 RELATIONSHIP BETWEEN REMOULDING FACTOR AND AVERAGE INCREASE IN MOISTURE CONTENT OF SOIL WITHIN 20 mm FROM PILE FACE

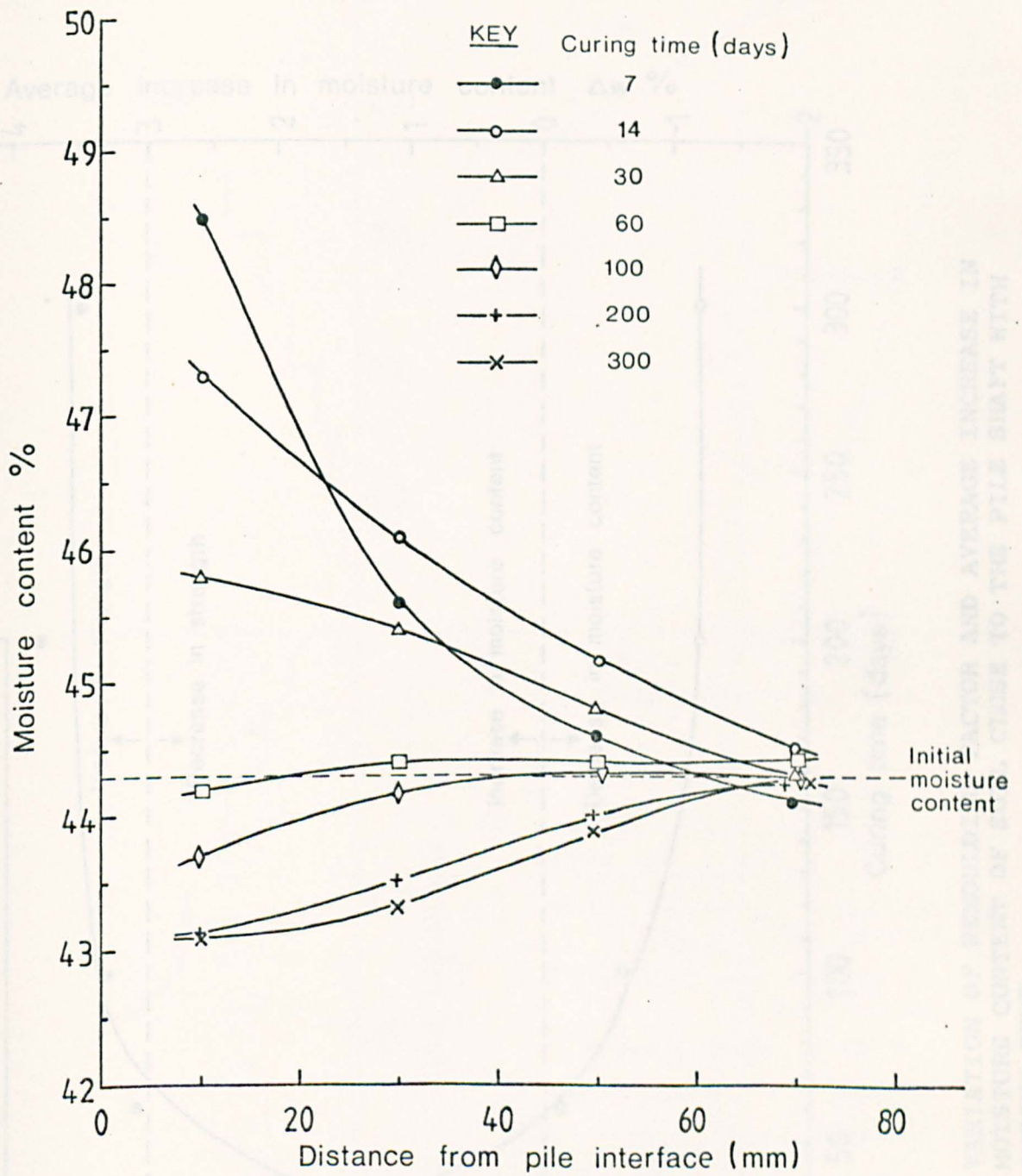


Fig.7.20 VARIATION OF MOISTURE CONTENT WITH CURING TIME

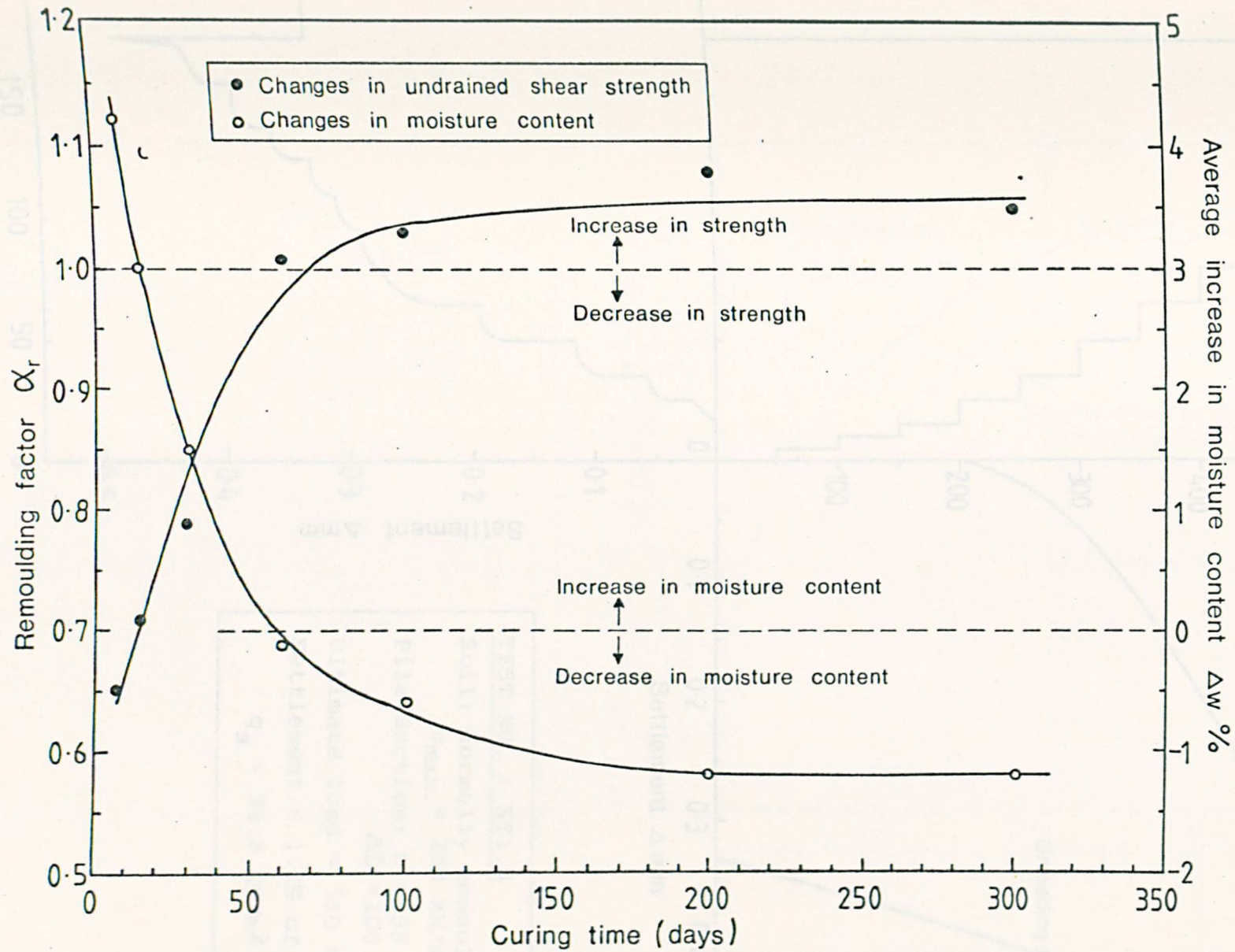


Fig.7.21 VARIATION OF REMOULDING FACTOR AND AVERAGE INCREASE IN MOISTURE CONTENT OF SOIL CLOSE TO THE PILE SHAFT WITH CURING TIME

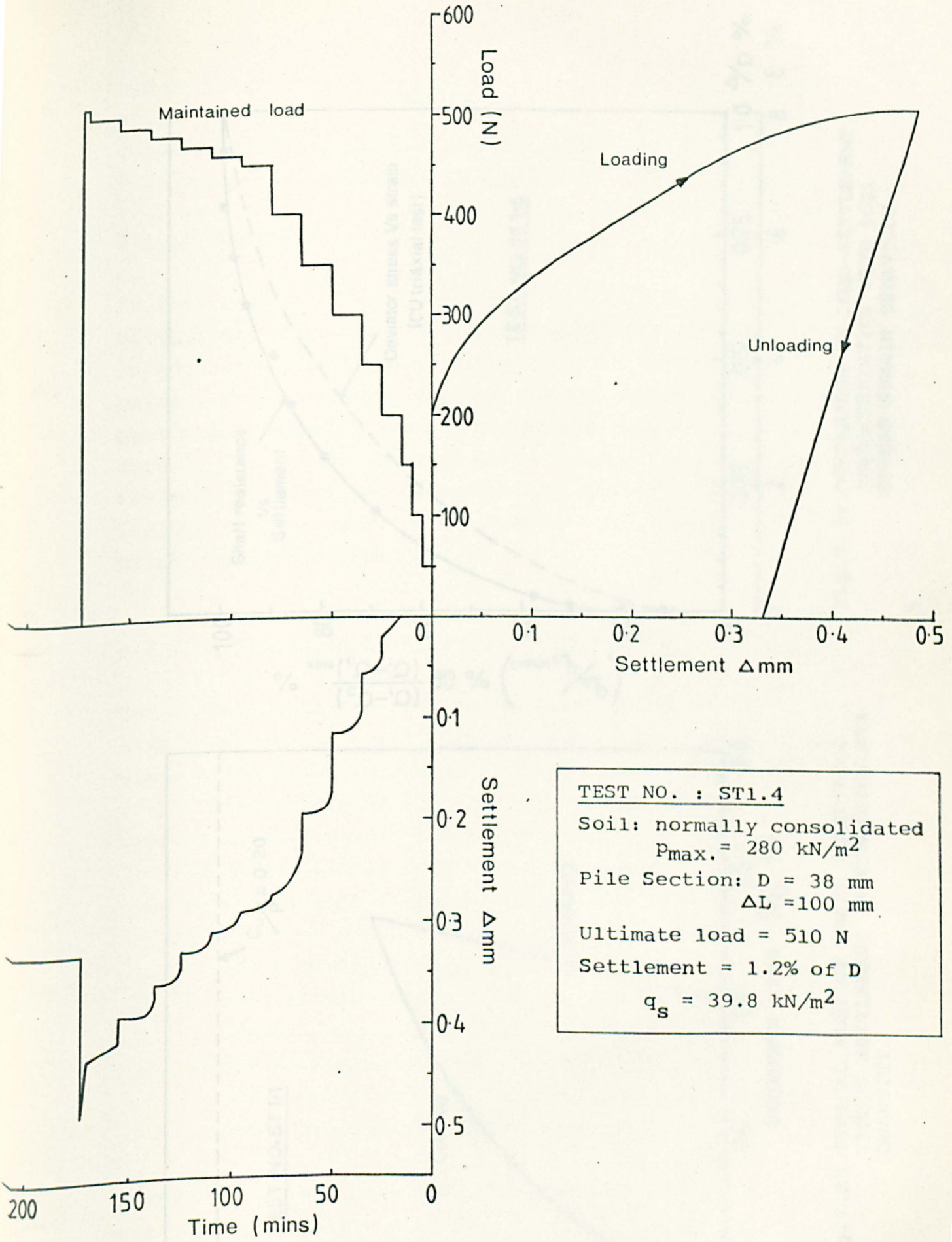


Fig. 7.22 TYPICAL LOAD/SETTLEMENT/TIME RELATIONSHIP

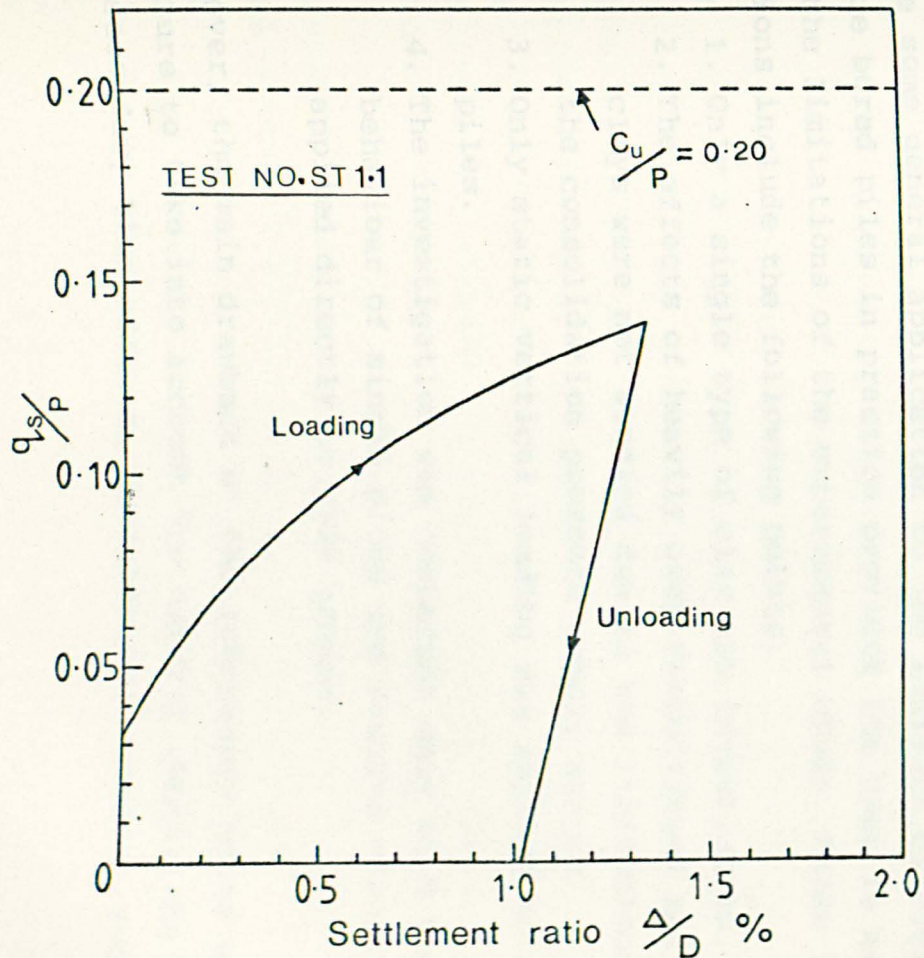


Fig. 7.23 TYPICAL PLOT OF SHAFT RESISTANCE VERSUS SETTLEMENT IN DIMENSIONLESS QUANTITY

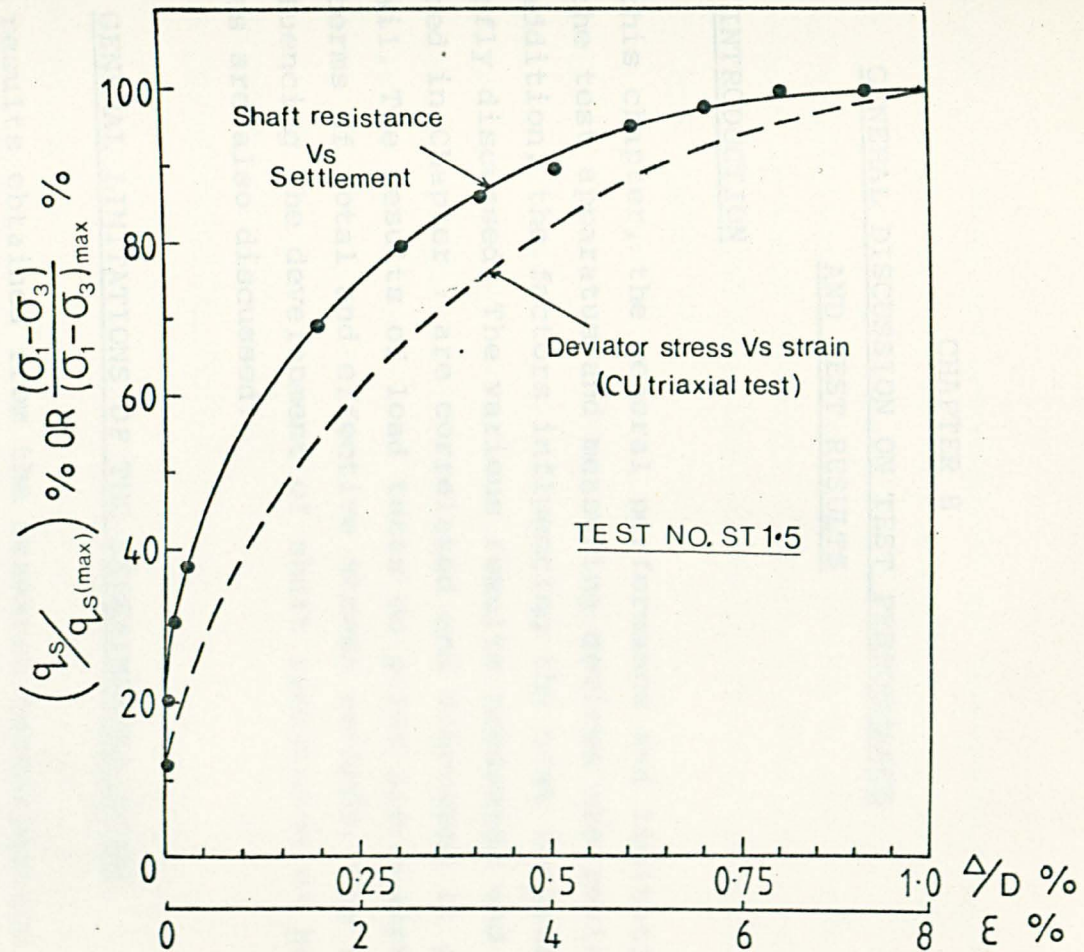


Fig. 7.24 COMPARISON OF LOAD-SETTLEMENT CHARACTERISTICS WITH SOIL STRESS-STRAIN BEHAVIOUR

## CHAPTER 8

### GENERAL DISCUSSION ON TEST PERFORMANCE AND TEST RESULTS

#### 8.1 INTRODUCTION

In this chapter, the general performance and limitations of the test apparatus and measuring devices are reviewed. In addition, the factors influencing the test results are briefly discussed. The various results presented and interpreted in Chapter 7 are correlated and discussed in greater detail. The results of load tests on piles are analysed in terms of total and effective stress methods. The factors influencing the development of shaft resistance of bored piles are also discussed.

#### 8.2 GENERAL LIMITATIONS OF THE EXPERIMENTAL STUDY

The results obtained from the research investigation can have some general application to the analysis of cast-in-place bored piles in practice provided the user is aware of the limitations of the experimental study. These limitations include the following points.

1. Only a single type of clay was investigated.
2. The effects of heavily over-consolidated and stiff clays were not studied due to the limitations of the consolidation pressure supply system.
3. Only static vertical loading was applied to the piles.
4. The investigation was concerned only with the behaviour of single piles and results cannot be applied directly to pile groups.

However, the main drawback of the laboratory tests was the failure to take into account the natural conditions such as secondary time effects, variable soil strata, and the

physical and chemical composition of the soil. Because the time for consolidation of laboratory samples is only a few weeks instead of hundreds of years, and because it is virtually impossible to simulate the physical and chemical environment in which the soil is formed, some differences can be expected between the behaviour in the laboratory and in the field.

In spite of these limitations, the study provided useful information regarding the performance of bored piles in saturated clay, with respect to the shaft resistance. Some results presented in the previous chapter have been shown to be compatible with results obtained in the field.

### 8.3 PERFORMANCE AND LIMITATIONS OF TEST APPARATUS

#### 8.3.1 Performance of Test Equipment

The test cell enabled uniform samples of clay beds to be prepared to the stress history required with the same consistency. The main shortcoming of the test cell was the need to remove the cell cover in order to obtain triaxial samples and samples for moisture content determination. This caused a relief of overburden even before samples were obtained and its effects have been discussed in Section 7.2.3. The size of the test apparatus limited the tests to relatively small samples and small test piles. However, a large test cell would have required a more cumbersome method of preparing the clay beds. One advantage of the test cell used in this study was the ease of handling which allowed the experimental procedures to be performed efficiently.

As regards the boring tools, the continuous flight auger (25mm diameter) had a considerable advantage over the single flight auger (38mm diameter) and the single plate auger (50mm diameter) in that cuttings were fed to the surface. For the latter two, it was necessary to pull out

the augers after every 20 to 30mm to remove the spoil. This may have caused a slight disturbance to the soil adjacent to the wall.

The pile loading system performed satisfactorily in transmitting the applied dead weights vertically onto the test pile. The construction of each pile was such that it was installed in a central position in the test cell. Since the pile loading frame was co-axially aligned with the centre of the test cell, it was most unlikely that eccentric loading occurred during the load tests.

There were no collapses in the 'voids', used to eliminate end-bearing capacity of the bored piles, under a head of fresh microconcrete. However, excess water from the fresh microconcrete could seep pass the 'void' into the base of the hole. If this happens, the zone of clay immediately beneath the base of the 'void' may be softened. However, it is unlikely that the softened clay below the 'void' will affect the development of shaft resistance. The successful use of the 'voids' dispensed with the need of a base load cell usually used in tests where there is a need to separate shaft resistance from the total load.

### 8.3.2 Repeatability of test results

As in any research project, the credibility of the results depends on the ability to reproduce the results under similar test conditions. In each of the Test Series, at least one test was repeated to check on the reproducibility of results. In all cases, it was possible to obtain similar results. The repeatability of test results is shown in Table 8.1 which summarizes the results of two pairs of identical tests. With the exception of the settlement prior to failure for Tests ST1.3 and ST2.1, it can be seen from the table that the differences between each set of parameters are within 4%.

The variation of stresses during consolidation and the load-settlement curves for Tests ST1.3 and ST2.1 are shown in Figs. 8.1 and 8.2 respectively to illustrate the degree of repeatability of test results. It can be seen from these figures that the trend is very similar, although the magnitudes differ slightly. Within the limits and accuracy of the measuring devices, the differences are very small.

Therefore, the behaviour of bored piles in saturated clay are reproducible under the same laboratory controlled conditions and any small difference in magnitudes are probably due to the sensitivity of the measuring devices.

### 8.3.3 Boundary effects of test cell

Friction in the walls of the test cell may affect the behaviour of the saturated clay. Two earth pressure cells were placed near the wall of the test cell (about 15mm from the centre of the pressure cell) opposite each other and another two were placed at a distance of about 50mm from the cell wall opposite each other; all the pressure cells being located at approximately mid-height of the sample. The pressure cells placed furthest away from the cell wall were able to record the full value of the total vertical stress applied on the clay bed implying that wall friction had no effect in this vicinity. Near the cell wall, both pressure cells showed a reduction in total vertical stress of the order of 3%, probably due to the wall friction. The ease of removal of the sample from the test cell after completion of the test also indicated that the wall friction between the soil and the test cell was probably very small and therefore negligible. This demonstrates the effectiveness of smearing the walls with silicone grease to reduce the frictional effect.

The study of moisture migration and undrained shear strength discussed in Section 7.3 and 7.4 indicates that the thickness

of the zone of soil affected by the installation of a bored pile is confined mainly to soil within a radial distance of 60mm from the pile shaft. For a 38mm diameter pile this gives a total radial thickness of about 80mm and the wall of the test cell is therefore unlikely to influence the effects of installation.

Piezometers were installed in the soil adjacent to the cell cover and the cell walls to monitor any development of excess pore pressure during pile loading. The purpose was to examine the effects of the rigid boundary of the cell wall and cover on the test results. Piezometer measurements taken during the duration of the load test showed no excess pore pressure being generated at the cell wall. However, excess pore pressure of the order of 10 to 20 kN/m<sup>2</sup> was measured for the soil adjacent to the cell cover. The results were based on measurements conducted in a clay bed consolidated at 420 kN/m<sup>2</sup>. The excess pore pressure therefore represents about 5% of the effective vertical stress and about 7% of the effective horizontal stress and hence is unlikely to significantly affect the shaft resistance developed.

#### 8.3.4 Effects of temperature

Temperature affects the soil behaviour as well as the performance of the measuring devices, especially where long term tests are concerned. However, only the problem of temperature effects on soil behaviour are discussed in this section, whilst the temperature effects on the stability of the measuring devices are discussed in Section 8.4.

For a saturated soil, a change in temperature causes a change in void ratio and/or change in effective stress. Mitchell (1976) investigated the problem of temperature effects on the strength of soil and found that there is a reduction in strength with increase in temperature.

This is attributed to the fact that an increase in temperature causes an increase in pore pressure and a decrease in effective stress and therefore reduces the strength of the soil structure. However, changes in soil strength are significant only when temperature variation exceeds  $10^{\circ}\text{C}$ .

A record of ambient temperature of the area in the research laboratory in which the tests were conducted was kept during the duration of the test programme. For the purpose of the discussion, the ambient temperature based on weekly averages for a complete year is shown in Fig. 8.3. The curve is divided into the summer months (beginning of April to the end of September) and the winter months (beginning of October to the end of March).

The location of the laboratory at the basement probably helped to keep the temperature at a fairly constant level of about  $19.5^{\circ}\text{C}$  with a variation of about  $\pm 1.5^{\circ}\text{C}$  during the summer months. However, during the winter months, the temperature dropped to an average of  $17.0^{\circ}\text{C}$  with a variation of  $\pm 3.5^{\circ}\text{C}$ . One temperature as low as  $12^{\circ}\text{C}$  was recorded. The greatest drop in temperature occurred towards the beginning of January and in mid-February as a result of the severe winter. Another reason was that the supply of heating to the research laboratory was switched off for about two weeks towards the end of December.

The temperature variation shown in Fig. 8.3 indicates the advantage of conducting tests during the summer months. For long term tests which continue into the winter period, temperature correction may be required for the test results if the temperature variation is significant. The alternative is to conduct these tests in a constant temperature room. However, the important point is the effect of the change in ambient temperature on the temperature of the soil.

In the case of the long term tests conducted in this study, temperature of the soil was taken with a laboratory thermometer

during the stages of the test when access to the clay bed was possible (i.e. slurry preparation, prior to boring and and after a pile test). Temperature in the clay which is in a closed system was fairly constant and showed a variation less than  $\pm 2^{\circ}\text{C}$ . However, this observation excludes the temperature effects of concrete hydration on the soil properties. An increase of temperature of the order of  $8^{\circ}\text{C}$  to  $10^{\circ}\text{C}$  is known to occur during the hydration process (Neville, 1973). Since the quantity of concrete used to construct the pile is very small, it is unlikely that the temperature increase due to the hydration process would affect the soil properties.

#### 8.3.5 Effects of creep in soil and concrete

Creep in soil is a complex stress-strain-time phenomenon depending mainly on the soil type, stress history, drainage conditions and type of loading. It is of particular interest in soils because evidence shows that many soils undergo a loss of strength as a result of creep [Barden (1969) and Wooley and Reese (1974)].

Mitchell (1976) conducted various experiments on creep properties of Kaolin and showed that in terms of effective stress, the soil strength does not change during creep. In this research where the stress levels in the clay beds were less than  $600 \text{ kN/m}^2$ , Mitchell's work suggest that the creep rates are very small and of little practical importance. Bjerrum (1973) also presented a discussion on the effect of time on the shear strength of clay and showed that time effect is primarily related to the cohesive element of shear strength while the frictional component is for the most part independent of time.

After casting, concrete changes in volume due to shrinkage and temperature changes. These volumetric strains have the effect of reducing the total horizontal pressure on the

pile shaft. In practice, it is difficult to evaluate these strains. However, in view of the small size of the pile constructed, it is reasonable to assume that the effects of shrinkage are insignificant in terms of the test results. Furthermore, unless the concrete is subjected to a sustained loading for an appreciable time period, creep is unlikely to occur.

#### 8.4 PERFORMANCE AND LIMITATIONS OF INSTRUMENTATION

##### 8.4.1 Introduction

Most of the measurements were made by the earth pressure cells and pore pressure transducers. Therefore, accuracy of the results is highly dependent on the reliability of these instruments as well as their effects on the soil behaviour. The method of installing the measuring devices prior to consolidation of the clays ensured minimum disturbance to the soil. In fact, the procedure ensured good contact with the clay particles as evidenced by the fact that the pressure cells were able to record the full total vertical stress applied to the clay sample. The performance and limitations of each type of measuring device are discussed separately in the following sections.

##### 8.4.2 General performance of EP and IF pressure cells

Under low pressures ( $140 \text{ kN/m}^2$  and  $280 \text{ kN/m}^2$ ), the EP pressure cells were able to record the full total vertical stress immediately after application of this stress to the clay sample. However, under higher pressures ( $420 \text{ kN/m}^2$  and  $560 \text{ kN/m}^2$ ) the immediate readings of the pressure cells were approximately 5% lower than the applied vertical stress although after some time the full values were measured. This behaviour can be attributed to a slight arching effect occurring during the initial stages of consolidation. As pore pressure dissipated and stresses became effective, this arching was

destroyed and the clay was able to deform fully to the deflected shape of the diaphragm.

In general, results from the EP pressure cells were very encouraging in that most of them remained operative throughout the test. Only about 10% of the EP pressure cells used became inoperative, mainly due to the seepage of moisture into the measuring devices causing a short circuit in the strain gauges. This was reflected by sudden erratic changes in the readings.

Compared to the EP devices, the IF pressure cells were less successful in terms of its operation and sensitivity, although reasonable and consistent readings were obtained. About 30% of the IF pressure cells became inoperative during tests. This was again due mainly to seepage of moisture causing short circuits, although in a few cases dislocation of the pressure cells occurred, usually by tilting from their intended positions. In all these cases, the tests had to be repeated. The displacement of the IF pressure cells probably occurred during the concreting stage. Improper tamping of the rod to compact the concrete may have disturbed the position of the IF pressure cells. Pressurising the fresh concrete to simulate the hydrostatic head may also have occasionally dislocate the device if the pressure was not applied slowly and uniformly.

The accuracy of the measurements is limited by the design and calibration of the pressure cells. For EP pressure cells the accuracy was of the order of 2 to 5 kN/m<sup>2</sup> depending on the diaphragm thickness and for IF cells, the order of accuracy was about 5 kN/m<sup>2</sup>. On this basis, it is reasonable to assume that in soft and firm clay, the pressure cells can give fairly accurate values of total stresses. However, where total stress change are small, the measurements become unreliable.

One limitation of the IF pressure cells was the inability of the cells to accommodate variations in borehole diameter. In other words, if the borehole diameter changes significantly as in the case of boreholes left opened for some time, the IF pressure cells cannot be used. Therefore, further improvements could be made to the IF pressure cells.

A limitation common with all strain-gauged type pressure cells is the stability of the strain gauges with respect to time and temperature. Since this factor has a major influence on the measurements, it is discussed separately in Section 8.4.4.

As a check to their performance, some pressure cells were recalibrated to observe any difference in strain readings at the same load level. In all cases, there was no significant difference, provided the re-calibrations were conducted under the same conditions in which the devices were initially calibrated.

#### 8.4.3 Compatibility of theoretical and measured readings

It can be shown that the maximum strain at the centre of the diaphragm can be calculated theoretically from the relationship,

$$\xi_r = 0.477 \cdot p/t^2 \quad \dots (8.1)$$

where  $\xi_r$  is in microstrain,  $p$  is the uniformly applied pressure ( $\text{kN/m}^2$ ) and  $t$  is the diaphragm thickness (mm). The above equation applies only to the EP pressure cells designed in this research study and its derivation is given in Appendix IV. For a diaphragm thickness of 10mm and a design pressure of  $420 \text{ kN/m}^2$ , the theoretical strain calculated from equation (8.1) is 200 microstrain.

At a vertical consolidation pressure of  $420 \text{ kN/m}^2$ , the output of the EP pressure cells was  $1404 \mu\text{V}$  (after correction

for cell action) for an input voltage of 3 volts. The output voltage is related to the strain by the relationship (derived in Appendix V),

$$\epsilon = \frac{2e}{KV} \quad \dots (8.2)$$

where  $\epsilon$  is in microstrain,  $e$  is the output in  $\mu V$ ,  $K$  is the Gauge Factor and  $V$  is the supply voltage in volts. Substituting values of  $e=1404\mu V$ ,  $K=2.07$  and  $V=3$  volts into the equation (8.2), the corresponding measured strain is 450 microstrain. However, this is the cumulative reading of two strain gauges that formed the active strain rosette. Thus, the measured strain for one strain gauge is 225 microstrain.

The theoretical and the measured strains are therefore of the same order. The slight difference may be attributed to possible errors associated with the determination of the calibration constants or to the assumptions made in the theoretical relationship. Although the above procedure applies to the EP pressure cells, the compatibility between measured and theoretical strains of IF pressure cells can similarly be shown.

The good compatibility of theoretical and measured results suggests that the problems and errors inherent in the use of the pressure cells in soil can be eliminated by proper design, installation and operation of the instruments.

#### 8.4.4 Stability of strain gauges

The term 'instability' in strain gauges generally refers to zero drift. Temperature variation can create considerable drift but it is felt that the provision of dummy gauges and the use of self-temperature compensating foil gauges helped to reduce this drift.

In order to determine stability of strain gauges in the pressure cells, readings of the devices at zero load were taken over the period of a complete test (i.e. from consolidation to pile loading). The experimental arrangement for the stability tests has been discussed in Section 6.8.3. Since results obtained from the EP pressure cells were similar to those of IF pressure cells, only the results of the former are discussed.

Since the pore pressure transducers also operate on strain-gauge principles, the stability of a typical transducer was investigated. The transducer was left exposed under ambient conditions, with no loads applied. The pressure cells and pressure transducer under investigation were powered continuously with supply voltages of 3 volts and 10 volts as used in the tests.

Typical drift curves of strain gauges for a complete short term test (usually about 30 days) are shown in Fig. 8.4. Graphs 1a and 1b represents the drift for the same pressure cell, designated EP6-1, based on readings taken during the day (between 1200 and 1400 hours) and during the night (between 2400 and 0200 hours). Graph 2 represents the maximum drift of the day for the pore pressure transducer while Graph 3 shows the variation of ambient temperature of the research laboratory over the same period. Graph 3 was plotted to indicate the effect of temperature variation on the zero drift.

In general, the trend of the drift curves for both the pressure cell and pressure transducer is similar to the temperature curve. For the case of the EP pressure cells, the drifts were all negative. This is due to the fact that the initial reading of the EP cell was taken at ambient condition. When the cell was embedded in clay, it is probable that the lower temperature of the clay (found to be  $2^{\circ}\text{C}$  less than the ambient temperature) caused the initial

negative drift. It can also be seen from Fig. 8.4 that the drift is greater for Graph 1b than for Graph 1a. This difference can be attributed to the lower temperature occurring during the night. For the whole period in which readings are shown, the maximum drift for the EP pressure cells was about  $12\mu\text{V}$ . In the worst case, this drift represents a false pressure of approximately  $10\text{ kN/m}^2$  in the reading. Therefore, where zero drifts are significant, corrections to the measured values are necessary. The actual reading is obtained by subtracting or adding the zero drift to the measured value, depending on whether the drift is positive or negative.

The maximum drift of  $12\mu\text{V}$  in the EP pressure cell was monitored over an ambient temperature variation of  $3^\circ\text{C}$ . Although the variation of the temperature in the clay and the ambient temperature need not be the same, as a rough guide, the zero drift per  $^\circ\text{C}$  is  $4\mu\text{V}$  or about  $3\text{ kN/m}^2$  per  $^\circ\text{C}$ . Therefore, for the case of long term tests where temperature variation is large between summer and winter months (see Fig. 8.3), the effects on the strain gauges become uncertain and results become speculative and unreliable even with corrections applied.

For the pore pressure transducer with four active gauges the readings were fairly stable (Graph 2). The maximum drift over a short term test was only  $5\mu\text{V}$  representing a false pressure of less than  $1\text{ kN/m}^2$ . For measurements taken over a period of 10 months, the maximum drift was only  $10\mu\text{V}$  representing less than  $2\text{ kN/m}^2$ . Therefore, corrections were not required in the pore pressure transducers readings for both short and long term tests.

#### 8.4.5 Response of piezometers

The response times of the soil and interface piezometers used in the tests were studied over different pressure

increments. Although the miniature pressure transducer was not used in the tests, its response was studied for the purpose of comparison between the laboratory-made piezometers and the commercially available miniature transducer. The time to record the peak value was achieved by closing the drainage tap and then applying the pressure increment. Readings were logged in the data system every second and the time taken to achieve response was noted.

The typical response of the piezometers is shown in Table 8.2. Results shown are based on the average of at least 3 readings for each increment. The theoretical time lag is also shown in the table and the calculations are given in Appendix VI. It can be seen that the miniature piezometer transducer gave almost instantaneous peak values. This is due to the fact that any change in pore pressure was transmitted directly to the sensing diaphragm without any intermediate system. In the case of the soil and interface piezometers, pore pressure changes were transmitted via a fluid medium and hence a longer response time was required to achieve peak values.

Although the measured response times are higher than the calculated time lag, the values are of the same order. The difference can be attributed to the fact that the theoretical values were calculated on the basis of 99% equalization. In addition there were two major limitations of the piezometer system. Firstly, the ability to achieve reliable measurements depends on the efficiency in de-airing the system. The presence of air or gas bubbles will increase the flexibility of the system and hence increase the time for full response. In some tests, minute air bubbles were observed in the transparent nylon tubing in the early stages of consolidation. However, these minute bubbles disappeared later in the test, probably dissolving in the water under high pressure.

The second limitation is the partial blockage of the probes, a common feature in most porous discs. When the probes are partially clogged with clay particles, a reduction in permeability occurs and hence a longer time lag. To minimize the possibility of this event occurring during a test, the porous plastic and porous stone were replaced after every test.

Another major limitation of importance to the interface piezometer (although it applies equally to the soil piezometer) is the inability to measure reliably negative pore pressures in excess of  $100 \text{ kN/m}^2$ . This limitation can be explained by the observation of Lambe and Whitman (1968). These authors studied the effects of negative pore pressure in a saturated soil and suggested that high negative pore pressure can sustain pure tension for only a short time. Cavitation, usually in the measuring system, will occur, resulting in measured values being lower than actual negative pore water pressure.

The above observations suggest that the soil and interface piezometers are not suited for tests where pore pressure changes rapidly or where negative pore pressure is in excess of  $100 \text{ kN/m}^2$ . For these cases, the use of the miniature pressure transducer is recommended, although its cost should be borne in mind. The advantage of the soil and interface piezometers are the ease in fabrication and if damaged, they can be cheaply replaced.

The drive-in piezometers have not been included in the above discussion because of their inconsistent measurements when used in a test. The drive-in piezometers were intended to be used to replace any soil piezometers which become inoperative, by driving a probe into the soil. Unlike the case of the soil and interface piezometers, installed prior to consolidation, the method of driving the probe into the soil proved inefficient. When the probes were forced into the ground, a gap between the nylon tubing and soil was

formed. This allowed leakage of water from the system into the gap as well as introducing bubbles into the system. As a result, the drive-in piezometers were not used for the tests.

#### 8.4.6 Tell tale devices

Measurements obtained during a pile load test showed no settlement of the soil. However, it is felt that this observation is inconclusive due to the limitations of the devices. The tell tale rod is not very sensitive to small changes. Also, temperature changes and possible friction between the rod and tubing could have influenced the performance.

### 8.5 STRESS CHANGES IN THE SOIL SURROUNDING THE PILE

#### 8.5.1 General

In order to appreciate the test results obtained, it is essential to follow the stress changes in the soil adjacent to the pile from the 'at-rest' condition after consolidation until the pile had failed in the load test.

The variations of total and effective horizontal stress and pore water pressure with time are shown in Figs. 8.5 and 8.6 for normally and lightly overconsolidated clay respectively. For all the tests in which measurements were recorded, the trends were consistent for both the normally consolidated and overconsolidated clays, although the magnitude of the stresses differed. This difference depends on the stress history of clay bed. For the purpose of discussion, only the variation in stresses of the normally consolidated clay ( $p_0 = 420 \text{ kN/m}^2$ ) shown in Fig. 8.5 is discussed. Where appropriate, the effects of overconsolidation are also discussed.

### 8.5.2 Consolidation and boring

The total and effective stress changes occurring during consolidation have been discussed in Section 7.2.5 and shown in Figs. 7.11 and 7.12. At the end of consolidation, the total horizontal stress was constant and a small residual pore water pressure of the order of 5 to 15 kN/m<sup>2</sup> was present. This is denoted by point A in the respective curves in Figs. 8.5 and 8.6. The residual pore pressure is thought to be the result of a threshold value of hydraulic gradient required to cause flow in a clay system [Miller and Low (1963)]. Below this threshold value, flow would not occur and therefore the pore pressure would not dissipate fully. Therefore, the effective horizontal stress was slightly less than the total horizontal stress.

With boring, relief of total lateral stresses on the walls of the borehole occurred. Therefore, when the load was removed from the saturated soil, the total stress in the soil at the surface of the borehole was zero, and the change in pore water pressure was equal to the magnitude of stress relief giving a negative value. Therefore, values at B represent the values immediately after boring.

In a fine grained soil like clay, viscous resistance to pore water flow prevents the soil structure from rapidly expanding by absorbing in pore water from the surrounding soil. This resistance together with the tension at the face of the borehole caused by the negative pore water pressure, provides the initial stability of the borehole. This stability is time-dependent. If the hole is not concreted after some time, then collapse of the hole may occur. It will be shown later in this chapter that a delay between concreting and the completion of boring has an effect on the stability of the borehole and the development of shaft resistance.

### 8.5.3 Casting and curing

When the microconcrete was cast in the borehole and pressurized (to simulate the hydrostatic head of fresh concrete), two significant changes in the soil stresses were observed. There was an immediate rise in the total horizontal stress from C to D and this stress then increased with time. The magnitude of D depends on the stress history of the soil; the higher the consolidation pressure or overconsolidation ratio, the higher is the immediate rise in total horizontal stress. At the same time, the negative pore pressure was dissipated by moisture migration into the stress-relieved zone from the excess water present in the fresh concrete and from the surrounding area of relatively higher pore pressure unaffected by the boring. This migration of pore pressure resulted in swelling and softening of the soil. It has been shown in Sections 7.3 and 7.4 that these effects were significant for soil within 20mm from the pile surface.

It can be seen from Figs. 8.5 and 8.6 that the dissipation of negative pore pressure for normally and lightly overconsolidated clays follow the same trend indicated by B-C-D, although differing in magnitudes. The point C represents the pore pressure measured after placement of the piezometer and the point D represents measurement after the concrete was placed and pressurized. The significant difference in negative pore pressure dissipation between the normally consolidated and overconsolidated clay indicated by B-C can be explained by the observation of Lambe and Whitman (1968) and the limitation of the interface piezometer in measuring negative pore pressures. As discussed in Section 8.4.5, Lambe and Whitman found that negative pore pressure greater than  $100 \text{ kN/m}^2$  can sustain pure tension for only a short time, after which cavitation in the measuring system will occur. Although both readings at C for Figs. 8.5 and 8.6 are slightly higher than  $100 \text{ kN/m}^2$ , they soon dropped to values below  $100 \text{ kN/m}^2$ .

As the concrete set, the total horizontal stress against the pile interface increased with time as shown by the rise in path D-E-F where points D and F represent the total horizontal stress after a curing time of 7 and 30 days respectively. Because of the limitation of the IF pressure cells as regards long term stability of the strain gauges (discussed in Section 8.4.4), they were not installed in piles in which the curing time exceeded 30 days. For the overconsolidated clays there is no point 'F' since measurements for total horizontal stress and pore pressure were only taken up to the 7 days curing time, after which the pile was tested. In general, the negative pore water pressure dissipated with time and approached an equilibrium value represented by a small residual pore pressure.

Total horizontal stress variation after a curing time of 30 days is shown in broken lines (Fig. 8.5) to indicate the expected trend. It is probable that the total horizontal stress may reach its undisturbed value. However, Chandler (1968) and Tomlinson (1977) suggest that this is unlikely to occur because of soil arching around the pile shaft and shrinkage in concrete. Although these phenomena are likely to occur with field piles, it is unlikely that they would have a significant effect in this research study. This is based on the fact that the circumference of the pile was relatively small and the volume of concrete used to construct the pile was very small. Therefore, neither soil arching or concrete shrinkage would prevent the total horizontal stress from approaching its undisturbed value.

In general, the horizontal effective stress for both the normally and lightly overconsolidated clay does not vary as much as the total horizontal stress and the pore water pressure. In the effective stress diagram, points B and C have been omitted since they are approximately similar in values to A and D respectively. Therefore, the path A-D represents the change in effective stress before boring and immediately after concrete was cast and pressurized.

With time, the effective stress also approaches its undisturbed value, although as shown in Fig. 8.5, the effective stress at 30 days curing is slightly less than the effective stress prior to pile installation. However, within limits of the sensitivities of the measuring devices, this difference is small. Therefore, it appears reasonable to assume that the horizontal effective stress in the soil before pile installation and some time after installation are approximately the same.

#### 8.5.4 Pile Loading

After a defined curing period, load tests were carried out on the piles at a relatively rapid rate. However, measurements by the interface piezometer showed that during loading, very small positive pore pressures ( $<20 \text{ kN/m}^2$ ) were generated in the soil. The small excess pore pressures were generally less than 8% of the effective horizontal stress at the interface.

Three possible explanations can be proposed for the above observation: (1) the interface piezometer was unreliable, (2) drainage occurred along the thin shear zone formed around the pile even during the short period between successive increments, and (3) the excess pore pressure due to loading is generally low.

The first explanation appears unlikely since prior to loading, the device performed satisfactorily. The blockage of the probe is also ruled out since after each test, the probe was re-tested for its response.

Excess pore pressure may dissipate quickly along the thin shear zone of soil adjacent to pile or into the porous concrete which may act as a vertical drain. However, it is not possible to verify or deny this inference apart from the observation that no excess water was found on or

near the 'top' of the pile after a load test.

The third explanation appears to be supported by a number of authors. Tomlinson (1970) observed that if the excess pore water pressure generated during installation was allowed to dissipate completely, then no significant changes occurred in the pore pressure during the loading of the piles. Measurements of pore water pressure at the pile-soil interface due to loading have been reported by Clarke and Meyerhof (1973). Based on the study of large model piles and some full-scale piles driven into insensitive clay, the authors found that the excess pore pressure were less than 15% of the effective horizontal stress for normally and lightly overconsolidated clay.

D'Appolonia and Lambe (1970) applied the finite element method to determine the change in stress due to loading an incompressible pile in an elastic medium. This analysis indicated that changes in total radial stresses at the pile-soil interface due to loading are small.

Kirby and Esrig (1979) summarized some published data on excess pore pressures generated during pile loading and found that they are generally in the range of 0 to 25% of the undrained shear strength and within 10% of the average normal effective stress (i.e.  $\frac{1+2K_0}{3} \sigma_{vo}'$ ). Elastic finite element analysis by the authors also yielded small changes in pore pressure due to loading.

On the basis of the reported literature, the small excess pore pressure observed in the study during loading therefore seems reasonable and suggests that effective stress conditions at the pile interface remain virtually unchanged by pile loading. This observation can be explained by considering a soil element adjacent to the pile. During loading, the soil element is subjected to a pure shear loading, and excess pore pressure due to the applied shear stresses is zero. Any change in pore pressure will be due to changes

in the total vertical and radial stresses at the pile-soil interface during loading. Since the total horizontal stress measured by the IF pressure cell during loading showed very small changes, the excess pore water pressure measured is therefore small. In fact, the small changes in total horizontal stress and excess pore pressure at the interface due to loading were of the same order.

## 8.6 ANALYSIS OF LOAD TEST RESULTS IN TERMS OF TOTAL AND EFFECTIVE STRESS

### 8.6.1 Introduction

In this section, the test results in Test Series ST1, ST2 and LT2 presented in Table 7.13 (Section 7.5) are analysed by the total and effective stress methods. General principles of these methods have been discussed in Chapter 3. The implications of these analyses are then compared with some reported results from laboratory and field tests.

### 8.6.2 Total Stress Analysis

The common procedure for correlating shaft resistance with undrained shear strength is to define an adhesion factor  $\alpha$ , that is,

$$q_s = \alpha c_u \quad \dots (8.3)$$

The value of  $\alpha$  calculated are based on the assumption that the values of undrained shear strength obtained from the reconsolidated-undrained triaxial tests (see Section 7.2.3) are representative of the prepared clay bed. Results of this analysis are presented in Table 8.3. The remoulding factor,  $\alpha_r$ , from the study on installation effects in Sections 7.3 and 7.4, are also shown in this table as a basis of comparison with the adhesion factor.

Values shown in Table 8.3 suggests that for piles tested 7 days after casting,  $\alpha$  varies between 0.58 and 0.76 for the normally consolidated clay and from 0.45 to 0.77 for the overconsolidated clay. These values are plotted against the undrained shear strength in Fig. 8.7. On the same figure, the recommended design curves by Skempton (1959) and Tomlinson (1977) are also plotted.

It can be seen from Fig. 8.7 that the values of  $\alpha$  for normally consolidated clay are higher than the upper limit of 0.6 suggested by Skempton for bored piles constructed in favourable conditions, but lower than Tomlinson's adhesion values which are based on driven piles in clay. The only agreement with the design curves given by Tomlinson is that  $\alpha$  increases with a decrease in undrained strength. The difference in magnitude of  $\alpha$  values may be attributed to the different methods of pile installation as well as the time in which the piles are tested. Chandler (1968) and Tomlinson (1977) have shown that the undrained shear strength increases with time after pile installation. An increase in undrained strength was also observed in this study as shown in Fig. 7.21. Therefore, results of load tests will depend on the time period between installation and testing.

Comparing the laboratory results with Skempton's design values, it is prudent to note that the design values are based mainly on load tests of bored piles in stiff overconsolidated London Clay. The low  $\alpha$  values in the field are to account for variation in soil properties and construction procedures. However, in this study, the laboratory-scale bored piles were constructed in conditions near to 'ideal', i.e. there was no delay between boring and concreting, and no adverse soil or ground water conditions existed. This may account for the high  $\alpha$  values.

The size of the laboratory piles, which has been discussed in Section 8.5.3, could be another reason for the high  $\alpha$  values. The relatively small circumference of the piles aided the rapid re-establishment of the effective horizontal

pressure. Therefore, even though laboratory piles were tested only 7 days after casting, the shaft resistance mobilized was relatively high.

For the case of overconsolidated clay,  $\alpha$  values obtained are lower than those for normally consolidated clay. Despite the fact that they are only lightly overconsolidated, the observation suggests that there is a greater degree of disturbance during installation of bored piles in overconsolidated clay. This may be attributed to the relatively higher swelling potential in overconsolidated clay when loads are removed during boring. Associated with swelling, as discussed in Section 8.5.2, is the softening of soil. The values of  $\alpha$  for the lightly overconsolidated clay appear to fall within the design limits of Skempton. However, based on long term tests carried out in normally consolidated clay, there is evidence to suggest that  $\alpha$ -values for overconsolidated clay will also increase with time.

For piles tested at 30 days, the increase in shaft resistance over the 7-day value was about 16%, after which further increase was small. For piles tested at great age (between 100 to 300 days), it appears that the values of  $\alpha$  approach a limit of about 0.80. This limit is in good agreement with the results of O'Neill and Reese (1972) who found from their laboratory and field studies that 70% to 85% of the undrained shear strength should be developed ultimately along the shafts of bored piles installed in dry. Skempton (1959) also found that the upper limit of  $\alpha$  for bored piles in London Clay is 0.80.

If the remoulding factor,  $\alpha_r$ , is plotted against the adhesion factor,  $\alpha$ , it can be seen in Fig. 8.8 that for the short term tests, values of  $\alpha_r$  agree well with  $\alpha$  values. However, for long term tests, values of  $\alpha_r$  and  $\alpha$  have no significant relationship apart from the fact that they approach a limit of about 1.0 and 0.8 respectively. The

implication of this result is that although the undrained shear strength had been 'restored' with age, the shaft resistance mobilized was still only 80% of the undrained shear strength.

There are three possible explanations to account for this loss in strength. Firstly, loss in strength could be the result of a reduction in effective stress due to excess pore water pressure generated during loading. However, it has been stated in Section 8.5.4 that the excess pore pressure due to loading is small and unlikely to significantly affect the effective stress condition at the pile shaft. A second possible reason is that loads were applied over a short period on the piles, and this procedure will undoubtedly have some influence in the development of shaft resistance. Had the loads been sustained over a longer period, the shaft resistance developed will be greater than that obtained from a quick load test. Due to this consolidation, the value of  $\alpha$  may approach unity [Wooley and Reese (1974)]. Another possible explanation is that a number of factors affect the development of shaft resistance apart from the undrained strength of the soil at the time of loading, such as surface roughness and the effects of installation on the soil structure at the interface. These factors could have contributed to a reduction in the shaft resistance developed.

### 8.6.3 Effective Stress Analysis

To analyse the problem using the effective stress method requires a knowledge of the effective stress parameters of the soil as well as the effective stress conditions in the soil before and after pile installation. In section 3.2 the difficulties associated with the application of the effective stress method have been discussed. The effective stress equation similar to that proposed by Chandler (1968) is commonly given as,

$$q_s = \sigma_H' \tan \delta \quad \dots (8.4)$$

$$\text{or } q_s = K_s \sigma_v' \tan \delta \quad \dots (8.5)$$

The results of the effective stress analysis are presented in Table 8.4.

The measured values of  $\sigma_{vo}'$  and  $\sigma_{Ho}'$ , the effective vertical and horizontal stresses after consolidation, and  $\sigma_H'$ , the effective horizontal stress at the pile interface prior to loading, are shown in columns 3 to 5 of the table. It has been shown in Section 8.5.4 that the effective horizontal stress,  $\sigma_H'$  showed no significant change after pile loading. For tests LT2.3 to LT2.6, the values of  $\sigma_H'$  are assumed to be  $260 \text{ kN/m}^2$  (the average value of  $\sigma_{Ho}'$  in the same tests) since the stress was not measured for reasons of instrument stability discussed in Section 8.4.4.

The values of  $K_o$  and  $K_s$  deduced from the measured stresses are shown in columns 6 and 7 where,

$$K_o = \sigma_{Ho}' / \sigma_{vo}' \quad \dots (8.6)$$

$$\text{and } K_s = \sigma_H' / \sigma_v' \quad \dots (8.7)$$

Since it was not possible to measure  $\sigma_v'$ , the effective vertical stress at the pile interface prior to loading, it was assumed that  $\sigma_v' = \sigma_{vo}'$ . This assumption should be borne in mind in the evaluation of the results.

If the shaft resistance,  $q_s$ , is plotted against the measured effective horizontal stress,  $\sigma_H'$ , for both the short and long term tests, it can be seen from Fig. 8.9 that a linear relationship exists and that the tangent of the angle of shearing resistance between the pile and soil is given by the gradient of the line.

If  $c'=0$  is assumed, then for the range of effective horizontal stress measured, the relationship given by a full line in Fig. 8.9 is,

$$q_s = 0.260\sigma_H'$$

and  $\delta = 14.6^\circ$

If no assumption is made regarding  $c'$ , then the best fit for the points plotted is shown by broken lines. In this case, the y-intercept gives a small effective cohesion and the equation of this line is,

$$q = 4.5 + 0.232\sigma_H'$$

giving  $c' = 4.5 \text{ kN/m}^2$

and  $\delta = 13.1^\circ$

The presence of a small effective cohesion may be due to the influence of the results of load tests in the overconsolidated clay. Nevertheless, it is usual to assume zero effective cohesion in the effective stress approach for reasons given in Section 3.3.5. Therefore, in the following discussions, the relationship given by the full line in Fig.8.9 will apply. However, it is prudent to note that where the maximum shaft resistance developed is low, the assumption that  $c'=0$  could represent a significant error in the analysis.

If the calculated angle of shearing resistance between the pile and soil is compared with the effective angle of friction  $\phi'$  measured by consolidated-undrained triaxial tests with pore pressure measurement and given in Section 7.2.4, then it can be seen that,

$$\delta/\phi' = 0.73$$

The implication of this result will be discussed further in the next section.

For bored piles, it has been suggested that because of the effects of installation,  $K_S < K_O$ . Test results in Table 8.4 indicate that it is possible that the  $K_O$  conditions may be restored after pile installation. Values of  $K_S$  measured at 7 days indicate that between 75% to 90% of the  $K_O$  conditions were 'restored'. Values of  $K_S$  measured at 30 days showed an increase of about 12% on the  $K_S$  value at 7 days.

This corresponds to an increase in shaft resistance of about 16% over the same period, thus giving further evidence that the shaft resistance is a function of the effective horizontal stress.

The fact that  $K_S$  approaches the value of  $K_0$  can also be attributed to the experimental procedure. The piles were formed in relatively 'favourable' conditions and the circumference of the piles were relatively small. Thus, the degree of disturbance due to pile installation was relatively small and coupled with the rapid re-establishment of the effective horizontal stress because of the size of pile, it is therefore not surprising that  $K_S$  may be equal to  $K_0$ .

#### 8.6.4 General discussion on total and effective stress analysis

From the analyses presented in the previous sections, there appears to be some correlation between total and effective stress methods. The trend whereby the remoulding factor  $\alpha_r$  approaches unity with time appears to correspond to the trend of  $K_S$  approaching  $K_0$ . Both these observations imply that for the case of the laboratory piles, original soil conditions are probably restored after a certain period.

The values of  $\beta$  calculated from  $q_s/\sigma_{v0}'$  and given in column 9 of Table 8.4 show much less variation than the  $\alpha$ -values. For the normally consolidated clay, the average value of  $\beta$  is 0.14 increasing to about 0.17 after 100 days. For the overconsolidated clay, the values of  $\alpha$  and  $\beta$  are plotted against the overconsolidation ratio in Fig. 8.10. However, no direct relationship between  $\alpha$  and  $\beta$  can be established apart from the obvious inference that with increasing overconsolidation ratio (for  $OCR \leq 4$ ),  $\beta$  increases in value while  $\alpha$  decreases in value.

The effective angle of friction between the pile and soil,  $\delta$ , obtained by back-calculation from the effective stress equation (8.4), has been found to be less than the effective angle of shearing resistance of the soil,  $\phi'$ . There are three possible reasons why the effective angle of shearing resistance,  $\phi'$ , was not fully mobilized. Firstly, the value of  $\delta$  could be the effective residual angle of friction,  $\phi_r'$ , suggested by Searle (1979). Secondly, the value of  $\delta$  could be the result of softening and remoulding on the clay close to the pile face. Thirdly, the physical condition of the pile surface could have influenced the mobilized effective angle of friction at pile failure.

Considering the first reason, Searle has shown that the adhesion is related to the effective angle of shearing resistance and derived the expression,

$$\alpha \simeq \tan \phi_r' \frac{1 - \sin \phi_p'}{\sin \phi_p'} \quad \dots (8.8)$$

where  $\phi_p'$  and  $\phi_r'$  are the effective peak and residual angles of friction respectively. Assuming  $\phi_p' = \phi' = 20^\circ$  (from consolidated-undrained test) and  $\phi_r' = \delta = 14.6^\circ$  (obtained by back analysis in this study), then equation (8.8) gives the result,

$$\alpha \simeq 0.50$$

However, this value is well below the ultimate adhesion factor of 0.80 deduced from the load tests. Moreover, it is unlikely that the normally consolidated clay or the lightly overconsolidated clay would have given residual values of  $\phi'$  which were significantly lower than the peak value. For these reasons, it is unlikely that the assumption  $\delta = \phi_r'$  is valid.

To check the validity of the second reason, four triaxial specimens were wrapped in filter paper and submerged in distilled water for about seven days. This procedure was similar to that used by Chandler (1968) to simulate the

remoulding and softening that occurs with bored pile construction. These specimens were then reconsolidated and sheared under undrained conditions at different cell pressures similar to the procedure described in Section 4.4.3. The effective stress parameters obtained for the 'softened' specimens are  $c'=0$  and  $\phi'=18.5$ . Therefore, although the value of  $\delta$  is not the 'softened' effective angle of friction it is possible that the softening and remoulding effects could have contributed to the reduction in the mobilized effective angle of friction.

Considering the third reason why  $\delta < \phi'$ , a stress condition similar to that shown in Fig. 8.11 has been discussed by Parry and Swain (1976). The physical condition of the pile surface could be such that when failure occurred, the maximum value of  $\delta$  which could be mobilized on the soil-pile interface was insufficient to induce failure in the soil element. Therefore, failure was not in the soil close to the pile, but at the interface. In fact, a close observation of the soil adjacent to the pile after a load test showed no definite failure plane in the soil.

At this juncture, it is appropriate to draw attention to the difference between piles constructed in the laboratory and piles cast in the field in terms of the precise regularity of the contact surface between concrete and the soil. Surface roughness in a field bored pile is difficult to simulate in the laboratory. Nevertheless, surface roughness would affect the mobilized effective angle of friction between the pile and the soil, and hence the mobilized shaft resistance.

Rice (1975) conducted pull-out tests on a 19mm diameter model underreamed pile made of mild steel embedded in kaolin. Using a load cell placed just above the underream, the shaft resistance of the anchor was obtained from the total pull-out load. For the normally consolidated clay, prepared anisotropically at a range of consolidation pressure from

150 to 570 kN/m<sup>2</sup>, the values of  $\beta$  could be calculated from the results of Rice's studies, and were found to vary between 0.14 and 0.20 for shaft resistance. Applying the effective stress equation of (8.5) to Rice's work and assuming  $K_0 = 0.64$  obtained from this study, an average relationship of  $\delta = 0.68 \phi'$  was obtained. Although the installation procedure was different in that the clay was consolidated around the underreamed pile, values of  $\beta$  and  $\delta/\phi'$  appear to be of the same order as these found in this study. One implication of this comparison is that in view of the similarity in the values of  $\delta/\phi'$ , it is possible that the surface of the microconcrete used may approximate to that of the smooth mild steel of the model underreamed pile.

It is also interesting to note that Potyondy (1961) obtained an angle of friction between concrete and clay less than the angle of shearing resistance of the soil. This conclusion was based on a number of shear box tests using various types of clay.

An electron microscope study of the soil fabric at the pile interface and in the soil mass may assist in the verification of the above explanations, particularly the reason concerning the physical condition of the pile.

Assuming that  $\delta < \phi'$  is because of the physical condition of the pile, the stress condition given by Parry and Swain (1976) and shown in Fig. 8.11 will be considered. At failure, the stress circle at the pile-soil interface is given by LMN where OM represents the failure envelope. From the geometry of Fig. 8.11,

$$q_s = r \cos \delta \quad \dots (8.9)$$

(a) if  $\sigma_1' = \sigma_{vo}'$  (i.e.  $\sigma_{vo}' > \sigma_v'$ ),

$$\sigma_{vo}' = \frac{r}{\sin \delta} + r \quad \dots (8.10)$$

eliminating  $r$ ,  $q_s = \sigma_{vo}' \frac{\sin \delta \cos \delta}{1 + \sin \delta} \quad \dots (8.11)$

[equation (8.11) can be rewritten as  $q_s = \sigma_{v0}'(1 - \sin \delta) \tan \delta$ ]

(b) if  $\sigma_v' = \sigma_{v0}'$ ,

$$\sigma_{v0}' = \frac{r}{\sin \delta} + r \sin \delta \quad \dots (8.12)$$

combining equations (8.9) and (8.12),

$$q_s = \sigma_{v0}' \frac{\sin \delta \cos \delta}{1 + \sin^2 \delta} \quad \dots (8.13)$$

Substituting the value of  $\delta = 14.6^\circ$  obtained from this study, equation (8.11) gives  $\frac{q_s}{\sigma_{v0}'}$  0.19 and equation (8.13) gives  $\frac{q_s}{\sigma_{v0}'}$  0.23. Case (a) where  $\sigma_1' = \sigma_{v0}'$  appears to give a better approximation to the values of  $q_s/\sigma_{v0}'$  obtained from this study i.e. 0.17. Therefore, assuming  $\sigma_v' = \sigma_{v0}'$  in the effective stress equation (8.5) may give an overestimation of the shaft resistance.

#### 8.6.5 Comparison of design methods

The observed maximum shaft resistance developed at failure allows a comparison to be made with that calculated, using various methods currently available for the design of bored piles in cohesive soils. The comparison between measured and predicted values is shown in Fig. 8.12.

In plotting the graphs in Fig. 8.12, the following assumptions have been made:

1. The measured shaft resistance plotted on the Y-axis is based on the results of load tests carried out 7 days after casting in normally consolidated clay (Test Series ST1).
2. In Skempton's method, two assumptions have been made. In the first case, the commonly used value of 0.45 for  $\alpha$  has been assumed (Graph 1). Since the laboratory bored piles were constructed in favourable conditions, the upper limit of 0.6 for  $\alpha$  has also been assumed (Graph 2).
3. In Chandler's method given by equation (3.11) for

normally consolidated clay,  $K_0$  and  $\delta$  have been assumed as  $(1-\sin\phi')$  and  $\phi'$  respectively. A further assumption has been made that the effective cohesion is zero. The value of  $\phi'$  has been taken as  $20^\circ$ , obtained from consolidated-undrained triaxial tests with pore pressure measurement, and the predicted relationship with measured values is shown in Graph 3.

4. In Burland's method  $\beta$  has been assumed as 0.3, the design value recommended by the author for shaft resistance in soft clay (Graph 4).
5. The assumed ultimate shaft resistance in Graph 5 is based on the results of short and long term load tests carried out in normally consolidated clay at a consolidation pressure of  $420 \text{ kN/m}^2$ . The ultimate shaft resistance developed at great age ( $>100$  days) represents an increase of about 23% over the shaft resistance developed at 7 days. On this basis, it has been assumed that the shaft-resistance developed 7 days after casting for normally consolidated clay at other pressures will assume a similar increase in shaft resistance at great age.

In general, the total stress methods gave predictions of shaft resistance less than the measured shaft resistance and the assumed ultimate shaft resistance. On the other hand, both the effective stress methods gave higher values of shaft resistance. The latter observation is not surprising since Chandler (1968) has shown that for bored piles, effective stress analysis applied with the above assumptions generally gives results which are an upper limit to the measured values.

To ascertain the degree in over- or under- estimation of the measured values, a typical example is taken for the case of piles tested in normally consolidated clay prepared at a consolidation pressure of  $420 \text{ kN/m}^2$  (Test ST1.1 and LT2.6). From the results given in Table 8.4, the shaft resistance at 7 days and 300 days have been found to be

55.0 kN/m<sup>2</sup> and 67.5 kN/m<sup>2</sup> respectively. Comparisons with values predicted by the various design methods are summarized in Table 8.5

It can be seen from the table that Skempton's method where  $\alpha$  is taken as 0.45 underestimates both the short and long term shaft resistance by about 30% and 45% respectively. Where  $\alpha$  is taken as 0.60, the predicted values are closer to the measured values. This indicates that Skempton's recommendation, that a value of  $\alpha$  equal to 0.60 to be used for piles constructed in favourable conditions, agrees well with recorded values. The comparison also suggests that  $\alpha$  equal to 0.45 may not be a suitable value for piles constructed in soft to firm clay. However, this inference should be treated with caution in view of the differences between laboratory and field piles which were briefly mentioned in the previous sections.

For the effective stress methods, Burland's approach gives predicted values about twice the measured values for the short and long term shaft resistance. The difference can be attributed to the fact that  $\beta$  equal to 0.3 has been based on load tests on driven piles. For bored piles in normally consolidated soil, it has been shown in Section 3.2.2 that this value will give an overestimation of the ultimate shaft resistance.

A better agreement is obtained between Chandler's method for long term results, where the predicted value is 1.4 times the shaft resistance at 300 days. However, as Chandler (1968) pointed out, this method represents the upper limit of the shaft resistance in normally consolidated clay, and in practice, it is likely that the ultimate shaft resistance at great age will be less than the values predicted by this method.

### 8.6.6 Implications of the analyses

If bored piles are constructed in favourable soil conditions with good site supervision and quality control, an adhesion factor as high as 0.8 may be achieved. The total stress analysis has shown that assuming an adhesion factor of 0.45 can result in an under-design of the pile. Because of the economic implication, especially in a major contract, an adhesion factor of 0.45 is considered to be unstable for bored piles in normally consolidated clay. An adhesion factor of 0.6 is considered to be more appropriate provided there are no adverse ground conditions and good construction practice is followed.

Since the effect of casing withdrawal on the development of shaft resistance was not studied, a brief discussion is appropriate in view of the fact that a substantial number of bored piles are constructed using temporary casing. If casing is used, it is likely that adhesion factors will be lower than those suggested in the previous paragraphs. This would be due to the greater degree of soil disturbance associated with the installation and withdrawal of casing as discussed in Section 2.3.4. Therefore, the commonly used adhesion factor of 0.45 is probably appropriate for design. This is in agreement with the design recommendation by O'Neill and Reese (1972) that when the casing method of construction is used, the adhesion factor assumed for piles installed by the dry method should be reduced by about one-third when applied to design of piles constructed by the casing method (Section 2.6.6).

In the effective stress analysis, it has been shown that the shaft resistance is a direct function of the effective horizontal stress acting on the pile shaft,  $\sigma_H'$ , and the effective angle of shearing resistance,  $\delta$ . Better agreement exists between the measured shaft resistance and that predicted by the effective stress approach in equation (8.4) when  $\delta$  is less than  $\phi'$ . In this study,  $\delta$  was found to be

0.73  $\phi'$ . However, more tests are required before any definite design guidelines can be established.

A further understanding of the effective stress design parameters is required to help facilitate extrapolation of results from research to actual pile design of piles. At the present state of knowledge in practice, it is more common to use  $K_0$  and  $\sigma_{v0}'$  than  $K_s$  and  $\sigma_H'$  in effective stress analysis because of the difficulties in determining the latter parameters in the field. This study has shown that if  $K_0$  and  $\sigma_{v0}'$  values are used in the analysis, the result represents an upper bound value for the shaft resistance of bored piles in normally consolidated clay. No definite conclusion can be drawn for the lightly overconsolidated clay from the effective stress analysis in view of the limited amount of test results.

In the present state-of-the-art, the effective stress methods of design may not represent a significant improvement over the total stress methods. Information on the effective stress condition of the soil before and after pile installation in practice is not presently available. Laboratory tests and theoretical analysis can only suggest the trend and possible changes in the effective stresses in the soil. Therefore, field measurements of effective stresses in the soil are urgently required to verify these observations and provide information for further development of the effective stress approach in design.

## 8.7 FACTORS INFLUENCING DEVELOPMENT OF SHAFT RESISTANCE OF BORED PILES

### 8.7.1 Introduction

The results of shaft resistance presented in the previous sections are influenced by a number of factors such as the stress history of the soil, the effects of installation and the age at which piles are tested. These factors are

discussed in this section with reference to the results presented in Tables 7.13, 8.3 and 8.4.

### 8.7.2 Effect of stress history of the soil

Only normally and lightly overconsolidated clays were investigated in this study. Limitations in the test equipment did not permit overconsolidated clay to be prepared to an overconsolidation ratio greater than 4.

It has been shown in Section 8.6.2 that the values of  $\alpha$  for overconsolidated clays are lower than those for normally consolidated clay. However, the behaviour in terms of load-settlement characteristics appears to be similar for both the normally and lightly overconsolidated clay as shown by a family of curves in Fig. 8.13 for different stress histories. The difference between the curves lies in the magnitude of the shaft resistance mobilized and the settlement prior to 'plunging' failure.

The curves indicate a quick build up of shaft resistance at low settlement. As overconsolidation ratio increases the maximum shaft resistance developed also increases. It has been stated in Section 7.2.5 that the coefficient of lateral earth pressure at rest,  $K_0$ , is related to the overconsolidation ratio. Since shaft resistance is controlled by the magnitude of the effective horizontal stress, it is therefore expected that as overconsolidation ratio increases,  $K_0$  and hence the shaft resistance increases.

### 8.7.3 Effect of pile dimensions.

Tests carried out in Series ST3 showed that pile dimensions do not affect the development of the shaft resistance. The load-settlement characteristics for three piles of diameters 25mm, 38mm and 50mm tested in beds of clay normally consolidated at  $420 \text{ kN/m}^2$  are shown in Fig. 8.14. Values of shaft

resistance for the three piles tested are generally of the order of 0.9% to 1.2% and the maximum shaft resistances developed are within 12% of each other. The significant difference lies in the magnitude of the settlement prior to plunging failure. The 50mm diameter pile showed relatively large settlement. In view of the limited number of piles tested with different diameters, no definite explanation can be given for this behaviour although, it is believed that the large settlement may be due to the higher loads it supports.

The implication from these tests is that the diameter of a pile does not significantly affect the development of shaft resistance and hence the results obtained from this study may be applicable for both small and large diameter bored piles, but this requires further study.

#### 8.7.4 Effect of delay between completion of boring and Concreting

Test Series ST4 was carried out to determine the effects of delay between boring and concreting on the development of shaft resistance. In these tests, the soil face of the borehole was allowed to be exposed for a longer time than usual prior to concrete placement. Delay times of 2, 12 and 24 hours were investigated. During these periods, the change in diameter of the borehole at the mid-height of the pile shaft was measured using a modified caliper capable of measuring to an accuracy of 0.1mm. After these delay periods, the hole was filled with microconcrete in the usual way and load tested after 7 days.

The changes in pile diameter and the shaft resistance developed are presented in Table 8.6. Also shown in the table is the ratio  $q_s/q_0$ , where  $q_s$  represents the maximum shaft resistance of the pile installed with a delay time between boring and concreting and  $q_0$  denotes the maximum shaft

resistance of the pile installed with a minimum delay time (i.e. 30mins). The variation of adhesion factor and pile diameter with delay time are shown in Fig. 8.15.

Measurements showed that the diameter of borehole decreased with increasing delay between boring and concreting implying radial soil movement towards the centre of the borehole. Relaxation of stress in the soil as load is removed during boring may result in plastic yielding, even at stresses well below those which would result in shear failure, causing the radial movement of the soil perimeter. However, the diameters of piles measured after the load tests showed a slight increase over that measured prior to casting. This observation can be attributed to the total lateral pressure exerted by the fresh concrete acting against the soil at the interface.

The cumulative effect of stress relaxation in the soil followed by pressure exerted by the concrete is reflected in the shaft resistance mobilized. With longer delay time, the adhesion factor decreases. It is interesting to note that the variations in the adhesion factor and the diameter of borehole prior to casting shown in Fig. 8.15 follow a similar trend although, it is prudent to note that the trend is a function of the scales of axes.

For delay time less than 2 hours, the effect on the shaft resistance is unlikely to be significant. However, delay times of 12 hours and 24 hours (not uncommon in practice) result in load reductions of about 10% and 20% respectively.

Fearenside and Cooke (1978) also investigated the effect of delay between boring and casting on the adhesion factor. No definite conclusions could be drawn from the field tests in view of the limited number of tests and the uncertainties in the number of variables affecting the pile behaviour.

The observations above have shown the importance of the delay between boring and concreting. Therefore, in pile tests, it is desirable as well as advantageous to keep a record of the time of each stage of pile construction especially the time lapse between boring and concreting.

#### 8.7.5 Influence of moisture migration

As shown in Sections 7.3 and 7.4, the effect of an increase in moisture content results in a corresponding reduction in shear strength in the soil. This relationship is illustrated in Fig. 8.16, and the reduction in shear strength is denoted by the remoulded factor,  $\alpha_r$ . The relationship between the remoulding factor,  $\alpha_r$ , and the adhesion factor,  $\alpha$ , has been discussed in Section 8.6.2.

It can be seen that the higher the increase in water content of soil close (within 20mm) to the pile, the lower is the value of the remoulding factor, and hence lower adhesion factor. Higher increase in water content of the soil close to the pile has been found to be associated with higher consolidation pressure, higher overconsolidation ratio and higher water-cement ratio.

In order to examine in detail the results of moisture migration studies presented in Sections 7.3 and 7.4, it is essential to consider the concept of water movement in the soil close to the pile. In this respect, the work of Chuang and Reese (1969) is considered. These authors have shown that moisture migration in soil is a function of the potential gradient. Consider a small element of soil at the wall of the shaft. From the theory of fluid flow, the direction of flow must be perpendicular to the hydraulic gradient of the potential gradient. Based on finite element analysis, the authors also showed that when the suction force of the soil is higher than the gravitational force, the effect of gravity can be neglected. Therefore, water from

the fresh concrete will move in a direction normal to the wall of the pile shaft as a result of a hydraulic gradient.

The influence of water-cement ratio of the concrete on the moisture migration has been shown to be of importance. The excess water in the concrete available for moisture migration can be calculated as demonstrated in Table 8.7. In this table, the example considers the case of a 38mm diameter pile constructed in a normally consolidated bed of clay at a consolidation pressure of  $420 \text{ kN/m}^2$ . The water-cement ratio of the concrete used is 0.6, which is the standard value used in the mix design. If other values of water-cement ratio are used in the calculations, it can be seen that the higher the water-cement ratio, the higher is the excess water available.

The observed increase in moisture content of soil within 20mm of the pile was found to be 4.2% (Table 7.7, Test ST5.3), 7 days after casting. Therefore, the increase in weight of water in this region of soil is 18 gm (calculated from  $4.2\% \times$  value in row 8 of Table 8.7) which represents about 80% of the excess water available in the concrete (23 gm). The remaining 20% of the excess water could be found in the outer region of the soil and probably even in the porous concrete as well.

In Section 7.4, it has been shown that with time, the moisture content in the soil close to the pile decreased. Since there was no significant increase in moisture content in the outer region of the soil, as indicated by Fig. 7.20, it is reasonable to assume that the concrete itself has a certain affinity for the excess water. The effects of long-term curing and the associated moisture and undrained shear strength changes on the development of shaft resistance are discussed in the next section.

### 8.7.6 Effect of long term curing of test piles

Results from Test Series LT2 showed that piles experienced a gradual increase in shaft resistance up to about 100 days, after which there is no further increase. The development of shaft resistance with time is shown in Fig. 8.17. The value of  $q_s/q_u$  is the ratio of the shaft resistance developed after a defined curing period and the ultimate shaft resistance that can be mobilized at great age. It can be seen that the shaft resistance developed 7 days after casting represents about 80% of the ultimate shaft resistance after 100 days. These results are based on tests on piles installed in clay beds prepared with a consolidation pressure of  $420 \text{ kN/m}^2$ .

These test results obtained may be compared with those found by other authors. Taylor (1966) found that there was an increase in shaft capacity of about 30% in piles tested at 180 days over those tested 7 days after casting. Whitaker and Cooke (1966) reported an increase in frictional resistance of piles in London Clay of the order of 13% over a period of about 430 days against a 100-day old pile. The time taken to achieve ultimate shaft resistance depends on a number of factors such as the stress condition of the soil, the method of pile installation and the load testing procedure.

The effect of age on the adhesion factor is plotted in Fig. 8.18. Field studies by Taylor (1966) and Rice (1975) are also shown. It has been stated in Section 8.3.2 that  $\alpha$  reaches a limit of about 0.80. Test results compare very well with the reported field studies of Taylor. The trend of the curve is similar to that of Rice, although magnitudes of  $\alpha$  differ. This is due to the different types of soil in which the piles were tested.

When the results are compared with the long term study of the effects of installation in Section 7.4, it is interesting

to note that the increase in shaft resistance is related to the increase in the shear strength of clay softened during installation and to the decrease in moisture content of the soil close to the pile. The remoulding factor,  $\alpha_r$ , is plotted in Fig. 8.18 to show the relationship with the measured adhesion factor. It can be seen in Fig. 7.21 that the moisture content and shear strength of the clay close to the pile achieved equilibrium in about 100 to 150 days and this observation compares reasonably well with the time taken for ultimate shaft resistance to be developed.

TABLE 8.1 REPEATABILITY OF TEST RESULTS

TEST NO.	MAXIMUM CONSOL. PRESSURE $\text{kN/m}^2$	STRESSES AT THE END OF CONSOLIDATION			AVERAGE SHEAR STRENGTH ( $\text{kN/m}^2$ )		PILE LOAD TESTS		
		$\sigma'_H$ $\text{kN/m}^2$	$\sigma'_V$ $\text{kN/m}^2$	$K_o$	VANE SHEAR TESTS	CU TRIAXIAL TESTS	FAILURE LOAD (N)	SHAFT RESISTANCE $q_s$ ( $\text{kN/m}^2$ )	SETTLEMENT $\Delta/D\%$
ST1.1	420	265	415	0.64	39.5	84	599	55.0	1.3
ST1.2	420	262	410	0.64	39	82	590	54.6	1.3
Difference (%)	-	1	1	0	1	2	1	1	0
ST1.3	140	85	135	0.63	13	30	260	22.0	0.8
ST2.1	140	88	138	0.64	13.5	29	265	22.3	0.9
Difference (%)	-	3	3	2	4	3	2	1	10

TABLE 8.2 RESPONSE OF PIEZOMETERS

PRESSURE INCREMENTS $\text{kN/m}^2$	$\Delta\sigma_v$ $\text{kN/m}^2$	MEASURED TIME TO PEAK (secs)			CALCULATED TIME LAG(sec.) (99% equalisation)	
		MINIATURE PIEZOMETER TRANSDUCER	SOIL PIEZOMETER	INTERFACE PIEZOMETER	SOIL	INTERFACE
					PIEZOMETER	PIEZOMETER
0 → 70	70	1	15	12	10	5
70 → 140	70	2	18	14	16	8
140 → 280	140	4	32	20	24	13
280 → 420	140	6	40	28	29	16
420 → 560	140	10	48	34	33	19.

TABLE 8.3 TOTAL STRESS ANALYSIS OF LOAD TEST RESULTS

TEST NO	MAXIMUM SHAFT RESISTANCE $q_s$ (kN/m <sup>2</sup> )	MEAN UNDRAINED SHEAR STRENGTH $C_u$ kN/m <sup>2</sup>	REMOULDED FACTOR $\alpha_r$	ADHESION FACTOR $\alpha$	MOBILIZATION OF ULTIMATE SHAFT RESISTANCE %
ST1.1	55.0	84	0.65	0.65	81
ST1.2	55.4	84	0.65	0.66	-
ST1.3	22.0	29	0.81	0.76	-
ST1.4	39.8	56	0.74	0.71	-
ST1.5	54.6	84	0.65	0.65	-
ST1.6	63.8	110	0.57	0.58	-
ST2.1	22.2	29	0.81	0.77	-
ST2.2	29.7	53	-	0.56	-
ST2.3	36.9	74	-	0.50	-
ST2.4	42.7	95	-	0.45	-
LT2.1	59.2	84	0.71	0.70	88
LT2.2	63.8	84	0.79	0.76	95
LT2.3	65.6	84	1.01	0.78	97
LT2.4	67.0	84	1.03	0.80	100
LT2.5	68.0	84	1.08	0.81	100
LT2.6	67.5	84	1.05	0.80	100

TABLE 8.4 EFFECTIVE STRESS ANALYSIS OF LOAD TEST RESULTS

TEST NO	MAXIMUM SHAFT RESISTANCE $q_s$ (kN/m <sup>2</sup> )	MEASURED VALUES			$K_o$	$K_s$	$K_o/K_s$	$\beta$
		$\sigma_{vo}'$ kN/m <sup>2</sup>	$\sigma_{Ho}'$ kN/m <sup>2</sup>	$\sigma_H'$ kN/m <sup>2</sup>				
1	2	3	4	5	6	7	8	9
ST1.1	55.0	405	260	220	0.64	0.54	0.84	0.14
ST1.2	55.4	410	260	225	0.64	0.55	0.86	0.14
ST1.3	22.0	135	90	80	0.65	0.59	0.90	0.16
ST1.4	39.8	275	175	155	0.64	0.56	0.88	0.14
ST1.5	54.6	415	265	220	0.63	0.53	0.83	0.13
ST2.1	22.2	135	85	80	0.64	0.59	0.92	0.16
ST2.2	29.7	130	110	100	0.82	0.69	0.84	0.22
ST2.3	36.9	135	145	130	1.06	0.96	0.90	0.27
ST2.4	42.7	130	160	145	1.21	1.11	0.92	0.32
LT2.1	59.2	405	260	230	0.64	0.56	0.88	0.15
LT2.2	63.8	410	255	245	0.63	0.60	0.95	0.16
LT2.3	65.6	410	260	↑	0.64	↑	-	0.16
LT2.4	67.0	405	260	ASSUME 260	0.64	ASSUME 0.64	-	0.17
LT2.5	68.0	405	265	↓	0.65	↓	-	0.17
LT2.6	67.5	410	260	↓	0.64	↓	-	0.17

TABLE 8.5 COMPARISON BETWEEN VALUES PREDICTED BY VARIOUS DESIGN METHODS AND THE MEASURED SHAFT RESISTANCE

REFERENCE	DESIGN VALUES	PREDICTED ULTIMATE SHAFT RESISTANCE (kN/m <sup>2</sup> )	(PREDICTED $q_s$ /MEASURED $q_s$ )	
			% of 7-day VALUE	% of 300-DAY VALUE
Skempton (1959)	$\alpha = 0.45$	37.8	68	55
	$\alpha = 0.60$	50.4	90	75
Chandler (1968)	$\phi' = 20^\circ$	97.0	175	140
Burland (1973)	$\beta = 0.3$	123	220	180

$$\left[ \begin{array}{l} \text{MEASURED SHAFT RESISTANCE : } q_s \text{ (7 days) = } 55.0 \text{ kN/m}^2 \\ q_s \text{ (300 days) = } 67.5 \text{ kN/m}^2 \end{array} \right]$$

TABLE 8.6 EFFECT OF DELAY TIME ON DEVELOPMENT OF SHAFT RESISTANCE

TEST NO	DELAY TIME $t$ (hrs)	PILE DIAMETER MEASURED AT MID-HEIGHT OF PILE (mm)			SHAFT RESISTANCE MOBILISED $q_s$ kN/m <sup>2</sup>	$\alpha$	$q_s/q_0$
		AFTER BORING	BEFORE CASTING	AFTER PILE TEST			
ST1.1	0.5	38.0	38.0	38.1	55.0	0.65	1.00
ST4.1	2	37.9	37.5	38.1	52.9	0.63	0.96
ST4.2	12	38.0	36.0	37.7	48.7	0.58	0.89
ST4.3	24	38.1	35.0	37.5	43.7	0.52	0.79

TABLE 8.7 CALCULATION OF EXCESS WATER IN CONCRETE AVAILABLE FOR MOISTURE MIGRATION

NO.	CALCULATION	VALUE	REMARKS
1	Wt. of water per m <sup>3</sup> of concrete (kg)	320	see Note (a)
2	Wt. of water per m <sup>3</sup> of concrete necessary for hydration (kg)	120	see Note (b) (0.38 x 320)
3	Excess water per m <sup>3</sup> of concrete (kg)	200	
4	Volume of concrete per 100mm of pile length (x 10 <sup>-6</sup> m <sup>3</sup> )	113	
5	Excess water per 100mm of pile length (gm)	23	(4)x(3)
6	Volume of soil in 20mm annular ring around pile per 100mm of pile length (x10 <sup>-6</sup> m <sup>3</sup> )	364	
7	Dry weight of soil in the volume calculated in No.6 (gm)	433	(6) x $\rho_d$
8	Wt. of water needed to increase water content in 20mm annular ring of soil by 1% (gm)	4.33	(7) ÷ 100

DATA: Pile diameter, d = 38mm; Density of concrete,  $\rho_c = 2.13 \text{ Mg/m}^3$   
 Water cement ratio = 0.60; Dry density of soil,  $\rho_d = 1.19 \text{ Mg/m}^3$

NOTES: (a) Calculated from  $\frac{\text{Water-cement ratio (0.6)}}{\text{Tot. Unit Wt. of Mix design (4.0)}} \times \rho_c$

(b) Assume theoretical water-cement ratio required for hydration is 0.38 (Neville, 1973)

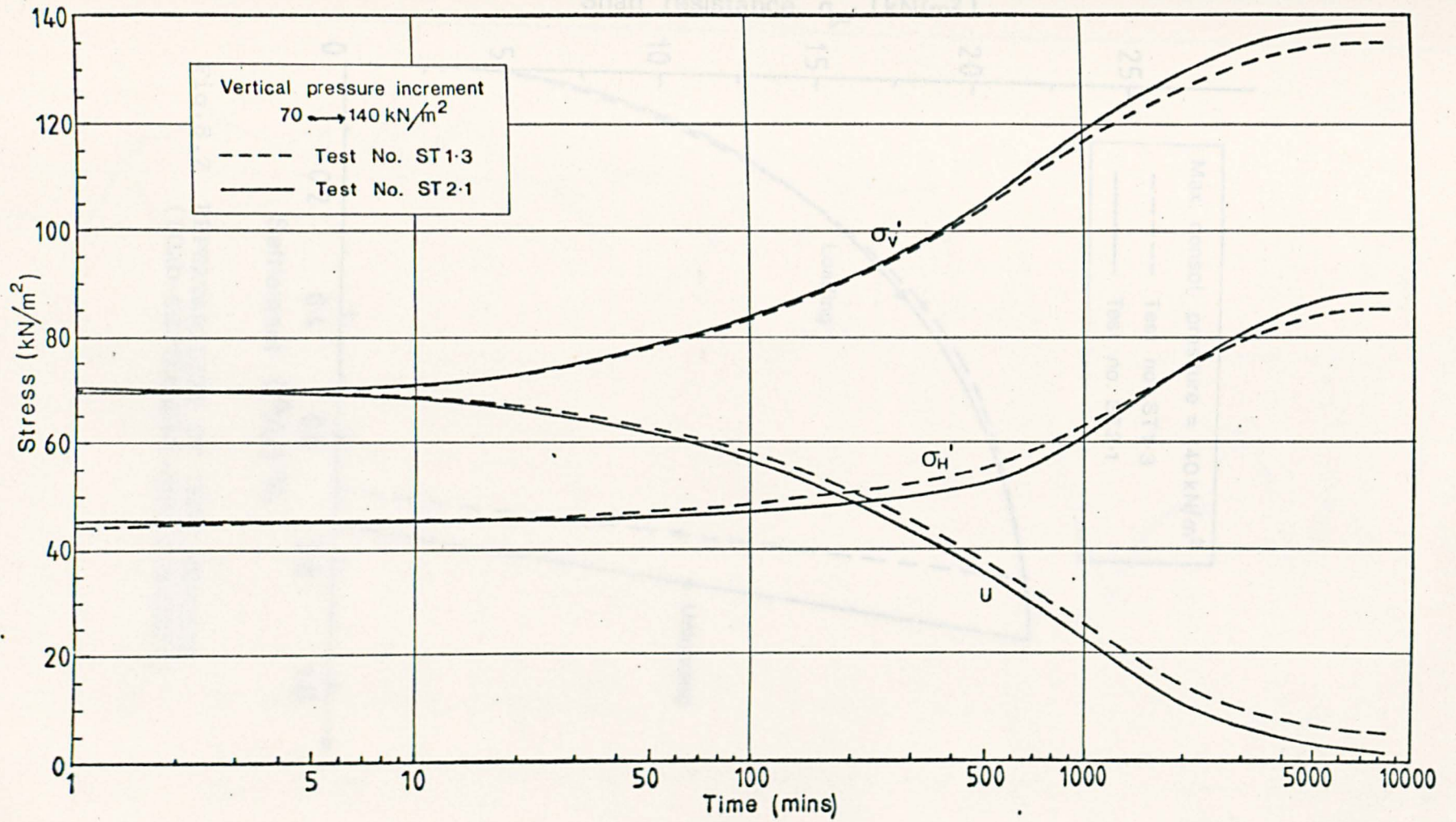


Fig.8.1 REPEATABILITY OF TEST RESULTS (VARIATION OF STRESSES DURING CONSOLIDATION)

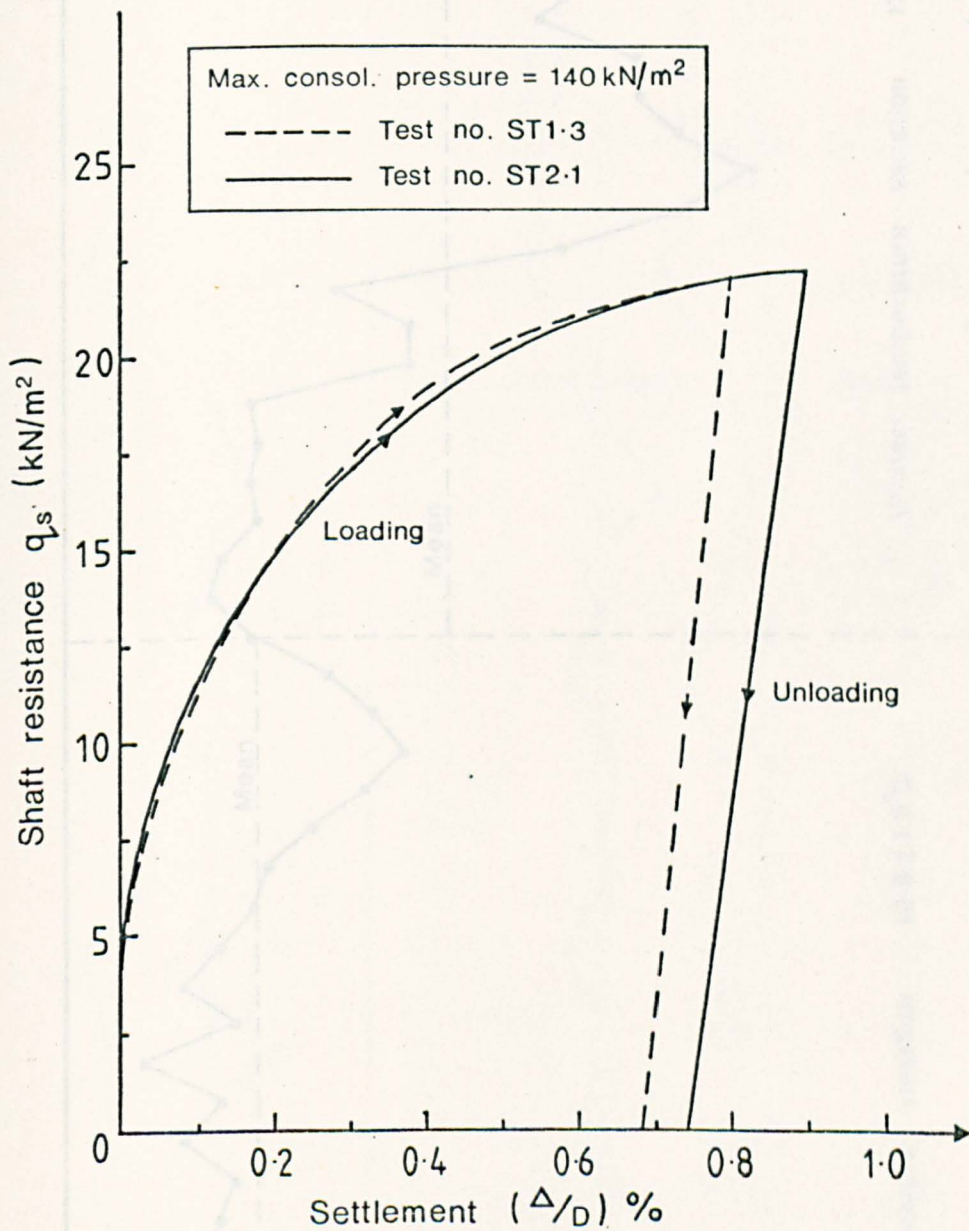


Fig.8.2 REPEATABILITY OF TEST RESULTS  
 (LOAD-SETTLEMENT RELATIONSHIP)

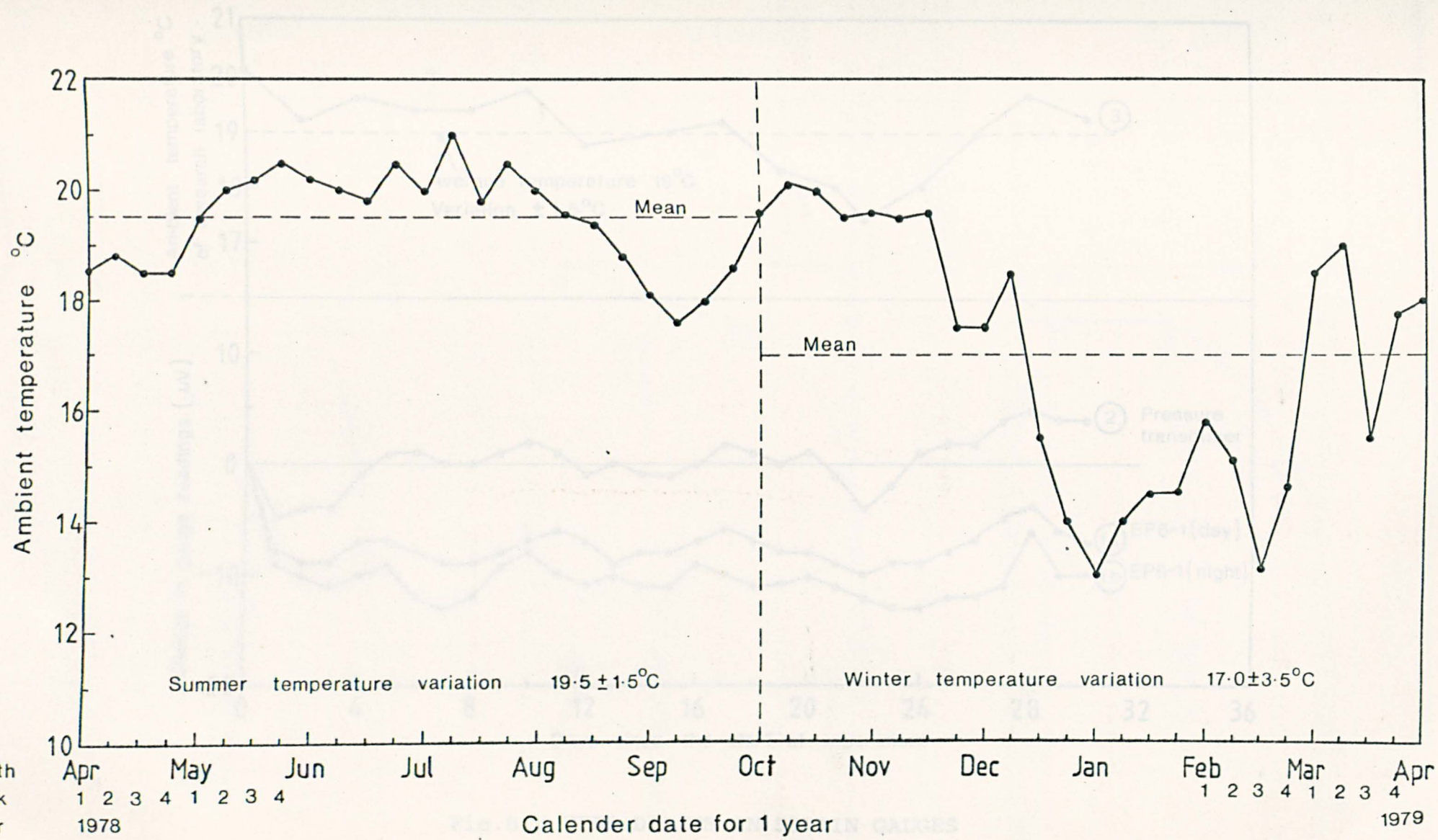


Fig.8.3 AMBIENT TEMPERATURE IN THE RESEARCH LABORATORY FOR A COMPLETE YEAR

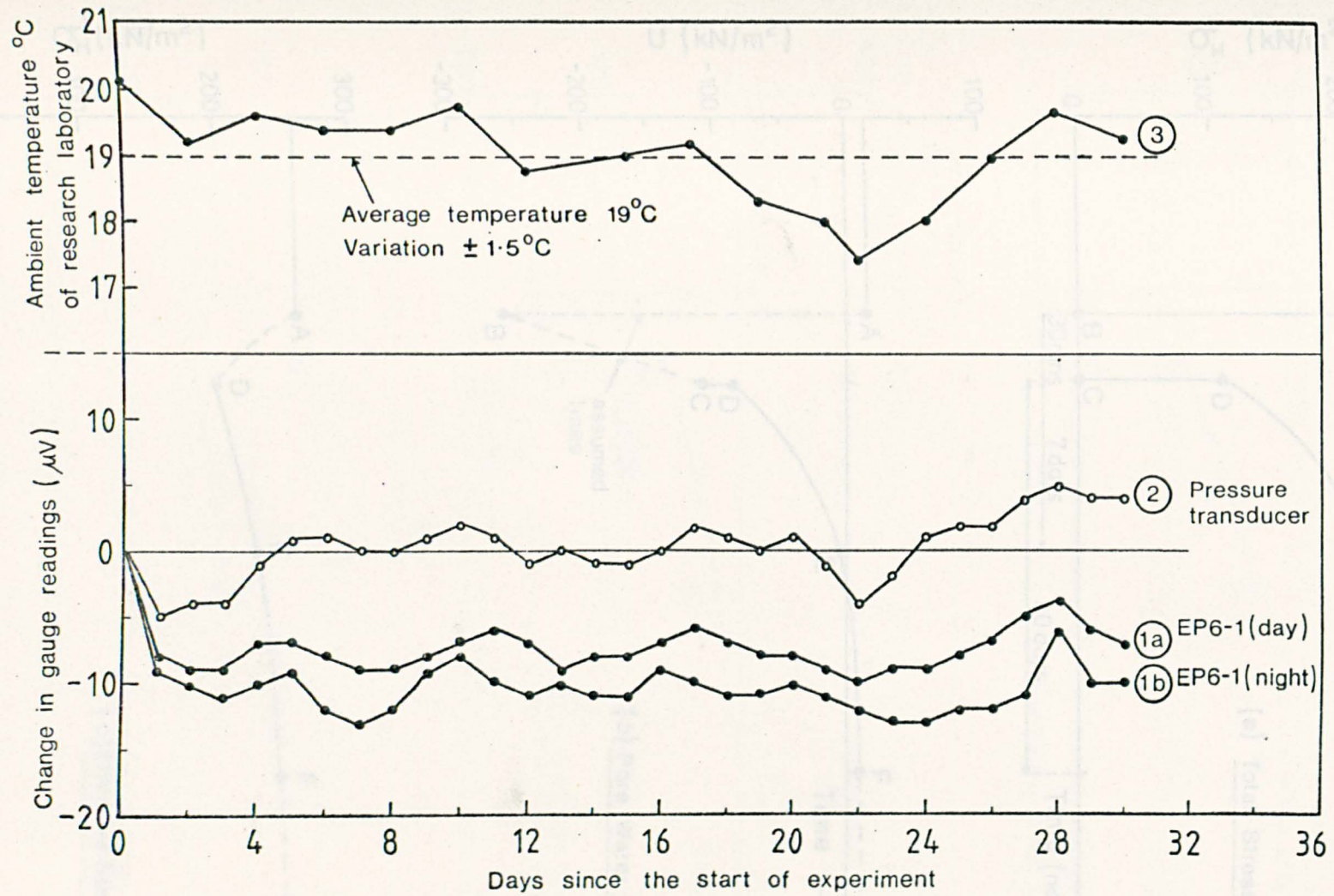


Fig.8.4 ZERO DRIFTS IN STRAIN GAUGES

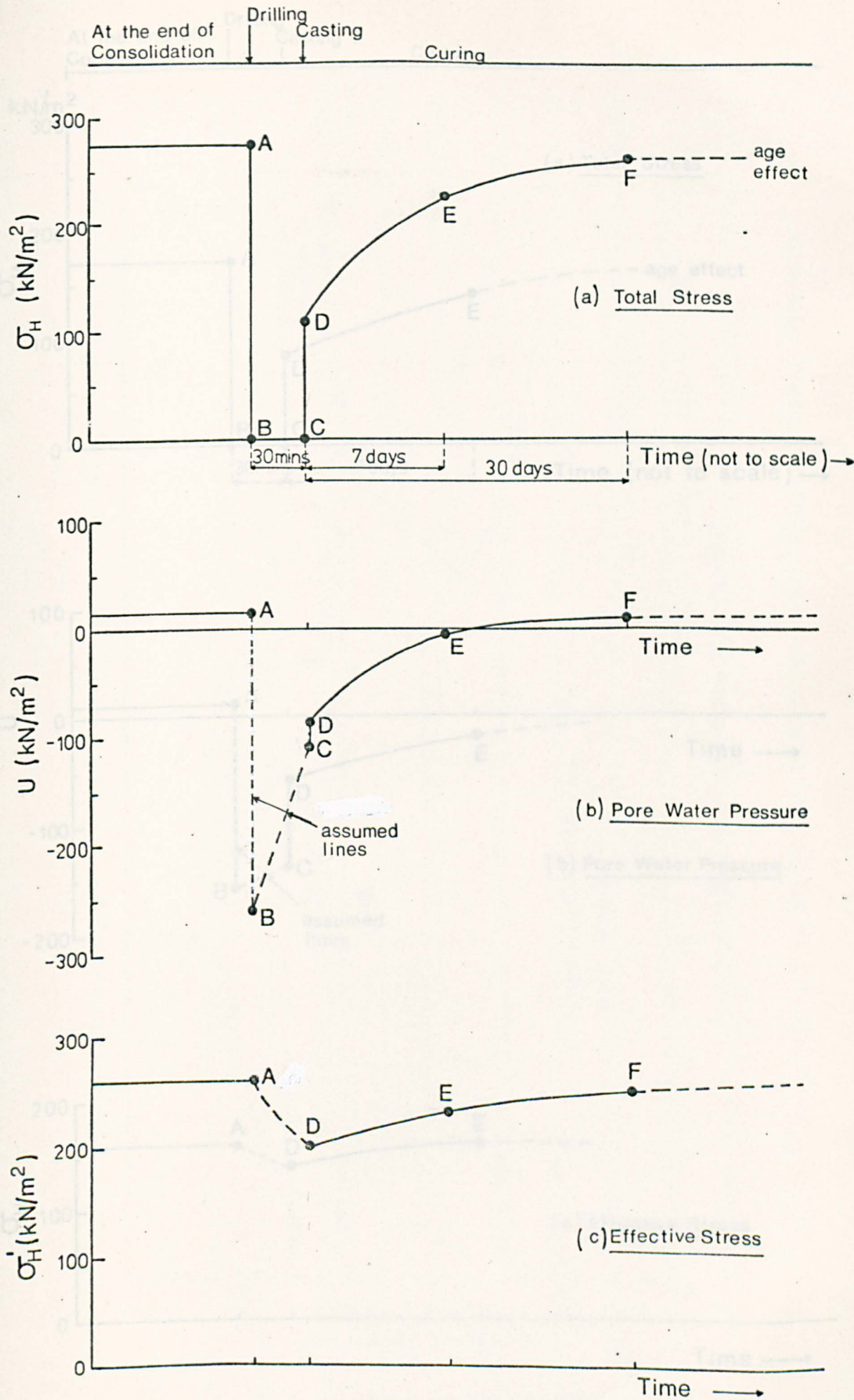


Fig.8.5 VARIATION OF TOTAL HORIZONTAL STRESS, PORE WATER PRESSURE AND EFFECTIVE HORIZONTAL STRESS WITH TIME (NORMALLY CONSOLIDATED CLAYS,  $p_o = 420 \text{ kN/m}^2$ )

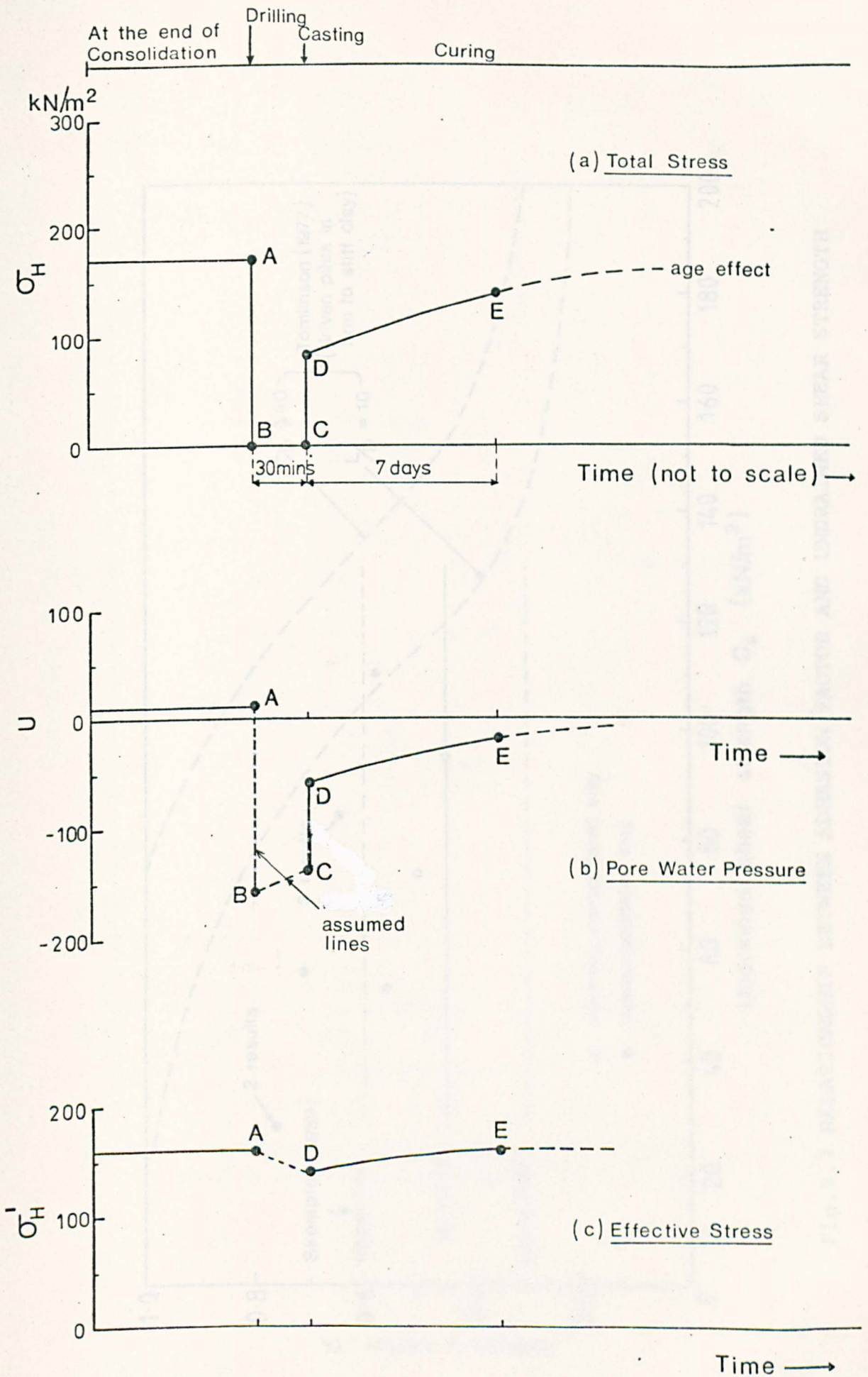


Fig.8.6 VARIATION OF TOTAL AND EFFECTIVE HORIZONTAL STRESS AND PORE WATER PRESSURE WITH TIME (OVERCONSOLIDATED CLAY, OCR=4)

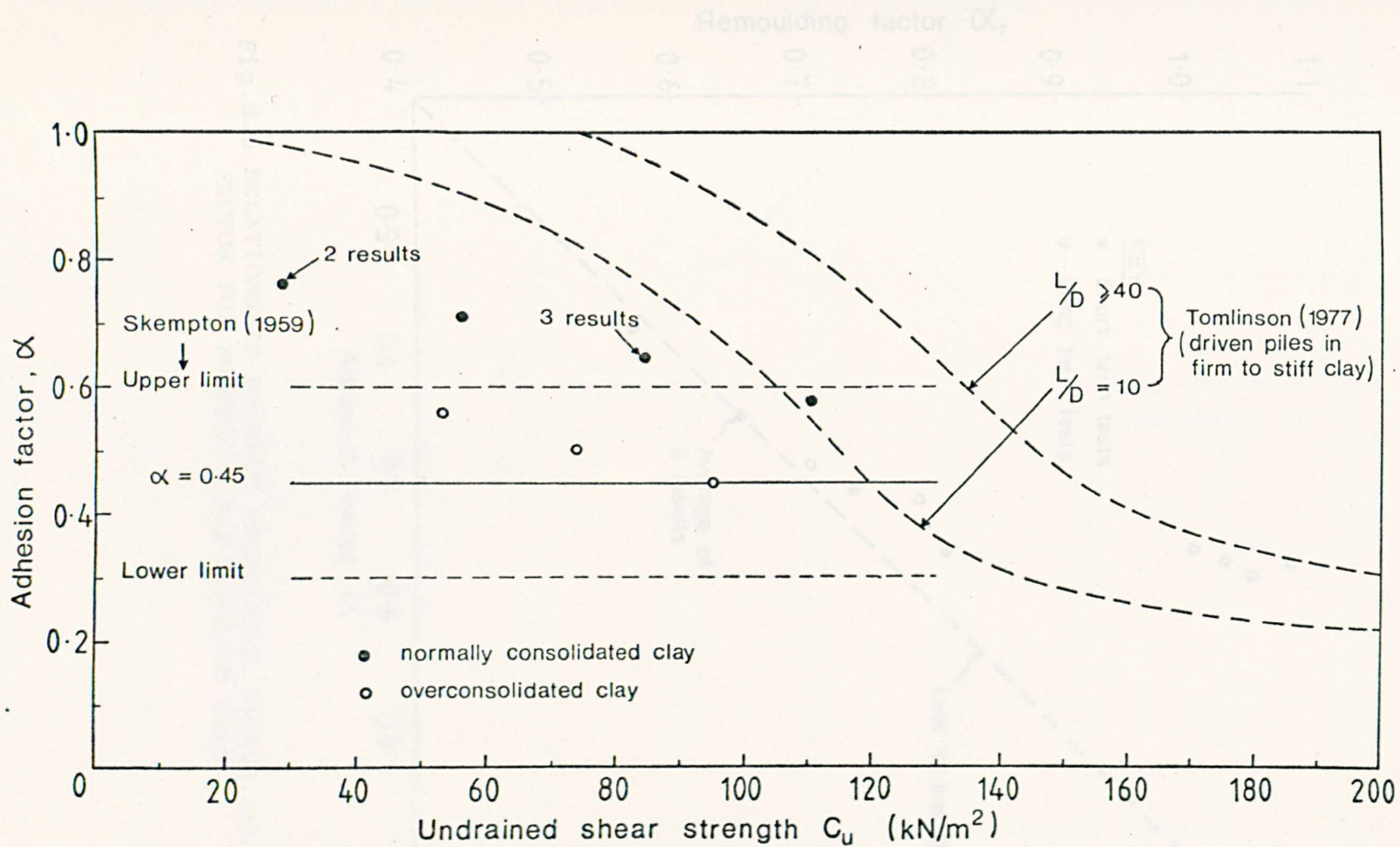


Fig.8.7 RELATIONSHIP BETWEEN ADHESION FACTOR AND UNDRAINED SHEAR STRENGTH

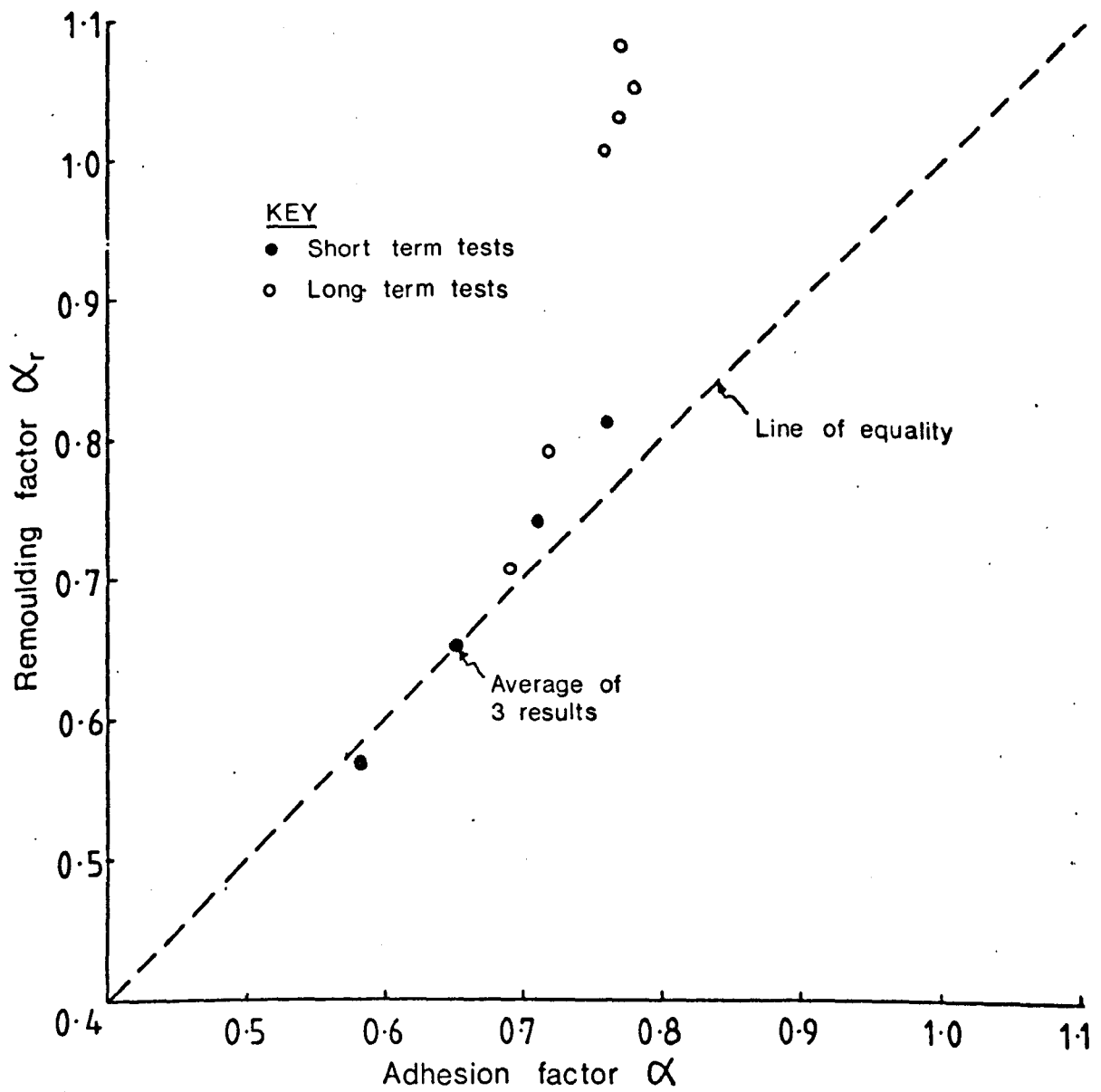


Fig.8.8 RELATIONSHIP BETWEEN REMOULDING FACTOR AND ADHESION FACTOR FOR NORMALLY CONSOLIDATED CLAY

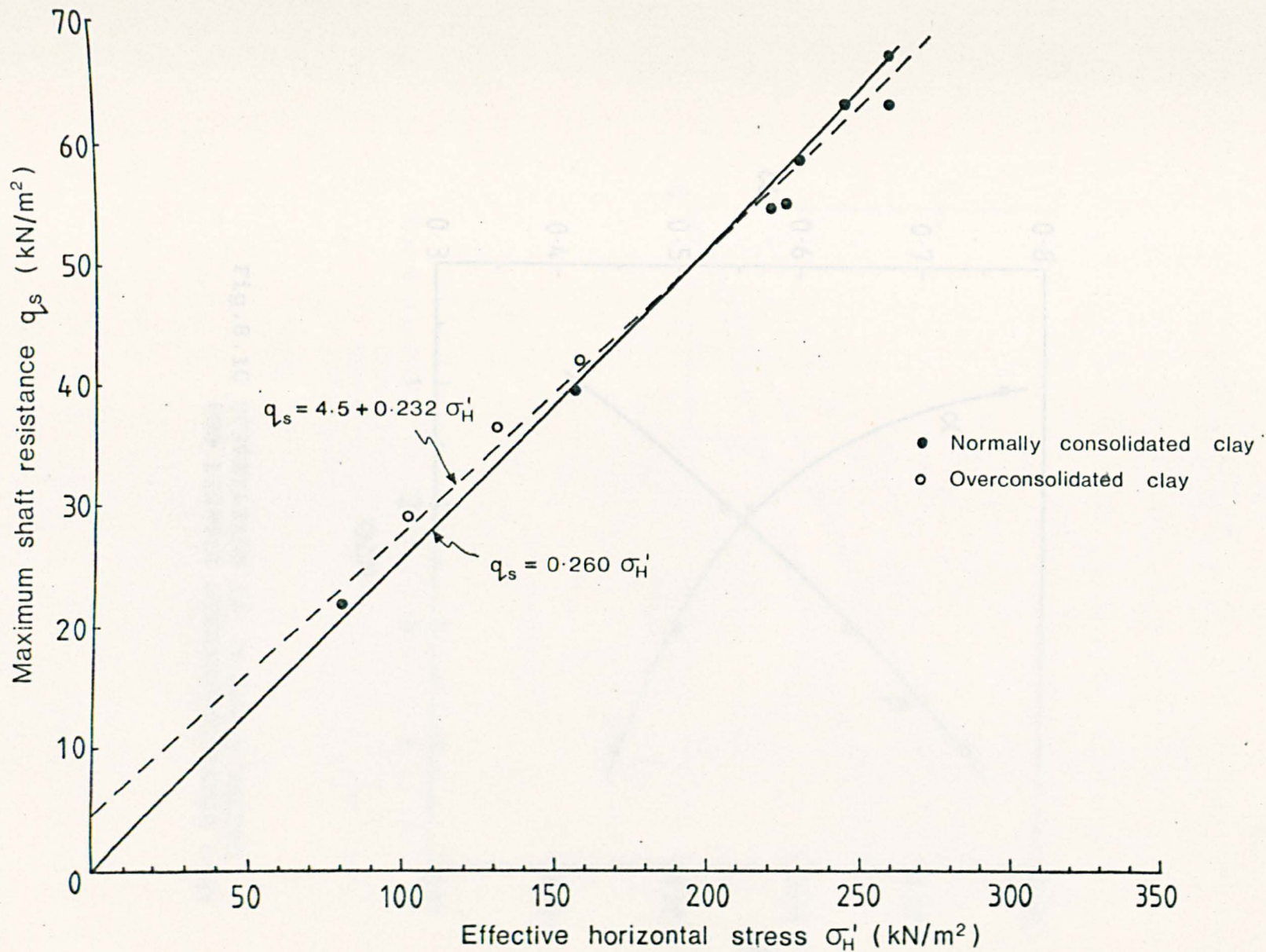


Fig.8.9 RELATIONSHIP BETWEEN SHAFT RESISTANCE AND EFFECTIVE HORIZONTAL STRESS

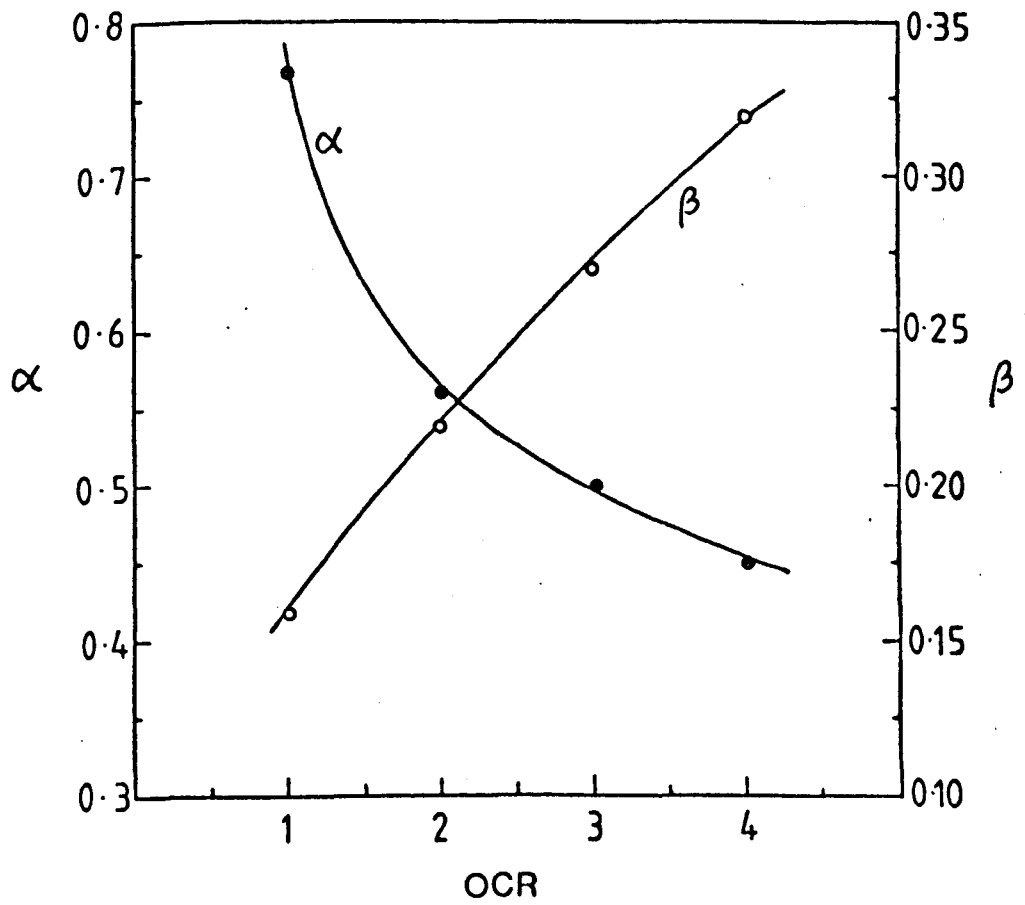


Fig.8.10 CORRELATION OF  $\alpha$  AND  $\beta$  VALUES FOR LIGHTLY OVERCONSOLIDATED CLAY

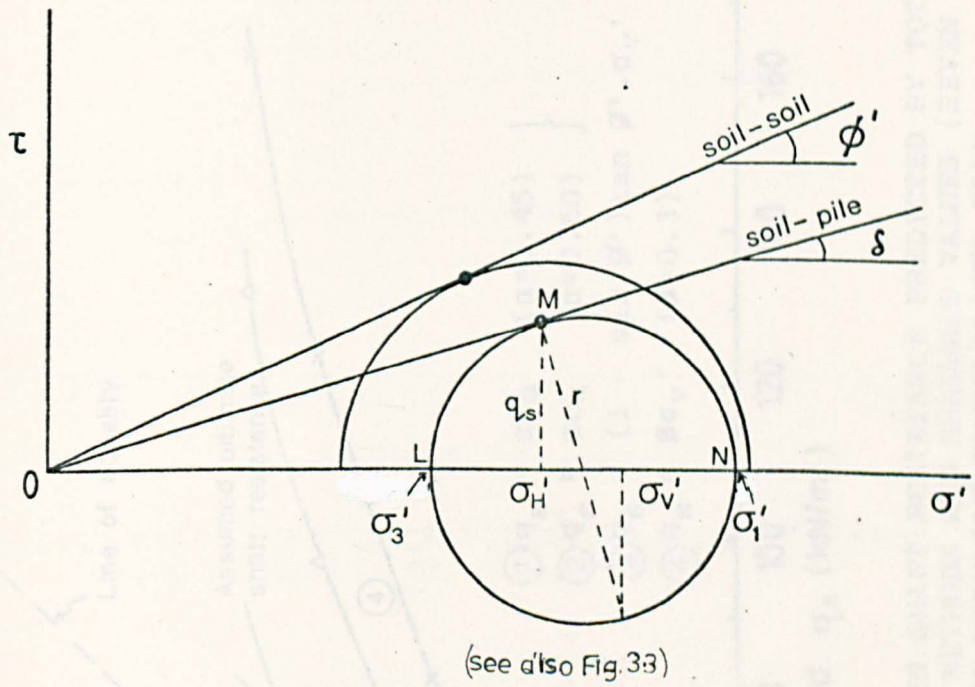


Fig.8.11 RANGE OF STRESS CONDITIONS IN NORMALLY CONSOLIDATED AND LIGHTLY OVERCONSOLIDATED SOILS WHERE  $\phi'$  IS NOT FULLY MOBILIZED (after Parry and Swain, 1976)

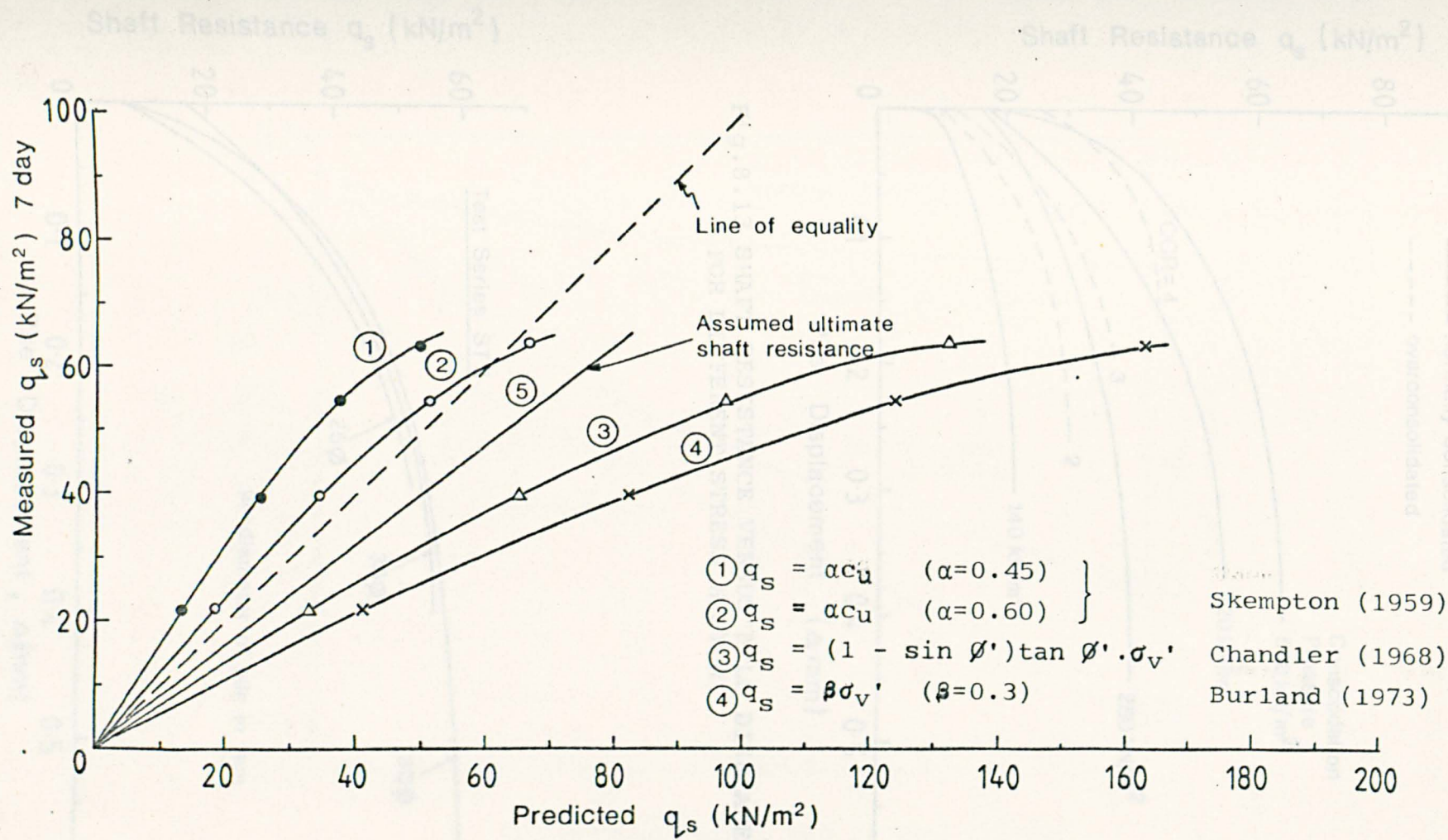


Fig. 8.12 COMPARISON BETWEEN SHAFT RESISTANCE PREDICTED BY TOTAL AND EFFECTIVE STRESS METHODS AND MEASURED VALUES (SEVEN DAYS AFTER CASTING) FOR NORMALLY CONSOLIDATED CLAY.

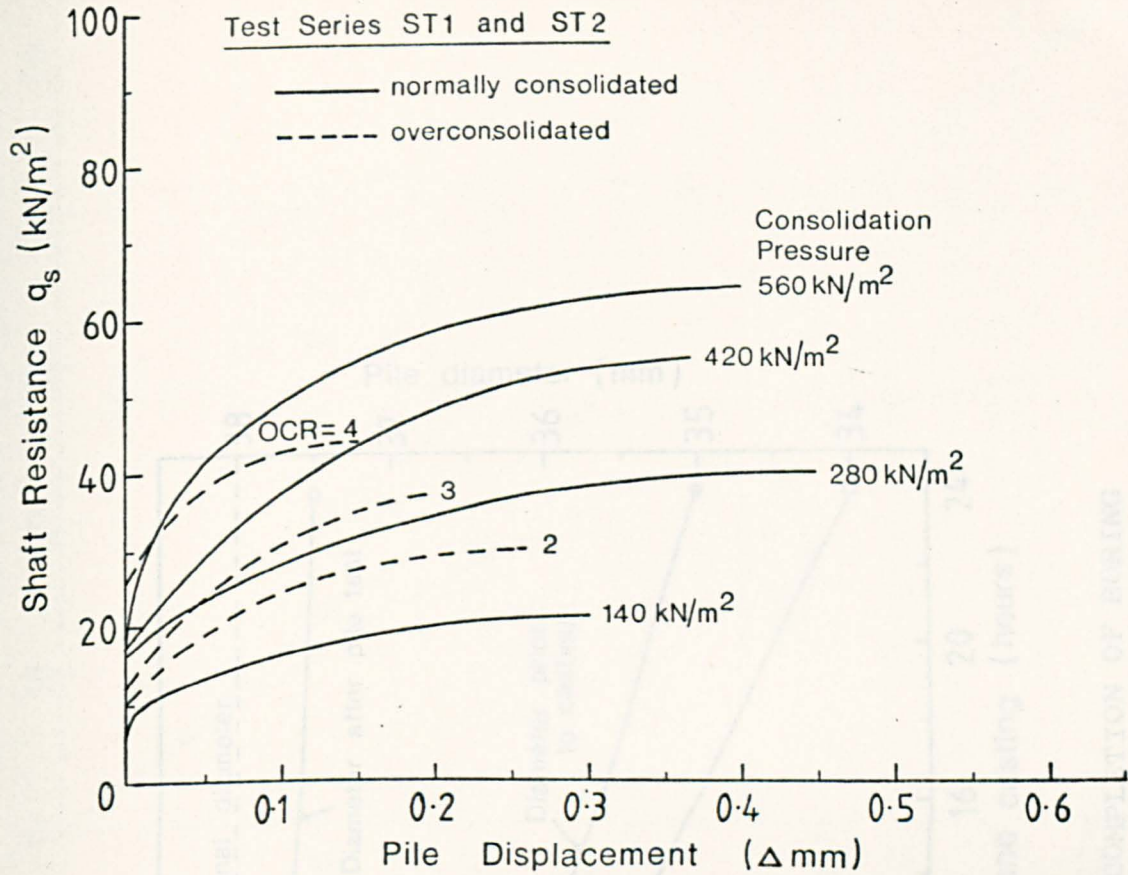


Fig.8.13 SHAFT RESISTANCE VERSUS PILE DISPLACEMENT FOR DIFFERENT STRESS HISTORY.

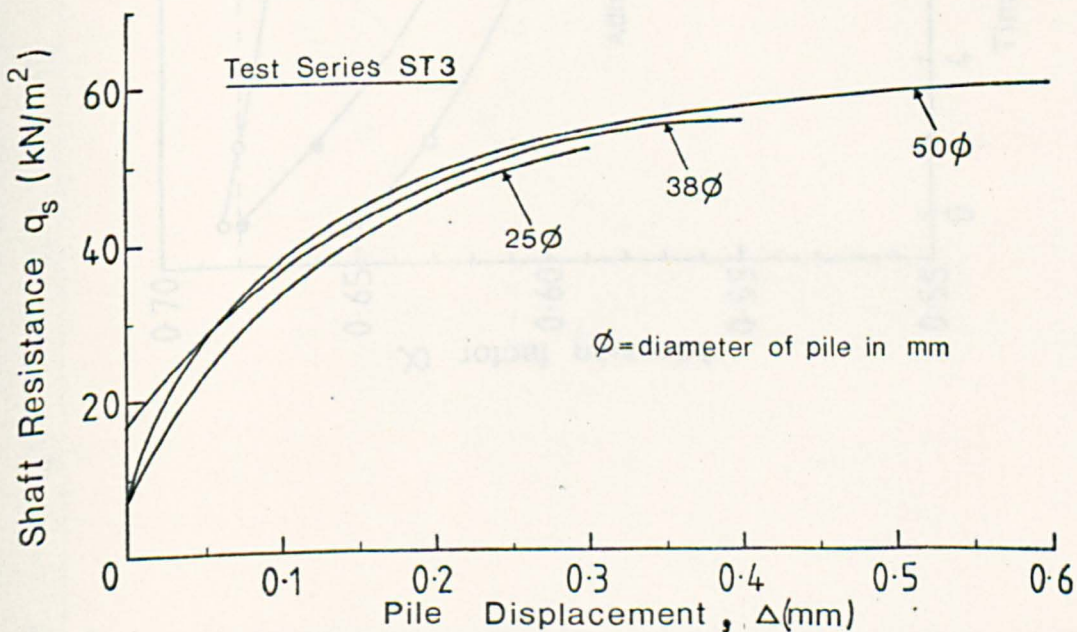


Fig.8.14 SHAFT RESISTANCE VERSUS PILE DISPLACEMENT FOR VARIOUS PILE DIAMETERS.

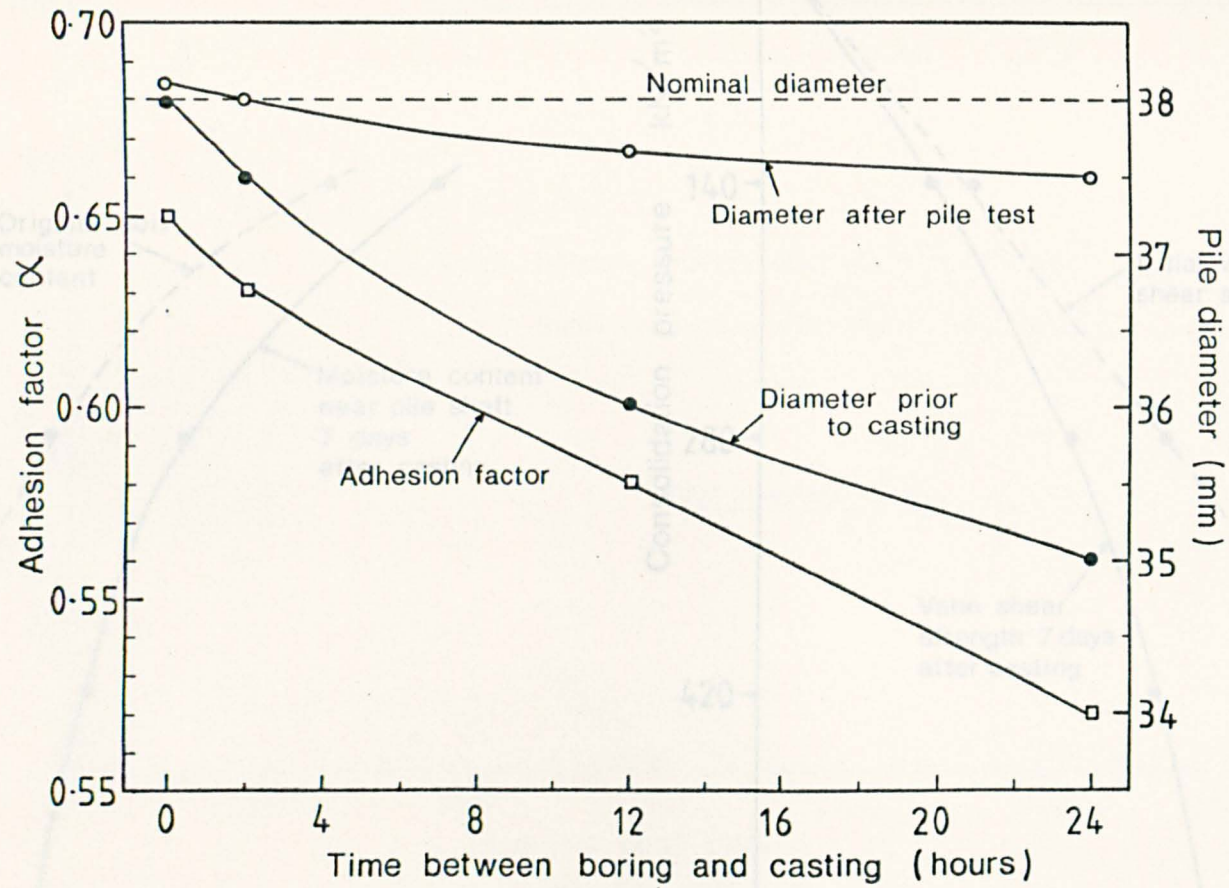


Fig. 8.15 EFFECT OF DELAY BETWEEN COMPLETION OF BORING AND CASTING ON THE ADHESION FACTOR

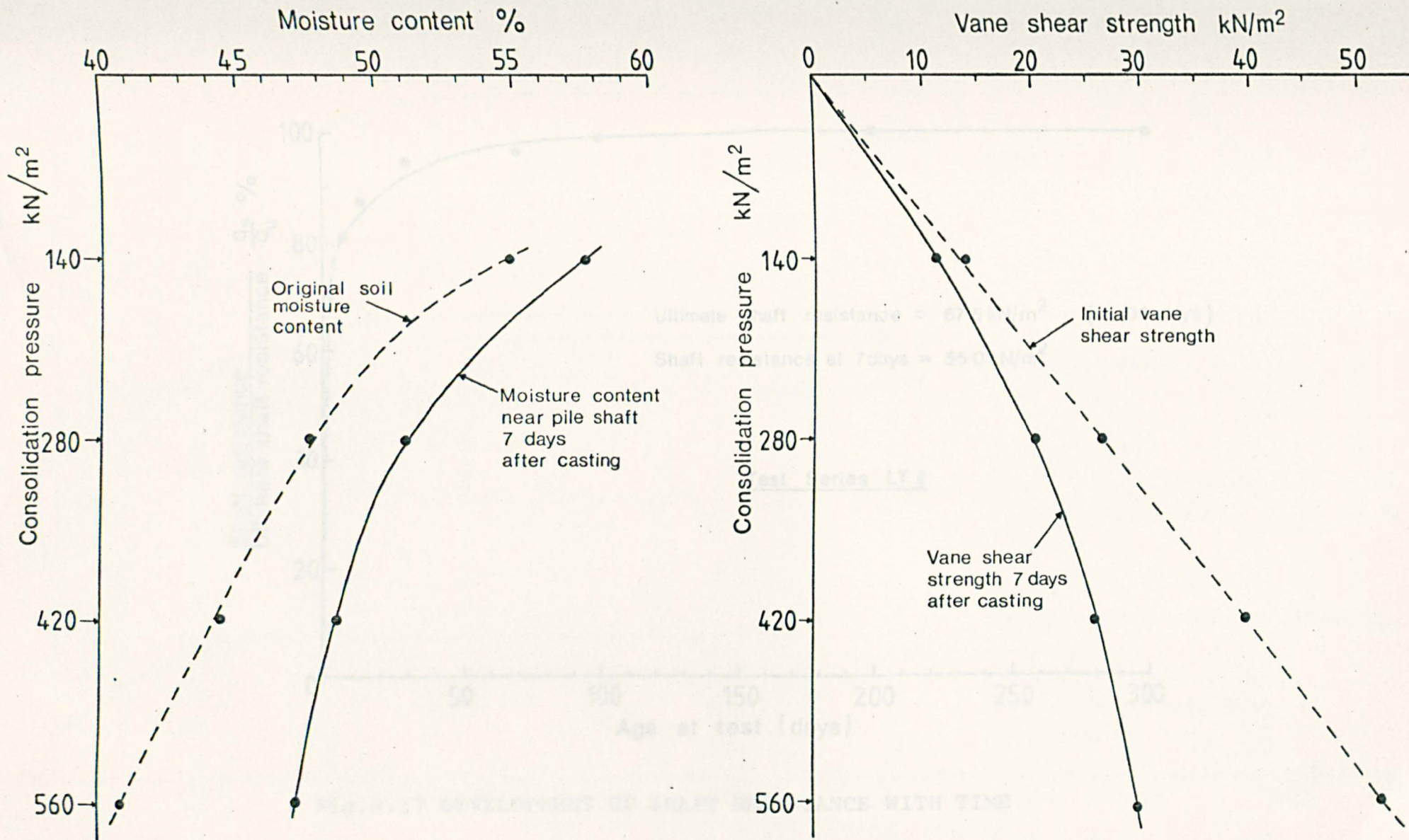


Fig.8.16 CHANGES IN MOISTURE CONTENT AND SHEAR STRENGTH AFTER PILE INSTALLATION

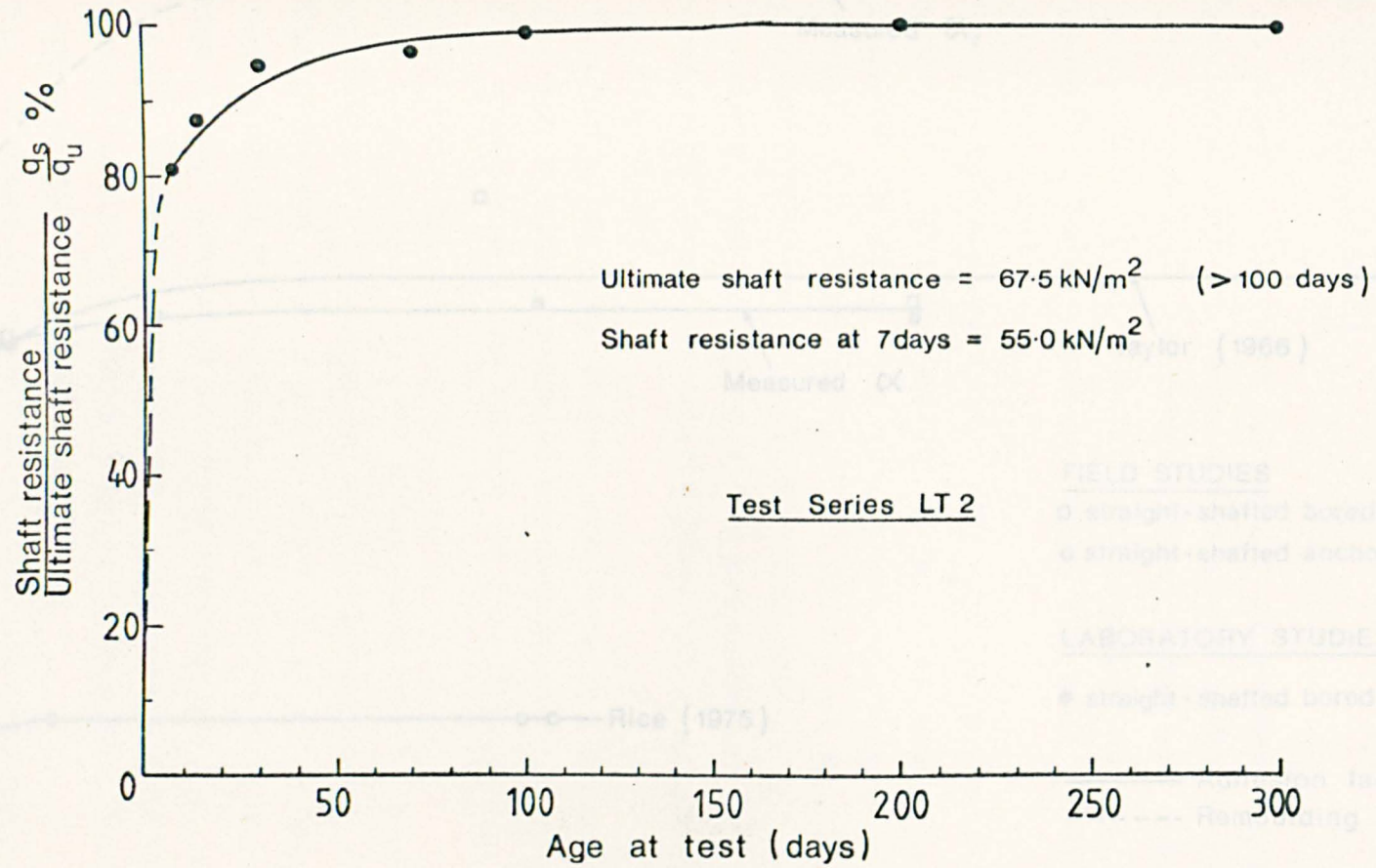


Fig.8.17 DEVELOPMENT OF SHAFT RESISTANCE WITH TIME

Fig.8.18 EFFECT OF AGE ON ADHESION FACTOR

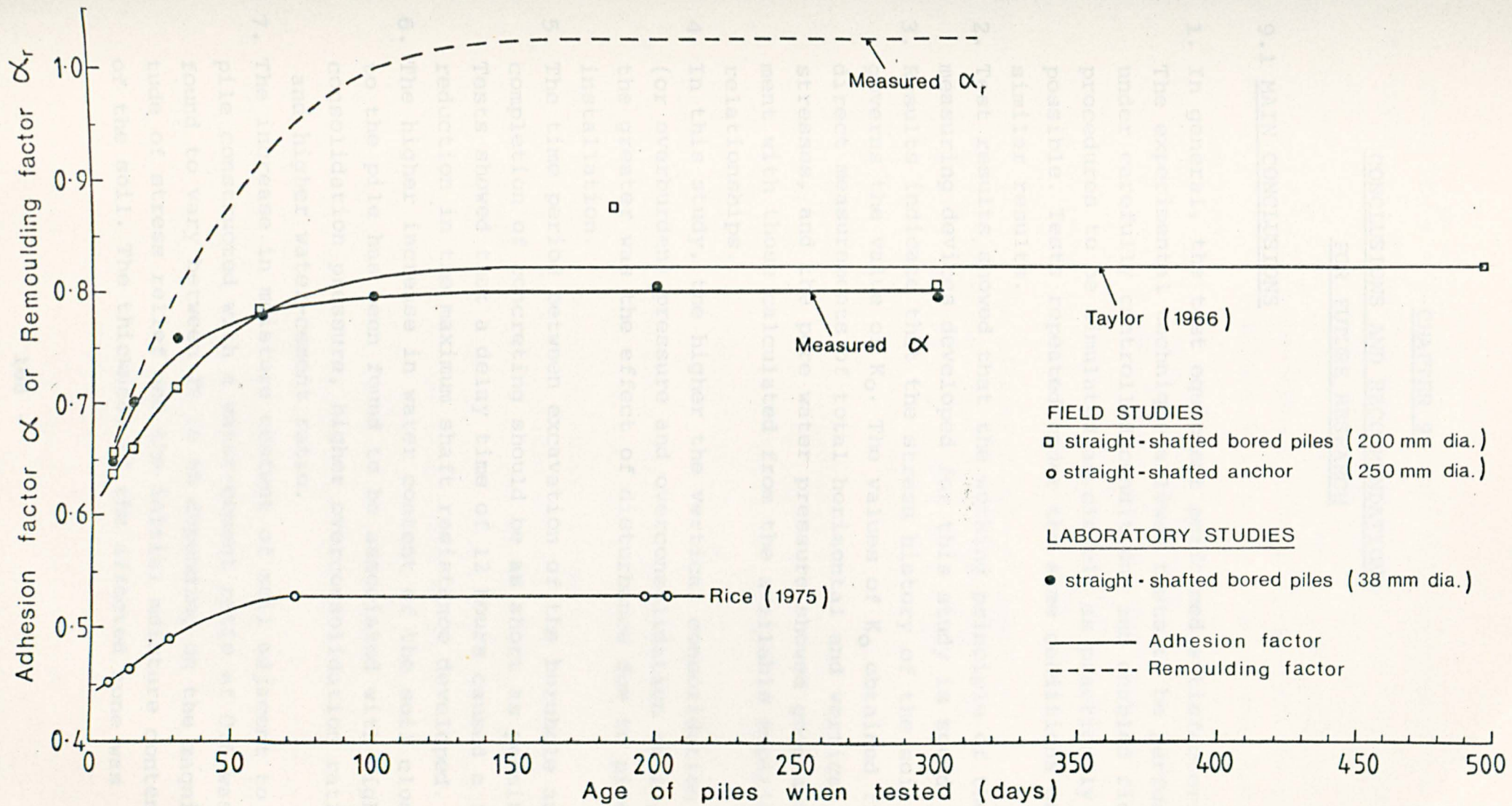


Fig.8.18 EFFECT OF AGE ON ADHESION FACTOR

CHAPTER 9  
CONCLUSIONS AND RECOMMENDATIONS  
FOR FUTURE RESEARCH

9.1 MAIN CONCLUSIONS

1. In general, the test equipment performed satisfactorily. The experimental technique allowed tests to be performed under carefully controlled conditions and enabled field procedures to be simulated as closely as practically possible. Tests repeated under the same conditions gave similar results.
2. Test results showed that the working principle of the measuring devices developed for this study is sound.
3. Results indicate that the stress history of the soil governs the value of  $K_0$ . The values of  $K_0$  obtained from direct measurements of total horizontal and vertical stresses, and the pore water pressure showed good agreement with those calculated from the available empirical relationships.
4. In this study, the higher the vertical consolidation (or overburden) pressure and overconsolidation ratio, the greater was the effect of disturbance due to pile installation.
5. The time period between excavation of the borehole and completion of concreting should be as short as possible. Tests showed that a delay time of 12 hours caused a 10% reduction in the maximum shaft resistance developed.
6. The higher increase in water content of the soil close to the pile has been found to be associated with higher consolidation pressure, higher overconsolidation ratio and higher water-cement ratio.
7. The increase in moisture content of soil adjacent to a pile constructed with a water-cement ratio of 0.6 was found to vary between 2% to 6% depending on the magnitude of stress relief and the initial moisture content of the soil. The thickness of the affected zone was

- found to be about 60mm from the pile interface.
8. There is a linear relationship between the water-cement ratio of the concrete used and the increase in water content of soil close (within 20mm) to the pile surface. An increase in water-cement ratio of 0.1 resulted in an increase in moisture content of 2.0% in soil close to the pile.
  9. There is a direct relationship between an increase in moisture content and changes in soil strength. An increase in 1% of moisture content resulted in an undrained strength reduction of about 7% for the type of clay investigated.
  10. In this study, the effective stress conditions of the soil were 'restored' some time after pile installation. During load testing the effective horizontal stress acting on the pile shaft varied little from that existing prior to loading.
  11. The settlement of the bored pile at failure was of the order of 0.5% to 1.5% of the shaft diameter.
  12. Test results showed that the diameter of the pile did not influence the magnitude of the shaft resistance mobilized.
  13. In this study, the shaft resistance continued to increase with curing time and the ultimate shaft resistance was achieved after about 100 days.
  14. In general, the total stress method of estimating the shaft resistance gave predictions less than the ultimate values measured, whereas effective stress methods predicted higher values than those measured.
  15. This study has shown that if  $K_0$  and  $\sigma_{v0}'$  values are used in the effective stress analysis for normally consolidated clay, the predicted shaft resistance represents an upper bound value.
  16. For the method of pile construction and the type of clay used in this research, the adhesion factor  $\alpha$  was found to have an ultimate value of 0.80 at about 100 days.

17. The shaft resistance of bored piles in clay was found to be a function of the effective horizontal stress acting on the pile shaft and the effective angle of friction between the pile and the soil.
18. In this study, the effective angle of friction between the piles and the soil,  $\delta$ , was found to be less than the effective angle of shearing resistance of the soil,  $\phi'$ .

## 9.2 RECOMMENTATIONS FOR FUTURE RESEARCH

Although the effects of installation and the factors influencing the development of shaft resistance have been investigated, and the changes in effective stress condition in the soil close to the pile have been documented, more work is required to provide a better understanding of the behaviour of bored piles in clay. The following research studies which have the potential of improving this understanding are suggested:

1. This investigation is limited to the study of bored piles in normally and lightly overconsolidated clays. The effects of heavily overconsolidated and stiff clays should be studied to form a complete understanding of the effects of stress history on pile behaviour.
2. It is apparent that the effects of installation influence the development of the shaft resistance of the piles. In this study, only the dry method of construction was investigated. Therefore, studies on the effects of slurry displacement method and the casing method of construction on the behaviour of bored piles will help in understanding the problems an engineer is likely to face in the field.
3. Since boring disturbs the soil fabric at the interface, an electron microscope study of the soil at the face of the borehole and in the soil mass will provide useful information on the degree of remoulding of the soil. Appearance of the clay skin taken from the pile face and

- examined by electron microscopy may aid the understanding of the shearing mechanism at the pile-soil interface.
4. Since shaft resistance of the pile is controlled by the effective lateral pressure, any expansion of the concrete will cause an increase in the effective lateral stress of the soil surrounding the pile. Therefore, the use of chemical additives to increase the concrete expansion could be examined.
  5. In this investigation, moisture migration studies were carried out from 7 days up to about 300 days in order to co-relate with load test results. However, daily changes in the moisture for the first 7 days were not studied. Therefore, it would be useful to know these changes immediately after pile installation in order to provide a complete record of moisture migration, and consequently a complete record of changes in the undrained strength of soil close to the pile.
  6. Since the effective angle of shearing resistance of the soil was not fully mobilized in this study, there is a need to examine the effects of surface roughness on the mobilization of the effective angle of shearing resistance.
  7. More field measurements of the effective stress conditions in the soil close to the pile before and during loading are required in order to provide information for further development of the effective stress approach in design. Correlation of some field studies with laboratory observations would allow extrapolation of laboratory findings to field situations. It would also be desirable to develop a simple field device for remote measurement of borehole diameter since it has been shown in this study that the diameter of the hole decreases with an increase in the time lapse between completion of boring and concreting.

## REFERENCES

- ABDEL-HAMID, M.S. and KRIZEK, R.J. (1976). At-rest lateral earth pressure of a consolidating clay. J. Geotech. Engng Div., Proc. ASCE, Vol.102, No.GT7, pp.721-738.
- AGARWAL, S.L. and VENKATESAN, S. (1965). An instrument to measure skin friction and normal earth pressure on deep foundations. ASTM STP392, pp.152-169.
- ALDRIDGE, W.W. and BREEN, J.E. (1968). Useful techniques in direct modelling of reinforced structures. Amer. Conc. Inst., Pub. No.24.
- ALPAN, I. (1967). The empirical evaluation of the coefficient  $K_0$  and  $K_{or}$ . Soil Fdn, Vol.7, No.1, p.31.
- AMERICAN CONCRETE INSTITUTE (1963). Recommended practice for concrete formwork. Amer. Conc. Inst. Stds, Detroit.
- AMERICAN PETROLEUM INSTITUTE (1977). Recommended practice for planning, designing, and constructing fixed offshore platforms. Amer. Petroleum Inst., Washington D.C.
- AMERICAN SOCIETY FOR TESTING AND MATERIALS (1968). The performance of deep foundations. ASTM STP444.
- AMERICAN SOCIETY FOR TESTING AND MATERIALS (1969). Standard method of test for load-settlement relationship for individual vertical piles under static axial load. ASTM D1143-69, Annual book of ASTM Stds, Part 11, pp.382-390.
- ARMAN, A., POPLIN, J.K. and AHMAD, N. (1975). Study of vane shear. Proc. ASCE Specialty Conf. on In-situ measurement of soil properties, Raleigh, North Carolina, Vol.1, pp.93-120.
- ARTHUR, J.R.F. and ROSCOE, K.H. (1961). An earth pressure cell for the measurement of normal and shear stresses. Civ. Engng and Pub. Wks Rev., Vol.56, pp.765-770.
- BAGUELIN, F., JEZEQUEL, J.F., LEMEE, E. and LE MEHAUTE, A. (1972). Expansion of cylindrical cavities in cohesive soils. J. Soil Mech. and Fdn Div., Proc. ASCE, Vol.98, No.SM11, pp.1129-1142.
- BAKER, C.N. and KHAN, F. (1971). Caisson construction problems and correction in Chicago. J. Soil Mech. and Fdn Div., Proc. ASCE, Vol.97, No.SM2, pp. 417-440.
- BARACOS, A (1976). Clogged filter discs. Geotechnique, Vol.26, No.4, pp. 634-636.
- BARDEN, L. (1969). Time dependent deformation of normally consolidated clays and peats. J. Soil Mech. and Fdn Div., Proc. ASCE, Vol.95, No.SM1, pp.1-31.

- BEA, R.G. (1975). Parameters affecting axial capacity of piles in clays. Proc. 7th Annual Offshore Techn. Conf., Houston, Texas, Vol.2, pp.611-623.
- BEARD, R.M. (1974). Development of an expedient site investigation tool and investigations in long term holding capacity. Civ. Engng Lab., Naval Construction Centre, Port Hueneme, California, 44 pps.
- BERRE, T. and BJERRUM, L. (1973). Shear strength of normally consolidated clays. Proc. 8th Int. Conf. Soil Mech. and Fdn Engng, Moscow, Vol.1, pp.39-49.
- BERRY, P.L. (1965). Primary and secondary consolidation of clay. M.Sc. thesis, University of Manchester.
- BHANOT, K.L. (1975). Performance of scaled cast-in-place instrumented concrete piles in silt. Proc. 5th Asian Regional Conf. on Soil Mech. and Fdn Engng, Bangalore, India, pp.213-215.
- BISHOP, A.W. (1958). Test requirements for measuring the coefficient of earth pressure at-rest. Proc. Brussels Conf. on Earth Pressure Problems, Brussels, Vol.1, pp.2-14.
- BISHOP, A.W. and HENKEL, D.J. (1962). The measurement of soil properties in the triaxial test. 2nd edition, Edward Arnold Ltd, London.
- BJERRUM, L. (1973). Problems of soil mechanics and construction on soft clays and structurally unstable soils. State-of-the-art report, Proc. 8th Int. Conf. Soil Mech. and Fdn. Engng, Moscow, Vol.3, pp.111-159.
- BJERRUM, L and ANDERSEN, K.H. (1972). in-situ measurement of lateral pressure in clay. Proc. 5th European Conf. on Soil Mech. and Fdn Engng, Madrid, Vol.1, pp.11-20.
- BRITISH STANDARDS INSTITUTION (1975). Methods of testing soils for engineering purposes. BS1377:1975, London.
- BRITISH STANDARDS INSTITUTION (1972). Code of practice for foundations. CP2004:1972, London.
- BROOKER, E.W. and IRELAND, H.O. (1965). Earth pressure at-rest related to stress history. Can. Geotech. J., Vol.2, No.1, pp.1-15.
- BURLAND, J.B. (1967). Deformation of soft clay. PhD thesis, University of Cambridge.
- BURLAND, J.B. (1973). Shaft friction of piles in clay: a simple fundamental approach. Ground Engng, Vol.6, No.3, pp.30-42.
- BURLAND, J.B. (1977). Some example of influence of field measurements of foundation design and construction. Ground Engng, Vol.10, No.7, pp.15-41.

- BURLAND, J.B. (1978). The function of research in the practice of ground engineering. Ground Engng, 10th year of publication, Nov., p.5.
- BURLAND, J.B. (1978a). Discussion on "Skin friction on pile". Ground Engng, Vol.11, No.8, pp.47.
- BURLAND, J.B. BUTLER, F.G. and DUNICAN, P. (1966). The behaviour and design of large diameter bored piles in stiff clay. Proc. Symp. Large Diameter Bored Piles, Instn Civ. Engrs, London, pp.51-71.
- BURLAND, J.B. and COOKE, R.W. (1974). The design of bored piles in stiff clays. Ground Engng, Vol.7, No.4, pp.28-35.
- CARDER, D.R. and KRAWCZYK, J.W. (1975). Performance of cells designed to measure soil pressure on earth retaining structures. Transport and Road Research Laboratory Report 689.
- CHANDLER, R.J. (1968). The shaft friction of piles in cohesive soils in terms of effective stress. Civ. Engng and Pub. Wks Rev., Vol.63, pp.48-51.
- CHANDLER, R.J. (1977). Discussion: "Abridged Proc. of DoE and CIRIA piling seminar" held at the Instn Civ. Engrs, on 11th Nov. 1976. CIRIA Publication.
- CHUANG, J.W. and REESE, L.C. (1969). Studies of shearing resistance between cement mortar and soil. Res. Rep. 89-3, Centre of Highway Res., Univ. of Texas at Austin, Texas.
- CLARK, J.I. and MEYERHOF, G.G. (1973). The behaviour of piles driven in clay: (II) Investigation of the bearing capacity using total and effective strength parameters. Can. Geotech. J., Vol.10, No.1, pp.86-102.
- COOKE, R.W. (1979). British Research Establishment report. Construction News/Piling and Ground Engng Supplement, Northwood Publications, London, pp.2-3.
- COOKE, R.W. and WHITAKER, T. (1961). Experiments on model piles with enlarged bases. Geotechnique, Vol.11, No.1, pp.1-13.
- COUTTS, J.A. and COOMBS, A.J. (1969). A method of installing a strain gauge. Strain, Vol.5, No.2, pp.101-103.
- COYLE, H.M. and REESE, L.C. (1966). Load transfer of axially loaded piles in clay. J. Soil Mech. and Fdn Div., Proc. ASCE, Vol.92, No.SM2, pp.1-26.
- CUMMINGS, A.E., KERHOFF, G.O. and PECK, R.B. (1950). Effects of driving piles into soft clay. Trans. ASCE, Vol.115, pp.275-285.
- D'APPOLONIA, D.J. and LAMBE, T.W. (1970). Method for predicting initial settlement. J. Soil Mech. and Fdn Div., Proc. ASCE, Vol.96, No.SM2, pp.523-544.

- D'APPOLONIA, D.J. and LAMBE, T.W. (1971). Performance of four foundations on end-bearing piles. J. Soil Mech. and Fdn Div., Proc. ASCE, Vol.97, No. SM1, pp.77-93.
- DEMELLO, V.F.B. (1969). Foundation of buildings in clay. State-of-the-art report, Proc. 7th Int. Conf. Soil Mech. and Fdn Engng, Mexico, Vol.2.
- DUBOSE, L.A. (1957). Small-scale load tests on drilled and cast-in-place concrete piles. Highway Res. Board, pp.132-145.
- DUNICAN, P. (1962). Large diameter bored piles. The Consulting Engr, pp.67-70.
- EID, M.M. (1978). Expansion of cylindrical cavities in clay. PhD thesis, University of Sheffield.
- EIDE, O., HUTCHINSON, N. and LANDVA, A. (1961). Short and long term test loading of a friction pile in clay. Proc. 5th Int. Conf. Soil Mech. and Fdn Engng, Paris, Vol.2, pp.45-53.
- ELLISON, R.D., D'APPOLONIA, E. and THEIRS, G.R. (1971). Load deformation mechanism for bored piles. J. Soil Mech. and Fdn Div., Proc. ASCE, Vol.97, No. SM4, pp.661-677.
- ENGELING, D.E. and REESE, L.C. (1974). Behaviour of three instrumented drilled shafts under short term axial loading. Res. Report No.176-3, Centre for Highway Res., Univ. of Texas at Austin, 118 pp.
- ESRIG, M.I., KIRBY, R.C. and BEA, R.G. (1977). Initial development of a general effective stress method for the prediction of axial capacity for driven piles in clay. Proc. 9th Offshore Techn. Conf., Houston, Vol.1, pp.495-506.
- FEARENSIDE, G.R. and COOKE, R.W. (1978). The skin friction of bored piles formed in clay under bentonite. CIRIA Report 77, 31 pp.
- FLAATE, K. (1966). Factors influencing results on vane test. Can Geotech. J., Vol.3, No.1, pp.18-31.
- FLAATE, K. and SELNES, P. (1977). Side friction of piles in clay. Proc. 9th Int. Conf. Soil Mech. and Fdn Engng, Tokyo, Vol.1, pp.517-522.
- FLEMING, W.G.K. and SLIWINSKI, Z. (1977). The use and influence of bentonite in bored pile construction. D.O.E. and CIRIA Piling Development Group Report PG3, 93 pp.
- FRISCHMANN, W.W. and FLEMING, W.G.K. (1962). The use and behaviour of large diameter piles in London Clay. The Structural Engr, Vol.40, pp.123-131.
- GARDNER, W.S. (1975). Considerations in the design of drilled piers. Lecture Series on Deep Foundations, Boston Soc. of Civ. Engrs, 42 pp.

- GIBSON, R.E. (1963). An analysis of system flexibility and its effects on time lag in pore water pressure measurements. *Geotechnique*, Vol.13, No.1, pp.1-11.
- GREEN, H. (1961). Long term loading of short bored piles. *Geotechnique*, Vol.11, No.1, pp.47-53.
- HADALA, P.F. (1967). The effect of placement method on the response of soil stress gauges. *Proc. Int. Symp. on Wave Propagation and Dynamic Properties of Earth Materials*, Univ. of New Mexico, Albuquerque, pp.255-263.
- HAGERTY, D.J. and GARLANGER, J.E. (1972). Consolidation effects around driven piles. *Proc. ASCE Specialty Conf. on Performance of Earth and Earth Supported Structures*, Purdue Univ., Vol.1, Pt.2, pp.1207-1222.
- HANNA, T.H. (1963). Model studies of foundation groups in sand. *Geotechnique*, Vol.13, No.4, pp.334-351.
- HANNA, T.H. (1973). Foundation Instrumentation. Series on Rock and Soil Mechanics, Vol.1, No.3, Trans Tech Publications.
- HUGHES, G.T. and TOWNSEND (1966). Probe for measurement of pore water pressure in varved clays. *Can. Geotech. J.*, Vol.3, No.1, pp.46-50.
- HVORSLEV, M.J. (1951). Time lag and soil permeability in ground water observations. *Waterways Expt Stn, Bulletin 36*, U.S. Corps of Engrs, Vicksburg.
- INSTITUTION OF CIVIL ENGINEERS (1978). Piling - model procedures and specifications. *Instn Civ. Engrs, London*.
- JAKY, J. (1944). The coefficient of earth pressure at rest. *Magyar Mernok es Epitesa Egylet Kozlonye* (in Hungarian).
- JANBU, N. (1976). Static bearing capacity of friction piles. *Proc. 6th European Conf. on Soil Mech. and Fdn Engng*, Vienna, Vol.1, Pt.2, pp.479-488.
- JOHNSON, R.P. (1962). Strength tests on scaled-down concretes suitable for models, with a note on mix design. *Magazine of Conc. Research*, Vol.14, No.40, pp.47-53.
- KALLSTENIUS, T. and BERGAU, W. (1956). Investigations of soil pressure measuring by means of cells. *Royal Swedish Geotech. Inst. Proc. No.12*, 50 pp.
- KEDZI, A. (1957). Bearing capacity of piles and pile groups. *Proc. 4th Int. Conf. on Soil Mech. and Fdn Engng*, London, Vol.2, pp.46-51.
- KEDZI, A. (1975). Pile Foundations. *Foundation Engineering Handbook*, edited by H.F. Winterkorn and H.Y. Fang, Van Nostrand Reinhold Co., New York, pp.556-600.

- KIRBY, R.C. and ESRIG, M.I. (1979). Further development of a general effective stress method for prediction of axial capacity for driven piles in clay. Proc. Conf. on Recent Developments in the Design and Construction of Piles, Instn Civ. Engrs, London, pp.245-254.
- KRAFT, L.M. and LYONS, C.G. (1974). State-of-the-art : ultimate axial capacity of grouted piles. Proc. 6th Annual Off-shore Techn. Conf., Houston, Vol.2, pp.485-502.
- KRIZEK, R.J., FARZIN, M.H., WISSA, A.E.Z. and MARTIN, R.T. (1974). Evaluation of stress cell performance. J. Geotech. Engng Div., Proc. ASCE, Vol.100, No. GT12, pp.1275-1296.
- LAMBE, T.W. and WHITMAN, R.V. (1968). Soil Mechanics. John Wiley and Sons Inc., New York.
- LEE, K.L. and BLACK, D.K. (1972). Time to dissolve air bubble in drain line. J. Soil Mech. and Fdn Div., Proc. ASCE, Vol.98, No. SM2, pp.181-194.
- LOWE, J. and JOHNSON, T.C. (1960). Use of back pressure to increase the degree of saturation of triaxial specimens. Proc. ASCE Conf. on Shear Strength of Cohesive Soils, Boulder, Colorado, pp.812-836.
- MACKEY, R.D. (1966). A three dimensional pressure cell. Civ. Engng and Pub. Wks Rev., Vol.61, pp.1487-1488.
- MASSARSCH, K.R. (1976). Soil movements caused by pile driving in clay. IVA Pile Res. Comm., Royal Acad. Engng Sci., Stockholm, Rapp.No.51, 261 pp.
- MATTES, N.S. and POULOS, H.G. (1969). Settlement of single compressible pile. J. Soil Mech. and Fdn Div., Proc. ASCE, Vol. 95, No. SM1, pp.189-207.
- McKINLAY, D.G. and ANDERSON, W.F. (1975). Determination of modulus of deformation of a till using a pressuremeter. Ground Engng, Vol.8, No.6, pp.51-54.
- MENARD, L.F. (1957). Apparatus for measuring the strength of soil in place. MSc. thesis, Univ. of Illinois, Illinois.
- MENARD, L.F. (1975). The interpretation of pressuremeter test results. Sols Soils No.26, pp.7-43.
- MEYERHOF, G.G. (1976). Bearing capacity and settlement of pile foundations. J. Geotech. Engng Div., Proc. ASCE, Vol.102, No. GT3, pp.196-228.
- MEYERHOF, G.G. and MURDOCK, L.J. (1953). An investigation of the bearing capacity of some bored and driven piles in London Clay. Geotechnique, Vol.3, No.7, pp.267-282.
- MILLER, R.J. and LOW, P.F. (1963). Threshold gradient for water flow in clay systems. Proc. Soil Sci. Soc. of America, Vol.27, pp.605-609.

- MITCHELL, J.K. (1976). Fundamentals of soil behaviour. John Wiley and Sons Inc., New York.
- MOHAN, D. and CHANDRA, S. (1961). Frictional resistance of bored piles in expansive clays. *Geotechnique*, Vol.11, No.4 pp.294-301.
- MOORE, P.J. and COLE, B.R. (1977). Discussion on "At-rest lateral earth pressure of a consolidating clay." *J. Geotech. Engng Div., Proc. ASCE*, Vol.103, GT7, pp.820-821.
- NEVILLE, A.M. (1973). Properties of concrete. 2nd Edition, John Wiley and Sons, New York.
- ØIEN, K. (1958). An earth pressure cell for use on sheet piles: Oslo subway. *Proc. Brussels Conf. on Earth Pressure Problems*, Brussels, Vol.2, pp.118-126.
- O'NEILL, M.W. and REESE, L.C. (1972). Behaviour of bored piles in Beaumont Clay. *J. Soil Mech. and Fdn Div., Proc. ASCE*, Vol.98, No.SM2, pp.195-213.
- PARRY, R.H.G. and NADARAJAH, V. (1974). Observation on laboratory prepared lightly overconsolidated specimens of kaolin. *Geotechnique*, Vol.24, No.3, pp.345-358.
- PARRY, R.H.G. and SWAIN, C. (1976). Skin friction of piles in clay. *Cambridge Univ. CUED/C - SOILS/TR 1976*, No.28.
- PARRY, R.H.G. and SWAIN, C. (1977). Effective stress methods of calculating skin friction on driven piles in clay. *Ground Engng*, Vol.10, No.3, pp.24-26.
- PARRY, R.H.G. and SWAIN, C. (1977a). A study of skin friction on piles in stiff clay. *Ground Engng*, Vol.10, No.8, pp.33-37.
- PEAKER, K.R. (1965). A hydraulic earth pressure cell. *ASTM STP392*, pp.75-81.
- PEATTIE, K.R. and SPARROW, R.W. (1954). The fundamental action of earth pressure cells. *J. of Mechanics and Physics of of solids*, Vol.2, pp.141-155.
- PECK, R.B. (1958). A study of the comparative behaviour of friction piles. *Highway Res. Board*, Special report 36, 72 pp.
- PECK, R.B., HANSON and THORBURN (1974). Foundation Engineering. 2nd edition, John Wiley and Sons Inc., New York.
- PEEKEL, C. (1972). Do we measure strain when we measure strain? *Strain*, Vol.8, No.3, pp.112-116.
- PENMAN, A.D.M. (1960). A study of the response time of various types of piezometers. *Proc. Conf. on Pore Pressure and Suction in Soils*, Instn Civ. Engrs, London, pp.53-58.
- POPLE, J. (1978). Some factors affecting the long-term stability of strain measurements using metal foil gauges. *Strain*, Vol.14, No.3, pp.93-103.

- POTYONDY, J.G. (1961). Skin friction between various soils and construction materials. *Geotechnique*, Vol.11, No.4, pp.339-353.
- POULOS, H.G. (1972). Load settlement prediction of piles and piers. *J. Soil Mech. and Fdn Engng, Proc. ASCE*, Vol.98, No.SM9, pp.879-897.
- POULOS, H.G. (1977). Estimation of pile group settlements. *Ground Engng*, Vol.10, No.2, pp.40-50.
- POULOS, H.G. and DAVIS, E.H. (1968). The settlement behaviour of single axially loaded incompressible piles and piers. *Geotechnique*, Vol.18, No.3, pp.351-371.
- PROCTER, E. (1977). Strain gauge practice. Monograph - British Soc. for Strain Measurement, Part 1, pp.5-11.
- RAYMOND, G.P., TOWNSEND, D.L. and LOJKACEK, M.J. (1971). Effect of sampling on the undrained soil properties of Leda soil. *Can. Geotech. J.*, Vol.8, No.4, pp.546-557.
- REDSHAW, S.C. (1954). A sensitive miniature pressure cell. *J. of Scientific Instruments*, Vol.31, pp.467-469.
- REESE, L.C. (1978). Design and construction of drilled shafts. *J. Geotech. Engng Div., Proc. ASCE*, Vol.104, No.GT1, pp.95-116.
- REESE, L.C., BROWN, J.C. and DALRYMPLE, H.H. (1968). Instrumentation for measurements of lateral earth pressure in drilled shafts. Res. Report No.89-2, Centre for Highway Res., Univ. of Texas at Austin, 125 pp.
- REESE, L.C. and HUDSON, W.R. (1968). Field testing of drilled shafts to develop design methods. Res. Report 89-1, Centre for Highway Res., Univ. of Texas at Austin.
- REESE, L.C., O'NEILL, M.W. and TOUMA, F.T. (1973). Bored piles installed by slurry displacement. *Proc. 8th Int. Conf. Soil Mech. and Fdn Engng*, Vol.2, pp.203-209.
- REESE, L.C., TOUMA, F.T. and O'NEILL, M.W. (1976). Behaviour of drilled piers under axial loading. *J. Geotech. Engng Div., Proc. ASCE*, Vol.102, No.GT5, pp.493-510.
- RICE, S.M.M. (1975). Field and model tests on anchors in clay. PhD thesis, Univ. of Sheffield.
- ROSCOE, K.H. (1968). Soils and model tests. *J. of Strain Analysis*, Vol.3, No.1, pp.57-58.
- ROWE, P.W. (1957).  $C_e=0$  Hypothesis for normally loaded clays at equilibrium. *Proc. 4th Int. Conf. Soil Mech. and Fdn Engng*, London, Vol.1, pp.189-192.

- SCHMERTMANN, J.H. (1975). Measurement of in-situ shear strength. Proc. ASCE Specialty Conf. on In-situ Measurements of Soil Properties, Vol. 2, pp. 57-138.
- SEARLE, I.W. (1979). The design of bored piles in overconsolidated clays using effective stresses. Proc. Conf. on Recent Developments in the Design and Construction of Piles, Instn Civ. Engrs, London, pp. 265-274.
- SEED, H.B. and REESE, L.C. (1957). The action of soft clay along friction piles. Trans. ASCE, Vol. 122, pp. 731-754.
- SELIG, E.T. (1964). A review of stress and strain measurement in soil. Proc. Symp. on Soil-Structure Interaction, Univ. of Arizona, Tusson, pp. 172-188.
- SHEERAN, D.E. and KRIZEK, R.J. (1971). Preparation of homogeneous soil samples by slurry consolidation. J. of Materials, Vol. 6, No. 2, pp. 356-373.
- SHERIF, M.A. and KOCH, D.E. (1970). Coefficient of earth pressure at rest as related to soil precompression ratio and liquid limit. Highway Res. Record No. 323, pp. 39-48.
- SKEMPTON, A.W. (1954). The bearing capacity of clays. Building Res. Congress, London, Div. 1, No. 3, pp. 180-189.
- SKEMPTON, A.W. (1959). Cast-in-situ bored piles in London Clay. Geotechnique, Vol. 9, No. 4, pp. 153-173.
- SKEMPTON, A.W. and SOWA, V.A. (1963). The behaviour of saturated clays during sampling and testing. Geotechnique, Vol. 13, No. 4, pp. 269-290.
- SOWA, V.A. (1970). Pulling capacity of concrete cast-in-situ bored piles. Can. Geotech. J., Vol. 7, No. 4, pp. 482-493.
- SOWERS, G.F., MARTIN, C.B. WILSON, L.L. and FAUSOLD, M. (1961). The bearing capacity of friction pile groups in homogeneous clay from model studies. Proc. 5th Int. Conf. Soil Mech. and Fdn Engng, Vol. 2, No. 3, pp. 155-159.
- TAVENAS, F.A. (1975). Discussion "In-situ measurement of initial stresses and deformation characteristics". Proc. ASCE Conf. on In-situ Measurements of Soil Properties, Vol. 2, pp. 263-269.
- TAYLOR, D.W. (1947). Pressure distribution theories, EP cell investigations and pressure distribution data. Fact-finding survey, Waterway Expt. Stn, Vicksburg, Miss.
- TAYLOR, P.T. (1966). Age effect on shaft resistance and effect of loading rate on load distribution of bored piles. PhD thesis, Univ. of Sheffield.
- TERZAGHI, K. (1943). Theoretical soil mechanics. John Wiley and Sons Inc., New York.
- THOMSON, W.J. (1963). Lateral pressure in one-dimension consolidation. Proc. 2nd Asian Conf. Soil Mech. and Fdn Engng, Tokyo, pp. 26-31.

- THORBURN, S. and THORBURN, J.Q. (1977). Review of problems associated with the construction of cast-in-place concrete piles. DoE and CIRIA Piling Development Grp Report PG2, 42 pp.
- THORLEY, A., CALHOON, M.L., ZEMAN, Z.P. and WATT, W.G. (1970). Bore-hole instruments for economical strength and deformation in-situ testing. Proc. In-situ Investigations in Soil and Rocks, British Geotech. Soc., London, pp.155-165.
- TIMOSHENKO, S.P. (1956). Strength of Materials. 3rd edition, Van Nostrand Reinhold, New Jersey.
- TOMLINSON, M.J. (1957). The adhesion of piles driven in clay soils. Proc. 4th Int. Conf. Soil Mech. and Fdn Engng, Vol. 2, pp. 66-71.
- TOMLINSON, M.J. (1961). The functions and principles of design of large diameter bored piles. Proc. Symp. on Large Diameter Bored Piles, Reinforced Conc. Rev., pp. 673-683.
- TOMLINSON, M.J. (1970). Adhesion of piles in stiff clays. CIRIA Report 26, 47 pp.
- TOMLINSON, M.J. (1977). Pile design and construction practice. A Viewpoint Publication, Cement and Conc. Assn .
- TORY, A.C. and SPARROW, R.W. (1967). The influence of diaphragm flexibility on the performance of an earth pressure cell. J. of Sci. Instruments, Vol. 44, pp. 781-785.
- TRIANDAFILIDIS, G.E. (1974). Soil-stress gauge design and evaluation. J. of Testing and Evaluation, ASTM, Vol. 2, No. 3, pp. 146-158.
- TROLLOPE, D.H. and LEE, I.K. (1961). The measurement of soil pressure. Proc. 5th Int. Conf. Soil Mech. and Fdn Engng, Paris, Vol. 2, pp. 493-499.
- VESIC, A.S. (1975). Principles of pile foundation design. Lecture Series on deep foundations, Boston Soc. of Civ. Engrs.
- VIJAYVERGIYA, V.N. and FOCHT, J.A. (1972). A new way to predict capacity of piles in clay. Proc. 4th Annual Offshore Techn. Conf., Houston, Vol. 2, pp. 865-874.
- WATERWAYS EXPERIMENT STATION (1944). Soil pressure investigation. Technical Memorandum 201-1, Waterways Expt Stn, Vicksburg, Miss., USA.
- WATT, W.G., KURFURST, P.J. and ZEMAN, Z.P. (1969). Comparison of pile load test skin friction values and laboratory strength tests. Can. Geotech. J., Vol. 6, No. 3, pp. 339-352.
- WELTMAN, A.J. (1977). Integrity testing of piles: a review. DoE and CIRIA Piling Development Group Report PG4, 36 pp.
- WELTMAN, A.J. and HEALY, P.R. (1978). Piling in boulder clay and other glacial tills. DoE and CIRIA Piling Development Group Report PG5, 78 pp.

- WELTMAN, A.J. and LITTLE, J.A. (1977). A review of bearing pile types. DoE and CIRIA Piling Development Group Report PG1, 82 pp.
- WHITAKER, T. (1957). Experiments with model piles in groups. *Geotechnique*, Vol.7, pp.147-167.
- WHITAKER, T. and COOKE, R.W. (1966). An investigation of shaft and base resistances of large bored piles in London Clay. Proc. Symp. Large Diameter Bored Piles, Instn Civ. Engrs, London, pp.7-49.
- WHITMAN, R.V., RICHARDSON, A.M. and HEALEY, K.A. (1961). Time lags in pore pressure measurements. Proc. 5th Int. Conf. Soil Mech. and Fdn Engng, Paris, Vol.1, pp.407-411.
- WILLIAMS, G.M.J. and COLMAN, R.B. (1965). The design of piles and cylindrical foundations in stiff fissured clay. Proc. 6th Int. Conf. Soil Mech. and Fdn Engng, Montreal, Vol.2.
- WOODWARD, R.J. (1972). Drilled Pier Foundations. McGraw-Hill Book Co. Inc., New York.
- WOOLEY, J.A. and REESE, L.C. (1974). Behaviour of an axially loaded drilled shaft under sustained loading. Res. Report 176-2, Centre for Highway Res., Univ. of Texas at Austin, 165 pp.
- WROTH, C.P. (1975). In-situ measurement of initial stresses and deformation characteristics. Proc. ASCE Specialty Conf. on In-situ Measurement of Soil Properties, Raleigh, Vol.2, pp.181-230.
- WROTH, C.P. and HUGHES, J.M.O. (1974). The development of a special instrument for the in-situ measurement of the strength and stiffness of soils. Cambridge Univ. Rep. CUED/C - SOILS TR18 .
- YONG, R.N. and WARKENTIN, B.P. (1975). Soil properties and behaviour. Elsevier Scientific Pub. Co., New York.
- ZEEVAERT, L. (1959). Reduction of point bearing capacity of piles because of negative friction. Proc. 1st Pan-American Conf. Soil Mech. and Fdn Engng, Mexico, Vol.3, pp.1145-1152.

APPENDIX I

DESIGN OF CONSOLIDATION AND TEST CELL

- References
1. BS4504:1969 (and Amendment Slip AMD 1481,28/6/74)
  2. BS1500:Part 1:1958 (incorporating Amendments)
  3. BS4190:1967
  4. BS449:Part 2:1969

Design Considerations

1. Test Requirements as listed in Section 4.3.1.
2. Availability of materials to construct cell.
3. Flexibility of design for modifications when required.
4. Construction considerations (practicality and ease of machining)

Data: Maximum working pressure,  $p_w = 560 \text{ kN/m}^2$   
 Design pressure,  $p = 840 \text{ kN/m}^2$   
 Factor of safety,  $F = 1.5$   
 Working temperature range,  $T = 0 \text{ to } 30^\circ\text{C}$   
 Tensile strength of carbon steel,  $f_t = 3.8 \times 10^5 \text{ kN/m}^2$   
 Modulus of carbon steel,  $E = 200 \times 10^6 \text{ kN/m}^2$

REFERENCE	DESIGN CALCULATIONS
1 BS1500 Table 2d Section 2/B2	Material to be used for test cell - carbon steel Permissible design stress of material, $f = f_t/5 = 0.76 \times 10^5 \text{ kN/m}^2$ Shear stress, $= 0.8f = 0.61 \times 10^5 \text{ kN/m}^2$ Assume internal diameter of cell = 200mm internal height of cell = 400mm
2 BS1500 Sect.3E,2(b), Eqn.(3)         Table 1	<u>Design of thickness of cylindrical shell</u> From code, $t = \frac{pD_i}{2fJ-p} + c \quad (\text{formula in terms Imperial units})$ $t = \text{minimum thickness in ins.}$ $p = 840 \text{ kN/m}^2 = 120 \text{ psi}$ $D_i = 200\text{mm} = 7.9 \text{ ins}$ $f = 0.76 \times 10^5 \text{ kN/m}^2: 11000 \text{ psi}$ $J = \text{joint factor} = 0.70 \text{ (from Table)}$ $e = \text{corrosion allowance} = 1/16 \text{ ins (recommended)}$

REFERENCE

DESIGN CALCULATIONS

$$t = \frac{120 \times 7.9}{2 \times 11000 \times 0.70 - 120} + \frac{1}{16} = 0.125 \text{ ins} = 3.2 \text{ mm}$$

t = 4mm was selected

3 BS4504:1969

Design of flanges and bolting

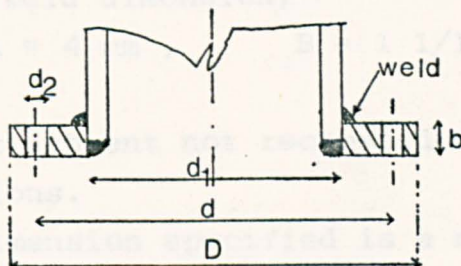


Table 6/3

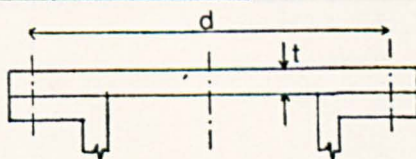
For nominal pressure of 600 kN/m<sup>2</sup>,  
internal diameter of 200mm,  
and d<sub>1</sub> = 208mm,

Table 6/3 recommends

- (a) Flange : D = 320mm, b = 20mm
- (b) Bolting: M16
- (c) holes : 8 Nos ; d<sub>2</sub> = 18mm ; d = 280

4 BS1500  
Sect.H Fig.23

Design of Flat covers



Eqn.20

Thickness of cell cover,  $T = d \sqrt{(P/Kf)} + c$   
(Imperial units)

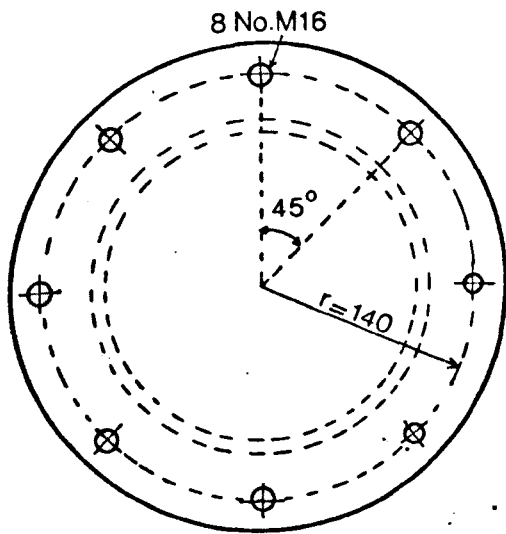
- T = minimum thickness in ins.
- d = 280 mm = 11.02 ins.
- p = 840 kN/m<sup>2</sup> = 120 psi
- f = 0.76 x 10<sup>5</sup> kN/m<sup>2</sup> = 11000 psi
- c = corrosion allowance = 1/16 ins (recommended)
- k = constant depending on method of attachment = 6

Substituting the values,

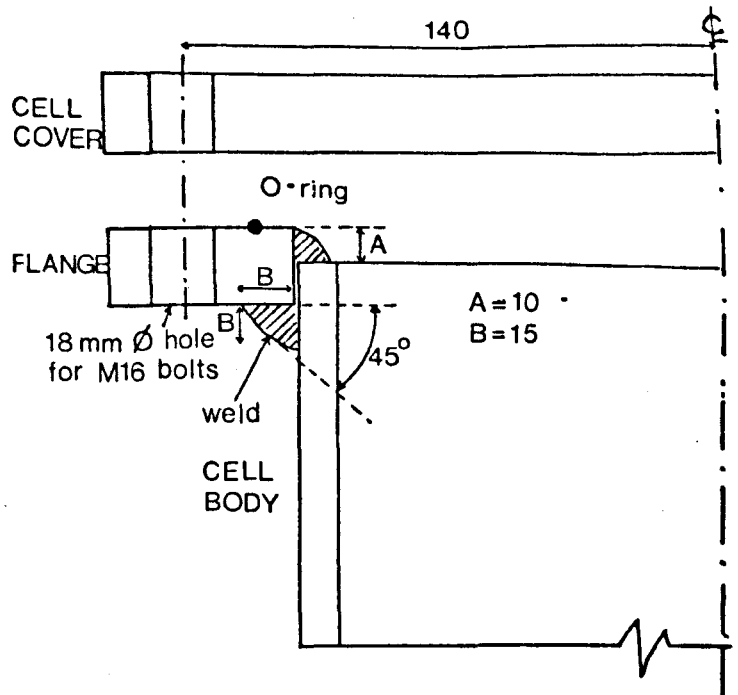
$$T = 0.532 \text{ ins} = \underline{13.5 \text{ mm}}$$

For ease of construction, let thickness of cell covers be the same as flange thickness, ie. T = 20 mm

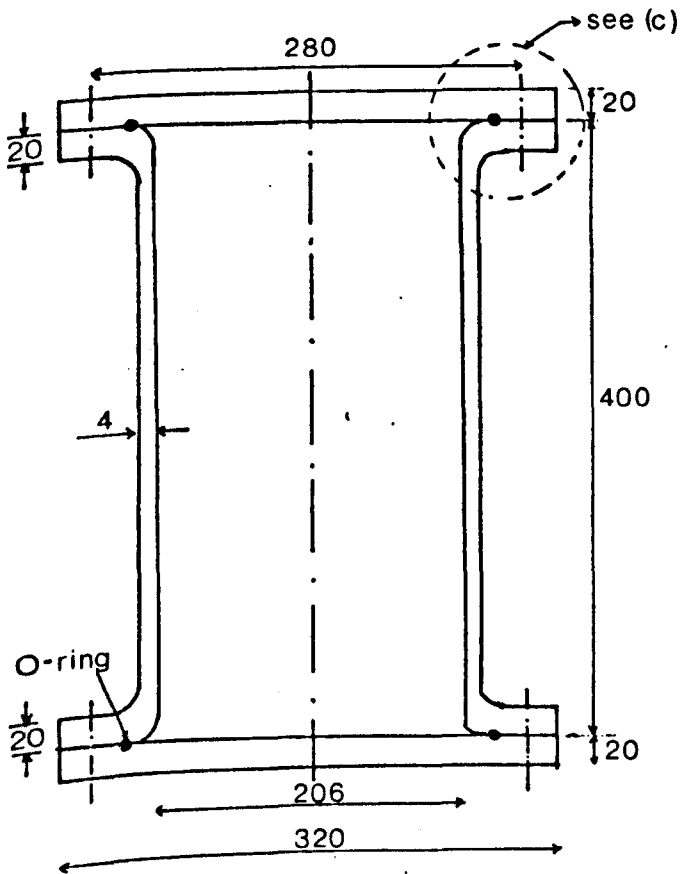




(a) PLAN



(c) FLANGE ATTACHMENT



(b) SECTION

Notes:

1. All dimensions in mm.
2. Material of test cell - carbon steel.
3. Design pressure =  $840 \text{ kN/m}^2$
4. Working (consolidation) pressure =  $560 \text{ kN/m}^2$
5. Number of cells constructed = 8.

Fig. I.1 TEST CELL.

## APPENDIX II

### MANUFACTURE OF RUBBER JACKS

The materials required for the manufacture of rubber jacks are shown in Fig. 4.10. The mould was made by cutting circular plates from a 25mm thick flat piece of plywood, then machining the plates to the required shape and finally joining them together with Araldite in several layers to form the required height. The edges were rounded off to prevent uneven concentrations of latex and the formation of air voids, as well as to ease the removal of the cured membrane. The surfaces were then polished and varnished to provide a smooth texture.

Before applying the Dunlop latex (Grade A360/W), the solution was first stirred to a uniform consistency because prolonged storage results in a thick skin formation at the surface and increased viscosity towards the bottom [Vaid and Campanella, (1973)]. Care was taken during stirring to avoid any formation of bubbles. After cleaning the surface of the mould with emery cloth, a coating of latex was applied with a brush and repeated at about 3-hourly intervals after the previous coating had dried at room temperature. Any air holes or particles formed during the painting were eliminated before the latex cured. After each coating, the brush was washed with plenty of soap and hot water and dried.

After about 20 to 25 coatings, the membrane was dusted with talcum powder and stripped off the mould and more talc was applied to the inner surface. The final rubber thickness was about 2mm and the total height of membrane when fully extended was 250mm. The quality of the rubber jacks depends on the surface texture and cleanliness of the mould, the concentration of solution and the uniformity of the coating.

## APPENDIX III

### DESIGN OF EARTH PRESSURE CELLS

#### 1. EP CELLS

##### Design considerations

1. Design requirements listed in Table 5.2
2. Physical requirements discussed in Section 5.3.4
3. Construction and machining considerations

##### Theory

For a circular plate clamped around its circumference and subjected to a uniformly distributed load normal to its surface, the plate will exhibit zones of positive and negative strain providing deflection everywhere does not exceed a small fraction of plate thickness. Therefore, if central deflection of the plate is limited to 1/5 of its thickness, Timonshenko's (1956) equation, may be applied with little error,

$$\delta = \frac{p a^4}{64 \bar{D}} \quad \dots (1)$$

where  $\delta$  is the central deflection

$p$  is the uniformly applied pressure

$a$  is the radius

$\bar{D}$  is the flexural rigidity given by  $\frac{Et^3}{12(1-\nu^2)}$

$E$  is the modulus of elasticity

$t$  is the diaphragm thickness

and  $\nu$  is Poisson's Ratio

For radial strain,  $\epsilon_r$ , and circumference strain,  $\epsilon_\theta$ , at a radius,  $r$ , from the centre of the diaphragm, Timoshenko showed that,

$$\epsilon_r = \frac{pta^2}{32\bar{D}} \left(1 - \frac{3r^2}{a^2}\right) \quad \dots (2)$$

$$\epsilon_\theta = \frac{pta^2}{32\bar{D}} \left(1 - r^2/a^2\right) \quad \dots (3)$$

substituting  $a = d/2$  where  $d$  is the diaphragm diameter and

$\nu = 0.33$  for aluminium alloy into equation(1),

$$\delta = \frac{pd^4}{96Et^3} \quad \dots (4)$$

For requirement (1) in Table 5.2,  $\frac{\delta}{d} \leq \frac{1}{2000}$  ... (5)

Eliminating  $\delta$  by equating (4) and (5),

$$\text{minimum thickness, } t = \left( \frac{2000}{96} p/E \right)^{\frac{1}{3}} \cdot d \quad \dots (6)$$

Substituting  $E = 70 \times 10^6 \text{ kN/m}^2$  for aluminium used, and assuming  $d = 20\text{mm}$ , equation (6) is reduced to

$$t = 0.132 p^{\frac{1}{3}} \quad \dots (7)$$

where  $t$  is in mm and  $p$  in  $\text{kN/m}^2$ . A plot of  $t$  against  $p$  has been given in Fig. 5.2. An overall cell diameter of 25mm and thickness 5mm were selected and found to satisfy all the design requirements (see Table 5.4).

## 2. IF CELLS

In the case of 'IF' pressure cells

$$\delta/d \leq \frac{1}{1000} \quad \dots (8)$$

Eliminating  $\delta$  by equating (8) and (4)

$$t = \left( \frac{1000}{96} p/E \right)^{\frac{1}{3}} \cdot d \quad \dots (9)$$

Substituting  $E = 70 \times 10^6 \text{ kN/m}^2$  and taking  $d = 12\text{mm}$ , equation (6) becomes

$$t = 0.064 p^{\frac{1}{3}} \quad \dots (10)$$

A plot of  $t$  against  $p$  has been shown in Fig. 5.2. The length of the casing depends on the diameter of the pile, while the overall diaphragm diameter was chosen as 14mm to satisfy construction considerations.

## APPENDIX IV

### THEORETICAL CALCULATION OF STRAIN IN THE CENTRE OF THE DIAPHRAGM

In Appendix III, the radial and circumferential strains have been given as

$$\epsilon_r = \frac{pta^2}{32\bar{D}} \left( 1 - \frac{3r^2}{a^2} \right)$$

$$\epsilon_\theta = \frac{pta^2}{32\bar{D}} \left( 1 - \frac{r^2}{a^2} \right)$$

At the centre of the diaphragm ( $r=0$ ) where strain is a maximum,

$$\epsilon_r = \epsilon_\theta = \frac{pta^2}{32\bar{D}} \quad \dots (1)$$

Substituting the formula for  $\bar{D}$  and the values of  $p$ ,  $a$ ,  $E$ , and  $\nu$  given in Appendix IV, equation (1) becomes

$$\epsilon_r = 0.477 p/t^2 \quad \dots (2)$$

where  $\epsilon_r$  is in microstrain,  $t$  is in mm and  $p$  is in  $\text{kN/m}^2$

Therefore, for various known design thicknesses and pressures, the maximum strain in the centre of diaphragm can be calculated.

#### Maximum skin friction in diaphragm

The maximum skin stress at the diaphragm centre is given by Hanna (1973) as

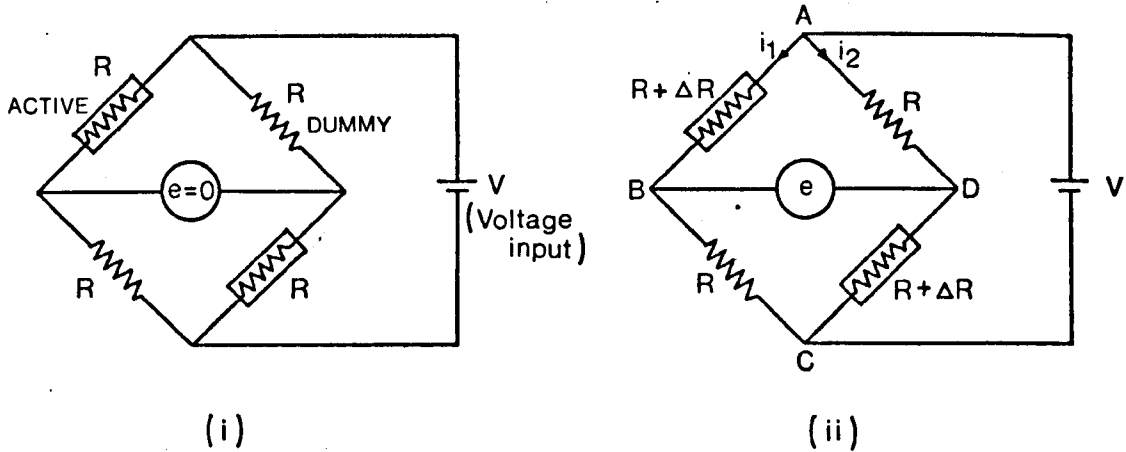
$$f_c = \frac{3}{16} (d/t)^2 p \quad \dots (11)$$

and this value should not exceed the allowable stress of the aluminium diaphragm ( $f_a = 59 \times 10^3 \text{ kN/m}^2$ )

APPENDIX V

PRINCIPLES OF STRAIN GAUGING

Theory



Strain gauges are usually connected to form a Wheatstone bridge circuit for the measurement of small resistance changes. For this study, two active arms were connected to two dummy arms to form a similar circuit with temperature compensation.

The strain sensitivity of metal material or gauge factor,  $K$  is related to the change in resistance and strain by

$$K = \frac{(\Delta R/R)}{(\Delta L/L)} = \frac{1}{\epsilon} \frac{\Delta R}{R}$$

Rearranging,

$$\frac{\Delta R}{R} = K \epsilon \quad \dots (1)$$

Now, for a balanced bridge [figure (i)], i.e. resistance of all arms are equal, the output voltage,

$$e = 0$$

Suppose the active strain gauges undergo a strain, then the resistance becomes  $R + \Delta R$  (assuming positive for tensile strain).

The current passing through the bridge arm ABC and ADC is

$$i_1 = i_2 = \frac{V}{2R + \Delta R} \quad \dots (2)$$

For loop ABD,

$$\begin{aligned} V_{BD} &= V_{AB} - V_{AD} \\ &= i_1(R + \Delta R) - i_2(R) \quad \dots (3) \end{aligned}$$

Substituting (2) into (3),

$$V_{BD} = \frac{V (\Delta R)}{2R + \Delta R}$$

$$\text{but } 2R \gg \Delta R \quad \therefore (2R + \Delta R) \simeq 2R$$

$$\text{hence } e = V_{BD} = \frac{V \Delta R}{2 R}$$

$$\text{or } e = \frac{V}{2} K \epsilon \quad \dots (4)$$

With K and V constant for a particular strain gauge and bridge circuit, the output voltage, e is proportional to the strain.

## APPENDIX VI

### CALCULATION OF TIME LAG FOR DESIGN PURPOSES

#### Theory

Hvorslev (1951) has given a method of calculating the response time of a piezometer. This theoretical method assumes that,

- (i) the soil surrounding the piezometer is uniform, isotropic, fully saturated and infinite,
- (ii) no swelling or consolidation occurs around the piezometer and
- (iii) no accumulation of air bubbles or hydraulic losses in the piezometer system occur.

Penman (1960) modified the method slightly to obtain the relationship,

$$Q = \left( \frac{Fk}{\gamma_w} \right) \Delta p t$$

where  $Q$  is the quantity of water which will flow into a tip under a pressure difference  $\Delta p$  in time  $t$ , and where

$F$  = intake factor (with dimension of length)

$k$  = permeability of soil

$\gamma_w$  = unit weight of water

If  $p_o$  is the true pressure,  $p$  is the out-of-balance pressure, and  $V$  is the volume of water entering the system per unit pressure increase, then

$$\frac{Q}{\Delta p} = \frac{V (p_o - p)}{p_o} = \frac{Fkt}{\gamma_w}$$

$$\therefore \frac{(p_o - p)}{p_o} = \frac{Fkt}{V\gamma_w}$$

The intake factors given by Hvorslev (1951) is shown in Table VIa while the system flexibility and pressure equalisation ratio given by Penman (1960) is shown in Table VIb

and Fig. VI. For the pressure equalisation, Penman (1960) suggested that electrical resistance transducers have relatively low flexibility and very small volume change, and therefore, the flexibility is neglected.

Example: Response to pressure increment of  $280 \text{ kN/m}^2$  to  $420 \text{ kN/m}^2$

		PIEZOMETER		REMARKS
		SOIL	INTERFACE	
DATA	Diameter, d (mm)	7	12.5	-
	Intake factor, F (mm)	19.3	34.4	$F=2.75d$
	Permeability, k (m/s)	$1.02 \times 10^{-9}$	$1.02 \times 10^{-9}$	Table 7.1
	Vol. flexibility factor, V (ml/(kN/m <sup>2</sup> ))	$1.47 \times 10^{-5}$	$1.47 \times 10^{-5}$	for 300mm tube length
	Unit Wt. of water, $\gamma_w$ (kN/m <sup>3</sup> )	9.8	9.8	-
RESULTS	For 99% equalization, $\frac{Fkt}{V\gamma_w}$ is	4.6	4.6	
	$\therefore$ time lag, t (secs)	22	12	

TABLE VIa (after Hvorslev, 1951)

SHAPE OF FILTER TIP	INTAKE FACTOR
Sphere: diameter, d	$2\pi d$
Flat disc: dia., d	$2.75d$
Cylindrical: diameter, d length, l	$\frac{2\pi l}{2.31 \log_{10} [1/d + \sqrt{1 + (1/d)^2}]}$

TABLE VIb (after Penman, 1960)

$\frac{Fkt}{V\gamma_w}$	0.11	0.36	0.69	1.20	2.30	3.00	4.60	6.91	9.21
$\frac{P_o - P}{p}$ %	10	30	50	70	90	95	99	99.9	99.99

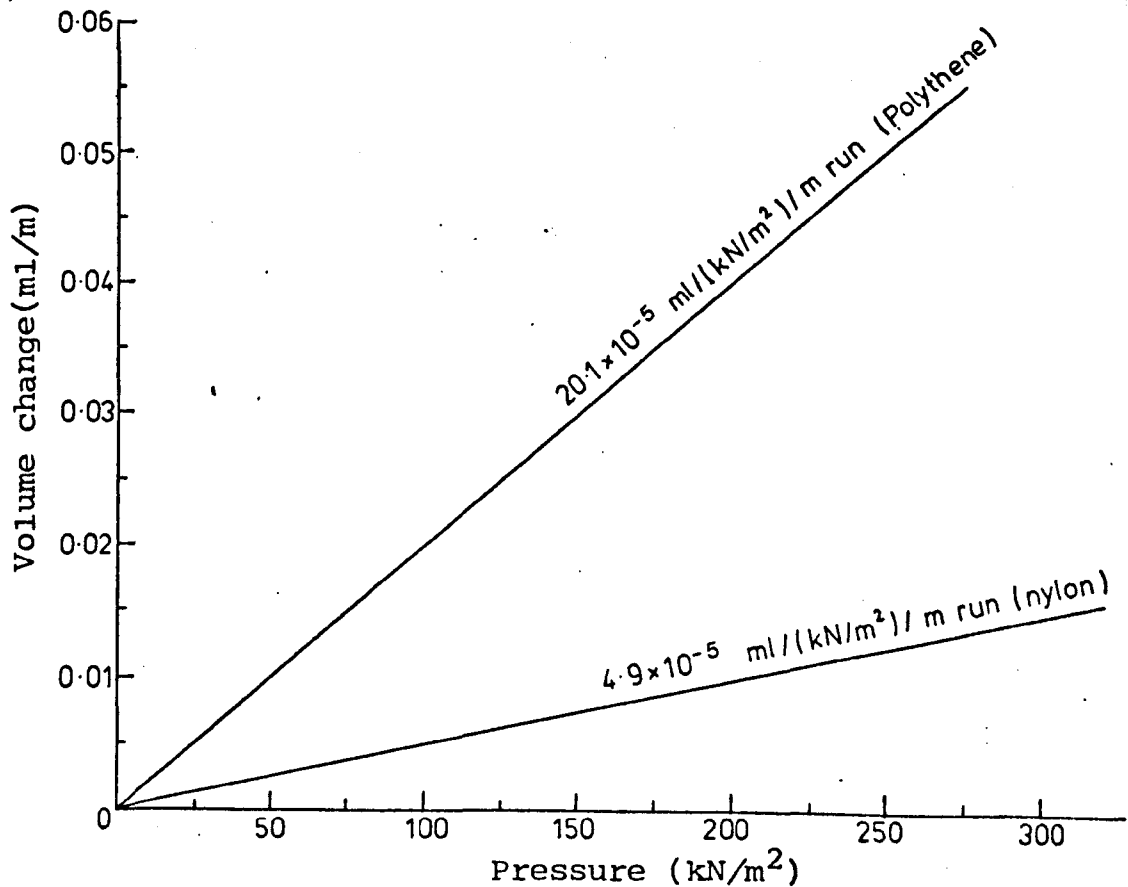


Fig. VI FLEXIBILITY - PRESSURE RELATIONSHIP  
(after Penman, 1960)

## APPENDIX VII

### LATERAL PRESSURE OF CONCRETE

#### Theory

Peurifoy (1965) gives a formula developed by the American Concrete Institute (1963) for calculating the lateral pressure of concrete on the formwork. The formula considered the effect of two variables: rate of placement and temperature.

Maximum pressure on column formwork expressed as,

$$P = 150 + \frac{1}{7} 9000R \quad \dots(\text{Imperial Units})$$

where maximum  $P = 3000\text{psf}$  ( $144\text{ kN/m}^2$ ) or  $150h$ , whichever is

less and

$P =$  maximum lateral pressure, psf

$R =$  rate of placement, ft/hr

$T =$  temperature of concrete in formwork, °F

$h =$  maximum height of fresh concrete, ft.

#### Calculations

Assuming that casting of the 100mm long 'model' pile took 5 mins, then rate of placement = 100mm in 5 mins

$$\approx 4 \text{ ft/hr}$$

The rate is similar to the American Concrete Code (1963) specifications of 5 ft/hr. Temperature during setting of fresh concrete measured with a thermometer was,  $T=24^\circ\text{C}=75^\circ\text{F}$ .

$$\begin{aligned} \therefore P &= 150 + \frac{1}{75}(9000 \times 4) \\ &= 630 \text{ psf} \\ &= \underline{30 \text{ kN/m}^2} \end{aligned}$$

Therefore, for unset concrete, the hydrostatic head is equivalent to approximately 3 metres. This is consistent with values assumed in practice, i.e. between 3 and 7 metres. The head of concrete calculated was applied during the initial setting of concrete. It should be pointed out that once the concrete hardens, the rigid structure of the concrete does not exert lateral pressure any longer.